



UNIVERSITÀ
DEGLI STUDI
DI PADOVA

Sede Amministrativa: Università degli Studi di Padova

Dipartimento di Agronomia Animali Alimenti Risorse naturali e Ambiente - DAFNAE

SCUOLA DI DOTTORATO DI RICERCA IN SCIENZE DELLE PRODUZIONI
VEGETALI

CICLO XXVIII

Characterization of a novel brachytic2 (*br2*) allele in maize

Direttore della Scuola: Ch.mo Prof. Antonio Berti

Supervisore: Ch.mo Prof. Serena Varotto

Dottoranda : Sara Balzan

Declaration

I hereby declare that this submission is my own work and that, to the best of my knowledge and belief, it contains no material previously published or written by another person nor material which to a substantial extent has been accepted for the award of any other degree or diploma of the university or other institute of higher learning, except where due acknowledgment has been made in the text.

A copy of the thesis will be available at <http://paduaresearch.cab.unipd.it/>

Dichiarazione

Con la presente affermo che questa tesi è frutto del mio lavoro e che, per quanto io ne sia a conoscenza, non contiene materiale precedentemente pubblicato o scritto da un'altra persona né materiale che è stato utilizzato per l'ottenimento di qualunque altro titolo o diploma dell'università o altro istituto di apprendimento, a eccezione del caso in cui ciò venga riconosciuto nel testo.

Una copia della tesi sarà disponibile presso <http://paduaresearch.cab.unipd.it/>

Table of contents

Table of contents	5
Riassunto	7
Summary	10
Chapter I: General introduction	13
1.1 Zea mays is both a plant model organism and an important crop species	13
1.1.1 The Maize stem development	17
1.1.2. The Maize root system	22
1.2. The role of auxin in plant development	25
1.2.1 Auxin biosynthesis and conjugation.....	25
1.2.2 Auxin signalling.....	28
1.2.3 Polar Auxin Transport (PAT).....	29
1.3 Plant transposable elements	58
1.3.1 The class I RNA retrotransposon.....	60
1.3.2 The class II DNA transposons.....	63
1.3.3 The miniature inverted-repeat transposable elements.....	64
1.3.4 Transposon activity.....	67
Chapter II: Morphological characterization of the <i>br2:NC238</i> line	70
2.1 Introduction	70
2.2 Materials and methods	73
2.3 Results	78
2.3.1 The <i>br2:NC238</i> root system at seedling stage.....	78
2.3.2 The <i>br2:NC238</i> root system at flowering stage.....	81
2.3.3 The stem of <i>br2:NC238</i> at flowering stage.....	85
2.3.4 Internode anatomy and auxin accumulation in <i>br2:NC238</i> plants	91
2.4 Discussion.....	94
Chapter III: Genetic characterization of the <i>br2:NC238</i> line mutation	100
3.1 Introduction	100
3.2 Materials and methods	104
3.3 Results	108
3.3.1 Genetic characterization of <i>br2:NC238</i> mutation.....	108

3.3.2 Study of <i>br2:NC238</i> line <i>abcb1</i> insertion	111
3.3.3 Analyses of <i>br2:NC238</i> line <i>abcb1</i> transcript.....	123
3.3.4 Expression analysis of auxin carriers in <i>br2:NC238</i> line.....	129
3.4 Discussion	133
Chapter IV: The <i>br2NC238:B73</i> line.....	139
4.1 Introduction	139
4.2 Materials and methods.....	141
4.3 Results.....	141
4.3.1 Genetic analyses of <i>br2NC238:B73</i> line.....	141
4.3.2 Morphological traits measurements.....	142
4.4 Discussion.....	148
5. General discussion and conclusions.....	149
References.....	152

Riassunto

A partire dalla "Rivoluzione verde" sono state selezionate varietà di colture a taglia ridotta, ad esempio riso e sorgo. Molti sono i vantaggi derivanti: un maggior utilizzo di energia per la produzione della granella rispetto alla crescita vegetativa, la possibilità di aumentare la densità delle piante per superficie, la maggior resistenza ai danni da vento e la minor perdita di granella durante raccolta e trasporto.

Molte linee mutanti nane sono caratterizzate da difetti in sintesi, metabolismo o trasporto di ormoni: brassinosteroidi e gibberelline soprattutto. Un difetto nel trasporto di auxina caratterizza le linee mutanti di mais *br2* e di sorgo *dw3*.

Test di allelismo condotti all'Università di Purdue (IN) incrociando la linea di mais NC238 a statura ridotta con altre piante a statura ridotta indicarono che la linea NC238 è un mutante di tipo *brachytic 2*.

Nel 2003 è stato clonato il gene *br2/pgp1/abcb1* responsabile del fenotipo a bassa statura dovuto alla riduzione della lunghezza degli internodi vicini alla base del fusto. Il gene *abcb1* codifica per la proteina ABCB1 che appartiene alla famiglia di trasportatori MDR (Multidrug Resistant), sottofamiglia B. Questa proteina è l'omologo della proteina trasportatrice di auxina di *Arabidopsis* ABCB1.

L'ormone auxina svolge molti ruoli nella regolazione dello sviluppo della pianta, sintesi, degradazione e coniugazione contribuiscono a modulare i livelli di auxina. Le proteine ABCB, assieme a PIN, PILS e AUX/LAX creano un flusso direzionale di auxina dai siti di sintesi (aree meristematiche, giovani tessuti) alle zone dove è necessaria. L'auxina svolge ruoli nello sviluppo embrionale, mantenimento delle cellule indifferenziate, architettura del fusto, risposta tropica, sviluppo e tropismo delle radici. La maggior parte di queste funzioni sono state studiate in *Arabidopsis*.

Questa tesi si focalizza sull'analisi fenotipica e morfologica della linea *br2:NC2382*. Una pianta alta era stata isolata in una popolazione di NC238. La mutazione infatti è dovuta a un'inserzione di un trasposone e a seguito di un fenomeno di reversione, in cui il trasposone si è reinserito in un altro locus del genoma, si era originato un revertente. Questa pianta revertente è stata auto-fecondata per ottenere una progenie da usare negli esperimenti come linea di riferimento *wild type*.

In parallelo, l'allele mutante *br2* di NC238 è stato introgresso nella linea di riferimento B73.

La presente tesi si suddivide in quattro parti.

Nel primo capitolo sono state introdotte la biologia, morfologia e genetica del mais (*Zea Maize*). Sono stati descritti la sintesi, il metabolismo e i ruoli dell'ormone auxina. In questa sezione è stata inserita la review dal titolo "The role of auxin transporters in monocot development" ("Il ruolo dei trasportatori di auxina nello sviluppo delle monocotiledoni") scritta durante il periodo all'estero presso il laboratorio del prof. Johal (Università di Purdue, IN). La review descrive le funzioni dei diversi trasportatori di auxina nelle monocotiledoni: mais, riso sorgo e brachipodio, comparandole con i rispettivi ruoli in *Arabidopsis*, quando trasportatori omologhi esistono. Inoltre una descrizione della struttura e classificazione degli elementi trasponibili delle piante è stata fatta.

Nel secondo capitolo viene descritta l'analisi dei tratti fenotipici. Le pubblicazioni che studiano e caratterizzano i mutanti *br2* descrivono difetti nell'allungamento del fusto dovuti alla ridotta lunghezza degli internodi alla base del fusto. Inoltre, difetti nella struttura dei vasi del fusto di *br2* sono stati osservati. In un altro caso alterazioni nelle cellule delle foglie e nell'angolo fogliare sono stati descritti. Nessun articolo descrive in dettaglio il sistema radicale di *br2*. La caratterizzazione della linea *br2:NC238* è stata fatta misurando i tratti dell'apparato radicale di piante allo stadio di una settimana. Inoltre sono state eseguite misure fenotipiche su piante in fioritura, coltivate in campo all'azienda agraria sperimentale dell'Università di Padova "L.Toniolo", per identificare eventuali alterazioni dei tratti della pianta. Sono state misurate: la statura delle piante, le distanze, i diametri e il numero dei nodi, l'altezza della spiga più alta, le ramificazioni del pennacchio. Inoltre, è stata fatta una analisi dell'apparato radicale fino a un metro di profondità di suolo. Le radici sono state estratte attraverso carotaggi del terreno alla base del fusto, lavate, scannerizzate e i dati elaborati con un software apposito. Inoltre l'anatomia delle cellule del fusto di *br2:NC238* e la loro localizzazione di auxina sono state osservate.

Il terzo capitolo riguarda la caratterizzazione della mutazione a livello genetico. Sono stati amplificati e sequenziati il clone genomico e il trascritto, delle linee *br2:NC238* e il suo revertente.

E' stato fatto lo studio dell'inserzione che causa la mutazione in *br2:NC238*. E' stata analizzata la struttura della sequenza e sono state interrogate anche dati di sequenze genomiche,

sequenze ripetute e elementi trasponibili. Inoltre, è stata fatta un'analisi di espressione dei geni codificanti trasportatori di auxina.

Il quarto capitolo riguarda lo studio della linea B73 nella quale l'allele mutato di NC238 è stato inserito. Il clone genomico di *abcb1* e il trascritto sono stati amplificati e sequenziati per confermare la mutazione e l'alterazione della trascrizione del gene. Sono state fatte le analisi fenotipiche per confermare che l'allele conferisce le caratteristiche morfologiche anche in linee genotipiche diversi.

In conclusione, le analisi hanno mostrato che il fenotipo di *br2:NC238* appare quando le piante hanno 7 foglie. Negli stadi precedenti, *br2:NC238* e il revertente sono indistinguibili. Allo stadio di fioritura, *br2:NC238* è caratterizzato da ridotta lunghezza degli internodi alla base del fusto e maggior diametro dei nodi bassi. Il resto della pianta è normale.

La mutazione *br2* nella linea NC238 è dovuta a un'inserzione di un trasposone in una regione intronica del gene. Il trasposone è caratterizzato da due regioni invertite terminali (TIR) ed è fiancheggiato da due sequenze target dirette duplicate (TSD) che sono presenti anche nelle sequenza genica del revertente. Nonostante la similarità con diversi elementi trasponibili, il trasposone non può essere allocato in nessuna delle famiglie trasposoniche note. A livello trascrizionale, il trasposone altera lo splicing del gene. L'analisi di espressione dei trasportatori di auxina nel fusto allo stadio di 3 e 7 foglie mostra alterazione nei profili di trascrizione. Inoltre, un aumento di espressione della forma di splicing predetta dal Maize Genome Database (T02) è stato osservato.

La presenza dell'allele *abcb1* mutato nella linea di riferimento B73 causa l'insorgenza del fenotipo tipico dei mutanti *br2*. Il risultato indica che l'introggressione dell'allele *abcb1* di *br2:NC238* in un'altra linea genetica produce una linea di altezza ridotta senza alterare gli altri tratti della pianta e suggerisce la possibilità di introdurre la linea NC238 nei programmi di breeding.

Summary

Starting from the Green Revolution era, cereals have been bred for dwarf or semi-dwarf phenotype for many advantages, such as increased allocation of energy to seed rather than stem, denser growth, increased resistance to storm damages and reduced loss during harvesting.

Many dwarf mutants are characterized by alteration in hormones biosynthesis and signaling, as brassinosteroids (BR) and gibberellins (GA) pathways, while a defect in polar auxin transport (PAT) causes the sorghum mutant *dwarf3* (*dw3*) and the maize *brachytic2* (*br2*) mutations. Many *br2* alleles have been isolated in maize. At Purdue University (Indiana USA), allelic tests conducted on the dwarf NC238 inbred line indicated that the NC238 dwarf phenotype is due to a new *br2* allele. The isolation of a tall NC238 plant indicated the mutation is due to a transposon insertion that originated the tall revertant plant in a transposition event. Both *dw3* and *br2* are mutations affecting the gene orthologue of *Arabidopsis thaliana ABCB1*, which functions in auxin PAT.

Auxin is a key regulator of plant growth: local biosynthesis, degradation and conjugation contribute to the modulation of IAA homeostasis at the cellular level. ABCBs, together with the PIN FORMED, the AUX1/LAX and the PILS auxin transporters, create a directional auxin flux from the site of synthesis - young tissues - to the site of action. Auxin transport, with local biosynthesis and conjugation, allows the establishment of an auxin gradient, and the local auxin maxima regulates many aspects of the embryonic development, stem cell maintenance, shoot architecture, and tropic growth responses, root development and gravitropism. To date, the majority of the studies on auxin PAT have been focused on *Arabidopsis*, while less is known in other species, such as maize. This thesis focuses on the characterization of *br2:NC238* brachytic maize inbred line. In order to better characterize this maize mutant line, both a phenotypic and genotypic analysis of the NC238 dwarf plants were performed. In parallel, the *brachytic 2* allele was introgressed in the B73 maize reference inbred line background.

The present thesis is composed of four chapters. The first chapter is an introduction on Maize biology and genetics and auxin synthesis, metabolism and roles. This section comprises the review I wrote when I was visiting scholar at Prof. Johal lab at Purdue University: "The role of auxin transporters in monocot development". The review describes the roles of auxin

transporters in monocot development: maize, rice, sorghum and brachypodium, making comparison with *Arabidopsis* auxin carriers, when possible. Moreover, a section describing the plant transposable elements structure and classification is present.

The second chapter describes the morphological characteristics of NC238 line. It was previously reported alterations in stem vasculature in *br2*. Other paper described alteration in leaf cell size and leaf angle. Literature lacks a root system characterization. The develop stage when the *br2:NC238* phenotype arise was identify. Seedlings' root system, and stem traits on field grown plants at anthesis (University of Padova farm "L.Toniolo") were measured. The internode length, node diameter, number of nodes, tassel branches and ear position along the stem were recorded. Moreover, 1m deep soil coring at the base of the stem were made, in order to study the root system profile. In addition the anatomy of the stem and auxin localization in stem tissues were observed.

The third chapter regards the genetic characterization of the mutation. Genomic clones and transcripts sequences from both *br2:NC238* and the revertant plants were amplified and sequenced. A study on the nature of the *br2:NC238* insertion was performed through analyses of the sequence and interrogation against genes, repeats and transposons databases. Moreover, expression analyses of auxin transporters encoding genes were performed.

Chapter four describes the genetic and phenotypic characterization of the *br2:B73* line obtained by introgression of the *br2:NC238* *abcb1* mutant allele in the B73 reference line.

In conclusion, *br2:NC238* short phenotype is due to the shortening and thickness of the lower internodes. The other parts of the plant are normal. Phenotype appeared when plants were 7-leaf-old. *br2:NC238* and the revertant plants were indistinguishable in the early stages of development.

The *br2:NC238* mutation is caused by a insertion in a intronic region of *abcb1* gene. The insertion is characterized by terminal Inverted repeats (TIRs) and Target Site Duplication (TSD) that are also present twice in the revert line. Despite the similarities with many known transposable elements, it was not possible to find the family the *br2:NC238* insertion sequence belongs to. The insertion caused alteration in the gene transcription and alteration in the expression analyses of auxin transporters encoding genes at 3- and 7-leaf-old plant stem tissues were observed. Moreover, an increase in T02 Maize GDB predicted splicing form was observed.

The introgression of *br2:NC238* *abcb1* mutant allele in B73 reference line genome originated a short stature plant, *br2* type. The result indicates the *abcb1* mutant allele was responsible for the *br2:NC238* phenotype and suggests the allele may be used in breeding programs to obtain lines with reduced height.

Chapter I

General introduction

1.1 *Zea mays* is both a model organism for plant research and an important crop species

Maize (*Zea mays* L. spp. *mays*, commonly called "corn" in the USA) is one of the world's most important crops, together with rice (*Oryza sativa*), sorghum (*Sorghum bicolor*), and wheat (*Triticum* spp.). It belongs to the grass tribe andropogoneae of the family Gramineae (Poaceae). The name *Zea* derived from Greek *zea* that means cereal or grain. Its closest wild relatives are the teosintes, annual perennial grasses of the genus *Zea*, indigenous to Mexico and Central America. Genetic studies identified *Zea mays* spp. *parviglumis* as the direct ancestor of modern maize and it is estimated that maize diverged from the teosintes ancestor between 6000 and 9000 years ago (Matsuoka et al., 2002; Strable and Scanlon, 2009). For western civilization, the story of maize began in 1492 when Columbus's men discovered this new grain in Cuba and exported it to Europe.

Maize is an annual monocot plant producing large, narrow, opposing leaves, borne alternately along the length of a segmented stem. Maize is a monoecious plant with a male inflorescence, the tassel, and a female inflorescence, the ear. The apex of the stem ends in the tassel, and at the midpoint of the stem the ears born at the apex of condensed, lateral branches known as shanks protruding from leaf axils. The tassel produces pairs of free spikelets each enclosing a fertile and a sterile floret. The ear, a spike, produces pairs of spikelets on the surface of a highly condensed rachis (central axis, or cob). The female flower is tightly covered over by several layers of leaves until emergence of the pale yellow silks - made from the stylus and stigma - from the leaf whorl at the end of the ear. Each of the female spikelets encloses two fertile florets, one of whose ovaries will mature into a maize kernel once sexually fertilized by wind-blown pollen. The maize tassel and ear, despite their differences, share a common developmental origin and become distinct through the formation of long branch primordia and the abortion of female floral organs in the tassel, and through the abortion of male floral organs in the ear. Each female flower has a single functional ovary that ends with silk and each silk can accept one pollen grain. After the germination of the pollen grain on silk, pollen tube moves downwards, carrying three haploid nuclei: a vegetative one, and two generative (sperms). In the embryo sac eight nuclei are present, three at one pole (egg and two synergids) two at the centre (polar nuclei), and three at the

opposite pole (antipodal). Fecundation consists in the fusion of a generative nucleus with the egg to form a zygote from which the diploid embryo generates, and in the fusion of the second generative nucleus with the two polar nuclei to give origin to a triploid cell that, by continuous mitosis, produces the endosperm in the process called double fecundation. Although it can happen that the pollen from a tassel fertilizes the silk on the same plant (self-pollination), in maize this is less likely than cross-pollination between different plants. This physical separation of the flowers also facilitates breeder pollinations. Ears can be covered and pollen collected from tassels to make the desired cross. The mature seed is attached to the cob, the entire ear is protected by modified leaves called bracts. Maize does not have effective systems for the dispersal of seeds. The indehiscent dry fruit, is called caryopsis.



Figure 1.1. Maize adult plant. The male inflorescence, the tassel, is at the top of the stem while female flowers are located in the ear (1). Tassel branches bear small flowering producing branches called spikelets (2). At anthesis, anthers shed pollen. One floret per ear spikelet develops to maturity. The mature ear floret contains a single ovary that ends in the silk where pollen germinates and grows to the ovary. After fertilization the ovary produces the kernel (3). Adapted from www.efloras.org

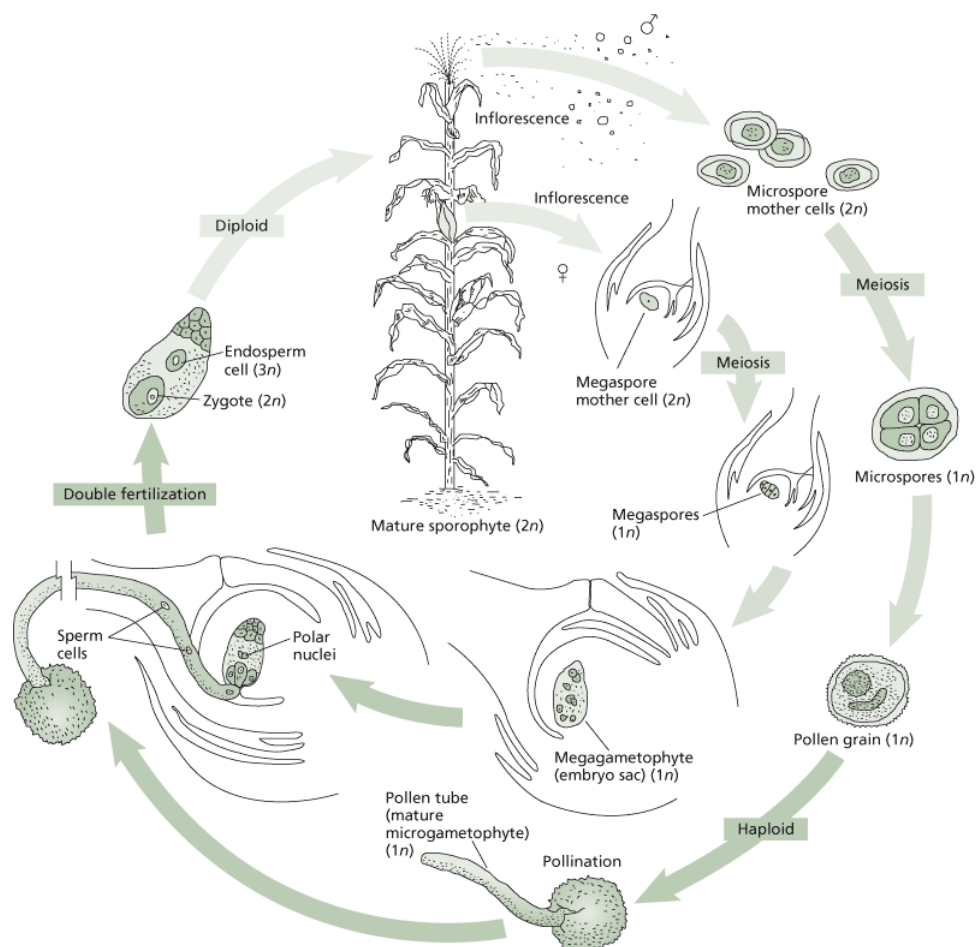


Figure 1.2. Life cycle of maize. The vegetative plant represents the diploid sporophyte generation. Meiosis occurs in the male and female flowers, represented by the tassels and ears, respectively. The haploid microspores (male spores) develop into pollen grains, and the single surviving haploid megaspore (female spore) divides mitotically to form the embryo sac (megagametophyte). The egg forms in the embryo sac. Pollination leads to the formation of a pollen tube containing two sperm cells (the microgametophyte). Finally, double fertilization results in the formation of the diploid zygote, the first stage of the new sporophyte generation, and the triploid endosperm cell. Adapted from <http://www.sinauer.com/plant-physiology-and-development.html>.

Maize is often classified as dent corn, flint corn, flour corn, popcorn, sweet corn, and waxy corn. It is not only an important human nutrient, but also a basic element of animal feed and raw material for manufacture of many industrial products. The products include corn starch, maltodextrins, corn oil, corn syrup and products of fermentation and distillation industries. It is also being used as biofuel.

In addition to its agronomic importance, maize has been a keystone model organism for basic research for nearly a century. Within the cereals, which include other plant model species such as rice (*Oryza sativa*), sorghum (*Sorghum bicolor*), wheat (*Triticum* spp.), and barley (*Hordeum vulgare*), maize is the most thoroughly researched genetic system. The use of maize as model

organism started in 1869 with Gregor Mendel's breeding experiments after his pea (*Pisum*) genetic researches. However, Correns and de Vrie are considered the pioneers of maize genetics research with their studies on *xenia*: the dominant influence exerted by the pollent parent on the phenotype of the endosperm. Emerson and East are considered the fathers of the modern maize genetics and Emerson was remembered as Beadle, Burnham, Rhoades and Mc Clintock's mentor. In maize, the genetic variation is represented by its inbred lines. Traditional maize inbred line development consists of rapid inbreeding through self-pollination with the primary selection criterion being grain yield in a process referred to as the pure-line method (Shull 1909, Bauman 1981). The aim during the development of inbred lines is to achieve homozygosis while ensuring plant vigor and performance, which usually decreases with the level of homozygosis. Historically, at least seven self-pollinations are needed to obtain a new inbred line. The inbreeding depression is the loss of performance of the inbreds due to the effect of inbreeding. It increases the homozygous recessive alleles leading to plants that are weaker and smaller and having other less desirable traits (reviewed in Charlesworth and Willis, 2009). Shool (1908) reported that inbred lines of maize showed general deterioration in yield and vigor. However, hybrids between two inbreds immediately and completely recovered; in many cases their yield exceeded that of the varieties from which the inbreds were derived. Furthermore, they had a highly desirable uniformity (reviewed in Crow, 1998). Thus, the word "heterosis" was introduced by Shull (1914) as shorthand for "stimulation of heterozygosis". Hundreds of maize inbred lines are described. B73, Mo17, W22 are the most widely used in the research studies, also thanks to the genome sequencing of B73 and Mo17. B73 is considered the *wild type* reference inbred line (Schnable et al., 2009). In many studies, the source of variation represented by inbred lines were used to evaluate differences in stress tolerance. Chen (2012) evaluated a selection of maize inbred lines for drought and heat stress tolerance under field conditions, and identified several inbred lines that showed high tolerance to drought.

Besides inbred line studies,, maize research has benefited from a vast collection of genetic mutants (Neuffer et al. 1997). Moreover, several mutants have been obtained thanks to TILLING project, as well as the use of Ac/Dc transposons for targeted mutagenesis (Bai et al. 2007) (Pohlman et al. 1984), the Mu Element (Slotkin et al. 2003, May et al. 2003), and the EMS mutagenesis. CIMMYT (International Maize and Wheat Improvement Centre) has taken the lead in preserving maize germplasm. It has the world's largest collection of maize accessions. The Maize Genetics Cooperation Stock Center (MGCSC) located at the University of Illinois in Urbana Champaign is the primary source for maize mutant stock for the research labs.

1.2 The maize stem development

Plant height and the height of the main ear are very important characteristics for breeding. The higher is the ear, the more ears can develop from the nodes below. However, if it is too high the weight of the ear may bend the stalk or even break it. Height adaptations are essential to plant fitness and agricultural performance. Most of the success of the Green revolution is due to the introduction of “semi dwarf” crop as wheat and rice (Multani et al., 2003) (a mano David and Keijiro Otsuka, 1994). These lines were able to support the heavy grain of the high yielding varieties. Over 40 maize genes at which mutations have large effects on plant height have been identified (Multani et al., 2003). These are involved in hormone synthesis, transport, and signaling. In addition to *brachytic 2* (Multani et al., 2003), maize height genes include *brachytic 1* (Avila Bolivar, 2015) and *brachytic 3* (Cassani et al., 2010); *dwarf 3* mediating gibberellin synthesis (Winkler, 1995); *dwarf 8* and *dwarf 9* regulating DELLA proteins of gibberellin signal transduction pathways (Winkler and Freeling, 1994); and *nana plant 1* impacting brassinosteroid synthesis (Hartwig et al., 2011).

The generalized grass shoot consists of a superposition of elementary units, the phytomers, each consisting of a leaf (sheath and blade), the internode below it, and the node and the axillary branch at the base of the internode. In most grasses, the lower internodes remain short. In maize, internode cell elongation occurs only after reproductive development has started (Siemer et al., 1969), and the lower internodes may remain short because they have already lost their ability to elongate by the time that reproductive development begins. The maize embryonic stem consists of a meristematic cone bearing five to seven leaf primordia, showing no differentiation of distinct internodes (Martin, 1988). The first internode forms below the coleoptile and elongates rapidly, leading the plant to emerge, before a light signal stops its extension (Kiesselbach, 1949). Higher internodes originate from intercalary meristems (Sharman, 1942). According to Martin (1988), intercalary growth occurs only after the transition of the apex to the reproductive phase. Before this transition, the whole stem (apical cone) elongates as a single entity, and at a very slow rate (Kiesselbach, 1949; Siemer et al., 1969). After tassel initiation, the stem elongates at a slightly higher rate (Siemer et al., 1969) and from ear initiation onwards, it elongates rapidly, up to anthesis and silking (Siemer et al., 1969). During the period of rapid elongation, plant height is linearly related to the phyllochron (the rate of leaf emergence from the apical bud) (Robertson et al., 1994).

Elongation of internodes is completed in four phases. In the first phase, division occurs at a constant cell size, and this 'stationary regime' results in an exponential rate of elongation, which is homogeneous over the internode. In the second phase, a gradient of cell length develop at the distal end of the internode, and there is an increase in the rate of internode elongation. Thirdly, the most distal cells matured, so that the region with a gradient of cell lengths move downwards, whereas the region of non-elongated cells, at the base of the internode, remains constant in length. This is a new 'stationary regime' of linear internode elongation, in which the production of new cells compensates for the maturation of older cells. In the fourth phase, the region of non-elongated cells at the base of the internode decreases in length, resulting finally in the cessation of elongation (Sachs et al., 1965, Martin et al., 1988, Morrison et al., 1994, reviewed in Fournier, 2000).

In the internodes, the course of the bundles is vertical, but at the level of the nodes they meet the horizontal strands and anastomose into elaborate plexus. The sap moves from the roots to the leaves passing through these complex plexuses. Despite the complexity of the bundles at the nodes, internodes vascular bundles are easily followed for their regular arrangement. For these reasons, transverse sections of internodes have been used as model of stem vascularization in most introductory texts (Shane, 2000). In fact, despite the lacking of node section images, literature is rich in maize internode section pictures. Evans (1928) defined nodes complexity as "to defy solution". Shane (2000) identify many node traits: axial bundles at nodes are anatomically different from those in internodes; about 3% of the hundreds of axial bundles in internodes are continuous through a node; special connecting elements join vessels within the axial bundles, and then join these connected vessels with vessels in the transverse bundles. In internodes, within axial bundles the large metaxylem vessels are always separated by parenchymatic cells. At plexuses these parenchyma cells are replaced by the connecting xylem elements, which join together the lumens of the large vessels (Shane, 2000). Tracers location experiments showed water and dye pass from the root vessels into the stem vascular bundles and along the vessels within axial bundles in internodes and upwards through plexuses for the length of the stem. The movements of the dye, that passes freely into almost all the bundles, and that of the water indicate the volume of the stem xylem is, for water, a continuous space. However, tracer assay showing small particles (20nm average diameter gold particles) do not enter the transverse bundles. The absence of particles from the vessels of all transverse bundles (except where a bifurcation of an axial vessel entered a transverse bundle) indicates the presence of vessel end walls that separated the vessels in axial bundles from the vessels in transverse bundles, and

the absence of particles from connecting elements within bundles indicates end walls also separate axial vessels from connecting elements (Shane, 2000).

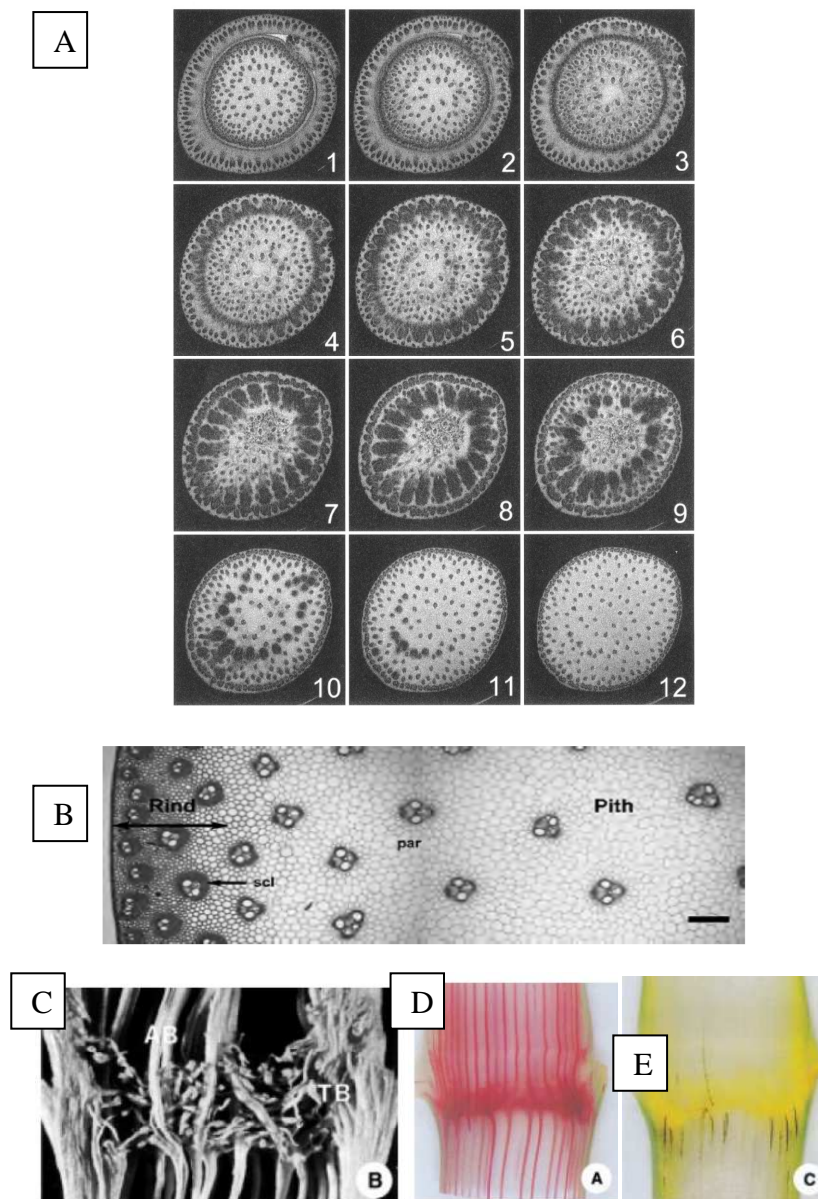


Figure 1.3. The maize stem. A) Series of 12 images of magnetic resonance imaging cross-sections through a node (the node below the main ear insertion) from field-grown maize stem (Odyssey sweet corn). Adapted from www.agron.missouri.edu_maize.node. B) Partial overview of the cross section of a elongated internode, vascular bundles are distinguishable and regularly distributed in the internode section. Bar=500mm, par=parenchyma, scl=sclerenchyma. Adapted from Jung & Casler, 2006. C) Optical microscopy image of the maize stem bisected longitudinally. The direction of the axial bundles that pass through the node may be slightly altered within the node. Axial bundles (AB) are enlarged at the base of each plexus and distorted where each is joined to transverse bundles (TB). Adapted from Shane, 2000. D) Nodal plexuses of maize stems during dye staining assay. Longitudinal sections through the first node above the cut surface, and portions of the adjoining internode.. The same number of axial bundles is highlighted by the dye above and below the node. Adapted from Shane, 2000. E) Tracer assay showing small particles (20nm average diameter gold particles) do not enter the transverse bundles. Adapted from Shane, 2000.

The maize plant initiates an axillary bud at each of the lower nodes in acropetal succession. During reproductive development, Axillary Meristems (AMs) give rise to flowering branches or to flowers. Once floral meristems are initiated on the flanks of the inflorescence, the final stages of reproductive development ensue and the floral organs are formed. Maize forms two distinct types of inflorescences after the transition to flowering. The shoot apical meristem gives rise to the terminal tassel, which has long branches and develops the male flowers. Bud initiation is stopped when the apical meristem starts to elongate and differentiate into a tassel. Ears derived from the axillary buds already formed at the lower nodes, have a prominent axis with no long branches, and develop the female flowers. By the time the tassel emerges from the top of the plant, usually only the topmost earshoot in non-prolific genotypes becomes functional. In the prolific genotypes, two or more earshoots at the top nodes can be functional. In either prolific or non-prolific genotypes, the topmost earshoot exhibits dominance over the ones at the lower nodes.

The inflorescence meristems (IMs) of the tassel and the ear each produce spikelet pair meristems (SPMs). Each SPM forms a short branch, bearing two SMs, which in turn produce a pair of floral meristems (FMs), though in the ear only one of these develops into a fertile flower reviewed in (Woodward and Bartel, 2005; Bommert, 2005).

Multiple and redundant genetic mechanisms contribute to SAM initiation, growth, and function. These include the CLAVATA/WUSCHEL pathway (Schoof et al., 2000) and the Knotted-1-like homeobox (KNOX) genes (Tsuda et al., 2011; Hay and Tsiantis, 2010), plant hormones (Murray et al., 2012) and chromatin remodeling factors (Shen and Xu, 2009).

Auxin biosynthesis, transport, and signaling are all required for axillary meristem initiation (Domagalska and Leyser, 2011). Connections between auxin transport and all branching events of maize shoot development have been observed. Auxin minimum is established at each leaf axil, where an AM will later initiate, and the cells within an auxin minimum have increased potential to form an AM (Wang et al., 2014). PIN1 localization experiments suggest that in axillary meristem the auxin minimum depends on auxin transport (Wang et al., 2014). Disruption of the auxin minimum, either by ectopic expression of an auxin biosynthetic gene or by local auxin application, compromised AM initiation (Wang et al., 2014).

Treating maize plants at the transition to the reproductive phase with the auxin transport inhibitor N-1-aphthylphthalamic acid (NPA) abolished the ability of the IM to form any axillary meristem. Moreover, the dynamic gradients of auxin, established by the activity of polar auxin transporters, are likely responsible for the formation of all vegetative and reproductive axillary meristems and

organs during maize development (Gallavotti et al., 2008). Auxin is also responsible for the apical dominance when travels basipetally from the shoot apex and suppresses the outgrowth of axillary buds (Thimann and Skoog, 1933; Leyser, 2003). Many auxin-related mutations have been identified. The maize BARREN INFLORESCENCE2 (BIF2) and BARREN STALK1 (BA1) control early developmental switches involved in the initiation of axillary meristems. *bif2* mutant tassels make fewer or no branches and spikelets, and the ears have fewer or no spikelets (McSteen and Hake 2001). Since the BMs, SPMs, SMs and FMs in weak *bif2* mutants are all defective, it appears that BIF2 is required for initiation and maintenance of all types of axillary meristems. *ba1* mutants lack vegetative branches and ears and have unbranched tassels also lacking spikelets (Gallavotti et al. 2004). The sparse inflorescence1 (*spi1*) mutant of maize has fewer branches and spikelets due to the absence of axillary meristems: SPI1 encodes a monocot-specific YUC gene family member required for localized auxin biosynthesis.

If auxin is required for axillary meristem initiation, then axillary meristem outgrowth required a complex interaction among auxin and other hormones (Domagalska and Leyser, 2011).

Beside auxin, many other hormones regulate the stem branching and the internodes elongation as well as the floral development. Cytokinins (CKs) play critical roles in cell proliferation and new organ creation and interact with auxin. CKs promote branching and increase spikelet numbers in rice. In the SAM, the CKs promote the proliferation of the stem cells and suppress the stem cell differentiation, whereas auxin plays a role in organ primordium initiation via the inhibition of the CK biosynthesis (Aloni et al., 2006; Naseem et al., 2015).

It is well known that applications of gibberellins (GAs) induce the plant stem to elongate, however GAs have also effects on inflorescences and ear development. In maize, GA application causes stem elongation and this elongation is reflected by longer internodes (Cherry et al. 1960). GA affects sex determination in maize flowers: higher GA concentrations favor the stamen abortion and thus feminization of flowers, while lack of GA causes masculinization of ears (Dellaporta, 1994, Irish, 2005). Higher GA concentrations inhibit the growth of early stage ears but slightly stimulated the growth of later stage ears in tissue culture (Bommineni and Greyson 1990). GA treatments promote internode elongation in both prolific and non-prolific genotypes, but also decrease ear development (Xu et al., 2004). Internode length is negatively correlated to ear number for a broad spectrum of corn germplasm, but plant height and ear number did not show this correlation (Xu et al., 2004). According to Ross and O'Neill model (2001) auxin promotes gibberellins biosynthesis. In tobacco and in pea, auxin from the shoot is required for normal GA biosynthesis (Ross et al., 2001). Auxin was shown to induce the expression of the GA

biosynthetic gene GA20ox in tobacco and Arabidopsis, whereas in pea, the hormone induced the expression of GA3ox and suppressed the expression of GA2ox, which is involved in GA deactivation (O'Neill and Ross, 2002; Frigerio et al., 2006). Moreover, loss of the auxin receptor TIR1, that mediates Aux/IAA degradation and the consequent ARF activation, suppresses auxin regulation of GA biosynthetic gene expression (Frigerio et al., 2006).

Auxin and strigolactone have the capacity to modulate each other's levels and distribution in a dynamic feedback loop required for the coordinated control of axillary branching. Agusti et al. (2011) showed that SL signaling interacts with auxin to stimulate the activity of vascular cambium in Arabidopsis and pea. In grasses, elongation and thickening of the stem is primarily due to activity of intercalary meristems located in nodes of the culm. The knockout mutation in an essential strigolactone (SL) biosynthetic gene that encodes CAROTENOID CLEAVAGE DIOXYGENASE8 (CCD8) originates short stature plant, similar to *br2* mutant, characterized by reduction in stem diameter and reduced elongation of internodes (Guan et al., 2012; Hayward et al., 2009).

Brassinosteroids (BRs) control sex determination in maize (Hartwig et al., 2011). BRs are also involved in internodes elongation, as the maize BR-deficient mutant, *brd1*, exhibits severe dwarfism (Makarevitch et al., 2012). BRs treatment increases sensitivity to exogenous auxin and enhances auxin-induced hypocotyl elongation (Vert et al., 2008).

1.2 The Maize root system

Root architecture is another plant morphological trait, frequently under estimated, mainly due to difficulties in its observation and measuring. However, root plasticity is crucial for plant acclimation under environmental stresses as low nitrogen stress (Gao et al., 2015), drought (Comas et al., 2013) and flooding (Justin, 1987).

Root architecture has traditionally been largely ignored by plant breeders in terms of potential yield increases, and was not a major selection criterion in the crop development programs of the Green revolution of the 1960s and 1970s that was carried out for the increasing food demands of a rapidly growing global population. The use of modern varieties as dwarfed cereal cultivars, fertilizers and pesticides, and a better irrigation were the basics of the Green revolution. However, for many aspects this first Green revolution was not a total success (S. Hallet, 2011). Food production was not enough for the increasing population and drop in food prices failure in increasing local people standards of life. Moreover, agricultural techniques caused the reduction of natural soil fertility and the lost of crop diversity. Many experts think root architecture will be

considered in the Second Green Revolution that is expected to consist of crop genotypes with superior yield at low soil fertility (Smith and De Smet, 2012). In fact, root system exploitation and modification in crops may enable plants to make more efficient use of existing soil nutrients and increase stress tolerance, improving yields while decreasing the need for heavy fertilizer application. Root branching is essential to increase the surface area of the root system, enabling the plant to tap more distant reserves of water and nutrients and improve soil anchorage (Hochholdinger and Tuberosa, 2009). For this reason, studies regarding crop yield and environmental responses more and more frequently include the root system physiology analyses (Lux and Rost, 2012; Maeght et al., 2013).

Arabidopsis has been the main plant model for the root system studies (States, 1994; Benfey and Schiefelbein, 1994; Smith and De Smet, 2012). However, crop species are mainly monocots and the root system varied from that of the dicot *Arabidopsis* (Smith and De Smet, 2012). Monocots root architecture is more complex, forming a 'fibrous' root system of many types of branched root. In cereals, shoot-borne 'crown and brace' roots, sometimes together with 'seminal' roots, constitute the majority of the monocot root system. In maize, the root system consists of roots that are spatially and temporary distinguishable, formed during embryogenesis and during post-embryonic development. The embryonic root system emerges a few days after germination and consists of a primary root that is formed at the basal pole of the embryo and variable number of seminal roots that emerge one week after germination and are laid down at the scutellar node. The post embryonic root system is composed of shoot-borne crown roots that form from consecutive underground nodes, brace roots that emerge late in development from aboveground nodes of the shoot, and lateral roots (LRs). Pericycle is the tissue layer located between the central vascular cylinder and the endodermis and represents the initiation site for LR branching. The pericycle cells adjacent to the xylem pole represent the precursors to LR founder cells. Lateral roots are highly branched, thus increasing enormously the absorbing surface of the root system. LRs are the main responsible of water and nutrient uptake. Brace and crown roots contribute to root lodging resistance and together with their lateral roots are responsible for most of the water uptake.

Central in root system development is auxin: auxin plays an important role in LR development.

Two separate sources provide auxin in specific stages of LR development: the root tip localized-auxin is important for primordia initiation, while the leaf derived-auxin is critical for primordial outgrowth. Following seed germination, free IAA is formed in a process that is regulated by light. Later on in development, auxin synthesis is initiated in the first developing true leaves and this

auxin is required for the first emergence of LR primordia. In fact, removal of cotyledons has only a minor effect on LR primordium emergence in contrast to removal of the leaves. As the root system becomes more developed, the amount of local synthesized auxin increases and the emergence of the latter primordia is less dependent on leaf-derived auxin. An increase in auxin levels in *Arabidopsis* roots at about 5 ± 7 DAG has been detected, which coincides with the emergence of LRs. The root system gradually reduces the dependence on apical tissue-derived auxin as evidenced by a major enhancement of its capacity to synthesize auxin by 10 DAG (Bhalerao et al., 2002). The fundamental role of localized auxin biosynthesis in roots has been demonstrated by the simultaneous inactivation of the *Arabidopsis* auxin biosynthesis genes YUCCA (YUC) that lead to short and agravitropic roots, while their over-expression cannot rescue auxin deficiencies in roots. Auxin synthesized in roots is required for normal root development and the auxin transported from shoots is not sufficient for supporting root elongation and root gravitropic responses (Chen et al., 2014).

Many types of LR mutants have been isolated in *Arabidopsis*, including excess of lateral roots production (King et al., 1995, Boerjan et al., 1995, Celenza et al., 1995) and defective in LR development. These mutants allowed proposing a fine model of LR development. Screening mutagenized *Arabidopsis* plants Celenza (1995) isolated three mutants: the *alf1-1* mutation causes hyperproliferation of lateral roots, *alf4-1* prevents initiation of lateral roots, and *alf3-1* is defective in the maturation of lateral roots. The *alf3-1* mutant could be rescued by IAA while the *alf4-1* mutant could not. These mutants allowed suggesting a model for LR development in which IAA is required to initiate cell division in the pericycle and both to promote cell division and maintain cell viability in the developing lateral root. In fact, auxin was originally defined as the "root forming hormones of plants" (Went, 1926). The *ALF1* gene product is believed to modulate the level of free, active auxin and therefore the number of LR. *ALF4* is directly involved in LR initiation by sensing or responding to indole-3-acetic acid (IAA), implied by the IAA resistant phenotype of the *alf4* mutant. In a second step the primordia require the *ALF3* gene product, which locally elevates the level of IAA necessary for cell division and subsequent maintenance of the LR meristem leading to LR elongation (Celenza et al., 1995).

1.2 The role of auxin in plant development

Auxins are a structurally diverse group of phytohormones involved in a large number of plant developmental processes. The term “auxin” is derived from the Greek word “auxein” meaning “to grow”. Its local accumulation triggers organ initiation and its dynamic and uneven distribution, so-called auxin gradients, within plant organs provide spatial information that is a major determinant of tissue patterning (Benková et al., 2003). Local biosynthesis, degradation and conjugation contribute to the modulation of IAA homeostasis at the cellular level. Availability of free IAA inside the cell is also controlled by auxin transport. Auxin influx and efflux carriers presence and their position at the cell membrane mediate the establishment of a polar auxin transport (PAT). Maintaining auxin homeostasis is crucial for normal plant growth and development.

1.2.1 Auxin biosynthesis and conjugation

Auxin biosynthesis in plants is fairly complex and plays an essential role in many developmental processes. Auxin is synthesized in the young parts of the plant, the shoot and root apices, and in the leaves, before being transported towards the sites it is needed.

Plants contain many natural auxins and generally three are the active auxins: Indole-3-acetic acid (IAA), 4-chloroindole-3-acetic acid (4-Cl-IAA), and phenylacetic acid (PAA) (Enders and Strader 2015; Simon and Petrasek 2011). Of these, IAA is the most abundant and the most studied natural auxin (Simon and Petrasek 2011).

Multiple pathways have been postulated that contribute to de novo IAA biosynthesis. Two major pathways for IAA biosynthesis have been proposed in plants: the tryptophan (Trp)-independent and Trp dependent pathways.

Little is known about the Trp-independent pathway that remains to be substantiated from genetic, biochemical, and functional studies. It was proposed two decades ago based on results from feeding plants with labeled Trp and Trp-biosynthetic intermediates: when the Arabidopsis and maize seedlings were fed with isotope-labeled precursor, IAA was more enriched than Trp, and the incorporation of label into IAA from Trp is low, suggesting that IAA can be produced de novo without Trp as an intermediate (Ouyang et al., 2000; Zhang et al., 2008). Only recently, Wang and colleagues gave evidence that the indole synthase (INS) is a key component in the long predicted Trp-independent auxin biosynthetic pathway and is critical for apical–basal pattern formation during early embryogenesis in Arabidopsis. INS shows cytosol-localized

spatiotemporal expression patterns during embryogenesis, and contributes to the establishment of an auxin gradient during embryogenesis. It is probable that local auxin biosynthesis through the tryptophan-dependent pathways include the indole-3-acetamide (IAM), the indole-3-pyruvic acid (IPyA), the tryptamine (TAM), and the indole-3-acetaldoxime (IAOx) pathways. Plant cells synthesize Trp from chorismate via indole-3-glycerol phosphate (IGP) in the chloroplast (Radwanski and Last 1995) and produce a large number of Trp metabolic intermediates as IAM, IPA, TAM, and IAOx.

The IPyA pathway is considered the main auxin biosynthesis pathways. IPyA has been isolated from a range of species. The Tryptophan Aminotransferase of Arabidopsis (TAA) family of enzymes converts tryptophan to IPyA and the YUCCA (YUC) family of enzymes converts IPyA to IAA creating a simple, two-step conversion of Trp to IAA (Cheng et al., 2006; Phillips et al., 2011). Mutations in TAA1, the founding member of a large Trp-independent and Trp-dependent pathways coordinately regulates the auxin gradient and orchestrates critical formative steps in the creation of apical–basal pattern during embryogenesis (Wang et al., 2015). The first YUC gene was identified as a key auxin biosynthesis gene a decade ago from an activation-tagging screen for long hypocotyl mutants in Arabidopsis. Overexpression of any of the YUC family members leads to auxin overproduction phenotypes in Arabidopsis. The dominant yucca (later renamed as yuc1D) mutant was caused by the insertion of four copies of the CaMV 35S transcriptional enhancer downstream of the YUC gene. yuc1D is an auxin overproduction mutant showing dramatic developmental defects (Zhao et al., 2001). AtYUC was later found to be a member of a gene family with 11 genes and its orthologous genes have been found in other plants, as the *spil* gene in maize (Cheng et al., 2006; Gallavotti, Yang, Schmidt, & Jackson, 2008; Zhao et al., 2001).

IAM has been identified as an endogenous auxin precursor in many species throughout the plant kingdom (reviewed by Korasick et al., 2013). The IAA biosynthetic pathway via IAM was initially thought to be a bacteria-specific pathway IAM is the key intermediate in the bacterial auxin biosynthesis pathway characterized in *Agrobacterium* and *Pseudomonas*: Trp is oxidized by the enzyme tryptophan-2-monooxygenase encoded by the *aux1/iaaM/tms1* gene. Then, IAM is converted to IAA by indole-3-acetamide hydrolase encoded by the *aux2/iaaH/tms2* gene to produce IAA. IAM have been detected also in plants, as Arabidopsis and maize, and have been shown to be involved in auxin pathway. The presence of IAM in growth media induces lightgrown Arabidopsis seedlings to have long hypocotyls and epinastic cotyledons. The IAM-induced phenotypes are identical to those observed in auxin overproduction mutants (Sugawara et

al. 2009, Yamada et al. 1985; Romano et al. 1995). Unlike the bacterial IAM pathway, the genes and enzymes responsible for producing IAM in plants have not been identified. Although IAM has been detected in Arabidopsis, tobacco, and maize in the model legume plant pea (*Pisum sativum* L.) tissues IAM was not detected and plants treated with IAM did not exhibit high-IAA phenotypes, and did not accumulate IAA indicating this pathway may not be universally used (Quittenden et al., 2014).

In Arabidopsis, there is evidence that IAM is mainly generated from IAOx. The conversion of tryptophan to IAOx is catalyzed by the cytochrome p450 enzymes CYP79B2 and CYP79B3. Some studies showed that IAO participated in the conversion of indole-3-acetaldehyde (IAD) to IAA in Arabidopsis and pea, however, rice, maize, and tobacco lack the CYP79B2/3 homologs and do not have detectable levels of IAOx (Mashiguchi et al., 2011; Seo et al., 1998; Zdunek-Zastocka, 2008).

The TAM pathway was first proposed in 1966 after observations of its auxin-like activity in *Avena* coleoptile elongation assays (Sirois, 1966). TAM pathway has also been found in tomato (*Solanum lycopersicum* L.), rice, Arabidopsis, barley (*Hordeum vulgare* L.), and pea. TAM was a proposed substrate for the YUC flavin monooxygenases. YUCs catalyze a rate-limiting step in the TAM pathway, the N-hydroxylation of TAM to produce N-Hydroxytryptamine (NHT) (Zhao et al., 2001).

Indole-3-pyruvic acid (IPyA) has been isolated from a range of species. the tryptophan aminotransferase TAA1 and its close homologues TAR1 and TAR2 convert L-Trp to IPyA and the YUC enzymes subsequently synthesize IAA from IPyA.

The regulation of auxin levels by *de novo* synthesis is one important homeostatic mechanism operating in plant cells, but the levels of IAA can also be modified by conjugation to molecules, as sugars, and degradation. While algae and fungi regulate free auxin concentration by its *de novo* synthesis and degradation, plants with elaborated vascular systems deposit excessive auxin in the form of IAA conjugates that are inactive storage auxin species and, when required, their hydrolysis provides plants with a potentially faster way to modulate free IAA levels than *de novo* biosynthesis (Cooke et al., 2002). For example, in the germinating seeds, large amount of IAA is released from the endosperm from its ester form to support the growth of developing seedlings and IAA conjugates that accumulate in large amounts in cotyledons of mature seeds may be considered to be only one of the possible sources of IAA required for the growth of bean seedlings (Bialek et al., 1992). More than 98% of total IAA in Arabidopsis is estimated to be present as conjugated forms, IAA esters or amide compounds. Conjugates are usually classified

according to the type of the attached molecule: ester conjugates (IAA–glucose, IAA–myoinositol), high-molecular-weight IAA–glycans, and amido conjugates (IAA–amino acid, IAA–peptide, or IAA–protein) (reviewed in Korasick, Enders, & Strader, 2013).

1.2.2 Auxin signaling

Auxin signaling involves thousands of auxin response genes. These include the Auxin/Indole-3-Acetic Acid family proteins (Aux/IAA), the Auxin-Response Factors (ARF) transcriptional factors and many other as SAUR, *Gretchen Hagen3 (GH3)* and ARG gene families (reviewed in Abel & Theologis, 1996).

Auxin signals can be perceived by two types of receptors, AUXIN BINDING PROTEIN1 (ABP1), localized in the endoplasmic reticulum and the cell surface; and TRANSPORT INHIBITOR RESPONSE 1/AUXIN SIGNALLING F-BOX (TIR1/AFB) nuclear F-box proteins. The best-characterized auxin binding protein is ABP1, which was first described in maize. ABP1 may sense changes in auxin levels at the cell surface and mediate rapid cellular responses (Napier et al., 2002; Robert et al., 2010; Xu et al., 2010), while TIR1/AFB proteins induce auxin-dependent transcriptional cascades (Ruegger et al., 1998; Dharmasiri et al., 2005).

ARF and Aux/IAA proteins contain a similar PB1 (Phox and Bem1) protein-protein interaction domain in their C-termini that facilitates the formation of ARF-ARF, ARF-Aux/IAA, and Aux/IAA-Aux/IAA homo- and hetero-oligomers (Guilfoyle, 2015, Han et al., 2014). Aux/IAA proteins function as active repressors by dimerizing with auxin response factors bound to auxin response elements (Tiwari et al., 2013). Aux/IAA are generally, Aux/IAA are nucleus-localized short lived proteins and auxin promotes their rapid degradation in proteasome-dependent way, by enhancing the interaction between the ubiquitin-ligase SCF^{TIR1} complex and the Aux/IAA proteins (Zenser et al., 2001). Tiwari's work indicate that auxin plays a dose-dependent role in modulating the lifetimes of Aux/IAA proteins and thus their capacity to repress early auxin response genes (Tiwari et al., 2013). In fact, the degradation of Aux/IAA directly or indirectly changes the transcription of thousands of early/primary auxin response genes (Zenser et al., 2001; Tiwari et al., 2013; Hayashi, 2012).

Different ARFs are involved in various developmental processes ranging from embryogenesis to floral development (Guilfoyle and Hagen, 2007). ARFs bind to the TGTCTC sequence on DNA sequences called Auxin Response Elements (AuxREs) in promoters of auxin response genes. (Guilfoyle and Hagen, 2007). Each ARF functions as a transcriptional activator or repressor. In

the absence of auxin, ARFs are bound to Aux/IAA repressor proteins. In *Arabidopsis*, there are 23 ARF and 29 Aux/IAA proteins (Quint and Gray, 2006).

SAUR and GH3 are two families of auxin-inducible genes. SAURs are a class of small, auxin induced RNAs. The function is still unknown, however they may play some role in an auxin signal transduction pathway that involves calcium and calmodulin (Yang and Poovaiah, 2000).

GH3 gene family maintains hormonal homeostasis by conjugating excess IAA, salicylic acid (SA), and jasmonic acids (JAs) to amino acids during hormone-and stress-related signaling pathways. Exogenous auxin application induces GH3 expression in soybean plant (Guilfoyle, 1999).

1.2.3 Polar Auxin Transport (PAT)

Compared with other plant hormones, auxin exhibits a unique property, as it is transported in a directional-polar flux from the sites of synthesis to the sites where it is needed. The localization of the auxin carriers leads the direction of the flux.

The dicotyledon plant *Arabidopsis* has been the most used model organism for auxin transport studies. A combination of phylogenetic and domain structural analyses showed that PIN and ABCB carriers functions were conserved between dicots and monocots (Yue et al., 2015). However, many different traits characterized monocots and dicots. Auxinic herbicides have been used for decades to control dicot weeds. Monocots have single cotyledons, whereas dicots have two, The vasculature in leaves of dicots is reticulate, whereas the vasculature in monocots is parallel. Dicots often produce a primary root that produces lateral roots, whereas, in monocots, shoot-borne adventitious roots are the main component of the root system. All these traits are regulated by auxin.

During my visiting at Purdue University, I have summarized the role of auxin transporters in monocot plant development in a review as part of my thesis.

The role of auxin transporters in monocots development

Sara Balzan,¹ Gurmukh S. Johal,² and Nicola Carraro^{3,*}

Edited by: Serena Varotto, University of Padova, Italy

Reviewed by: Enrico Scarpella, University of Alberta, Canada;

Patrick H. Masson, University of Wisconsin–Madison, USA

*Correspondence: Nicola Carraro, Department of Agronomy, Purdue University, 915 West State Street, West Lafayette, IN 47907, USA e-mail: ncarraro@purdue.edu

This article was submitted to Plant Evolution and Development, a section of the journal *Frontiers in Plant Science*.

Abstract

Auxin is a key regulator of plant growth and development, orchestrating cell division, elongation and differentiation, embryonic development, root and stem tropisms, apical dominance, and transition to flowering. Auxin levels are higher in undifferentiated cell populations and decrease following organ initiation and tissue differentiation. This differential auxin distribution is achieved by polar auxin transport (PAT) mediated by auxin transport proteins. There are four major families of auxin transporters in plants: PIN-FORMED (PIN), ATP-binding cassette family B (ABCB), AUXIN1/LIKE-AUX1s, and PIN-LIKES. These families include proteins located at the plasma membrane or at the endoplasmic reticulum (ER), which participate in auxin influx, efflux or both, from the apoplast into the cell or from the cytosol into the ER compartment. Auxin transporters have been largely studied in the dicotyledon model species *Arabidopsis*, but there is increasing evidence of their role in auxin regulated development in monocotyledon species. In monocots, families of auxin transporters are enlarged and often include duplicated genes and proteins with high sequence similarity. Some of these proteins underwent sub- and neo-functionalization with substantial modification to their structure and expression in organs such as adventitious roots, panicles, tassels, and ears. Most of the present information on monocot auxin transporters function derives from studies conducted in rice, maize, sorghum, and *Brachypodium*, using pharmacological applications (PAT inhibitors) or down-/up-regulation (over-expression and RNA interference) of candidate genes. Gene expression studies and comparison of predicted protein structures have also increased our knowledge of the role of PAT in monocots. However, knockout mutants and functional characterization of single genes are still scarce and the future

availability of such resources will prove crucial to elucidate the role of auxin transporters in monocots development.

Keywords: IAA, PIN, ABCB, AUX/LAX, PILS, PAT

INTRODUCTION

Plants exhibit an astonishing variety of shapes and develop multicellular bodies able to live for hundreds of years and reach considerable size. They rely on continuous growth and are able to regenerate organs from undifferentiated meristematic cells populations. Plant growth and organ differentiation, as well as response to environmental stimuli, are regulated, among other factors, by endogenous compounds called phytohormones. They control the plant developmental program by regulating cell division and expansion, tissue differentiation, and senescence. Phytohormones can act within the cell of origin or move to other sites in the plant, where they are perceived as a signal by hormone receptors (Davies, 2004).

The plant hormone auxin was first isolated as Indol-3-acetic acid (IAA) by Went (1926), as he studied the tropic response of *Avena sativa* coleoptiles. Subsequently, during the first half of the twentieth century, other four phytohormones were identified, including abscisic acid, cytokinins, gibberellins, and ethylene (Kende and Zeevaart, 1997). More recently, several additional compounds have been recognized as hormones including brassinosteroids (BR), jasmonate (JA), salicylic acid (SA), nitric oxide (NO), and strigolactones (SLs) (Tarkowská et al., 2014). Auxin is a regulator of many aspects of plant development, including cell division, elongation, differentiation, embryonic development, root and stem tropisms, apical dominance, and flower formation (Young et al., 1990; Woodward and Bartel, 2005; Tanaka et al., 2006; Möller and Weijers, 2009; Leyser, 2010; Müller and Leyser, 2011; Christie and Murphy, 2013; Gallavotti, 2013; Geisler et al., 2014). Besides IAA, which is the most abundant natural form of auxin, several auxin-like molecules have been identified. While 4-chloroindole-3-acetic acid (4-Cl-IAA), indole-3-butyric acid (IBA), and phenylacetic acid (PAA) are all found in plants, 2,4-dichlorophenoxyacetic acid (2,4-D) and naphthalene-1-acetic acid (NAA) are synthetic compounds that have biological activity similar to IAA (Bertoni, 2011; Simon and Petrášek, 2011).

Local biosynthesis, degradation and conjugation contribute to the modulation of IAA homeostasis at the cellular level. Availability of free IAA inside the cell is also controlled by auxin transport, which occurs in two distinct pathways: a passive diffusion through the plasma membrane (PM) and an active cell-to-cell transport, depending on the protonation state of IAA. IAA is a weak acid

with a dissociation constant of $pK = 4.8$. In a neutral or basic environment IAA^- will be the most abundant form (99.4% ionized at $pH = 7.0$), whereas in the acidic extracellular space $IAAH$ is predominant (about 20% protonated at $pH = 5.5$) (Delbarre et al., 1996; Estelle, 1998; Kramer and Bennett, 2006). $IAAH$ can enter into the cell through the PM by passive diffusion or active transport by PM importers. Once inside the cytoplasm, which has a neutral pH , IAA^- becomes the predominant form and it cannot freely move out of the cell unless actively transported by efflux carrier proteins (**Figure 1**). The differential localization of transporters at specific sites on the PM creates a directional auxin flow that eventually establishes a polar auxin transport (PAT) stream through adjacent cells. Four classes of auxin transporters have been identified: the PIN-FORMED (PIN) exporters, the ATP-binding cassette (ABC)-B/multi-drug resistance/P-glycoprotein (ABCB/MDR/PGP) subfamily of ABC transporters, the AUXIN1/LIKE-AUX1 (AUX/LAX) importers, and the newly described PIN-LIKES (PILS) proteins.

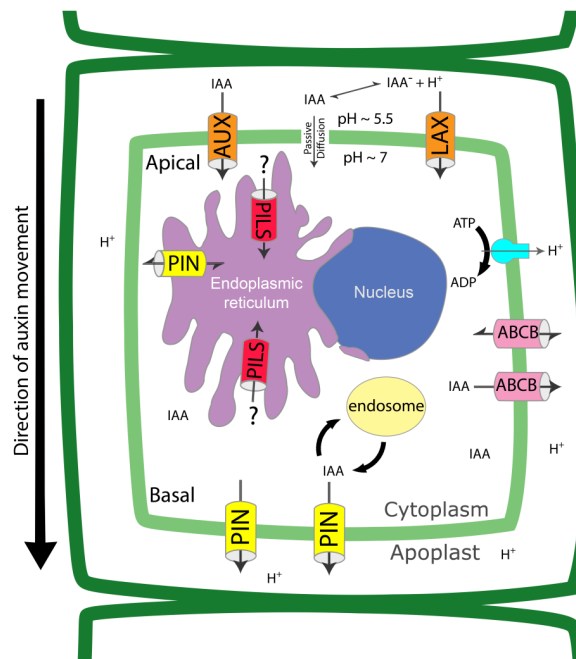


FIGURE 1. Auxin transport proteins regulate intracellular and cell to cell auxin fluxes. Auxin (IAA) crosses the plasma membrane through passive diffusion, as protonated form, or through PM transporters, as deprotonated form. PINs are efflux carriers located at the PM and ER and can be re-inserted in the lipid bilayer by recycling via the endocytic pathway. AUX/LAXs and PILs are influx carriers located at PM and ER, respectively. ABCBs are located at the PM and use energy from ATP to translocate IAA . The coordinated localization of the different transporters determines the overall directionality of the auxin flux and contributes to the regulation of intracellular auxin levels.

Despite the fact that auxin was first isolated and studied in the monocot *A. sativa*, characterization of auxin transport proteins derives mostly from forward genetic studies of mutants with defects in development, organ morphogenesis, and gravitropism in the dicot *Arabidopsis thaliana*. In recent years, the number of studies on the biological role of PAT in monocots has increased. This has been facilitated by the lower cost of deep sequencing of whole plant genomes and transcriptomes and by the availability of tools such as transgenic lines carrying proteins with fluorescent tags, which are used in subcellular localization studies and PAT fluxes modeling (Mohanty et al., 2009; Egan et al., 2012; Yu et al., 2012). In this work, we present a comprehensive description of monocots auxin transporters and provide, where possible, functional comparison between monocot and *Arabidopsis* proteins.

MATERIALS AND METHODS

PIN and PILS protein sequences of *Arabidopsis*, rice, maize sorghum, and *Brachypodium* (gene accession numbers are listed in Table S1) were aligned using the ClustalW 2.0 software (Larkin et al., 2007). The alignment file was used to generate an unrooted tree with MEGA 6.0 (Tamura et al., 2013), applying the Neighbor-joining method, the Poisson model and 500 bootstrap replications. Bootstrap analysis values >60 are indicated at each node.

PINs

PINs are the most studied family of auxin transporters in plants. PIN genes are present in eight copies in *Arabidopsis* and encode integral membrane proteins with two conserved domains formed by transmembrane helices, typically five at both the N and C termini, and a less conserved central hydrophilic loop of variable length (Křeček et al., 2009; Ganguly et al., 2012). Their subcellular localization has been correlated with the length of the hydrophilic domain. In *Arabidopsis*, PIN1, -2, -3, -4, and -7 have a longer loop (ranging in size from 298 to 377 amino acid residues), PIN5 and -8 have a shorter loop (27–46 residues) and PIN6 contains an intermediate form (Křeček et al., 2009; Ganguly et al., 2010; Viaene et al., 2013). “Long” PINs are generally inserted into the PM while “short” PINs are located in the endoplasmic reticulum (ER) and they are thought to contribute to intracellular auxin homeostasis (Mravec et al., 2009; Ding et al., 2012; Cazzonelli et al., 2013). More recently, it has been demonstrated that PIN5 is also PM localized, depending on the cell type and developmental stage, and that PIN5, -6, and -8 function in polar cell-to-cell transport of auxin by regulating coordinated influx and efflux of IAA into and out of the ER (Bender et al., 2013; Sawchuk et al., 2013; Ganguly et al., 2014).

Several auxin transporters show polar localization in the cell, but it is only in the case of PIN proteins that polar targeting occurs more frequently (**Figure 1**). Shifting PIN polarity results in the alteration of PAT which leads to developmental defects in Arabidopsis (Löfke et al., 2013). The polar localization of PIN proteins is established by cycling between the PM and endosomal compartments such as the trans-Golgi network/early endosomes (TGN/EE). PIN recycling can take place via endocytosis of clathrin-coated vesicles and depends on phosphorylation and ubiquitination (Robert et al., 2010; Kleine-Vehn et al., 2011; Löfke et al., 2013). Unphosphorylated PINs, or those dephosphorylated by the PP2A/PP6 phosphatase, are recycled to the PM by the brefeldin A (BFA)-sensitive ADP-ribosylation factor-guanine nucleotide exchange factor (ARF-GEF) GNOM. Phosphorylation of PIN proteins by the protein kinase PINOID (PID) results in their GNOM-independent recycling to the PM on the opposite side of the cell (Friml et al., 2004; Dhonukshe et al., 2010). Monoubiquitination and subsequent polyubiquitination of PIN proteins induce their endocytosis, followed by trafficking from the TGN/EE to late endosomes, from where the SNX1/BLOC-1 complex mediates transfer to multivesicular bodies (MVBs) for vacuolar degradation (Habets and Offringa, 2014). Recently, another Arabidopsis kinase, D6 PROTEIN KINASE (D6PK), has been demonstrated to regulate PIN phosphorylation and, together with PID, D6PK promotes PINs-mediated auxin transport at the PM by maintaining their phosphorylation status. D6PK PM localization is essential to establish and maintain PIN phosphorylation, and *d6pk* mutants have defects in both negative gravitropism and phototropism due to impaired auxin transport (Zourelidou et al., 2009; Willige et al., 2013; Barbosa et al., 2014).

Phylogenetic studies on the origin and evolution of PIN proteins have demonstrated that their general structure is highly conserved across the plant kingdom and suggest that the last common ancestor of land plants had at least one “long” (canonical) PIN protein (Carraro et al., 2012; Bennett et al., 2014). Strong selective pressure maintained PINs function as auxin carriers while they underwent sub- and neo-functionalization with substantial modification to protein structure, possibly due to selective loss of phosphorylation sites in their central loop (Dhonukshe et al., 2010; Fozard et al., 2013; Bennett et al., 2014). This generated several clades of non-canonical proteins with shorter and divergent structure, leading to altered localization and biological function. Monocot PIN families are often enlarged due to whole genome duplications and the retention of multiple copies of similar proteins. Both *Oryza sativa* and *Zea mays* contain four PIN1 copies and present at least one monocot-specific gene, PIN9, which is divergent in sequence and expression pattern from the closest dicot PINs (Xu et al., 2005; Forestan et al.,

2012; Bennett et al., 2014; Clouse and Carraro, 2014). The PIN9 protein profile prediction shows an intermediate hydropathic profile in between the “long” and the “short” PINs.

AtPIN1 is expressed early during embryonic development and later both in the primary root and in the inflorescence stem. Disruption of AtPIN1 expression leads to the formation of naked, pin-shaped inflorescences and abnormalities in the number, size, shape, and position of lateral organs (Okada et al., 1991; Gälweiler et al., 1998). As suggested by the *pin1* phenotype, PIN1 plays an important role in establishing the plant developmental plan and is involved in floral bud formation, phyllotaxis (the arrangement of leaves and flowers around the stem), vascular development, vein formation, embryogenesis, lateral organ formation, anther development, and root negative phototropism (Gälweiler et al., 1998; Benková et al., 2003; Reinhardt et al., 2003; Weijers et al., 2005; Feng et al., 2006; Scarpella et al., 2006; Lampugnani et al., 2013; Zhang et al., 2014). *Arabidopsis pin2* was the first pin mutant identified in a screen for agravitropic seedlings by Bell and Maher (1990). Initially, it was called *agr1*, and the gene responsible for the phenotype was cloned independently by four research groups and named AGR1/EIR1/PIN2/WAV6 (Chen et al., 1998; Luschnig et al., 1998; Müller et al., 1998; Utsuno et al., 1998). AtPIN2 functions in auxin-regulated root gravitropic response and its expression levels and polar cellular localization are altered by salt stress (Abas et al., 2006; Sun et al., 2008). AtPIN3 is expressed during embryo development and the *Atpin3* mutant shows reduced growth, and decreased apical hook formation (Friml et al., 2002b; Zádňíková et al., 2010). It has been shown that AtPIN3 plays an important role in root gravitropism, as in vertically grown seedlings AtPIN3 is positioned symmetrically at the PM in the columella cells, but rapidly relocalizes laterally to the lower PM of the statocytes following gravistimulation. AtPIN3 relocalization determines the direction of the auxin flux, which leads to asymmetric auxin accumulation and subsequent differential cell growth (Friml et al., 2002b). AtPIN3 is also involved in root negative phototropic response, as blue-light induced AtPIN3 polarization is needed for asymmetric auxin distribution (Zhang et al., 2013).

AtPIN4, as well as AtPIN7, are involved in auxin controlled embryo, primary root, and apical hook development (Friml et al., 2002a, 2003; Vieten et al., 2005; Kleine-vehn et al., 2010; Zádňíková et al., 2010). AtPIN7 also undergoes relocalization similar to AtPIN3 in response to gravistimulation in a subgroup of the columella cells (Rosquete et al., 2013). AtPIN5 is involved in auxin homeostasis, and it has been demonstrated that it can export auxin from yeast cell (Mravec et al., 2009). AtPIN6 is involved in stamen development, and microarray and reporter assays have demonstrated that it is necessary for nectaries development (Bender et al.,

2013). Expression analysis of pPIN6::PIN6-GFP lines during leaf development has demonstrated that AtPIN6 localizes to the ER and expression is initiated in broad sub-epidermal domains that later on narrow to sites of vein formation (Bender et al., 2013; Sawchuk et al., 2013). Moreover, AtPIN6 is implicated in processes such as shoot apical dominance, lateral root primordia development, adventitious root formation, root hair outgrowth, and root waving where it regulates auxin homeostasis (Cazzonelli et al., 2013). AtPIN8 is expressed in the male gametophyte, and has a crucial role in pollen development and functionality (Ding et al., 2012). AtPIN8, together with AtPIN5 and AtPIN6, also take part into leaf vein network patterning by regulating intracellular auxin transport between the cytoplasm and the ER lumen. Their action is exerted coordinately with AtPIN1, in order to modulate intracellular auxin levels in extending veins (Sawchuk et al., 2013).

PINs IN *Oryza sativa*

Rice has 12 PINs (Table S1) and OsPIN1 was first described by Xu et al. (2005). Transmembrane motif analysis of the deduced amino acid sequence shows that OsPIN1 is a “long” (canonical) PIN protein, which harbors a long hydrophilic loop and two transmembrane regions composed of five helices each. Protein structure, phylogenetic, and functional analysis identify OsPIN1 as the closest ortholog of AtPIN1 (Xu et al., 2005; Carraro et al., 2012; Wang et al., 2014). The three OsPIN1s, -a, -b, and -c are expressed in roots, stem base, stem and, at a lower level, in leaves and young panicles. In these last two organs, OsPIN1 expression is lower than in the other tissues (Xu et al., 2005; Wang et al., 2009). Over-expression of OsPIN1 in 35S::OsPIN1 transgenic plants increases primary root length and lateral root number. Suppression of OsPIN1 expression obtained by RNA interference (RNAi) reduces the number of adventitious roots and increases the number of tillers and the tiller angle. Thus, OsPIN1 is involved in auxin transport in primary and adventitious roots, which are more abundant in rice compared to Arabidopsis. The role of OsPIN1 in PAT was confirmed by treating wild type plants collars with 1-N-Naphthylphthalamic acid (NPA), which blocks initiation and growth of adventitious and lateral roots, while application of the auxin NAA rescues the RNAi-induced phenotype (Xu et al., 2005). OsPIN2 is the most recently characterized PIN gene of rice and shows a different expression pattern compared to OsPIN1 (Chen et al., 2012). Wang et al. reported that OsPIN2 is highly expressed in roots and at the base of the stem, less in young panicles and exhibits no expression in adult stem and leaves (Wang et al., 2009). Over-expression of OsPIN2 results in a larger tiller angle, reduced plant height and an increase in tillers number compared to wild type. OsPIN2 over-expression increases auxin transport from the shoot to the

root–shoot junction and transgenic plants are less sensitive to root growth inhibition by NPA (Chen et al., 2012). Overall, the results indicate that OsPIN2 acts in a specific auxin-dependent pathway which includes OsPIN1b and OsTAC1 (TILLER ANGLE CONTROL 1), and controls rice shoot rather than root architecture (Chen et al., 2012). Three OsPIN5 homologs are present on chromosomes 1, 8, and 9 of rice. The expression patterns of OsPIN5a and OsPIN5c are very similar: while only weakly expressed in roots, they show very high expression levels in leaves, shoot apex, and panicle. Small amounts of OsPIN5b transcript are detected in the shoot apex, roots of 6-week-old plants and 4-week-old callus tissue (Wang et al., 2009; Miyashita et al., 2010). One AtPIN8 homolog has been identified in rice but it has not been characterized yet (Miyashita et al., 2010). OsPIN9 is highly expressed in adventitious root primordia and pericycle cells at the base of the stem (Wang et al., 2009). OsPIN9 expression levels in roots are decreased by IAA and increased by cytokinin [6-benzylaminopurine (6-BA)] application (Wang et al., 2009; Shen et al., 2010). Expression analysis shows that OsPIN10a is present in the stem, leaves, and young panicle, but not in the roots. OsPIN10b is mainly expressed in leaves but also at the stem base and in lateral root primordia and both genes are up-regulated by IAA, 6-BA, and JA treatments (Wang et al., 2009).

PINs IN *Zea mays*

The PIN family in maize includes 12 members characterized by often overlapping but sometimes organ-specific expression domains (Forestan et al., 2010). ZmPINs consist of both “long” (ZmPIN1a, -b, -c, -d, ZmPIN2, ZmPIN10a, -b) and “short” forms (ZmPIN5a, -b, -c, ZmPIN8), with ZmPIN9 having a protein structure in between the two classes (Forestan et al., 2012; Table S1). The ZmPIN1 homologs were among the first identified in maize and are expressed at the PM, supposedly functioning in PAT at different stages of plant development. The ZmPIN1a, -b, and -c loci are located in duplicated regions on chromosomes 9, 5, and 4, respectively, and, along with ZmPIN1d, are characterized by a six exons/five introns gene structure. This gene organization is similar to that of AtPIN1 and OsPIN1. The proteins encoded by ZmPIN1a, -b, -c, and -d present higher sequence similarity to AtPIN1 than other PINs from Arabidopsis and they should be considered as different orthologs of AtPIN1. In monocot species such as maize, the presence of paralogs encoding protein isoforms derived from duplication and neo-functionalization cannot be ruled out, but so far there is no conclusive evidence in the case of ZmPINs. ZmPIN1a, -b, -c are ubiquitously expressed but differentially modulated in maize vegetative and reproductive tissues and during kernel development. ZmPIN1 plays an important role during embryogenesis, where detectable hormone activity inside the developing maize

embryo appears much later than in *Arabidopsis* (Forestan et al., 2010; Chen et al., 2014). In situ hybridization showed that ZmPIN1a localizes in the root apical meristem (RAM) and the calyptragen, which is a specialized layer of meristematic cells that continuously generate replacements for the root cap cells that die during primary root growth. Immunolocalization experiments locate ZmPIN1 in the central cylinder, vasculature, and cortex of the primary root (Carraro et al., 2006; Forestan et al., 2012). NAA application to a ZmPIN1a-YFP reporter line causes a more diffuse localization of ZmPIN1a and leads to changes in root anatomy, reducing the size of both root cap and meristem and developing of a pluristratified epidermis (Forestan et al., 2012). ZmPIN1a also interacts with KNOTTED1 (KN1) in shaping leaves and leaf veins patterns and regulates PAT during ear, tassel, and spikelet differentiation (Carraro et al., 2006; Gallavotti et al., 2008; McSteen, 2010; Bolduc et al., 2012). ZmPIN1a was shown to rescue the *Atpin1* phenotype and the application of NPA to plants at different stages of development leads to PAT disruption related defects (Gallavotti et al., 2008; Gallavotti, 2013). ZmPIN1b is mainly expressed in the epidermis, root cap, and vasculature. ZmPIN1c localizes in the epidermis and vasculature of the root central cylinder, while ZmPIN1d is specifically expressed in the tassel, ear, and in the fifth node of adult plants. ZmPIN1d is also expressed in the L1 layer of the shoot apical meristem (SAM) and inflorescence meristem during the transition to flowering (Forestan et al., 2012). ZmPIN2 is expressed in the root tip, male and female inflorescences and is involved in kernel development (Forestan et al., 2012). Interestingly, ZmPIN2 is up-regulated in the roots of the *brachytic2* mutant, which is characterized by reduced shoot-ward auxin transport at the root apex and reduced root gravitropic growth (McLamore et al., 2010). ZmPIN5a is highly expressed in roots and ZmPIN5b is expressed in the 5th node of the stalk. ZmPIN8 is up-regulated during the early phase of kernel development and in the 7th and 8th internodes. ZmPIN9 is expressed in the root epidermis and pericycle and NAA treatment increases its transcript levels in the root segment just before the root apex. There are two PIN10 homologs in maize, ZmPIN10a and ZmPIN10b. Both genes are expressed in the male inflorescence, with ZmPIN10a also up-regulated during the early phases of kernel development (Forestan et al., 2012).

PINs IN *Sorghum bicolor*

In *Sorghum bicolor*, PINs have been identified and their expression pattern described, but results from functional analysis are still missing (Shen et al., 2010; Wang et al., 2011). The nomenclature for sorghumPIN genes does not match the one followed for *Arabidopsis*, rice, and maize therefore, we include the gene identifier together with the common name (Table S1). In sorghum,

“long” PIN proteins have a conserved canonical architecture, with two hydrophobic domains divided by a hydrophilic loop (Zazimalová et al., 2007; Shen et al., 2010). Their chromosomal distribution, expression profile and up- or down-regulation following treatment with auxin transport inhibitors [NPA, 1-naphthoxyacetic acid (1-NOA) and 2,3,5-triodobenzoic acid (TIBA)] have been described (Shen et al., 2010). The SbPIN1 (Sb02g029210) transcript, similar to ZmPIN5c, is predicted to localize to the tonoplast and to be constitutively expressed in all tissues (Shen et al., 2010). SbPIN2 (Sb03g029320), one of the sorghum proteins predicted to be located at the PM, shows high sequence similarity to ZmPIN10a. SbPIN3 (Sb03g032850), similar to At/Os/ZmPIN8, is highly expressed in flowers (Shen et al., 2010). SbPIN4 (Sb03g037350) is the sorghum gene that shares most similarity with ZmPIN9 and it is also highly expressed in roots, although not exclusively (Shen et al., 2010). However, its expression is down-regulated by IAA application and increased by BR, while ZmPIN9 is up-regulated by auxin treatments (Shen et al., 2010; Forestan et al., 2012). SbPIN5 (Sb03g043960), similar to Zm/OsPIN5a, is expressed at low levels in untreated plants while IAA treatment suppresses expression in leaves and roots (Shen et al., 2010). The gene named SbPIN6 (Sb04g028170) encodes a “long” form similar to PIN1 proteins (Wang et al., 2011). The gene named SbPIN8 (Sb07g026370) is the most similar to ZmPIN5b having a predicted protein structure of a “short” PIN (Shen et al., 2010). Protein sequence alignment and expression pattern of SbPIN9 (Sb10g004430) suggest homology to ZmPIN10b. The SbPIN11 (Sb10g026300) sequence is orthologous to Zm/OsPIN2 and is more expressed in roots and seedling shoots.

PINs IN *Brachypodium distachyon*

In the genome of the grass *Brachypodium distachyon* there are both “long” and “short”/“intermediate” PIN forms (Bennett et al., 2014; O’Connor et al., 2014; Wang et al., 2014a). Two PIN1 paralogs have been identified: BdPIN1a (Genebank ID XM_003563990.1) and BdPIN1b (Genebank ID XM_003570618.1). BdPIN1a and BdPIN1b are highly expressed in internal tissues, with BdPIN1b spanning a broader domain. Transgenic *Brachypodium* lines carrying pPIN1a:PIN1a-YFP and pPIN1b:PIN1b-YFP constructs show expression in developing spikelets, suggesting a role in vascular patterning (O’Connor et al., 2014). The newly identified “Sister-of-PIN1” (SoPIN1)/PIN11 clade contains *Brachypodium* genes that are divergent in sequence from BdPIN1s and have no representatives in Brassicaceae. SoPIN1 is highly expressed in the stem epidermis and is consistently polarized toward regions of high expression of the DR5 auxin-signaling reporter, which suggests a role in the localization of new primordia (O’Connor et al., 2014).

ABCBs

The ABC superfamily of membrane proteins includes more than a hundred different members in plants (Kang et al., 2011). The subfamily B (ABCB) includes homologs of the mammalian MDRs/PGPs, several of which are involved in auxin transport (Geisler and Murphy, 2006; Cho and Cho, 2013). ABCB transporters are integral membrane proteins that actively transport chemically diverse substrates across the lipid bilayers of cellular membranes (Figure 1). The core unit of a functional ABC transporter consists of four domains: two nucleotide-binding domains (NBDs) and two transmembrane domains (TMDs). The two NBDs unite to bind and hydrolyze ATP, providing the driving force for transport, while the TMDs are involved in substrate recognition and translocation across the membrane (Jasinski et al., 2003; Higgins and Linton, 2004; Bailly et al., 2011). Arabidopsis has 22 ABCBs and the first ABCBs characterized as functioning in IAA translocation were identified in seedlings (Sidler et al., 1998; Noh et al., 2001). ABCB1, ABCB4, ABCB14, ABCB15, ABCB19, and ABCB21 are associated with auxin transport, although not exclusively (Geisler and Murphy, 2006; Titapiwatanakun and Murphy, 2009; Kaneda et al., 2011; Kamimoto et al., 2012; Cho and Cho, 2013). To date, the best-characterized ABCBs are AtABCB1, AtABCB4, and AtABCB19. They all function in auxin driven root development and require the activity of the immunophilin TWISTED DWARF1 (TWD1)/FKBP42 to be correctly inserted at the PM (Wu et al., 2010). AtABCB1/PGP1 was the first plant MDR-like gene cloned from Arabidopsis and it is localized at the PM in the root and the shoot apex of seedlings (Dudlers and Hertig, 1992; Noh et al., 2001). The *atpgp1* original mutant exhibits only a subtle phenotype compared to wild type plants, but a new allele designated as *atpgp1-2*, shows a shorter hypocotyl and dwarf phenotype under long-day conditions (Geisler et al., 2005; Ye et al., 2013). Disruption of *AtABCB19/AtMDR1* expression results in partial dwarfism and reduced PAT in hypocotyls and inflorescences (Noh et al., 2001). AtABCB19 functions together with AtABCB1 in long distance transport of auxin along the plant main axis in coordination with AtPIN1, and regulates root and cotyledon development and tropic bending response (Lin and Wang, 2005; Bandyopadhyay et al., 2007; Rojas-Pierce et al., 2007; Nagashima et al., 2008; Lewis et al., 2009; Christie et al., 2011). AtABCB4 is a root-specific transporter involved in auxin transport during root gravitropic bending, root elongation, and lateral root formation (Santelia et al., 2005; Terasaka et al., 2005; Kubeš et al., 2011; Cho et al., 2012). This transporter is substrate-activated and functions as an auxin importer at low substrate concentration, switching to auxin export as the availability of auxin increases (Yang and Murphy, 2009; Kubeš et al., 2011). AtABCB21 encodes a protein that is the closest homolog to

AtABCB4 and is expressed in the aerial parts of the seedling and in the root pericycle cells. Just like AtABCB4, AtABCB21 functions as a facultative importer/exporter that controls cellular auxin levels (Kamimoto et al., 2012). AtABCB14 was first described as a malate importer that functions in the control of stomata aperture according to CO₂ levels (Lee et al., 2008). More recently, AtABCB14 and 15 have been shown to be active in the vascular tissue of the primary stem, which shows anatomical alterations in *abcb14* and *abcb15* mutants. Since IAA transport along the inflorescence is reduced in both mutants, it was proposed that AtABCB14 as well as AtABCB15 participate in auxin transport (Kaneda et al., 2011).

ABCBS IN *Oryza sativa*

Homologs of ABCBs have been described in monocots. In rice, Garcia et al. identified 24 putative ABCB sequences, with OsABCB22 and OsABCB14/16 being homologs of AtABCB19 and AtABCB1, respectively (Garcia et al., 2004; Knöller et al., 2010). OsABCB14 is expressed in all plant organs, including roots, stem, leaves, nodes, root-stem transition region, filling seeds, panicle, and flowers (Xu et al., 2014). Spatial expression analysis shows that OsABCB14 expression is higher in root tips than in the basal root zone. Knockout mutants of OsABCB14 have decreased PAT rates, conferring insensitivity to 2,4-D and IAA. A role for OsABCB14 in auxin uptake and iron (Fe) homeostasis has been demonstrated. Acropetal auxin transport in rice *abcb14* plants root system is significantly lower than in wild type. The iron concentrations in shoots, roots, and seeds are significantly enhanced, and the expression level of iron deficiency-responsive genes was significantly upregulated in rice *abcb14* mutants (Xu et al., 2014). Recent evidence also suggests that N-glycosylation of ABCB proteins in rice might be important for root development. In an EMS-generated mutant line for OsMOGS, which encodes a mannosyl-oligosaccharide glucosidase, root PAT is altered due to under-glycosylation of OsABCB2 and OsABCB14 (Wang et al., 2014b).

ABCBS IN *Zea mays* AND *Sorghum bicolor*

In maize and sorghum, loss-of-function mutations in the AtABCB1 orthologous genes *ZmABCB1* and *SbABCB1* result in short stature plants designated as *brachytic2* (*br2*) and *dwarf3* (*dw3*), respectively (Multani et al., 2003). *br2* and *dw3* are characterized by reduced basipetal auxin transport and greatly reduced stalk height (Multani et al., 2003). BR2 is expressed in nodal meristems, and analyses of auxin transport and content indicate that BR2 function in monocot-specific meristems is the same as that of AtABCB1, which is an auxin transporter. Thus ABCB1/BR2 auxin transport ability is conserved between dicots and monocots, but should be considered in the context of distinct architectures of monocot versus dicot plants,

which have unsegmented (*Arabidopsis*) and segmented stems (maize, rice, sorghum, *Brachypodium*) (**Figure 2**; Multani et al., 2003; Knöller et al., 2010). The dwarfing phenotype of *dw3* is very similar to that of *br2* and it is the result of a 882-bp tandem duplication in exon 5 that disrupts protein function and the plant's ability to establish an auxin flux in the intermediate internodes (Multani et al., 2003). These mutants are of particular interest because of the agronomic importance in terms of their ability to resist to lodging and to dramatically enhance the harvest index of the plant. Thus dwarfing traits are important due to the potential distribution of nutrients and energy to grain production rather than vegetative growth. Given that *br2*, which has a defect in *ZmABCB1*, causes the stunting of lower internodes mostly, it raises the possibility that other brachytic mutants may arise from defects in other ABCB transporters. In maize, there are three putative *AtABCB19* homologs: *ZmABCB10-1* (GRMZM2G125424) and *ZmABCB2-1* (GRMZM2G072850), present closest sequence similarity to *OsABCB16*, while *ZmABCB10-2* (GRMZM2G085236), is more similar to the true auxin transporter *OsABCB14* (Knöller et al., 2010). *ZmABCB10-1* (GRMZM2G125424) is expressed in actively growing tissues, especially in pre-pollination ears at the flowering stage (Pang et al., 2013). In sorghum, *SbABCB16* (Sb06g018860) and *SbABCB18* (Sb06g030350) present the closest protein sequence similarity to *ABCB19* from *Arabidopsis*. *SbABCB16* expression is highest in the roots and is not responsive to IAA and 1-NOA treatments, while *SbABCB18* is mostly expressed in leaves and is up-regulated by IAA, 1-NOA, and BR applications (Shen et al., 2010).



FIGURE 2. The *br2* maize mutant shows dramatically impacted stalk architecture. The *br2* adult plant shows altered stalk height due to reduction in internode length, which is caused by the

disruption of IAA transport mediated by ZmABCB1. The same phenotype is present in the sorghum dw3 mutant, which carries a tandem duplication in the SbABCB1/Dw3 gene.

AUX/LAXs

The existence of auxin importers in plants was first demonstrated studying the Arabidopsis auxin insensitive 1 (aux1) mutant, which carries defects in roots gravitropic response. AtAUX1 belongs to a small gene family composed of four highly conserved proteins that share similarities with amino acid transporters: AtAUX1, AtLAX1, -2, and -3 (Péret et al., 2012). AtAUX1 encodes a protein similar to fungal amino acid permeases and is expressed in columella, lateral root cap, epidermis, and stele tissues of the primary root where it acts as an auxin importer (Bennett et al., 1996; Swarup et al., 2001, 2004; Carrier et al., 2008). AtAUX1 is involved in auxin-regulated root gravitropic response together with the auxin exporter AtPIN2. The coordinated action of these two proteins forms a lateral auxin gradient which inhibits the expansion of epidermal cells on the lower side of the root relative to the upper side, eventually causing the downward root curvature (Swarup et al., 2005). aux1, as well as pin2 Arabidopsis mutants are agravitropic and aux1 also presents a decreased number of lateral roots due to defects in lateral root initiation (Marchant et al., 2002). AtAUX1 and AtLAX1, act redundantly in regulating the phyllotactic pattern in Arabidopsis although AtLAX2 is not expressed in the SAM L1 layer. Since AtLAX2 is expressed in the forming primordium vasculature, one hypothesis is that AtLAX2 enhances the strength of the primordium as an auxin sink by pulling IAA from the L1 layer of the SAM (Bainbridge et al., 2008; Kierzkowski et al., 2013). AtLAX2 is involved in vascular development in cotyledons and it is also expressed in young vascular tissues, the quiescent center and columella cells in the primary root (Péret et al., 2012). AtLAX3 is expressed in the columella and stele of the primary root and it is involved in lateral root development, as Arabidopsis lax3 mutants show delayed lateral root emergence (Swarup et al., 2008). No root growth-related defects or lateral root-related defects are observed in either lax1 or lax2 single mutants while aux1lax3 double mutant shows a severe reduction in the number of emerged lateral roots (Swarup et al., 2008). Auxin binding and import activity of AUX/LAX proteins has been demonstrated using an oocyte expression system for AtAUX1 (Yang et al., 2006), AtLAX3, and AtLAX1 or a yeast-based heterologous expression system in the case of AtLAX2 (Yang et al., 2006; Carrier et al., 2008; Péret et al., 2012).

AUX/LAXs IN MONOCOTS

Recently, the expression profile of a putative AUX1 homolog in rice (OsAUX1, Genebank ID AK068536) has been published (Song et al., 2013). The study investigates lateral roots developmental pattern, auxin distribution, PAT and expression of auxin transporter genes in the rice cultivars “Nanguang” and “Elio,” under different nitrogen availability. Expression of OsAUX1 results higher in the lateral root initiation and emergence zone of “Nanguang” roots in response to partial NO_3^- nutrition rather than to NH_4^+ alone. OsAUX1 is up-regulated in the lateral root elongation zone in the roots of both cultivars in response to phosphorus–nitrogen–nitrogen (PNN) compared to NH_4^+ alone (Song et al., 2013).

ZmAUX1, the closest maize homolog of AtAUX1, has 7–10 predicted TMDs and it's 73% identical to AtAUX1 (Hochholdinger et al., 2000). Northern blot experiments show expression in the tips of primary, lateral, seminal, and crown roots. In situ hybridization shows that ZmAUX1 expression is tissue-specific and confined to the endodermal and pericycle cell layers of the primary root, as well as to the epidermal cell layer (Hochholdinger et al., 2000). ZmAUX1 and AtAUX1 exhibit a preference for IAA and 2,4-D over NAA as substrate and are subject to differential transport inhibition by hexyloxy and benzyloxy derivatives of IAA (Parry et al., 2001; Tsuda et al., 2011). Transcriptome analysis indicates a role for ZmAUX1 in leaf primordia differentiation, although evidence is still not conclusive (Brooks et al., 2009).

Five LAX genes, named SbLAX1-5, have been identified in sorghum. The corresponding proteins present a highly conserved core region with 10 predicted transmembrane helices and their transcript levels are higher in leaves and stems rather than in roots and inflorescence tissues (Shen et al., 2010). Expression analysis of 3-weeks-old sorghum seedlings indicates that IAA treatment induces SbLAX2 and SbLAX3, but it inhibits SbLAX1 and SbLAX4 expression in leaves and roots, as well as it down-regulates SbLAX5 expression in leaves. BR treatment induces the expression of all five SbLAX genes in roots while it down-regulates SbLAX1 and -4 in leaves. ABA, salt, and drought treatments alter the expression profile of all SbLAXs (Shen et al., 2010; Wang et al., 2011).

PILS

PIN-LIKES represent the most recently characterized family of plant auxin transport proteins and include seven members in Arabidopsis. PILS show low (10–18%) sequence identity with PINs and they are all capable of transporting auxin across the PM in heterologous systems (Barbez et al., 2012). PILS regulate intracellular auxin accumulation at the ER and thus reduce the availability for free auxin that can reach the nucleus, possibly exerting a role in auxin signaling that is comparable to that of AtPIN5 (Barbez et al., 2012; Barbez and Kleine-Vehn, 2013).

The PILS family is conserved throughout the plant lineage, having representatives in several taxa including unicellular algae, where PINs have not been found yet. This indicates that PILS could be evolutionarily older than PINs (Feraru et al., 2012; Viaene et al., 2013). Six PILS have been identified in rice, 10 in maize, 7 in sorghum, and 8 in *Brachypodium* (**Figure 3**; Feraru et al., 2012). Forestan et al. (2012) identified two maize proteins that in sequence comparison analysis do not cluster with *Arabidopsis* PINs: ZmPINX and ZmPINY. Our sequence comparison verified that the two proteins are more similar to PILS rather than PINs, as previously hypothesized (**Figure 3**). Expression analysis for these genes shows that they are ubiquitously expressed and differentially up-regulated in maize organs. In detail, ZmPINX is up-regulated in root apex and male and female inflorescences, while ZmPINY is highly expressed during kernel development (Forestan et al., 2012).

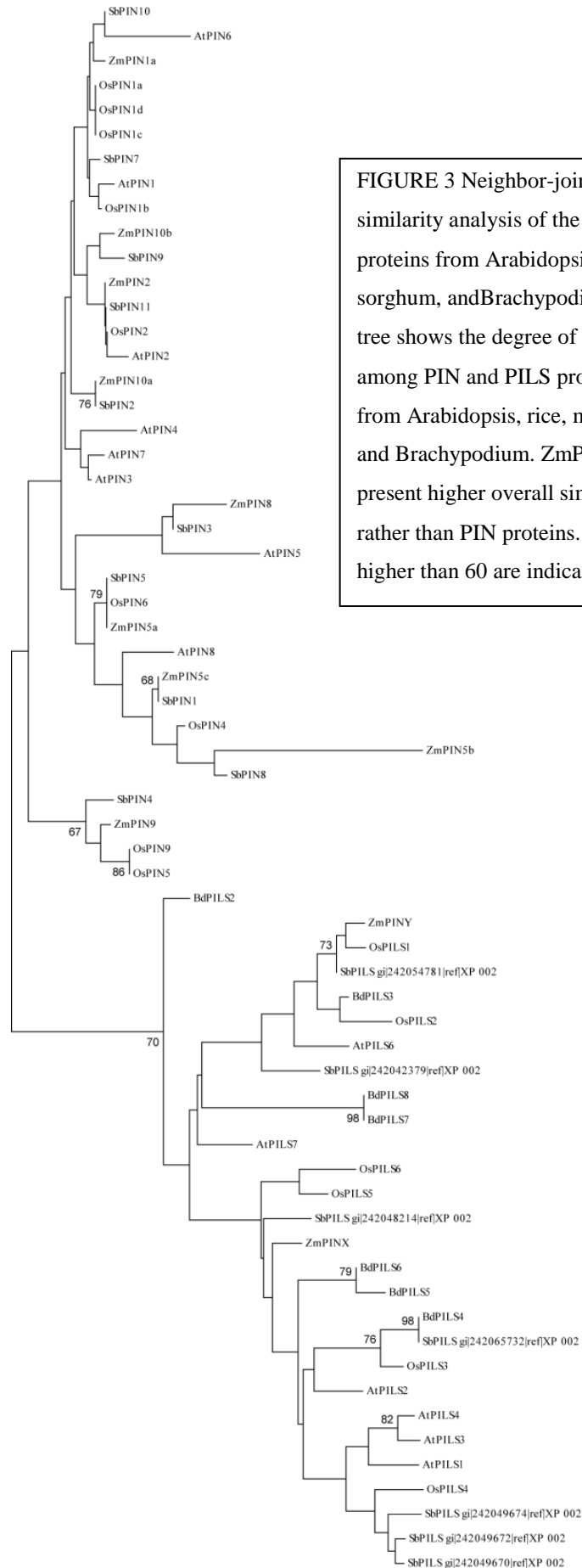


FIGURE 3 Neighbor-joining sequence similarity analysis of the PIN and PILS proteins from Arabidopsis, rice, maize, sorghum, and Brachypodium. The unrooted tree shows the degree of sequence similarity among PIN and PILS proteins from Arabidopsis, rice, maize, sorghum, and Brachypodium. ZmPINX and ZmPINY present higher overall similarity to PILS rather than PIN proteins. Bootstrap values higher than 60 are indicated at each node.

CONCLUSION

Auxin has a fundamental role in plant organs formation and its polar transport across cellular membranes is crucial for the correct development and response to external stimuli. Master regulators of PAT are auxin transport proteins, which have been extensively studied in *Arabidopsis* but not in other species, mainly due to the difficulty to obtain loss-of-function mutants. In monocots, only a few of these transporters have been characterized, mainly in rice and maize and most of the information available has been obtained by expression analyses without functional characterization. There are substantial divergences in development and plant structure between monocots and dicots. Differences are present in seed, vascular system, and leaf developmental programs (Tsiantis, 1999; Scarpella and Meijer, 2004; Coudert et al., 2010; Sreenivasulu and Wobus, 2013). The monocot root system architecture and cellular organization also differ considerably from those of dicots (Hochholdinger et al., 2004; Smith and De Smet, 2012). In addition, monocots have a segmented stem as opposed to the unsegmented stem of dicots. Auxin transporter families are larger in monocots allowing for the possibility of functional redundancy, but also for neo- and sub-functionalization of specific proteins. Monocot-specific and organ-specific proteins exist and they have a distinct role in regulating auxin driven organ development (PIN9). In some cases, alterations in PAT result in interesting new traits, such as dwarfism in maize and sorghum *br2* and *dw3* mutants respectively, which can be exploited to generate more productive lines through breeding programs. Moreover, many more short-statured mutants exist in maize that may have defects in auxin transport, although none of these mutants have been characterized in any detail. Interestingly, quite a few of these mutants exhibit dominant inheritance (Johal, unpublished) that makes them interesting in at least two ways. First, they can help side step gene redundancy problems and allow the functional exploration of additional genes. Second, they can be used in MAGIC (mutant-assisted gene identification and characterization)-based enhancer suppressor screens to unveil natural variation in a trait of interest (Johal et al., 2008). Even transgenic reporters for auxin activity can be used in lieu of bona fide dominant mutants for such MAGIC screens. The traditional enhancer/suppressor screens based on mutagenesis can also be employed to identify additional genes that encode auxin transporters. One such resource already exists in sorghum, where a line carrying a *dw3* mutation in *SbABCB1* was EMS mutagenized to produce and sequence M2 populations for both forward and reverse genetics (Krothapalli et al., 2013). These M2 populations can be screened to identify

other genes in the network with the ability to suppress or enhance the dw3 phenotype. Finally, there is the exciting possibility of using new genome editing and reverse genetics tools such as CRISPR/Cas9, which has been shown to work in rice and maize (Miao et al., 2013; Liang et al., 2014). Technologies like this can be used to alter the expression and function of genes encoding auxin transporters in monocots and this may lead to important new breakthroughs in our understanding of their roles in development and response to the environment.

Conflict of Interest Statement

The authors declare that the research was conducted in the absence of any commercial or financial relationships that could be construed as a potential conflict of interest.

Acknowledgments

The authors would like to thank Antje Klempien and Cristian Forestan for helpful comments on the manuscript.

SUPPLEMENTARY MATERIAL

The Supplementary Material for this article can be found online at: <http://www.frontiersin.org/journal/10.3389/fpls.2014.00393/abstract>

REFERENCES

- Abas L., Benjamins R., Malenica N., Paciorek T., Wiśniewska J., Wirniewska J., et al. (2006). Intracellular trafficking and proteolysis of the Arabidopsis auxin-efflux facilitator PIN2 are involved in root gravitropism. *Nat. Cell Biol.* 8 249–256 10.1038/ncb1369 [PubMed] [Cross Ref]
- Bailly A., Yang H., Martinoia E., Geisler M., Murphy A. S. (2011). Plant lessons: exploring ABCB functionality through structural modeling. *Front. Plant Sci.* 2:108 10.3389/fpls.2011.00108 [PMC free article] [PubMed] [Cross Ref]
- Bainbridge K., Guyomarc'h S., Bayer E., Swarup R., Bennett M., Mandel T., et al. (2008). Auxin influx carriers stabilize phyllotactic patterning. *Genes Dev.* 22 810–823 10.1101/gad.462608 [PMC free article] [PubMed] [Cross Ref]
- Bandyopadhyay A., Blakeslee J. J., Lee O. R., Mravec J., Sauer M., Titapiwatanakun B., et al. (2007). Interactions of PIN and PGP auxin transport mechanisms. *Biochem. Soc. Trans.* 35 137–141 10.1042/BST0350137 [PubMed] [Cross Ref]
- Barbez E., Kleine-Vehn J. (2013). Divide Et Impera – cellular auxin compartmentalization. *Curr. Opin. Plant Biol.* 16 78–84 10.1016/j.pbi.2012.10.005 [PubMed] [Cross Ref]
- Barbez E., Kubeš M., Rolèk J., Béziat C., Pěňčík A., Wang B., et al. (2012). A novel putative auxin carrier family regulates intracellular auxin homeostasis in plants. *Nature* 485 119–122 10.1038/nature11001 [PubMed] [Cross Ref]
- Barbosa I. C. R., Zourelidou M., Willige B. C., Weller B., Schwechheimer C. (2014). D6 PROTEIN KINASE activates auxin transport-dependent growth and PIN-FORMED phosphorylation at the plasma membrane. *Dev. Cell* 29 674–685 10.1016/j.devcel.2014.05.006 [PubMed] [Cross Ref]

Bell C. J., Maher E. P. (1990). Mutants of *Arabidopsis thaliana* with abnormal gravitropic responses. *Mol. Gen. Genet.* 220 289–293 10.1007/BF00260496 [Cross Ref]

Bender R. L., Fekete M. L., Klinkenberg P. M., Hampton M., Bauer B., Malecha M., et al. (2013). PIN6 is required for nectary auxin response and short stamen development. *Plant J.* 74 893–904 10.1111/tpj.12184 [PubMed] [Cross Ref]

Benková E., Michniewicz M., Sauer M., Teichmann T., Seifertová D., Jürgens G., et al. (2003). Local, efflux-dependent auxin gradients as a common module for plant organ formation. *Cell* 115 591–602 10.1016/S0092-8674(03)00924-3 [PubMed] [Cross Ref]

Bennett M. J., Marchant A., Green H. G., May S. T., Ward S. P., Millner P. A., et al. (1996). *Arabidopsis* AUX1 gene: a permease-like regulator of root gravitropism. *Science* 273 948–950 10.1126/science.273.5277.948 [PubMed] [Cross Ref]

Bennett T., Brockington S. F., Rothfels C., Graham S., Stevenson D., Kutchan T., et al. (2014). Paralagous radiations of PIN proteins with multiple origins of non-canonical PIN structure. *Mol. Biol. Evol.* 1–42 10.1093/molbev/msu147 [PMC free article] [PubMed] [Cross Ref]

Bertoni G. (2011). Indolebutyric acid-derived auxin and plant development. *Plant Cell* 23 845–845 10.1105/tpc.111.230312 [Cross Ref]

Bolduc N., O'Connor D., Moon J., Lewis M., Hake S. (2012). How to pattern a leaf. *Cold Spring Harb. Symp. Quant. Biol.* 77 47–51 10.1101/sqb.2012.77.014613 [PubMed] [Cross Ref]

Brooks L., Strable J., Zhang X., Ohtsu K., Zhou R., Sarkar A., et al. (2009). Microdissection of shoot meristem functional domains. *PLoS Genet.* 5:e1000476 10.1371/journal.pgen.1000476 [PMC free article] [PubMed] [Cross Ref]

Carraro N., Forestan C., Canova S., Traas J., Varotto S. (2006). ZmPIN1a and ZmPIN1b encode two novel putative candidates for polar auxin transport and plant architecture determination of maize. *Plant Physiol.* 142 254–264 10.1104/pp.106.080119 [PMC free article] [PubMed] [Cross Ref]

Carraro N., Tisdale-Orr T. E., Clouse R. M., Knöller A. S., Spicer R. (2012). Diversification and expression of the PIN, AUX/LAX, and ABCB families of putative auxin transporters in *Populus*. *Front. Plant Sci.* 3:17 10.3389/fpls.2012.00017 [PMC free article] [PubMed] [Cross Ref]

Carrier D. J., Bakar N. T. A., Swarup R., Callaghan R., Napier R. M., Bennett M. J., et al. (2008). The binding of auxin to the *Arabidopsis* auxin influx transporter AUX1. *Plant Physiol.* 148 529–535 10.1104/pp.108.122044 [PMC free article] [PubMed] [Cross Ref]

Cazonelli C. I., Vanstraelen M., Simon S., Yin K., Carron-Arthur A., Nisar N., et al. (2013). Role of the *Arabidopsis* PIN6 auxin transporter in auxin homeostasis and auxin-mediated development. *PLoS ONE* 8:e70069 10.1371/journal.pone.0070069 [PMC free article] [PubMed] [Cross Ref]

Chen J., Lausser A., Dresselhaus T. (2014). Hormonal responses during early embryogenesis in maize. *Biochem. Soc. Trans.* 42 325–331 10.1042/BST20130260 [PubMed] [Cross Ref]

Chen R., Hilson P., Sedbrook J., Rosen E., Caspar T., Masson P. H. (1998). The *Arabidopsis thaliana* AGRVITROPIC 1 gene encodes a component of the polar-auxin-transport efflux carrier. *Proc. Natl. Acad. Sci. U.S.A.* 95 15112–15117 10.1073/pnas.95.25.15112 [PMC free article] [PubMed] [Cross Ref]

Chen Y., Fan X., Song W., Zhang Y., Xu G. (2012). Over-expression of OsPIN2 leads to increased tiller numbers, angle and shorter plant height through suppression of OsLAZY1. *Plant Biotechnol. J.* 10 139–149 10.1111/j.1467-7652.2011.00637.x [PubMed] [Cross Ref]

Cho M., Cho H.-T. (2013). The function of ABCB transporters in auxin transport. *Plant Signal. Behav.* 8:e22990 10.4161/psb.22990 [PMC free article] [PubMed] [Cross Ref]

- Cho M., Lee Z.-W., Cho H.-T. (2012). ATP-binding cassette B4, an auxin-efflux transporter, stably associates with the plasma membrane and shows distinctive intracellular trafficking from that of PIN-FORMED proteins. *Plant Physiol.* 159 642–654 10.1104/pp.112.196139 [PMC free article][PubMed] [Cross Ref]
- Christie J. M., Murphy A. S. (2013). Shoot phototropism in higher plants: new light through old concepts. *Am. J. Bot.* 100 35–46 10.3732/ajb.1200340 [PubMed] [Cross Ref]
- Christie J. M., Yang H., Richter G. L., Sullivan S., Thomson C. E., Lin J., et al. (2011). phot1 inhibition of ABCB19 primes lateral auxin fluxes in the shoot apex required for phototropism. *PLoS Biol.* 9:e1001076 10.1371/journal.pbio.1001076 [PMC free article] [PubMed] [Cross Ref]
- Clouse R. M., Carraro N. (2014). A novel phylogeny and morphological reconstruction of the PINgenes and first phylogeny of the ACC-oxidases (ACOs). *Front. Plant Sci.* 5:29610.3389/fpls.2014.00296 [PMC free article] [PubMed] [Cross Ref]
- Coudert Y., Périn C., Courtois B., Khong N. G., Gantet P. (2010). Genetic control of root development in rice, the model cereal. *Trends Plant Sci.* 15 219–226 10.1016/j.tplants.2010.01.008[PubMed] [Cross Ref]
- Davies P. J. (ed.). (2004). *Plant Hormones Biosynthesis, Signal Transduction, Action!* 3rd Edn. Dordrecht: Kluwer Academic Publishers
- Delbarre A., Muller P., Imhoff V., Guern J. (1996). Comparison of mechanisms controlling uptake and accumulation of 2,4-dichlorophenoxy acetic acid, naphthalene-1-acetic acid, and indole-3-acetic acid in suspension-cultured tobacco cells. *Planta* 198 532–541 10.1007/BF00262639 [Cross Ref]
- Dhonukshe P., Huang F., Galvan-Ampudia C. S., Mähönen A. P., Kleine-Vehn J., Xu J., et al. (2010). Plasma membrane-bound AGC3 kinases phosphorylate PIN auxin carriers at TPRXS(N/S) motifs to direct apical PIN recycling. *Development* 137 3245–3255 10.1242/dev.052456 [PubMed][Cross Ref]
- Ding Z., Wang B., Moreno I., Dupláková N., Simon S., Carraro N., et al. (2012). ER-localized auxin transporter PIN8 regulates auxin homeostasis and male gametophyte development in Arabidopsis. *Nat. Commun.* 3 941 10.1038/ncomms1941 [PubMed] [Cross Ref]
- Dudlers R., Hertig C. (1992). Structure of an mdr-like Gene from Arabidopsis thaliana. *J. Biol. Chem.* 267 5882–5888 [PubMed]
- Egan A. N., Schlueter J., Spooner D. M. (2012). Applications of next-generation sequencing in plant biology. *Am. J. Bot.* 99 175–185 10.3732/ajb.1200020 [PubMed] [Cross Ref]
- Estelle M. (1998). Polar auxin transport. New support for an old model. *Plant Cell* 10 1775–1778 10.1105/tpc.10.11.1775 [PMC free article] [PubMed] [Cross Ref]
- Feng X.-L., Ni W.-M., Elge S., Mueller-Roeber B., Xu Z.-H., Xue H.-W. (2006). Auxin flow in anther filaments is critical for pollen grain development through regulating pollen mitosis. *Plant Mol. Biol.* 61 215–226 10.1007/s11103-006-0005-z [PubMed] [Cross Ref]
- Feraru E., Vosolsobé S., Feraru M. I., Petrášek J., Kleine-Vehn J. (2012). Evolution and structural diversification of PILS putative auxin carriers in plants. *Front. Plant Sci.* 3:22710.3389/fpls.2012.00227 [PMC free article] [PubMed] [Cross Ref]
- Forestan C., Farinati S., Varotto S. (2012). The maize PIN gene family of auxin transporters. *Front. Plant Sci.* 3:16 10.3389/fpls.2012.00016 [PMC free article] [PubMed] [Cross Ref]
- Forestan C., Meda S., Varotto S. (2010). ZmPIN1-mediated auxin transport is related to cellular differentiation during maize embryogenesis and endosperm development. *Plant Physiol.* 152 1373–1390 10.1104/pp.109.150193 [PMC free article] [PubMed] [Cross Ref]
- Fozard J. A., King J. R., Bennett M. J. (2013). Modelling auxin efflux carrier phosphorylation and localization. *J. Theor. Biol.* 319 34–49 10.1016/j.jtbi.2012.11.011 [PubMed] [Cross Ref]

- Friml J., Benková E., Blilou I., Wisniewska J., Hamann T., Ljung K., et al. (2002a). AtPIN4 mediates sink-driven auxin gradients and root patterning in Arabidopsis. *Cell* 108 661–673 [PubMed]
- Friml J., Wiśniewska J., Benková E., Mendgen K., Palme K. (2002b). Lateral relocation of auxin efflux regulator PIN3 mediates tropism in Arabidopsis. *Nature* 415 806–809 10.1038/415806a[PubMed] [Cross Ref]
- Friml J., Vieten A., Sauer M., Weijers D., Schwarz H., Hamann T., et al. (2003). Efflux-dependent auxin gradients establish the apical-basal axis of Arabidopsis. *Nature* 426 147–153 10.1038/nature02085 [PubMed] [Cross Ref]
- Friml J., Yang X., Michniewicz M., Weijers D., Quint A., Tietz O., et al. (2004). A PINOID-dependent binary switch in apical-basal PIN polar targeting directs auxin efflux. *Science* 306 862–865 10.1126/science.1100618 [PubMed] [Cross Ref]
- Gallavotti A. (2013). The role of auxin in shaping shoot architecture. *J. Exp. Bot.* 64 2593–2608 10.1093/jxb/ert141 [PubMed] [Cross Ref]
- Gallavotti A., Yang Y., Schmidt R. J., Jackson D. (2008). The relationship between auxin transport and maize branching. *Plant Physiol.* 147 1913–1923 10.1104/pp.108.121541 [PMC free article][PubMed] [Cross Ref]
- Gälweiler L., Guan C., Müller A., Wisman E., Mendgen K., Yephremov A., et al. (1998). Regulation of polar auxin transport by AtPIN1 in Arabidopsis vascular tissue. *Science* 282 2226–2230 10.1126/science.282.5397.2226 [PubMed] [Cross Ref]
- Ganguly A., Lee S.-H., Cho H.-T. (2012). Functional identification of the phosphorylation sites of Arabidopsis PIN-FORMED3 for its subcellular localization and biological role. *Plant J.* 71 810–823 10.1111/j.1365-313X.2012.05030.x [PubMed] [Cross Ref]
- Ganguly A., Lee S. H., Cho M., Lee O. R., Yoo H., Cho H.-T. (2010). Differential auxin-transporting activities of PIN-FORMED proteins in Arabidopsis root hair cells. *Plant Physiol.* 153 1046–1061 10.1104/pp.110.156505 [PMC free article] [PubMed] [Cross Ref]
- Ganguly A., Park M., Kesawat M. S., Cho H.-T. (2014). Functional analysis of the hydrophilic loop in intracellular trafficking of Arabidopsis PIN-FORMED proteins. *Plant Cell* 1–17 10.1105/tpc.113.118422 [PMC free article] [PubMed] [Cross Ref]
- Garcia O., Bouige P., Forestier C., Dassa E. (2004). Inventory and comparative analysis of rice and Arabidopsis ATP-binding cassette (ABC) systems. *J. Mol. Biol.* 343 249–265 10.1016/j.jmb.2004.07.093 [PubMed] [Cross Ref]
- Geisler M., Blakeslee J. J., Bouchard R., Lee O. R., Vincenzetti V., Bandyopadhyay A., et al. (2005). Cellular efflux of auxin catalyzed by the Arabidopsis MDR/PGP transporter AtPGP1. *Plant J.* 44 179–194 10.1111/j.1365-313X.2005.02519.x [PubMed] [Cross Ref]
- Geisler M., Murphy A. S. (2006). The ABC of auxin transport: the role of p-glycoproteins in plant development. *FEBS Lett.* 580 1094–1102 10.1016/j.febslet.2005.11.054 [PubMed] [Cross Ref]
- Geisler M., Wang B., Zhu J. (2014). Auxin transport during root gravitropism: transporters and techniques. *Plant Biol. (Stuttg.)* 16(Suppl. 1) 50–57 10.1111/plb.12030 [PubMed] [Cross Ref]
- Habets M. E. J., Offringa R. (2014). Tansley review PIN-driven polar auxin transport in plant developmental plasticity: a key target for environmental and endogenous signals. *New Phytol.* 203 362–377 10.1111/nph.12831 [PubMed] [Cross Ref]
- Higgins C. F., Linton K. J. (2004). The ATP switch model for ABC transporters. *Nat. Struct. Mol. Biol.* 11 918–926 10.1038/nsmb836 [PubMed] [Cross Ref]
- Hochholdinger F., Park W. J., Sauer M., Woll K. (2004). From weeds to crops: genetic analysis of root development in cereals. *Trends Plant Sci.* 9 42–48 10.1016/j.tplants.2003.11.003 [PubMed][Cross Ref]

- Hochholdinger F., Wulff D., Reuter K., Park W. J., Feix G. (2000). Tissue-specific expression of AUX1 in maize roots. *J. Plant Physiol.* 157 315–319 10.1016/S0176-1617(00)80053-X [Cross Ref]
- Jasinski M., Ducos E., Martinoia E., Boutry M. (2003). The ATP-binding cassette transporters?: structure, function, and gene family comparison between. *Plant Physiol.* 131 1169–1177 10.1104/pp.102.014720.ABC [PMC free article] [PubMed] [Cross Ref]
- Johal G. S., Balint-Kurti P., Weil C. F. (2008). Mining and harnessing natural variation: a little MAGIC. *Crop Sci.* 48:2066 10.2135/cropsci2008.03.0150 [Cross Ref]
- Kamimoto Y., Terasaka K., Hamamoto M., Takahashi K., Fukuda S., Shitan N., et al. (2012). Arabidopsis ABCB21 is a facultative auxin importer/exporter regulated by cytoplasmic auxin concentration. *Plant Cell Physiol.* 53 2090–2100 10.1093/pcp/pcs149 [PubMed] [Cross Ref]
- Kaneda M., Schuetz M., Lin B. S. P., Chanis C., Hamberger B., Western T. L., et al. (2011). ABC transporters coordinately expressed during lignification of Arabidopsis stems include a set of ABCBs associated with auxin transport. *J. Exp. Bot.* 62 2063–2077 10.1093/jxb/erq416 [PMC free article][PubMed] [Cross Ref]
- Kang J., Park J., Choi H., Burla B., Kretschmar T., Lee Y., et al. (2011). Plant ABC transporters. *Arabidopsis Book* 9:e0153 10.1199/tab.0153 [PMC free article] [PubMed] [Cross Ref]
- Kende H., Zeevaart J. A. D. (1997). The five “Classical” plant hormones. *Plant Cell* 9 1197–1210 10.1105/tpc.9.7.1197 [PMC free article] [PubMed] [Cross Ref]
- Kierzkowski D., Lenhard M., Smith R., Kuhlemeier C. (2013). Interaction between meristem tissue layers controls phyllotaxis. *Dev. Cell* 26 616–628 10.1016/j.devcel.2013.08.017 [PubMed][Cross Ref]
- Kleine-vehn J., Ding Z., Jones A. R., Tasaka M., Morita M. T. (2010). Gravity-induced PIN transcytosis for polarization of auxin fluxes in gravity-sensing root cells. *Proc. Natl. Acad. Sci. U.S.A.* 107 22344–22349 10.1073/pnas.101314510 [PMC free article] [PubMed] [Cross Ref]
- Kleine-Vehn J., Wabnik K., Martinière A., Łangowski Ł., Willig K., Naramoto S., et al. (2011). Recycling, clustering, and endocytosis jointly maintain PIN auxin carrier polarity at the plasma membrane. *Mol. Syst. Biol.* 7:540 10.1038/msb.2011.72 [PMC free article] [PubMed] [Cross Ref]
- Knöllner A. S., Blakeslee J. J., Richards E. L., Peer W. A., Murphy A. S. (2010). Brachytic2/ZmABCB1 functions in IAA export from intercalary meristems. *J. Exp. Bot.* 61 3689–3696 10.1093/jxb/erq180 [PMC free article] [PubMed] [Cross Ref]
- Kramer E. M., Bennett M. J. (2006). Auxin transport: a field in flux. *Trends Plant Sci.* 11 382–386 10.1016/j.tplants.2006.06.002 [PubMed] [Cross Ref]
- Křeček P., Skůpa P., Libus J., Naramoto S., Tejos R., Friml J., et al. (2009). Protein family review The PIN-FORMED (PIN) protein family of auxin transporters. *Genome Biol.* 10 1–11 10.1186/gb-2009-10-12-249 [PMC free article] [PubMed] [Cross Ref]
- Krothapalli K., Buescher E. M., Li X., Brown E., Chapple C., Dilkes B. P., et al. (2013). Forward genetics by genome sequencing reveals that rapid cyanide release deters insect herbivory of Sorghum bicolor. *Genetics* 195 309–318 10.1534/genetics.113.149567 [PMC free article] [PubMed][Cross Ref]
- Kubeš M., Yang H., Richter G. L., Cheng Y., Młodzińska E., Wang X., et al. (2011). The Arabidopsis concentration-dependent influx/efflux transporter ABCB4 regulates cellular auxin levels in the root epidermis. *Plant J.* 69 640–654 10.1111/j.1365-313X.2011.04818.x [PubMed] [Cross Ref]
- Lampugnani E. R., Kilinc A., Smyth D. R. (2013). Auxin controls petal initiation in Arabidopsis. *Development* 140 185–194 10.1242/dev.084582 [PubMed] [Cross Ref]
- Larkin M. A., Blackshields G., Brown N. P., Chenna R., McGettigan P. A., McWilliam H., et al. (2007). Clustal W and Clustal X version 2.0. *Bioinformatics* 23 2947–2948 10.1093/bioinformatics/btm404 [PubMed] [Cross Ref]

- Lee M., Choi Y., Burla B., Kim Y.-Y., Jeon B., Maeshima M., et al. (2008). The ABC transporter AtABCB14 is a malate importer and modulates stomatal response to CO₂. *Nat. Cell Biol.* 10 1217–1223 10.1038/ncb1782 [PubMed] [Cross Ref]
- Lewis D. R., Wu G., Ljung K., Spalding E. P. (2009). Auxin transport into cotyledons and cotyledon growth depend similarly on the ABCB19 Multidrug Resistance-like transporter. *Plant J.* 60 91–101 10.1111/j.1365-313X.2009.03941.x [PubMed] [Cross Ref]
- Leyser O. (2010). The power of auxin in plants. *Plant Physiol.* 154 501–505 10.1104/pp.110.161323 [PMC free article] [PubMed] [Cross Ref]
- Liang Z., Zhang K., Chen K., Gao C. (2014). Targeted mutagenesis in *Zea mays* using TALENs and the CRISPR/Cas System. *J. Genet. Genomics* 41 63–68 10.1016/j.jgg.2013.12.001 [PubMed][Cross Ref]
- Lin R., Wang H. (2005). Two homologous ATP-binding cassette transporter proteins, AtMDR1 and AtPGP1, regulate Arabidopsis photomorphogenesis and root development by mediating polar auxin transport. *Plant Physiol.* 138 949–964 10.1104/pp.105.061572.1 [PMC free article] [PubMed][Cross Ref]
- Löfke C., Luschnig C., Kleine-Vehn J. (2013). Posttranslational modification and trafficking of PIN auxin efflux carriers. *Mech. Dev.* 130 82–94 10.1016/j.mod.2012.02.003 [PubMed] [Cross Ref]
- Luschnig C., Gaxiola R. A., Grisafi P., Fink G. R. (1998). EIR1, a root-specific protein involved in auxin transport, is required for gravitropism in *Arabidopsis thaliana*. *Genes Dev.* 12 2175–2187 10.1101/gad.12.14.2175 [PMC free article] [PubMed] [Cross Ref]
- Marchant A., Bhalerao R., Casimiro I., Eklöf J., Casero P. J., Bennett M., et al. (2002). AUX1 promotes lateral root formation by facilitating indole-3-acetic acid distribution between sink and source tissues in the *Arabidopsis* seedling. *Plant Cell* 14 589–597 10.1105/tpc.010354.2 [PMC free article][PubMed] [Cross Ref]
- McLamore E. S., Diggs A., Calvo Marzal P., Shi J., Blakeslee J. J., Peer W. A., et al. (2010). Non-invasive quantification of endogenous root auxin transport using an integrated flux microsensor technique. *Plant J.* 63 1004–1016 10.1111/j.1365-313X.2010.04300.x [PubMed] [Cross Ref]
- McSteen P. (2010). Auxin and monocot development. *Cold Spring Harb. Perspect. Biol.* 2:a001479 10.1101/cshperspect.a001479 [PMC free article] [PubMed] [Cross Ref]
- Miao J., Guo D., Zhang J., Huang Q., Qin G., Zhang X., et al. (2013). Targeted mutagenesis in rice using CRISPR-cas system. *Cell Res.* 23 1233–1236 10.1038/cr.2013.123 [PMC free article][PubMed] [Cross Ref]
- Miyashita Y., Takasugi T., Ito Y. (2010). Identification and expression analysis of PIN genes in rice. *Plant Sci.* 178 424–428 10.1016/j.plantsci.2010.02.018 [Cross Ref]
- Mohanty A., Luo A., DeBlasio S., Ling X., Yang Y., Tuthill D. E., et al. (2009). Advancing cell biology and functional genomics in maize using fluorescent protein-tagged lines. *Plant Physiol.* 149 601–605 10.1104/pp.108.130146 [PMC free article] [PubMed] [Cross Ref]
- Möller B., Weijers D. (2009). Auxin control of embryo patterning. *Cold Spring Harb. Perspect. Biol.* 1:a001545 10.1101/cshperspect.a001545 [PMC free article] [PubMed] [Cross Ref]
- Mravec J., Skúpa P., Bailly A., Hoyerová K., Krecek P., Bielach A., et al. (2009). Subcellular homeostasis of phytohormone auxin is mediated by the ER-localized PIN5 transporter. *Nature* 459 1136–1140 10.1038/nature08066 [PubMed] [Cross Ref]
- Müller A., Guan C., Gälweiler L., Tänzler P., Huijser P., Marchant A., et al. (1998). AtPIN2 defines a locus of *Arabidopsis* for root gravitropism control. *EMBO J.* 17 6903–6911 10.1093/emboj/17.23.6903 [PMC free article] [PubMed] [Cross Ref]
- Müller D., Leyser O. (2011). Auxin, cytokinin and the control of shoot branching. *Ann. Bot.* 107 1203–1212 10.1093/aob/mcr069 [PMC free article] [PubMed] [Cross Ref]

- Multani D. S., Briggs S. P., Chamberlin M. A., Blakeslee J. J., Murphy A. S., Johal G. S. (2003). Loss of an MDR transporter in compact stalks of maize *br2* and sorghum *dw3* mutants. *Science* 302 81–84 10.1126/science.1086072 [PubMed] [Cross Ref]
- Nagashima A., Uehara Y., Sakai T. (2008). The ABC subfamily B auxin transporter AtABCB19 is involved in the inhibitory effects of N-1-naphthylphthalamic acid on the phototropic and gravitropic responses of Arabidopsis hypocotyls. *Plant Cell Physiol.* 49 1250–1255 10.1093/pcp/pcn092[PubMed] [Cross Ref]
- Noh B., Murphy A. S., Spalding E. P. (2001). Multidrug resistance-like genes of Arabidopsis required for auxin transport and auxin-mediated development. *Plant cell* 13 2441–2454 10.1105/tpc.010350[PMC free article] [PubMed] [Cross Ref]
- O'Connor D. L., Runions A., Sluis A., Bragg J., Vogel J. P., Prusinkiewicz P., et al. (2014). A division in PIN-mediated auxin patterning during organ initiation in grasses. *PLoS Comput. Biol.* 10:e1003447 10.1371/journal.pcbi.1003447 [PMC free article] [PubMed] [Cross Ref]
- Okada K., Ueda J., Komaki M. K., Bell C. J., Shimura Y. (1991). Requirement of the auxin polar transport system in early stages of Arabidopsis floral bud formation. *Plant Cell* 3 67710.2307/3869249 [PMC free article] [PubMed] [Cross Ref]
- Pang K., Li Y., Liu M., Meng Z., Yu Y. (2013). Inventory and general analysis of the ATP-binding cassette (ABC) gene superfamily in maize (*Zea mays* L.). *Gene* 526 411–428 10.1016/j.gene.2013.05.051 [PubMed] [Cross Ref]
- Parry G., Delbarre A., Marchant A., Swarup R., Napier R., Perrot-Rechenmann C., et al. (2001). Novel auxin transport inhibitors phenocopy the auxin influx carrier mutation *aux1*. *Plant J.* 25 399–406 10.1046/j.1365-313x.2001.00970.x [PubMed] [Cross Ref]
- Péret B., Swarup K., Ferguson A., Seth M., Yang Y., Dhondt S., et al. (2012). AUX/LAX genes encode a family of auxin influx transporters that perform distinct functions during Arabidopsis development. *Plant Cell* 24 2874–2885 10.1105/tpc.112.097766 [PMC free article] [PubMed][Cross Ref]
- Reinhardt D., Pesce E.-R., Stieger P., Mandel T., Baltensperger K., Bennett M., et al. (2003). Regulation of phyllotaxis by polar auxin transport. *Nature* 426 255–260 10.1038/nature02081[PubMed] [Cross Ref]
- Robert S., Kleine-Vehn J., Barbez E., Sauer M., Paciorek T., Baster P., et al. (2010). ABP1 mediates auxin inhibition of clathrin-dependent endocytosis in Arabidopsis. *Cell* 143 111–121 10.1016/j.cell.2010.09.027 [PMC free article] [PubMed] [Cross Ref]
- Rojas-Pierce M., Titapiwatanakun B., Sohn E. J., Fang F., Larive C. K., Blakeslee J., et al. (2007). Arabidopsis P-glycoprotein19 participates in the inhibition of gravitropism by gravacin. *Chem. Biol.* 14 1366–1376 10.1016/j.chembiol.2007.10.014 [PubMed] [Cross Ref]
- Rosquete M. R., von Wangenheim D., Marhavý P., Barbez E., Stelzer E. H. K., Benková E., et al. (2013). An auxin transport mechanism restricts positive orthogravitropism in lateral roots. *Curr. Biol.* 23 817–822 10.1016/j.cub.2013.03.064 [PubMed] [Cross Ref]
- Santelia D., Vincenzetti V., Azzarello E., Bovet L., Fukao Y., Düchtig P., et al. (2005). MDR-like ABC transporter AtPGP4 is involved in auxin-mediated lateral root and root hair development. *FEBS Lett.* 579 5399–5406 10.1016/j.febslet.2005.08.061 [PubMed] [Cross Ref]
- Sawchuk M. G., Edgar A., Scarpella E. (2013). Patterning of leaf vein networks by convergent auxin transport pathways. *PLoS Genet.* 9:e1003294 10.1371/journal.pgen.1003294 [PMC free article][PubMed] [Cross Ref]
- Scarpella E., Marcos D., Berleth T. (2006). Control of leaf vascular patterning by polar auxin transport. *Genes Dev.* 20 1015–1027 10.1101/gad.1402406.gree [PMC free article] [PubMed][Cross Ref]
- Scarpella E., Meijer A. H. (2004). Pattern formation in the vascular system of monocot and dicot plant species. *New Phytol. Tansley Rev.* 164 209–242 10.1111/j.1469-8137.2004.01191.x [Cross Ref]

- Shen C., Bai Y., Wang S., Zhang S., Wu Y., Chen M., et al. (2010). Expression profile of PIN, AUX/LAX and PGP auxin transporter gene families in *Sorghum bicolor* under phytohormone and abiotic stress. *FEBS J.* 277 2954–2969 10.1111/j.1742-4658.2010.07706.x [PubMed] [Cross Ref]
- Sidler M., Hassa P., Hasan S., Ringli C., Dudler R. (1998). Involvement of an ABC transporter in a developmental pathway regulating hypocotyl cell elongation in the light. *Plant Cell* 10 1623–1636 10.1105/tpc.10.10.1623 [PMC free article] [PubMed] [Cross Ref]
- Simon S., Petrášek J. (2011). Why plants need more than one type of auxin. *Plant Sci.* 180 454–460 10.1016/j.plantsci.2010.12.007 [PubMed] [Cross Ref]
- Smith S., De Smet I. (2012). Root system architecture: insights from *Arabidopsis* and cereal crops. *Philos. Trans. R. Soc. Lond. B Biol. Sci.* 367 1441–1452 10.1098/rstb.2011.0234 [PMC free article][PubMed] [Cross Ref]
- Song W., Sun H., Li J., Gong X., Huang S., Zhu X., et al. (2013). Auxin distribution is differentially affected by nitrate in roots of two rice cultivars differing in responsiveness to nitrogen. *Ann. Bot.* 112 1383–1393 10.1093/aob/mct212 [PMC free article] [PubMed] [Cross Ref]
- Sreenivasulu N., Wobus U. (2013). Seed-development programs: a systems biology-based comparison between dicots and monocots. *Annu. Rev. Plant Biol.* 64 189–217 10.1146/annurev-arplant-050312-120215 [PubMed] [Cross Ref]
- Sun F., Zhang W., Hu H., Li B., Wang Y., Zhao Y., et al. (2008). Salt modulates gravity signaling pathway to regulate growth direction of primary roots in *Arabidopsis*. *Plant Physiol.* 146 178–188 10.1104/pp.107.109413 [PMC free article] [PubMed] [Cross Ref]
- Swarup K., Benková E., Swarup R., Casimiro I., Péret B., Yang Y., et al. (2008). The auxin influx carrier LAX3 promotes lateral root emergence. *Nat. Cell Biol.* 10 946–954 10.1038/ncb1754 [PubMed] [Cross Ref]
- Swarup R., Kargul J., Marchant A., Zadnik D., Rahman A., Mills R., et al. (2004). Structure-function analysis of the presumptive *Arabidopsis* auxin permease AUX1. *Plant Cell* 16 3069–3083 10.1105/tpc.104.024737.2 [PMC free article] [PubMed] [Cross Ref]
- Swarup R., Kramer E. M., Perry P., Knox K., Leyser H. M. O., Haseloff J., et al. (2005). Root gravitropism requires lateral root cap and epidermal cells for transport and response to a mobile auxin signal. *Nat. Cell Biol.* 7 1057–1065 10.1038/ncb1316 [PubMed] [Cross Ref]
- Swarup R., Marchant A., Ljung K., Sandberg G., Palme K., Bennett M., et al. (2001). Localization of the auxin permease AUX1 suggests two functionally distinct hormone transport pathways operate in the *Arabidopsis* root apex. *Genes Dev.* 15 2648–2653 10.1101/gad.210501 [PMC free article][PubMed] [Cross Ref]
- Tamura K., Stecher G., Peterson D., Filipowski A., Kumar S. (2013). MEGA6: molecular evolutionary genetics analysis version 6.0. *Mol. Biol. Evol.* 30 2725–2729 10.1093/molbev/mst197 [PMC free article] [PubMed] [Cross Ref]
- Tanaka H., Dhonukshe P., Brewer P. B., Friml J. (2006). Spatiotemporal asymmetric auxin distribution: a means to coordinate plant development. *Cell. Mol. Life Sci.* 63 2738–2754 10.1007/s00018-006-6116-5 [PubMed] [Cross Ref]
- Tarkowská D., Novák O., Floková K., Tarkowski P., Turečková V., Grúz J., et al. (2014). Quo vadis plant hormone analysis? *Planta* 240 55–76 10.1007/s00425-014-2063-9 [PubMed] [Cross Ref]
- Terasaka K., Blakeslee J. J., Titapiwatanakun B., Peer W. A., Bandyopadhyay A., Makam S. N., et al. (2005). PGP4, an ATP binding cassette P-glycoprotein, catalyzes auxin transport in *Arabidopsis thaliana* roots. *Plant Cell* 17 2922–2939 10.1105/tpc.105.035816.2 [PMC free article] [PubMed][Cross Ref]
- Titapiwatanakun B., Murphy A. S. (2009). Post-transcriptional regulation of auxin transport proteins: cellular trafficking, protein phosphorylation, protein maturation, ubiquitination, and membrane composition. *J. Exp. Bot.* 60 1093–10107 10.1093/jxb/ern240 [PubMed] [Cross Ref]

- Tsiantis M. (1999). The maize rough sheath2 gene and leaf development programs in monocot and dicot plants. *Science* 284 154–156 10.1126/science.284.5411.154 [PubMed] [Cross Ref]
- Tsuda E., Yang H., Nishimura T., Uehara Y., Sakai T., Furutani M., et al. (2011). Alkoxy-auxins are selective inhibitors of auxin transport mediated by PIN, ABCB, and AUX1 transporters. *J. Biol. Chem.* 286 2354–2364 10.1074/jbc.M110.171165 [PMC free article] [PubMed] [Cross Ref]
- Utsuno K., Shikanai T., Yamada Y., Hashimoto T. (1998). Agr, an agravitropic locus of *Arabidopsis thaliana*, encodes a novel membrane-protein family member. *Plant Cell Physiol.* 39 1111–1118 10.1093/oxfordjournals.pcp.a029310 [PubMed] [Cross Ref]
- Viaene T., Delwiche C. F., Rensing S. A., Friml J. (2013). Origin and evolution of PIN auxin transporters in the green lineage. *Trends Plant Sci.* 18 5–10 10.1016/j.tplants.2012.08.009 [PubMed][Cross Ref]
- Vieten A., Vanneste S., Wisniewska J., Benková E., Benjamins R., Beeckman T., et al. (2005). Functional redundancy of PIN proteins is accompanied by auxin-dependent cross-regulation of PIN expression. *Development* 132 4521–4531 10.1242/dev.02027 [PubMed] [Cross Ref]
- Wang J.-R., Hu H., Wang G.-H., Li J., Chen J.-Y., Wu P. (2009). Expression of PIN genes in rice (*Oryza sativa* L.): tissue specificity and regulation by hormones. *Mol. Plant* 2 823–831 10.1093/mp/ssp023 [PubMed] [Cross Ref]
- Wang P., Cheng T., Wu S., Zhao F., Wang G., Yang L., et al. (2014a). Phylogeny and molecular evolution analysis of PIN-FORMED 1 in angiosperm. *PLoS ONE* 9:e89289 10.1371/journal.pone.0089289 [PMC free article] [PubMed] [Cross Ref]
- Wang S., Xu Y., Li Z., Zhang S., Lim J. -M., Lee K. O., et al. (2014b). OsMOGS is required for N-glycan formation and auxin-mediated root development in rice (*Oryza sativa* L.). *Plant J.* 78 632–645 10.1111/tj.12497 [PMC free article] [PubMed] [Cross Ref]
- Wang S., Shen C., Zhang S., Xu Y., Jiang D., Qi Y. (2011). Analysis of subcellular localization of auxin carriers PIN, AUX/LAX and PGP in *Sorghum bicolor*. *Plant Signal. Behav.* 6 2023–2025 10.4161/psb.6.12.17968 [PMC free article] [PubMed] [Cross Ref]
- Weijers D., Sauer M., Meurette O., Friml J., Ljung K., Sandberg G., et al. (2005). Maintenance of embryonic auxin distribution for apical-basal patterning by PIN-FORMED-dependent auxin transport in *Arabidopsis*. *Plant Cell* 17 2517–2526 10.1105/tpc.105.034637.1 [PMC free article] [PubMed] [Cross Ref]
- Went F. (1926). On growth-accelerating substances in the coleoptile of *Avena sativa*. *Proc. K. Ned. Akad. van Wet.* 30 10–19
- Willige B. C., Ahlers S., Zourelidou M., Barbosa I. C. R., Demarsy E., Trevisan M., et al. (2013). D6PK AGCVIII kinases are required for auxin transport and phototropic hypocotyl bending in *Arabidopsis*. *Plant Cell* 25 1674–1688 10.1105/tpc.113.111484 [PMC free article] [PubMed][Cross Ref]
- Woodward A. W., Bartel B. (2005). Auxin: regulation, action, and interaction. *Ann. Bot.* 95 707–735 10.1093/aob/mci083 [PMC free article] [PubMed] [Cross Ref]
- Wu G., Otegui M. S., Spalding E. P. (2010). The ER-localized TWD1 immunophilin is necessary for localization of multidrug resistance-like proteins required for polar auxin transport in *Arabidopsis* roots. *Plant Cell* 22 3295–3304 10.1105/tpc.110.078360 [PMC free article] [PubMed] [Cross Ref]
- Xu M., Zhu L., Shou H., Wu P. (2005). A PIN1 family gene, OsPIN1, involved in auxin-dependent adventitious root emergence and tillering in rice. *Plant Cell Physiol.* 46 1674–1681 10.1093/pcp/pci183 [PubMed] [Cross Ref]
- Xu Y., Zhang S., Guo H., Wang S., Xu L., Li C., et al. (2014). OsABCB14 functions in auxin transport and iron homeostasis in rice (*Oryza sativa* L.). *Plant J.* 79 106–117 10.1111/tj.12544 [PubMed] [Cross Ref]

- Yang H., Murphy A. S. (2009). Functional expression and characterization of Arabidopsis ABCB, AUX 1 and PIN auxin transporters in *Schizosaccharomyces pombe*. *Plant J.* 59 179–191 10.1111/j.1365-313X.2009.03856.x [PubMed] [Cross Ref]
- Yang Y., Hammes U. Z., Taylor C. G., Schachtman D. P., Nielsen E. (2006). High-affinity auxin transport by the AUX1 influx carrier protein. *Curr. Biol.* 16 1123–1127 10.1016/j.cub.2006.04.029 [PubMed] [Cross Ref]
- Ye L., Liu L., Xing A., Kang D. (2013). Characterization of a dwarf mutant allele of Arabidopsis MDR-like ABC transporter AtPGP1 gene. *Biochem. Biophys. Res. Commun.* 441 782–786 10.1016/j.bbrc.2013.10.136 [PubMed] [Cross Ref]
- Young L. M., Evans M. L., Hertel R. (1990). Correlations between gravitropic curvature and auxin movement across gravistimulated roots of *Zea mays*. *Plant Physiol.* 92 792–796 10.1104/pp.92.3.792 [PMC free article] [PubMed] [Cross Ref]
- Yu C., Han F., Zhang J., Birchler J., Peterson T. (2012). A transgenic system for generation of transposon Ac/Ds-induced chromosome rearrangements in rice. *Theor. Appl. Genet.* 125 1449–1462 10.1007/s00122-012-1925-4 [PMC free article] [PubMed] [Cross Ref]
- Zádníková P., Petrásek J., Marhavy P., Raz V., Vandenbussche F., Ding Z., et al. (2010). Role of PIN-mediated auxin efflux in apical hook development of *Arabidopsis thaliana*. *Development* 137 607–617 10.1242/dev.041277 [PubMed] [Cross Ref]
- Zazimalová E., Krecek P., Skůpa P., Hoyerová K., Petrásek J. (2007). Polar transport of the plant hormone auxin – the role of PIN-FORMED (PIN) proteins. *Cell. Mol. Life Sci.* 64 1621–1637 10.1007/s00018-007-6566-4 [PubMed] [Cross Ref]
- Zhang K.-X., Xu H.-H., Gong W., Jin Y., Shi Y.-Y., Yuan T.-T., et al. (2014). Proper PIN1 distribution is needed for root negative phototropism in *Arabidopsis*. *PLoS ONE* 9:e85720.1371/journal.pone.0085720 [PMC free article] [PubMed] [Cross Ref]
- Zhang K.-X., Xu H.-H., Yuan T.-T., Zhang L., Lu Y.-T. (2013). Blue-light-induced PIN3 polarization for root negative phototropic response in *Arabidopsis*. *Plant J.* 76 308–321 10.1111/tj.12298 [PubMed] [Cross Ref]
- Zourelidou M., Müller I., Willige B. C., Nill C., Jikumaru Y., Li H., et al. (2009). The polarly localized D6 PROTEIN KINASE is required for efficient auxin transport in *Arabidopsis thaliana*. *Development* 136 627–636 10.1242/dev.028365 [PubMed] [Cross Ref]

1.3 Plant transposable element

Transposable elements (TEs) are defined as DNA fragments able to translocate into other positions in the genome causing effects on genome structure and gene function.

Plant TEs were first discovered in maize by Barbara McClintock who originally named the maize transposons "jumping genes" or "controlling elements" because of their ability to alter the expression of genes near or at the site of TE insertion (Comfort, 2001; Bennetzen, 2000; McCLINTOCK, 1950).

Later in the 70s, measuring the reannealing kinetics of denaturated DNA fragments Flavell et al. (1974) demonstrated a large portion of the genome of several plant species, such as *Triticum aestivum* and *Zea mays*, was made of repetitive sequences. This genome fraction was initially proposed to be genes spacers and was called "junk DNA" (Ohno, 1972). In the 80s, Doolittle and Sapienza (1980) renamed it "selfish DNA" due to the absence of evident function. We now know that they represent an important, or even the major, evolutionary force in shaping the genomes. In fact, TEs can promote transposition, insertion, excision, chromosome breakage, and ectopic recombination. A TE does not need to be inserted in a coding sequence to affect the function of the gene. Modified gene expression can also occur if TEs are incorporated into a cis-regulatory region.

The term TE refers to various genomic transposable elements. The first TE classification system was proposed by Finnegan (1989, 1982) and has been updated in the following decades. According to Finnegan, TEs are classified based on their transposition intermediate: RNA (class I retroelements) or DNA (class II transposons). The transposition method of class I is commonly called "copy-and-paste", and that of class II, "cut-and-paste" (Finnegan, 1989).

After the Finnegan proposal, Repbase and the Wicker classifications were proposed based both on DNA and amino acid sequence features. Both classifications divide all TEs into two groups, the retrotransposons and the DNA transposons. Each group is divided in levels, called "type" for the Repbase and "class" for the Wicker, and each level is divided in classes or orders, for Repbase or Wicker respectively (Wicker et al., 2007; Jurka et al., 2005; Piégu et al., 2015)

With rare exceptions, transposons are found in virtually all genomes and they are often the largest component of non-coding sequence; in some large-genome plants, mobile DNAs make up the majority of the nuclear genome. In many grasses with genomes >2000 Mb, most genes exist as single-gene islands that are surrounded by TEs (Sanmiguel and Bennetzen, 1998). Among the completed eukaryotic genome sequences, TE content ranges from 0% in *Plasmodium falciparum* to 85% in maize (Gardner et al., 2002; Schnable et al., 2009) where it was estimated TEs have

increased the maize genome two - to five - fold (Sanmiguel and Bennetzen, 1998). Despite a significant range in genome sizes, land plants displayed much lower overall variability in TE diversity as compared to animals. However, fungi and protists have the lowest average TE diversity and the smallest total genome sizes. (Elliott and Gregory, 2015; Thon et al., 2006). According to a recent study that compared the TE content and the genome size, no simple relationship was found between TE diversity and genome size. Differences in genome size are thought to arise primarily through accumulation of TEs, but beyond a certain point (~500 Mbp), TE diversity does not increase with genome size. Maximum TE diversity (39 superfamilies present) occurs in genomes around 500Mbp in size, for both Class I (retrotransposons) and Class II (DNA transposons) TEs (Elliott and Gregory, 2015) (figure 1.4). These content variations correspond, in part, to the disparate histories of TE invasion experienced by different plant lineages, in addition to how an organism copes with these invasions, which is greatly influenced by host biology (Barker et al., 2012).

An in-silico analysis revealed GC-rich class I TEs is the predominant class of TEs in animal, but the AT-rich class II TEs is prevalent in plants. The GC-rich class I TEs appears to be evolved within the animals. On contrary, the preserved in AT-rich in class II TEs is believed to be contributed in host defence systems (Huang et al., 2014).

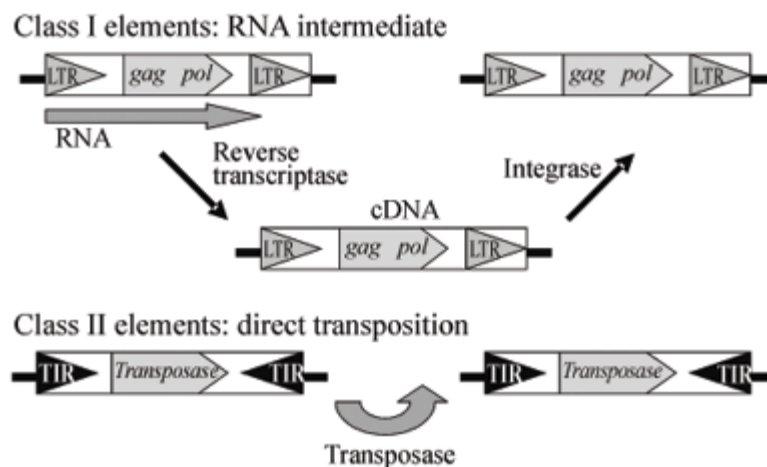


Figure 1.4. TE classification in class I and class according to the transposition mechanism: RNA or DNA intermediate (De Lima Favaro, 2005).

1.3.1 The class I RNA retrotransposon

All retroelements transpose through reverse-transcription of an RNA intermediate. Retrotransposons have two open reading frames (ORFs) in common with retroviruses: the group specific antigen (GAG) and the functional polyprotein (POL). GAG gene encodes structural proteins that form the virus-like particle (VLP), inside which reverse transcription takes place (Schmidt, 1999; Casacuberta and Santiago, 2003; Havecker et al., 2004; Irwin and Voytas, 2001). Pol is a polyprotein and is auto-processed by its aspartatic proteinase (AP) domain. It contains reverse transcriptase (RT) and RNase H, a bifunctional polypeptide carrying out reverse transcription and integrase (INT), which inserts the new LTR retrotransposon copy into the genome (Suoniemi et al., 1998). A retrotransposon's RNA template is first transcribed by the cellular encoded RNA polymerase II from the 5' LTR. The RNA is then translated to the proteins that form a virus-like particle (VLP) analogous to the retroviral virion core. VLPs encapsulate the RNA template, the reverse transcriptase responsible for producing the double-stranded DNA copy, and the integrase involved in the transfer of the linear DNA copy to the nucleus and its insertion into the genome.

According to Wicker's proposition, retrotransposons can be divided into four classes: long terminal repeat (LTR), DIRS, Penelope, long interspersed nuclear elements (LINEs) and short interspersed elements (SINEs).

LTR-retrotransposons are the major components of the plant genome and they are more prevalent than non-LTR. LTR-retrotransposons occupy mainly the constitutive heterochromatic regions, such as pericentromeric regions, knobs, and subtelomeres (Miller et al. 1998; Lippman et al. 2004; Kejnovsky et al. 2006). Despite they are present in all eukaryotic genomes, their recent activity seems higher in plant kingdom. Many plants LTR retrotransposons insertions have occurred within the past few million years. (Pereira, 2004). The characteristics of LTR retrotransposons make them a useful tool to analyze genomes. The LTRs from each element are identical at the time of insertion. After insertion, both LTRs accumulate mutations independently and by comparing the two LTRs of a given element, the insertion time can be estimated (Sanmiguel and Bennetzen, 1998).

In maize in particular, LTR constitute 60% of the genome, that would be 2-fold or more smaller without LTR retrotransposon amplifications over the last 2–3 million years (Sanmiguel and Bennetzen, 1998). Most LTR retrotransposons families exist in low copy numbers (Sanmiguel and Bennetzen, 1998).

LTR range from a few hundred base pairs to several kilo bases (5–7 kb long) and known LTRs start with nucleotides of 5'-TG-3' and end with 5'-CA-3'. Because the LTR retrotransposons

integrate into 4- to 6-bp staggered cut sites, they produce 4- to 6-bp target site duplication (TSD) upon integration.

According to GAG and POL position retrotransposon are divided in two superfamilies, Ty1-copia and Ty3-gypsy.

LTR-retrotransposons were classified as intact when they possessed two LTRs flanked by TSDs, a recognizable primer binding site, and a polypurine tract. Intact elements were additionally classified as autonomous if they contained intact Gag and Pol ORFs. Intact elements lacking complete Gag and Pol ORFs were classified as nonautonomous.

Some eukaryotic LTR retrotransposons do not encode the proteins necessary for transposition, they lack all coding capacity but have retained LTRs (Feschotte and Wessler, 2002). LTRs contain the promoter needed to produce a template RNA and the primer binding site and the polypurine tract needed to prime reverse transcription (Schulman, 2013; Havecker et al., 2004). For most non-autonomous retrotransposons, it is unclear which autonomous element is involved in mobilization. Large non autonomous elements like Dasheng have now been named 'large retrotransposon derivatives' (LARDS). The LARDS identified in barley and other members of the Triticeae have LTRs of 4.5 kb and an internal domain of 3.5 kb. The internal domain of the LARDS contains conserved non coding DNA that may provide important secondary structure to the mRNA. LARDS appear to be members of the gypsy class of LTR retrotransposons. Although apparently non autonomous, LARDS appear to be transcribed (Kalendar et al., 2004).

LTR retrotransposons commonly mutate to solo LTRs by unequal recombination, especially in regions where homologous recombination is a frequent process.(Ma and Bennetzen, 2006)

Another class of non-autonomous LTR retrotransposons has been identified in plants, called 'terminal-repeat retrotransposons in miniature' (TRIMs). TRIMs are short in size (mostly ≈ 350 bp), have terminal direct repeats (TDRs) of 100–250 bp (on average < 140 bp) and contain a primer binding site (PBS) and a polypurine tract (PPT) within the region between the repeats. TRIMs internal domain lack coding capacity and probably require the help of mobility-related proteins encoded by other retrotransposons. There are TRIMs in both monocotyledonous and dicotyledonous plants, but no autonomous partner has been found or proposed. TRIM elements seem to be involved actively in the restructuring of plant genomes, affecting the promoter, coding region and intron-exon structure of genes. In solanaceous species and maize, TRIM elements provided target sites for further retrotransposon insertions. In *Arabidopsis*, evidence is provided that the TRIM element also can be involved in the transduction of host genes (Witte et al., 2001).

Unlike LTR, non-LTR retrotransposons have no terminal repeats. Non-LTR retrotransposons are very variable in structure. Non-LTR were originally discovered in mammalian genomes (Schmidt, 1999), but non-LTR retrotransposons has been also isolated in plants (Schmidt, 1999; Noma et al., 1999; Wright et al., 1996).

Central to retrotransposon mobilization is reverse transcriptase (RT) activity, and thus all autonomous non-LTR retrotransposons contain an RT domain. The reverse transcriptase (RT) domain is the only common structure among all non-LTR retrotransposons. The 5' and 3' untranslated regions (UTRs) of non-LTR retrotransposons are quite variable.

LINEs, also designated L1 or LINE-like sequences, possess a poly(A) tail which defines the terminus of the element. LINEs are several kilobases long and contain two ORFs encoding a *gag* protein (ORF1), and endonuclease and reverse transcriptase domains (ORF2) together conferring the element's ability for autonomous retrotransposition. In many LINEs, both ORFs contain cystein-rich, zinc-finger-like regions which are considered as putative nucleic acid-binding domains. In general, sequence divergence and extreme heterogeneity is a typical feature of plant LINEs (Schmidt, 1999).

L1 retrotransposons comprises about 17% of the human genome. In general, L1 retrotransposons carry two ORFs: the protein encoded by ORF1 (ORF1p) usually contains an RNA recognition motif (RRM) while ORF2 encodes a polyprotein (ORF2p) that exhibits apurinic/apyrimidinic endonuclease (APE) and reverse transcriptase (RT) activities. In some plant L1 retrotransposons, an additional domain can also be found within ORF2p that is homologous to ribonuclease H (RNH). It has been speculated that retrotransposons may play a role in the horizontal transfer of RNH between plants, Archaea, and bacteria, as L1s carry an active Archaea-like ribonuclease H (RNH) domain. L1- encoded proteins are also thought to be responsible for the transposition of other repetitive elements and processed pseudogenes. Pseudogenes are sequences present in essentially all animal genomes that have many characteristics of genes, but are defective for production of protein. Processed pseudogenes generally lack introns, end in a 3' poly A, and are flanked by target site duplications. Copies of the Alu and SVA transposable elements and processed pseudogenes are also believed to have inserted into the genome by borrowing the endonuclease and reverse transcriptase proteins encoded by L1 (Szak et al., 2003; Kazazian, 2014).

A second type of non-LTR retrotransposons are SINEs. SINEs are a moderately to highly amplified sequence class of eukaryotes which have been most extensively studied in mammalian species. SINEs are up to several hundred base pairs in length and have a composite structure.

SINEs are terminated by a poly(A) tract, or A- or T-rich sequences. The 5' region of SINE is similar to tRNA and contains two sequences, called box A and box B, that serve as an internal promoter for the element transcription by RNA polymerase III. SINEs do not encode their own reverse transcriptase and are not autonomous. However, similar to LINEs, they move by retrotransposition and generate short target site duplications upon reintegration (reviewed in Schmidt, 1999).

The predominant SINEs in humans and other primates are known as Alu elements because they contain a site for the restriction enzyme AluI. They are made up of two 7SL RNA related sequences, the first of which contains a Pol III promoter, and a 3' poly(A) sequence. SVA elements form a further family of non-autonomous retroelements in humans and non-human primates present at a relatively low copy number of a few thousand per genome (Wang et al., 2005). MIR elements in mammals, have a 5' sequence derived from a tRNA gene and a 3' sequence similar to the 3' end of a LINE element (Finnegan, 2012).

Part of the success of retrotransposons is due to their replicative mode of transposition, where in principle, a small number of copies can produce hundreds or thousands of daughter copies during a single amplification event.

1.3.2 The class II DNA transposons

The class II elements group includes autonomous, non autonomous, MITEs, and other unclassified elements as *foldback* and *helitrons*. Most DNA transposons, and MITEs especially, are found at higher density in euchromatic regions where they often reside within or in close proximity to genes (Bureau and Wessler, 1992).

Autonomous class II TEs transpose through a DNA intermediate with the majority excising from the chromosome using the transposase enzyme and then integrating elsewhere in the genome by the action of this same transposase. Autonomous class II TE have fully intact copies that encode all of the element specific activities, such as transposase for cut and paste elements, replicase/helicase for Helitrons and GAG packaging proteins and reverse transcriptase for retroelements (Feschotte et al., 2002).

Wicker (2007) classified class II TEs in superfamilies as CACTA, Mutator, PIF/Harbinger, hAT, Tc1/mariner, Merlin, Transib, P, PiggyBac, and Crypton (Wicker et al., 2007). PIF/Harbinger, ISL2EU, and Spy were classified into the same superfamily that is designated as "PHIS". The PHIS transposon superfamily is high polymorphism in the target sequences, coding

capacity, and conserved motifs of transposase. Recently, three new types of PHIS transposons distinct from the previous PHIS transposons in TSDs, called *Pangu*, *NuwaI*, and *NuwaII*, have been found and a total of 380 families of PHIS superfamily were identified in 112 sequenced eukaryotic genomes (Han et al., 2015).

The maize element Activator (Ac), the *Drosophila melanogaster* element hobo, and the *A. majus* Tam3 elements form a superfamily of eukaryotic TEs referred to as the hAT (hobo-Ac-Tam3) superfamily. This family is widely distributed in all eukaryotic kingdoms. Members of the family are characterized by a 50 nucleotides conserved C-terminus domain, short TIRs and 8-bp host duplication upon insertion (Kempken and Windhofer, 2001). *hAT* transposable elements are ancient in their origin. They are widespread across the plant and animal kingdoms and are found in all eukaryotes except ciliates, diatoms, and the protozoan *Trichomonas*. They are the most abundant human superfamily of class II transposons found but represent only the 0.46% of the monocotyledon genomes (representing 8.2% of the total genomic DNA transposons) (Muehlbauer et al., 2006; Moreno-Vázquez et al., 2005; Holyoake and Kidwell, 2003).

1.3.3 The Miniature Inverted-repeat Transposable Elements (MITEs)

The most numerous class 2 elements in characterized plant genomes and in several animal species are miniature inverted-repeat transposable elements (MITEs).

The majority of reported MITEs are either *Stowaway* or *Tourist* elements that belong to the *Tc1/mariner* and *PIF/Harbinger* superfamilies, respectively.

MITEs are defined as small size elements, non-coding, carrying TIR and DR signals sequence, of potential to form a stable RNA secondary structure, and tendency to insert into A+T-rich regions. However, exceptions of these features have been reported.

MITEs are short, less than 600 pb. One of the shorter MITEs, *Nezha*, identified in cyanobacteria *Anabaena variabilis*, is 135 base pairs long (Zhou et al., 2008). MITEs are present in high copy numbers in many eukaryotic genomes. There is no discernible positive correlation between the percentage of TEs and MITEs. In maize, they contribute only for the 0.3% of the genome (Schnable et al., 2009). However, some MITEs families are present in moderate copy number as *Vege* in *D. willistoni* (Holyoake and Kidwell, 2003).

MITEs are mainly distributed on chromosome arms and are highly associated with plant genes (Kuang et al., 2009). Cases of MITE insertions in exon, intron, promoter and near the 5' or 3' ends of genes have been reported. In a few cases, they have been suggested to supply *cis*-acting domains involved in gene expression (Bureau et al., 1996). Studying the location of the matrix

attachment region (MARs) in rice and sorghum, brought to the discover that most of them co-localize with MITEs, suggesting that MITEs preferentially insert near MARs and/or that they can serve as MARs isolating their neighbouring genes (Tikhonov et al., 2000).

MITEs are characterized by terminal inverted repeats (TIRs) that can be 10–30 bp long. TIRs are almost perfectly reverse complementary to each other and they are highly conserved among multiple copies of the same MITE family. Thanks to the TIRs, MITEs usually have the potential to form a hairpin-like secondary structure. Typically the region between the TIRs is A+T rich, but not in all cases. The TIR signals may play an important role in the maintenance and proliferation of a MITE (Feschotte et al., 1870; Tu, 1997; Petersen and Seberg, 1999). A MITE insertion into the potato flavonoid 3'-5' hydroxylase gene first exon causes its gain of function and produce purple skin. The function of the gene was restored by transposition of the MITE after activation in protoplast culture (Kuang et al., 2009). The insertion of a MITE into ahFAD2A gene in two different insertion sites causes a high-oleate phenotype in two peanut mutants (Patel et al., 2004). MITEs show target site preference and TIRs are flanked by small direct repeats (target site duplication, TSD). Nezha MITE in cyanobacteria *Anabaena variabilis* generates a pair of 2-10 bp direct repeats signals when inserting into the target site. Together with Glider with 6–11-bp direct repeats in *Xenopus laevis*, Nezha generates the longest DR signals out of all the known MITEs.

Based on shared TIRs and TSD sequences, that could be TA or TAA respectively, MITEs are classified in two main subfamilies, Stowaway and Tourist but MITEs have also been reported from the hAT and MULE superfamilies (Kuang et al.) and other minor families that are typically taxa specific.

MITEs lack coding capacity and rely on DNA transposons that code for a transposase. Their TIR sequences sometimes resemble those of DNA transposons (Morgan 1995; Unsal and Morgan 1995; Yeadon and Catchside 1995). Through homology searches, some MITEs have been proposed to be truncated derivatives of autonomous larger DNA transposons. The only sequence shared between described MITEs and their related autonomous transposable elements is the TIRs; the core region of known MITEs has no similarity to known TEs (Feschotte et al., 2002). Feschotte proposed a model in which MITEs are seen as non-autonomous elements that originated from autonomous DNA TE in two steps process: first, production of various internally deleted non autonomous derivatives after DNA transposition, and second, amplification of the derivatives copy numbers (Feschotte et al., 1870, 2002). According to this theory, Stowaway and Tourist families probably arose from the activity of related, but distinct, mariner-like and PIF-like autonomous elements, respectively (Feschotte and Wessler, 2002; Zhang et al., 2001; Grzebelus

et al., 2007; Momose et al., 2010). However, the origins of many are unknown as the vast majority of characterized MITEs are not deletion-derivatives of existing autonomous TE and borrow the transposase of distantly related elements by cross mobilization.

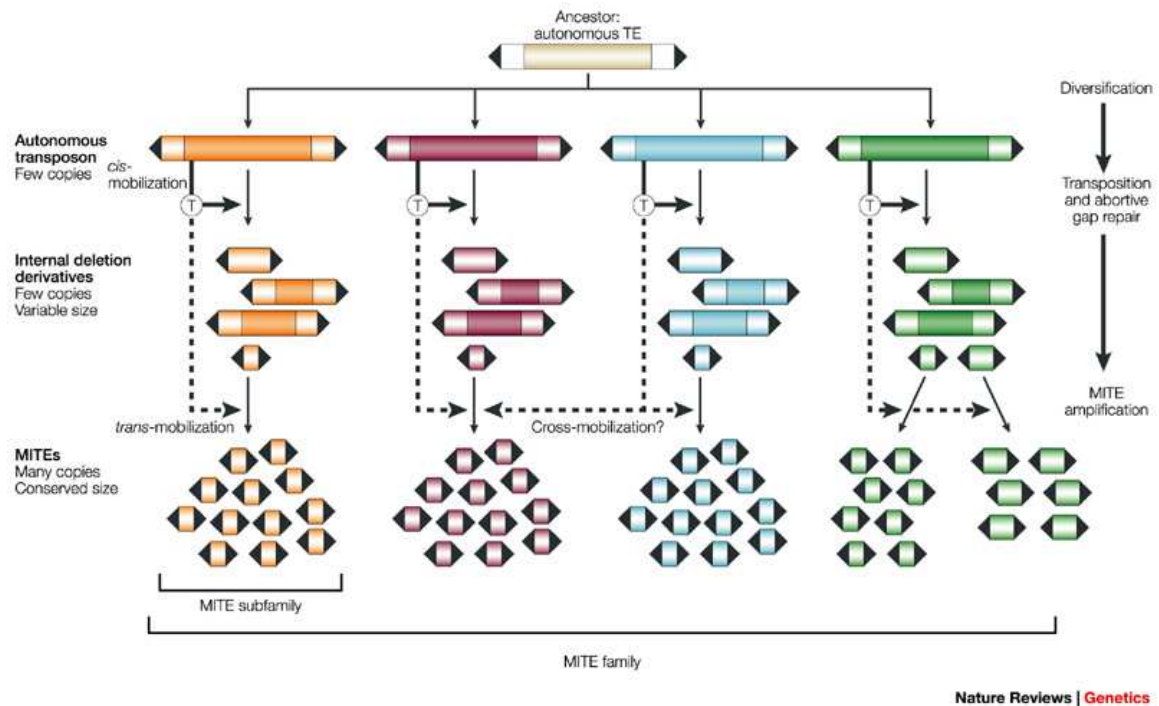


Figure 1.5. Hypothesis of origin of MITEs families from a common autonomous TE ancestor, through accumulation of internal deletions (Feschotte, 2002)

After the publication of draft sequences for the two subspecies of *Oryza sativa*, japonica (cv. Nipponbare) and indica (cv. 93-11) the first active DNA transposons from rice and the first active miniature inverted-repeat transposable element mPING from any organism were identified. Searching for repeat families with the structural features of MITEs and with very low intrafamily sequence divergence brought to the identification of the MITE mPing. The 430 bp length, the TSDs (the trinucleotide TAA or TTA) and TIRs of mPing indicated that it is a Tourist-like MITE. mPING is the first identified mobile MITE: its movement was activated during long-term cell culture (Jiang et al., 2003) and by anther culture (Kikuchi et al., 2003). When mPing was inserted into the gene for rice ubiquitin-related modifier-1 (Rurm1), its excision resulted in reversion of the mutation. Ping transposon was identified using mPing as query in rice genomic Nipponbare. Ping is 5,341 bp and shares 253 bp and 177 bp, respectively, of its terminal sequences with mPing, suggesting that mPing arose very recently from Ping by internal deletion and it is an autonomous element responsible for its mobilization. Further BLAST searches using Ping as the

query led to the identification of Pong (5.166 bp), with identical 15-bp TIRs and similar subterminal regions to those of mPing and Ping. At least five copies of Pong were found in the cultivar Nipponbare while three were found in the cultivar 93-11 (Jiang et al., 2003; Yang et al., 2007). The Mariner-like autonomous element Osmar that shares TIRs and TDS with rice Stowaway MITEs, was identified as the Stowaway MITEs transposition catalyst (Yang et al., 2009).

Helitrons are another category of class II DNA TE. They are presumed to transpose as a rolling circle replicon, similar to some known prokaryotic rolling circle transposons. Helitrons were discovered by computational analysis of genomic sequences from Arabidopsis, rice, and *Caenorhabditis elegans*. They constitute over 2% of the maize genome. Helitron-like transposons have conservative 5'-TC and CTRR-3' termini and do not have terminal inverted repeats. They contain 16- to 20-bp hairpins separated by 10–12 nucleotides from the 3'-end and transpose precisely between the 5'-A and T-3', with no modifications of the AT target sites (Kapitonov and Jurka, 2001).

TRIM elements are similar to SINEs and MITEs in their short size as they typically possess short overall length which consists of two 100 to 250 bp terminal direct repeats (TDRs) or LTRs and an internal domain of 100 to 300 bp. It has been reported that TRIMs also seem to be involved actively in altering gene structure, regulating gene expressing, reshaping genomes, and mediating horizontal transfer of DNA (Witte et al., 2001; Yang et al., 2007).

1.3.4 Transposon activity

Both class 1 and class 2 TEs can be either autonomous or non-autonomous. Autonomous TEs can move on their own, while non-autonomous elements require the presence of other TEs in order to move. This is because non-autonomous elements lack the gene for the transposase or reverse transcriptase that is needed for their transposition, so they must "borrow" these proteins from another element in order to move (Huang et al., 2012; Jiang et al., 2003). Non-autonomous elements can arise from premature stop codons, frame shifts or partial deletions of the coding sequence (CDS).

In general, transposon activity can be detected in two ways. First, identifying the novo insertions in offspring but not present in parents. Second, identifying polymorphic insertions between two individuals (transposon insertion polymorphisms (TIPs)) presumed to reflect insertions occurring after divergence from a common ancestor. The presence of polymorphic insertions between closely related species or individuals suggests that the element has been recently active and is

most likely currently active. In order to estimate the transposition frequency, the number of polymorphic elements in combination with the time from the common ancestor can be used. (Lisch, 2013; Huang et al., 2012). Transposition assays using cell lines are another method for proving and quantifying current retrotransposon activity. They use a reporter cassette added to a recombinant transposable element construct; this cassette is in antisense orientation with respect to the transposon and is interrupted by a sense-oriented intron. The intron is spliced out of the transposon transcript, and the presence of daughter integrants is detected by expression of the now uninterrupted reporter from genomic DNA (Huang et al., 2012).

Insertion of TEs usually originates a target site duplication (TSD) at the insertion site and occurs in both classes of TEs. TE insertion causes a double strand breakage at the insertion site caused by the transposase. Upon TE insertion, the complementary sequence is completed and thereby duplicated. This creates a copy of the target site on both sides of the element. The size of the TSD can range from 2 bps up to 16 or more bp. TE superfamilies are characterized by similarity in the TSD. For example, Mariner elements TSD is the dinucleotide TA while the TSD for Mutator elements is between 9–12 bp long and starts with GC (reviewed by Wicker et al. 2007).

Some exception have been found: TEs of the order DIR (Class I), Crypton and Helitron (both Class II) do not originate TSD after insertion. Moreover, recently, a new group of evolutionarily related DNA transposons, called *Spy*, have been reported in 21 invertebrate species. These include TIRs and DDE motif containing transposase but surprisingly do not create TSDs upon insertion. *Spy* transposons appear to transpose precisely between 5'-AAA and TTT-3' host nucleotides, without duplication or modification of the AAATTT target sites (Han et al., 2014).

The chromosomal distribution of TEs is often governed by the status of chromatin compaction and rates of recombination of particular genomic regions. In general, regions with suppressed or no recombination tend to accumulate repetitive DNA sequences. Most cereal LTR retrotransposon copies are inserted into intergenic islands (Sanmiguel and Bennetzen, 1998) and maize knob DNA is characterized by high density of retrotransposons (Ananiev et al., 1998). Yeast retroelements (Tys) are preferentially distributed into "silent" chromosomal regions (Boeke and Devine, 1998). A *Chlorella* LINE family is inserted in telomeric regions (Higashiyama et al., 1997). The *Drosophila* telomere is composed of one or more LINE (long interspersed DNA element)-like retrotransposable elements. In contrast, the small, non-autonomous Miniature Inverted Repeat Transposable Element (MITE) transposons prefer to insert into genes and gene-rich regions (Bureau and Wessler, 1994).

Chapter II

Morphological characterization of the *br2:NC238* line

1. Introduction

Maize (*Zea mays* L. spp. mays) is one of the world's most important grain crops, together with rice (*Oryza sativa*), wheat (*Triticum spp.*) and sorghum (*Sorghum bicolor*). Starting from the Green Revolution era, cereals have been bred for dwarf or semi-dwarf phenotype for many advantages. Plant stems act as sinks for assimilates and nutrients and may serve as reserves for grain filling. Stem growth and extension may compete with that of leaves, but their growth and extension determine, to a large extent, the ability of plants to compete for light, as well as the relationships between vegetative and reproductive growth. Stem dimensions are also closely related to resistance to lodging, which can be an important factor in determining yield.

Thus, manipulating plant height, through selection or the use of growth regulators, is of economic importance.

Many maize dwarf mutants have been isolated. The *brachytic* mutants (*br*) are characterized by the shortening of specific internodes. An instance, *br5* has short internodes just below the uppermost internode and normal internode length in the rest of the stem. In *br2*, the shortening of the stem length regards only the internodes at the base of the stem (figure 2.1).

Allelic tests performed crossing NC238 inbred line with *brachytic* mutants indicated NC238 line is a *br2* mutant (Johal, unpublished). *br2/pgp1/abcb1* encodes for an auxin transporter gene of the multidrug resistance/p-glycoproteins (MDRs/PGPs) subfamily B (Multani et al., 2003). It has been reported *br2* mutants are characterized by short stature due to shortening of the lower internodes (Multani et al., 2003; Pilu et al., 2007). Moreover, alteration in stem vasculature was eventually observed (Multani et al., 2003). Alteration in length and width of leaf epidermal cells were reported (Pilu et al., 2007). Moreover, leaves appeared to be more erectile in the *br2* mutant (Pilu et al., 2007). Literature lacks a characterization of the root system.

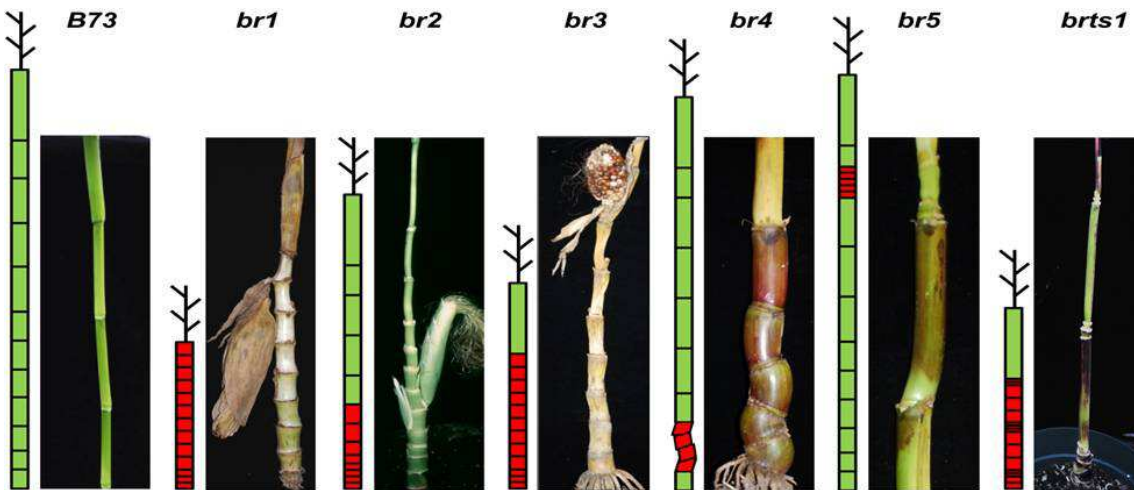


Figure 2.1. Comparison between the different brachytic lines stem structure. brachytic 2 mutant are characterized by the shortening of the lower internodes (Johal, unpublished)

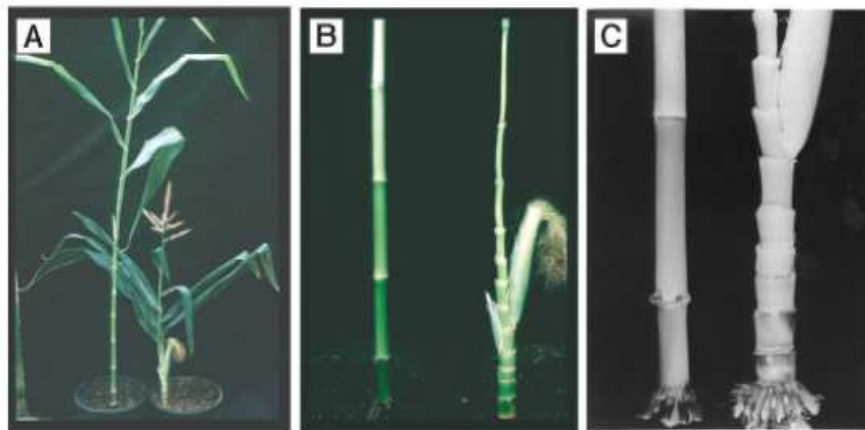


Figure 2.2. Wild type (left) and brachytic 2 (right) lines before (A) and after leaves removal (B, C) (Multani, 2003)

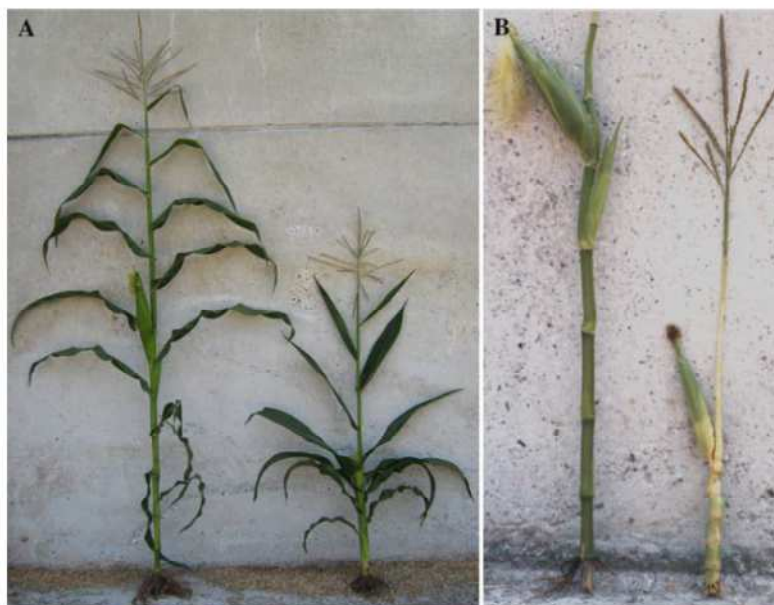


Figure 2.3. Wild type (left) and brachytic 2 (right) lines before (A) and after leaves removal (B) Pilu (2007)

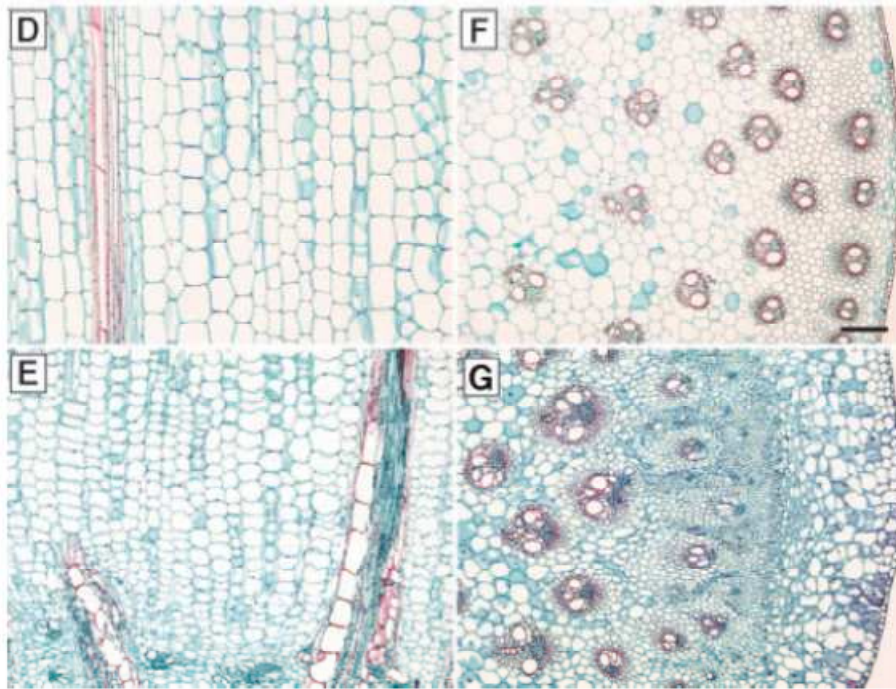


Figure 2.4. Alteration in the *br2* vasculature: *br2* stem is characterized by smaller cells (E) and 10 cell layers below the epidermis more than the revertant line (D, F) Adapted from Multani (2003).

A spontaneous tall plant was isolated in a NC238 population field, indicating the mutation was due to a transposable element in *abcb1* gene (Johal, unpublished). This tall revertant line was used as reference line.

Morphological traits measurements were performed at seedling stage, focusing on the root system. In fact, auxin plays important roles in root development and gravitropic response (Bhalerao et al., 2002; Müller et al., 1998; Peer et al., 2011). The root trait measurements of *br2:NC238* and the revertant lines were performed at optimal growth conditions using an aeroponic growth chamber. Moreover, the response of the two lines after treatments with auxin analog and auxin transport and action inhibitor were tested.

The developmental stage when the *br2* phenotype arise was identify.

Morphological trait measurements of plants at adult stage were performed in order to verify possible alterations in other plant traits in addition to the shortening of the internodes.

2.2. Materials and methods

Plant material and growth conditions

The present study uses the following maize lines provided by Prof. Johal (Purdue University): the NC238 inbred line and a revertant NC238 line isolated in a NC238 field at Purdue University, the Maize Genetics Cooperation Stock center and propagated by prof. Varotto's lab group.

For root traits measurements at seedling stage, an aeroponic growth system was set up at the greenhouse at the Botany and Plant Pathology Department at Purdue University. The system consisted of 24 tanks with 8 seedlings placed on the tank cover. From the bottom of the tank a nutrition medium (Hoagland Solution) was automatically sprayed toward the roots for 3 seconds every 10 minutes. Seeds were pre-germinated in paper rolls before transferring the seedlings in the growth chambers. Seedling were grown for one week in the system.

For histological observation and auxin immunolocalization analyses, plants were grown in pots (1:2 sand and general soil) in the University of Padua greenhouse until 7-leaf-old stage.

For morphological trait measurement of NC238 line, plants were growth at the "L. Toniolo" experimental farm of the University of Padova in Legnaro (PD) during Summer 2015.

Tests with auxin analogs and inhibitors

Seeds were germinated in wet paper rolls. The day the primary roots were 2-5cm long, seedlings were transferred to paper roll embedded with solutions containing auxin analog or auxin action/transport inhibitors. 1-naphthaleneacetic acid (NAA, Sigma Aldrich) was used as auxin analog, p-chlorophenoxyisobutyric acid (PCIB, Sigma Aldrich) as auxin action inhibitor, 1-N-naphthylphthalamic acid (NPA, Sigma Aldrich) and (2-[4-(diethylamino)-2-hydroxybenzoyl] benzoic acid (BUM, Sigma Aldrich) as auxin transport inhibitors. Treatments lasted one week. Pictures of roots were taken daily with digital camera (Olympus). Picture measurements were elaborated using ImageJ® open source software. Doses are listed in the following table.

Compound	NAA	NPA	PCIB	BUM
Concentrations	10 μ M	0.5 μ M, 50 μ M, 100 μ M	10 μ M, 50 μ M, 100 μ M	0.5 μ M, 10 μ M

Table 2.1. Compound and concentrations used in the auxin analog and auxin inhibitors treatments.

Statistical analyses

Statistical analyses were performed using R® open source software. Data distribution was tested with the function `shapiro.test`, variances of two samples were tested using `var.test` function. The Student test (`t.test`) was used as parametric test, while Wilcoxon test (`wilcox.test`) was used as non-parametric test. Null hypothesis referred to lack of difference, $p\text{-value} > 0.05$ suggested data were likely with a true null, $p\text{-value} < 0.05$ suggested to reject the null hypothesis.

Analyses of the root system of field growth plants

Plants were grown at the University of Padova farm in Legnaro (PD) during plant season 2015. Soil coring 100x7cm size was made at the base of the plant stem at flowering stage (figure 2.7, A, B). 6 plants per line were analyzed. Soil core was cut into 10cm long cylinders, corresponding to the soil horizons. Roots were separated from soil particle by centrifugation: soil cylinder was put into tanks filled with continuous flowing tap water, centrifugation force allowed roots to float and fall through the hole in the middle of the tank onto filters above the tank (figure 2.7, D). Washed roots were then cleaned (figure 2.7 E) and stored in ethanol 15% at 4°C until data analyses. Roots were scanned (EPSON Expression 11000XL PRO) and scans analyzed with Zeiss® software (figure 2.8). Objects with < 20 pixel length and < 30 perimeter/area rate were excluded from the analyses. Root surface and length have been expressed as the projected area and projected length of the root during the scanning. Data from the analyses were used to calculate root traits: the root diameters, the RLD (Root Length Density) expressed as projected length of the root per volume of soil, the RSD (Root Surface Density) expressed as the projected area of the root per volume of soil, and the RAI (Root Area Index) expressed as the root area within the soil horizon surface.

Analyses of the morphological traits of field growth plants

br2:NC238 and revertant plants were grown at the University of Padova farm in Legnaro (PD) during plant season 2015. Before analyses, plants were checked by genotyping with primers 4BS (table 3.1). At anthesis, plant stature measurement - from the base of the stem to the uppermost stem node - was recorded. After cutting the plant at the base of the stem, leaves were removed from the stem (figure 2.6). The following traits were measured: length of internodes, diameter of nodes, number of tassel branches, number of ears, length of tassel and length of the uppermost ear, position of the node where the ear was inserted. Two replicates (in two fields) during Summer 2015 were performed. 25 plants per line/per replica were measured.

IAA-immunolocalization and histological observations

Tissues from 7-leaf-old *br2:NC238* and revertant plant were collected, prefixed 1 hour at 4°C in 3% EDAC (N-Ethyl-N'-(3- dimethylaminopropyl) carbodiimide hydrochloride, Sigma Aldrich) in 1x PBS (137mM NaCl, 2.7mM KCl, 10mM Na₂HPO₄, 2mM KHPO₄, pH 7.4), and postfixed in 4% paraformaldehyde (Sigma Aldrich) in 1x PBS. Tissues were dehydrated at 4°C at ascending ethanol in 1x PBS series. Tissues were then transferred into glass tubes and 4 room temperature xylene washes 60' long were performed: ethanol:xylene 3:1, ethanol:xylene 1:1, ethanol:xylene 1:3, xylene 100%. Tissues were incubated overnight at room temperature with 1/4 volume of Paraplast chips (Sigma Aldrich) per tube. The following day, every 3 hours, 1/4 tube volume of Paraplast chips were added and the same volume of solution was discarded while increasing temperature from 37 to 47°C by the end of the day. The second day 1/4 tube volume of fresh melted Paraplast was added and same volume of solution discarded while increasing temperature from 47 to 57°C by the end of the day. Tissues were then transferred into Petri dishes containing melted Paraplast and every three hours, for two days, 1/4 tube volume of fresh melted Paraplast was added and same volume of solution discarded. The following day the dishes were moved at room temperature. Sectioning of the embedded tissues were performed with a Leica RM2135 microtome in 8-10µm slices. Slices were arranged on pre-warmed Polysine® slides (Menzel-Gläser) with a few drops of distilled water. Slides were de-waxed by two washes at room temperature in xylene 100%, and rehydrated through room temperature ethanol series at: 2x 20' in 100% ethanol, 20' in 90% ethanol in 1x PBS, 20' in 50% ethanol in 1x PBS, 2x 5' in 1x PBS.

- For auxin immunolocalization, slides were then covered with 400µL of blocking solution (0.1% Tween 20, 1.5% glycine, 5% Bovine Serum Albumin (BSA), in 1x PBS, pH 7) for 1 hour. Slides were washed 5' with Regular Rinse Solution (0.88 NaCl, 0.1% Tween 20, 0.8% BSA, in PBS) and 5' 0.8% BSA in 1x PBS. Slides were then incubated with a mouse monoclonal anti-IAA primary antibody (Biofords-Agdia, France - PMD09346/0096) used at a concentration of 0.05 mg mL⁻¹, for 5 hours, in humid chambers for slides at room temperature. Slides were washed 2x 10' in High Salt Rinse solution (2.9% NaCl, 0.1% Tween 20, 0.1% BSA in 1x PBS) and again 10' in Regular Rinse Solution. Slides were incubated overnight at 4°C in 0.8% BSA in 1x PBS. The following day slides were incubated 3 hours in humid chambers with 100µl/ slide of the secondary antibody: a donkey anti-mouse alkaline phosphatase conjugated secondary antibody (IgG-AP-SC2097 (Santa Cruz Biotechnology) used at a 1:250 dilution.

Slides were washed 2x 15' in Regular Rinse Solution, 15' in H₂O, and 5' in *in-situ* buffer (1M Tris pH 9.5, 5M NaCl, 1M MgCl₂, in H₂O) before signal detection. Coloring reaction was made 15-20' in *in-situ* buffer containing 2µl/ml of NBT (Nitro blue tetrazolium chloride in 70% formamide, stock 75mg/ml) and 1.5µl/ml of BCIP (5-Bromo-4-Chloro-3-indolyl-phosphate, 4-toluidine salt, stock 50mg/ml). Reaction was stopped in H₂O. Slides were mounted applying two drops of DPX (Distyrene-Plasticizer-Xylene, Fluka Biochemika) mounting medium and placing the coverslips.

- For histological observations, slides were stained 5' in 0.01% Calcofluor (Fluorescent Brightener - SIGMA) in tap water and mounted with DPX and coverslips.

Microscopy observations

Histological analysis and anti-IAA immunolocalization images were observed and taken with a Leica DM4000B Digital microscope, equipped with a Leica DC300F Camera and Leica Image Manager 50 software (Leica Microsystems - England).

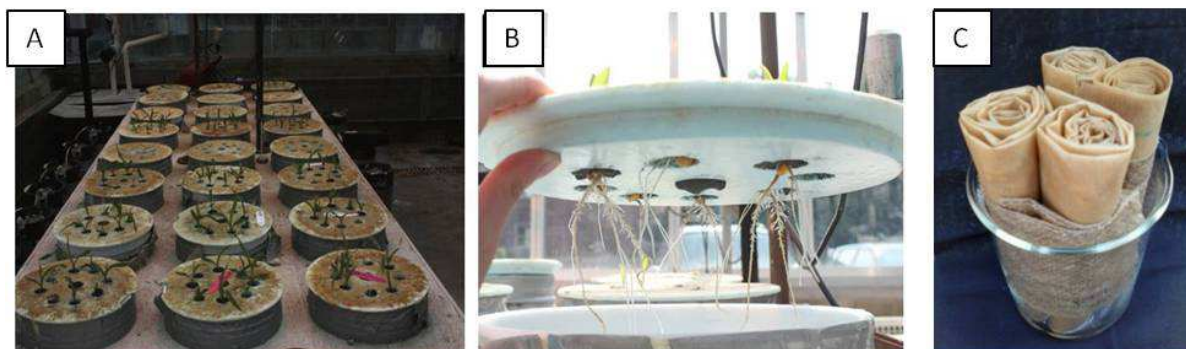


Figure 2.5. The aeroponic growth system. A) seedling growth in the chambers; B) particular of the seedling roots located on the cover of the chamber; C) paper rolls for seeds germination.

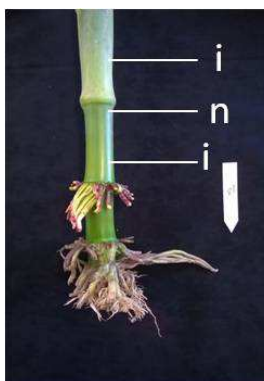


Figure 2.6. Adult plant stem structure after leaves removal: node (n) and internodes (i) are indicated.



Figure 2.7. Study of the root system of field grown plants at adult stage. After soil coring (A, B), soil core was cut in 10cm long small soil cylinders (C). Roots were separated from soil particle by centrifugation: soil cylinder was put into tanks filled with continuous flowing tap water, centrifugation force allowed roots to float and fall through the hole in the middle of the tank onto filters above the tank (D). Washed roots were handmade pincer cleaned from small retained soil particles (E), and stored in ethanol 15% solution at 4°C until scanning.

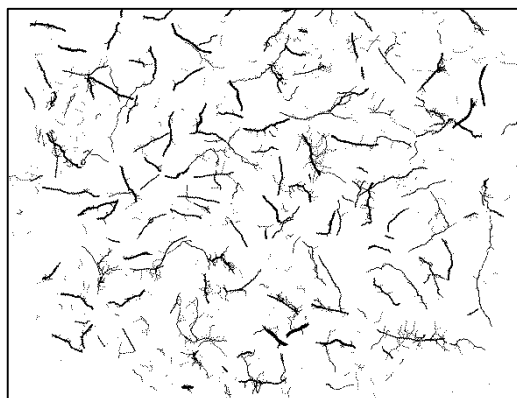


Figure 2.8. Example of the file from scanning of the roots from soil coring. Scans were analyzed with Zeiss® software. Objects with <20 pixel length and <30 perimeter/area rate were consider to be retained soil particles and indeed were excluded from the analyses. The software was used to calculate the total roots length, diameter, RLD, RSD, and RAI.

2.3 Results

2.3.1 The *br: NC238* root system at seedling stage

Previous works of characterization of *br2* mutants described the stem traits (Multani et al., 2003; Pilu et al., 2007; Cassani et al., 2010; Knöller et al., 2010) but lacked a detailed characterization of the root system. Auxin plays a major role in root development (Rahman et al., 2007; Swarup et al., 2008; Rahman et al., 2010; Kitomi et al., 2012). Thus, a detailed study of *br2:NC238* root system was performed on the roots of seedlings and adult field grown-plants.

At seedling stage, maize is characterized by the seminal root system composed of the primary root, the seminal and the lateral roots and the root hairs (Hochholdinger and Tuberosa, 2009). Using the aeroponic growth system at Purdue University campus, maize seedlings were grown for one week before taking pictures and measuring root traits. At this stage plants are not distinguishable (figure 2.9). Primary root length, number of seminal roots and length of seminal roots in respect of the primary root length are listed in table 2.1. The measurements showed no difference between *br2:NC238* and the revertant NC238 plants roots for the measured traits.

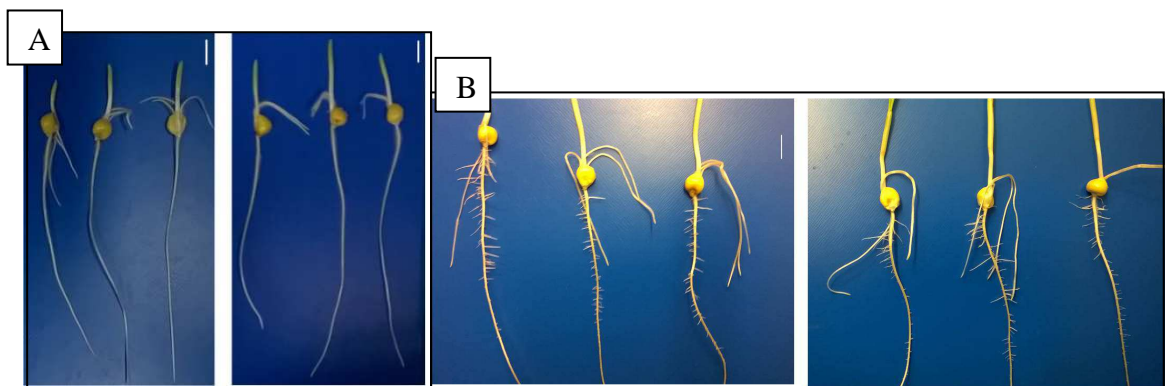


Figure 2.9. At seedling stage, the two lines are indistinguishable. A) 3-days-old paper roll-grown seedlings of revertant plant (left) and *br2:NC238* (right); B) One-week-old paper roll-grown seedlings of revertant plant (left) and *br2:NC238* (right).

Trait	<i>br2:NC238</i>	revertant NC238
primary root length (cm)	12,68±3,32 a	13,52±4,52 a
seminal roots number	2,33±0,97 a	2,53±0,74 a
seminal roots length/primary root length (%)	51,18±26,30 a	54,01±20,81 a

Table 2.2. Root traits measurements: at seedling stage, no differences were observed between the *br2:NC238* and the revertant NC238 lines (same letter indicates similarity of the groups, statistical tests p-value>0.05) at least 14 plants per line/per replica have been measured, three replicated have been measured, table refers to one of the tree replicates.

The gravitropic response of *br2:NC238* and revertant line primary root was also investigated. Pictures were taken before and after 4 hours of 90° rotation. No alteration in the gravity vector direction root growth was observed for both the lines (figure 2.10).



Figure 2.10. *br2:NC238* (up) and the revertant line (bottom) seedlings after 90° rotation. No differences were observed in the gravitropic response of *br2:NC238*.

Alteration in the expression levels of *PIN* mRNAs was already observed in *br2* mutant roots (Forestan et al., 2012). Moreover, it was previously demonstrated that IAA treatment alters auxin transporter expression, increasing many *PIN* encoding genes expression levels in maize shoot while reducing the expression of other *PINs*, *LAXex* and *ABCBs* (Yue et al., 2015). Thus, the expression of auxin transporter encoding genes in the root tip were verified before and after the seedling rotation. Four genes were selected. Forestan (2012) reported *PIN2* was strongly

expressed in the root apex, PIN1a and PIN9 were expressed in root apex and root elongation zone, while PIN8 expression was not detected in roots (Forestan et al., 2012). Results indicated similar transcript expression profiles in the two lines.

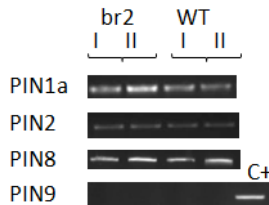


Figure 2.11. Expression profile of PINs in *br2:NC238* (*br2*) and the revertant tall (WT) NC238 root apex before (I) and after (II) rotation.

To examine if alteration in auxin accumulation induces different effects in *br2:NC238* roots compared to the NC238 revertant line, paper rolls grown seedlings were treated with auxin analog (NAA) and auxin transport or action inhibitors (NPA, PCIB, BUM). Treatments induced the same response in the two lines. NAA (10uM) reduced the primary root growth and increases the number of root hair in both the lines. Moreover, it caused defect in the gravitropic response of the primary root (figure 2.12). NPA 0.5 μ M induced slightly agravitropic growth of both the primary and the seminal roots. Higher doses of NPA treatments (>50 μ M) reduced the primary root growth and caused severe gravitropic defect in seminal roots (figure 2.13). PCIB treatments at concentrations from 10 μ M up to 100 μ M did not induce any visible effect on the two lines. BUM - an ABCBs inhibitor - has lethal effect at the low concentration of 0.5 μ M.



Figure 2.12. NAA (10 μ M) effects on revertant (left) and *br2:NC238* (right) seedling. Long and thick root hair and short primary root was visible in the two lines.



Figure 2.13. NPA (50 μ M) effects on revertant NC238 (left) and *br2:NC238* (right) seedlings. Severe gravitropic defects of the seminal roots are visible in the two lines.

2.3.2 The *br2:NC238* root system at flowering stage

Our results showed no alteration in *br2:NC238* plant root system at seedling stage. However, auxin plays important roles in root development (McSteen, 2010; Swarup et al., 2008; Hochholdinger et al., 2000; Müller et al., 1998). Thus, in order to assess any alterations in root traits - in a later stage of the plant development - a depth study of the root system was performed on adult plants at anthesis stage. Soil coring was made at the base of the stem, 10 cm depth soil horizons were separated and roots were isolated and scanned (figure 2.7 and figure 2.8). Scans were elaborated to obtain root length and root surface at each soil horizon as well as the average root diameter, the Root Length Density (RLD), the Root Surface Density (RSD) and the Root Area Index (RAI).

Analyses of the average RLD at each soil horizon indicated high difference in RLD along the first soil horizons for both the lines.

RLD in the first horizon was 9.21 ± 4.01 in *br2:NC238* line and 12.26 ± 3.97 in the revertant line. RLDs decreased to 3.47 ± 0.5 and 4.08 ± 1.86 in the second horizon, to 2.15 ± 1.07 and 1.86 ± 0.78 in the third one, and to 1.54 ± 0.78 and 1.37 ± 0.71 for *br2:NC238* line and revertant line respectively. Then, RLD was lower than $1 \text{ cm}^2/\text{cm}^3$ for all the rest of the horizons (2.14). On average, the *br2:NC238* plant RLD was $1.88 \pm 0.38 \text{ cm}^2/\text{cm}^3$, while the revertant plant RLD was $2.34 \pm 0.54 \text{ cm}^2/\text{cm}^3$. On average, the *br2:NC238* plant RLD was 20% lower than the revertant plant one (figure 2.15). Statistical analyses in order to test whether there was a difference between population means were performed. Data was not normally distributed (Shapiro-Wilk test, $p\text{-value} < 0.05$) and thus a non parametric test was applied (Wilcoxon test). Results indicated that

RLD values of br2:NC238 and the revertant lines were not statistically significantly different, for each soil horizon measurements (p-value>0.05).

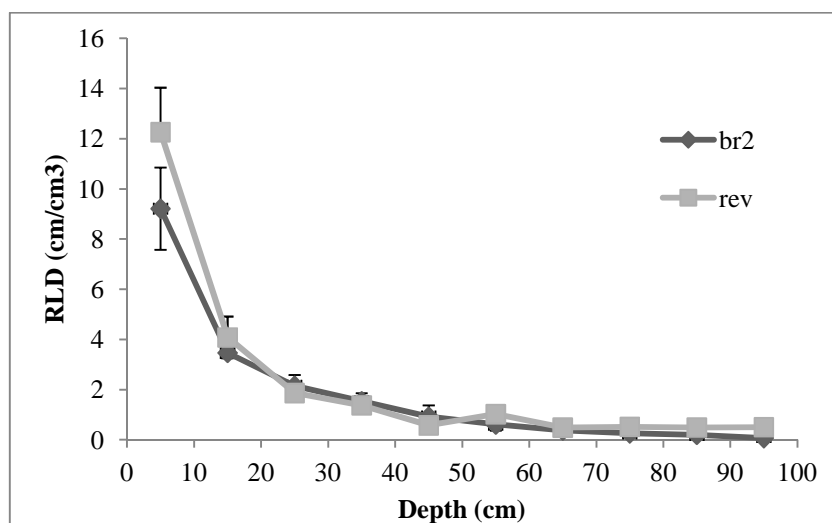


Figure 2.14. RLD profile of the *br2:NC238* (br2 in the graph) and the revertant line (rev) in the ten horizons. For both the lines, RLD profile was visible higher in the first horizons (ground to 40cm depth) and then it formed a plateau.

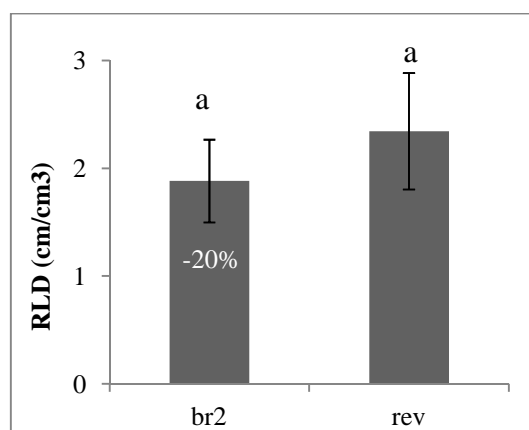


Figure 2.15. Total average RLD from the ten horizons of the *br2:NC238* (br2) and the revertant line (rev). Same letters refers to similarity of data, p-value 0.05).

The root diameter was also calculated. Root diameter is an important root trait: thinner roots contribute to higher surface area values and form the exchange site between plant and soil for water and nutrient absorption. Measurements indicated a general decreased in root diameter from the first to the deepest horizon for both lines (figure 2.16). However, the average root diameter profiles were similar in the two lines, as the statistical analyses confirmed (Wilcoxon test, p-valued >0.05 at each horizon).

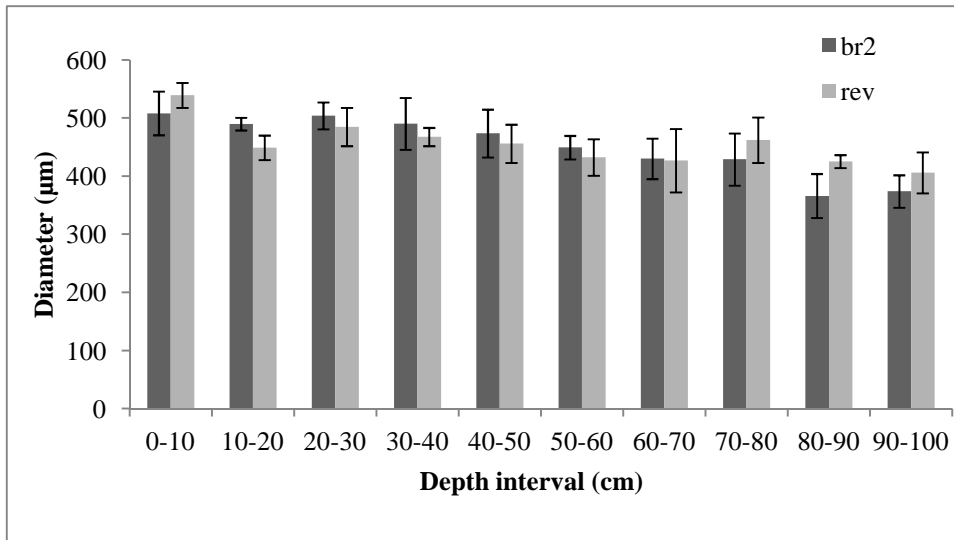


Figure 2.16. The profile of the root diameters at each horizon in *br2:NC238* (br2 in the graph) and the revertant line (rev) the two lines. Roots were thinner in the deeper horizons. Bars represent standard errors.

The RSD (Root Surface Density) represents the projected area of the root per volume of soil. The average RSD of *br2:NC238* was lower than that of the revertant line. As for RLD, for both the lines, RSD profile was visible higher in the first horizons (ground to 40cm depth) and then it reached a plateau (figure 2.17). Average RSD was 0.09 cm²/cm³ for the *br2:NC238* and 0.12 cm²/cm³ for the revertant line. Statistical analyses to test differences between population means (Wilcoxon test) indicated there was no statistically significant difference between *br2:NC238* and the revertant line RSD at each horizon (p-values >0.05).

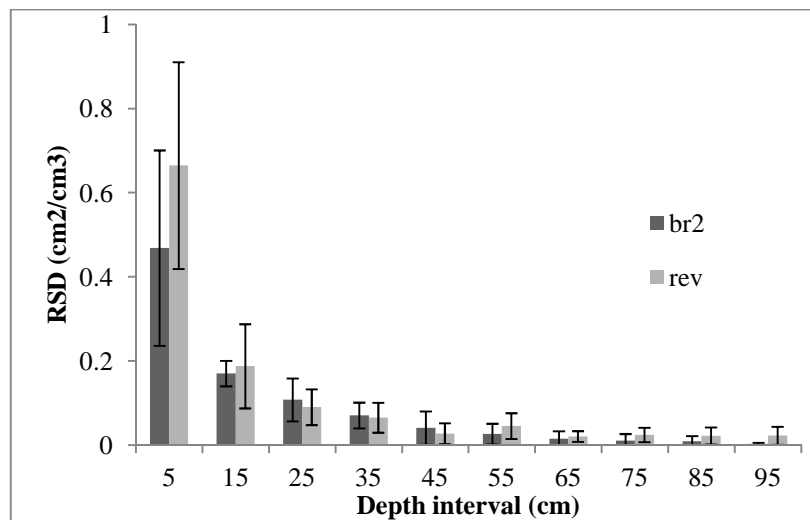


Figure 2.17. RSD profile of the *br2:NC238* (br2 in the graph) and the revertant line (rev) along the ten horizons. RSD profiles were similar to those of the RLD, decreasing in the first 40cm and then forming a plateau. Bars represent standard deviation.

The RAI (Root Area Index) represents the relative root surface. RAI is a measure of rooting density in a soil. Local soil and climate strong influence this plant parameter (Bischetti, 2005). Average RAI of *br2:NC238* was lower than that of the revertant line at each horizon. In deepest horizons, average RAI of *br2:NC238* were similar while the average RAI of the revertant plant slightly increased up to 100cm depth (figure 2.18). The average RAI of the two lines did not statistically differ as indicated by the statistical analyses to test differences between population means (Wilcoxon test, $p\text{-value} > 0.05$ for each horizon).

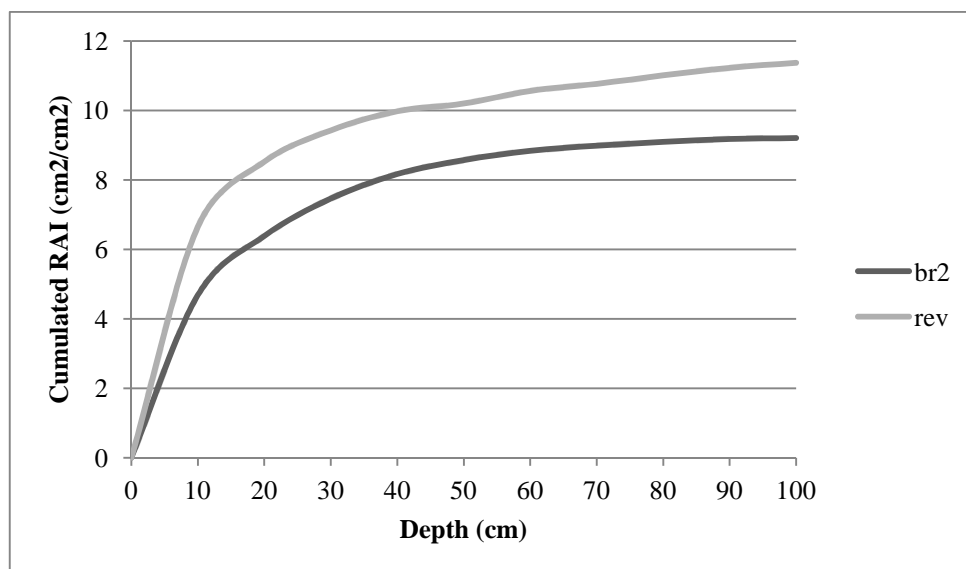


Figure 2.18. The average RAI of *br2:NC238* (br2 in the graph) and the revertant line (rev) along ten soil horizons.

In conclusion, root system analyses indicated both the *br2:NC238* and the revertant line root systems are mainly distributed in the first 40cm of soil depth and roots were thinner in the deeper horizons. The plant total length, RLD and RAD were not statistically different than those of the revertant plant.

Altogether these data indicate that there are not important differences in the root system of *br2:NC238* and revertant line.

2.3.3 The stem of *br2:NC238* at flowering stage

Literature lacks a description of the short NC238 inbred line. Allelic tests at Purdue University indicated NC238 is a *br2* mutant allele. *br2* gene encodes a auxin carrier protein. In 2003, phenotypic analyses on *br2* plant obtained with Mu-transposon tagging were performed (Multani et al., 2003). In 2007, a novel *br2* allele was isolated in a B73 wild type population (Pilu et al., 2007). These *br2* mutant lines are characterized by short stature due to the shortening of the internodes. Moreover, alterations in vascular bundle structure were observed (Multani et al., 2003). Alterations in the leaf epidermal size and leaf angle were also reported (Pilu et al., 2007).

The root system analyses performed in the present theses indicated root systems of *br2:NC238* and the revertant line at seedling stage were indistinguishable. Also at adult stage, the root systems of the two lines did not show statistically significant differences.

With the aim to elucidate if the *br2* mutation determines specific morphological/structural stem alterations, which might be responsible for shorter lower internodes, a characterization of plant stems structure both at phenotypic and cytological level was performed. Cross and longitudinal sections of plant stem were use to immunolocalize auxin, to assess its distribution along the stem.

At seedling stage, *br2:NC238* and the revertant plants are indistinguishable. 20 days after sowing the two lines were still similar in stature and leaf number: 100% of the *br2:NC238* plants and 100% of the revertant plants had 3 collared leaves (figure 2.20). Phenotype arose when plants had 6-7 collared leaves. At this stage, *br2:NC238* plants stature was reduced compared to the revertant plants, and after leaves removal *br2:NC238* 5th, 6th and 7th internodes were visible shorter than the revertant plants internodes (figure 2.19, 2.20).



Figure 2.19. *br2NC238* (left) and the revertant plant (right) stems at 7-leaf-old stage after leaves removal.

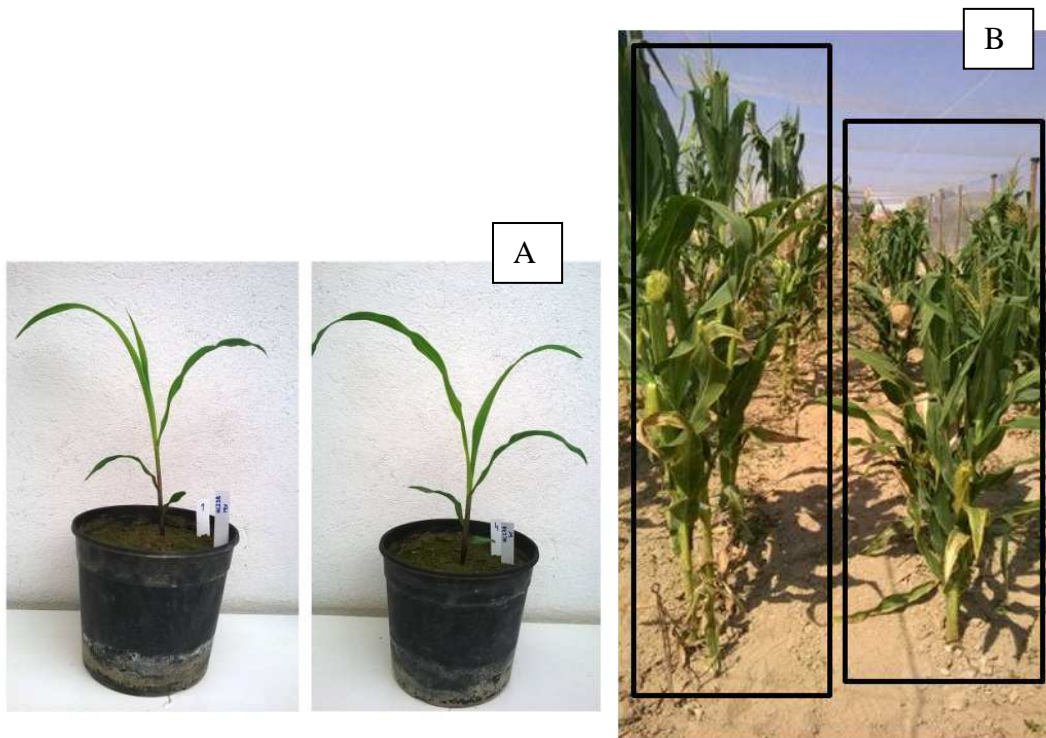


Figure 2.20. A) At 3-leaf-old stage *br2:NC238* (right) and the revertant line (left) plants were indistinguishable. B) Phenotype of the revertant plant (left) and the *br2:NC238* line (right) at adult stage at the University of Padova "L.Toniolo" farm.

The morphological characteristics of *br2:NC238* and its revertant line were measured and compared at anthesis stage. After stature measurement plants were cut and all the leaves removed from stem before measurements.

Tassel and ears became visible in the two lines simultaneously, and plant reach anthesis at the same time (table 2.3). Number of ears per plant and tassel ramifications were similar in the two lines (T-test, p-value>0.05). Results indicated *br2:NC238* short stature was not due to a reduction of the plant life cycle length.

	Days to flowering*	Ears per plant**	Tassel branches
<i>br2:NC238</i>	99.75±1.67 a	4.39±0.96 a	29.79±5.55 a
Revertant NC238	99.87±1.87 a	4.25±0.90 a	29.83±5.01 a

Table 2.3. Morphological trait related to reproduction measurements (* days to anthesis, ** including young ears with no silks emerged).

On average, *br2:NC238* stature was 36% shorter than the revertant plant.

The number of nodes of the two lines did not differ significantly (T-test, p-value=0.01), thus the short stature was due to the shortening of the internodes, rather than the number of leaves.

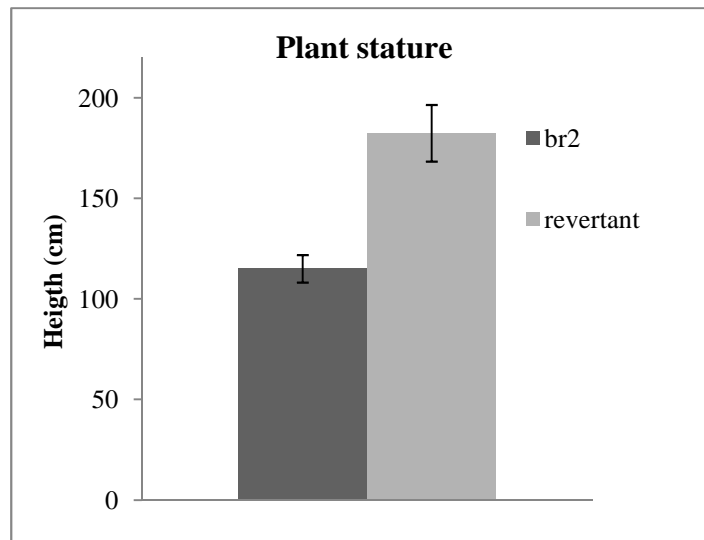


Figure 2.21. On average, *br2:NC238* stature was 36% shorter than the revertant plant.

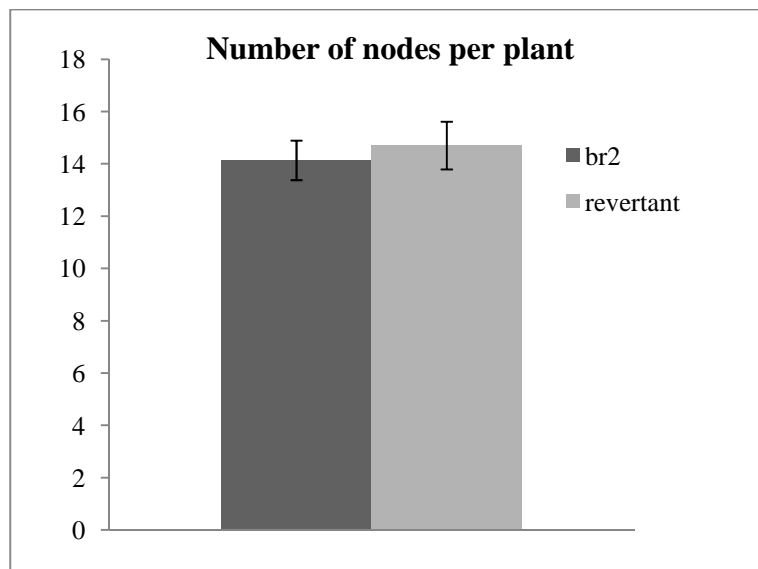


Figure 2.22. The number of nodes of the two lines did not differ significantly.

The length of the 1st and 2nd internode above the brace root node and the first internode above the uppermost ear are statistically different between the two lines, with *br2:NC238* internodes shorter than the revertant ones. However, the length of the lower internodes is the trait that is mostly affected in the *br2* semi-dwarf line. In monocots, the internode elongation is attributed to the development of intercalary meristems at the base of the growing internode, which are capable of cell division and cell elongation (Sauter and Kende, 1992). The reason why *br2* mutant is characterized by severe shortening of the lower internodes in particular is still unknown. Knoller (2010) observed *abcb1* expression in *br2* nodes and reduced free [³H]-IAA

levels in *br2* internodes compared to the wild type B73 suggesting a reduced amount of auxin due to the defect in transport from the sites of synthesis - young tissues and leaves - to the lower internodes at the base of the stem (Knöller et al., 2010).

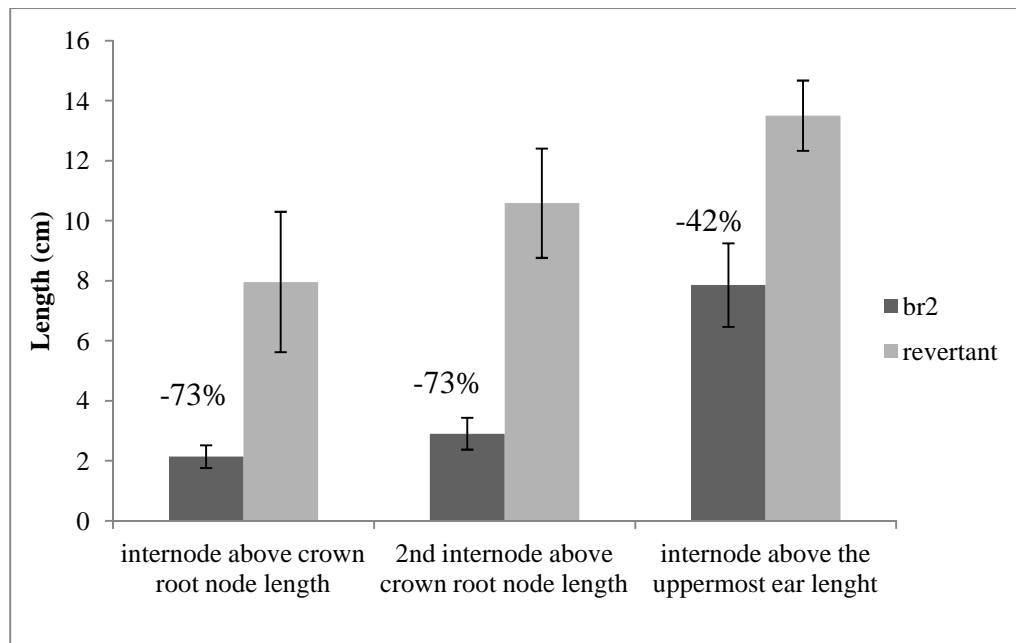


Figure 2.23. Comparison between internode lengths of *br2:NC238* and the revertant plant. Length of the lower internodes is the trait that mostly affects *br2* stature.

Shortening of the lower internodes caused the *br2:NC238* crown root nodes to be very close each other, near to the ground or even inside the soil, while two or three brace root nodes of the revertant plants are visible above the ground (figure 2.25). In wild type plants at optimal growth condition, brace roots emerge from above-ground stem nodes approximately 6 weeks after germination (Hochholdinger et al., 2004). Brace roots, together with the shoot-borne roots grown from nodes under the soil line - the crown roots - provide stability and support to plants, while lateral roots provide the major surface water and nutrient uptake. The *br2NC238* dwarf stature and the short distance between brace roots and soil surface could be an advantage during windy weather increasing the anchoring of the plant to the soil. Moreover, brace roots that enter the ground can take up water and nutrients improving yields while decreasing the need for heavy fertilizer application (Hoppe, 1986).

Also the diameter of the node above the uppermost brace root node differs between the two lines: the *br2* plant node is slightly thicker (p-value lower than 0.05). Instead, the diameter of

the node above the uppermost ear node in *br2* was no significantly thicker than the revertant line.

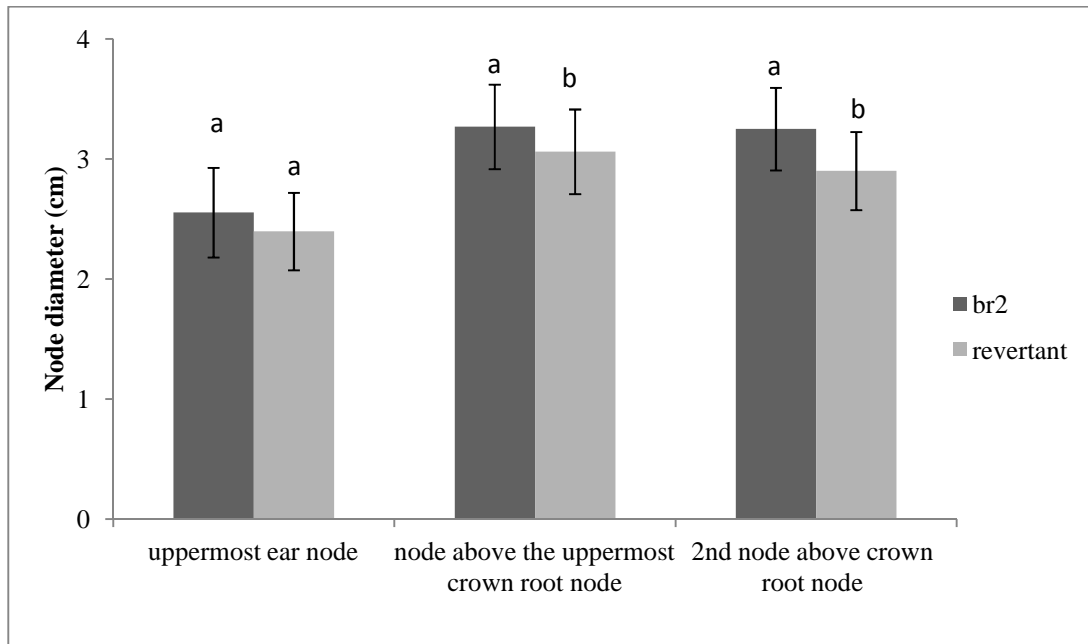


Figure 2.24. Comparison between node diameters of *br2:NC238* and the revertant plant. Lower nodes are thicker in *br2* stem. No difference was reported in the uppermost nodes. Different letters refer to statistically significant difference.

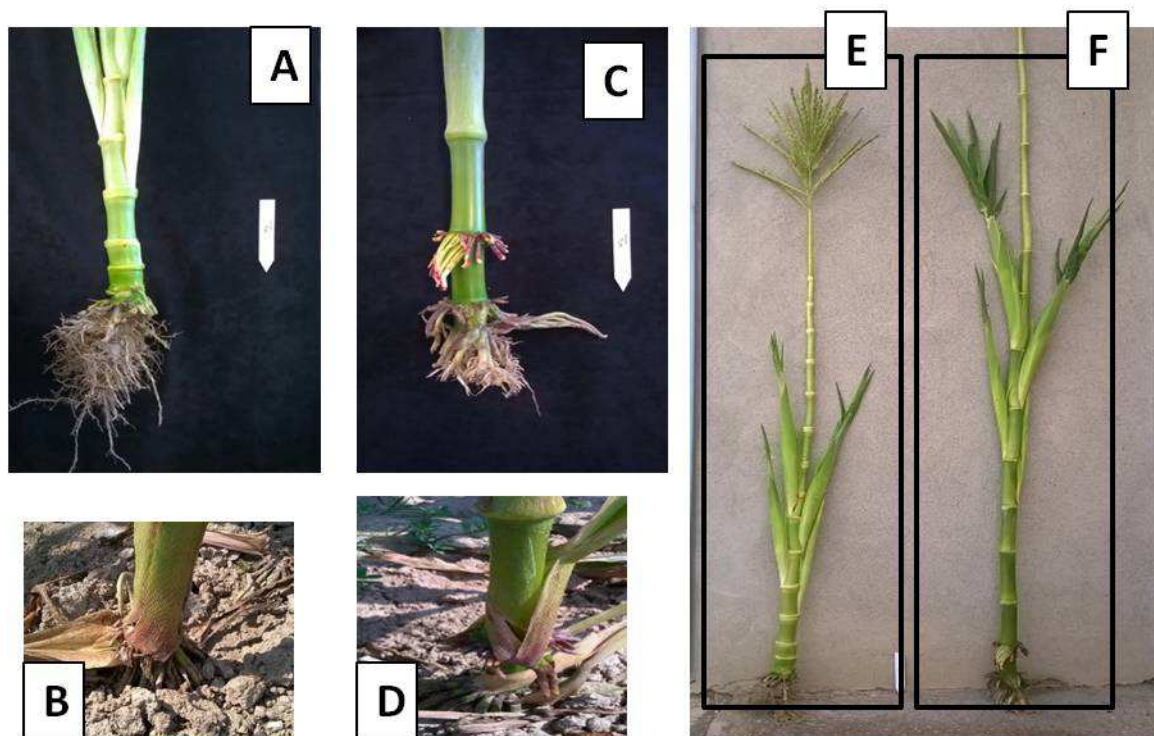


Figure 2.25. Phenotype of the *br2:NC238* (A, B, E) and the revertant line (C, D, F). *br2:NC238* crown root nodes are very close each other, near to the ground or even inside the soil, while two or three brace root nodes of the revertant plants are visible above the ground (B, D).

Reduced stem dimensions are an advantage for the plant in terms of energy allocation. Moreover, *br2:NC238* is characterized by thick lower nodes. Nodes thickness could increase plant resistance to lodging during windy weather and storms and can be an advantage in determining yield.

2.3.4 Internode anatomy and auxin accumulation in *br2:NC238* plants

As reported above, the length of the lower internodes is the trait that mostly affects the *br2* short stature. Length of the internodes depends both on the number and size of the cells in the stem tissues. Alterations both in stem parenchyma and vasculature bundles were previously observed in *br2* plants (Multani et al., 2003).

Monocot stem is characterized by vascular bundles scattered throughout the ground tissue. The vascular bundles occurring nearer the rind of the stem are smaller and are closer to one another (Heckwolf et al., 2015). Vascular bundles comprise the xylem vessels - that transports water and dissolved ions from the root system to the stem - and the phloem, composed of thin-walled cells (sieve tubes and companion cells), that transports organic molecules from the leaves to other parts of the plant (Shane, 2000).

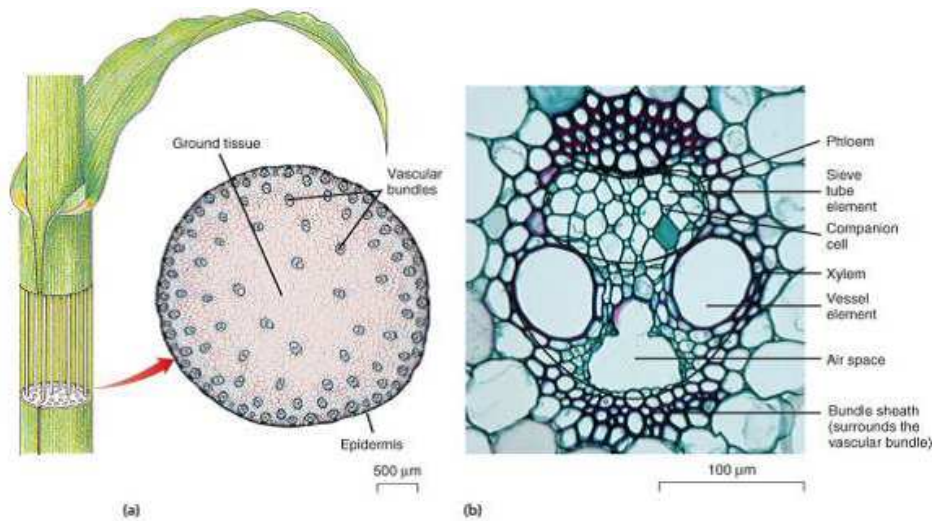


figure 2.26. The monocot stem tissues organization (a) and particular of the vascular bundles (b) (from www.studyblue.com)

Cross sections of *br2:NC238* and the revertant line stems were analyzed. Sampling were performed at 7-leaf-old stage, when *br2:NC238* plants became visible different from the

revertant line plants. Stems were cut in 0.5cm height cylinders. Tissues were ethanol dehydrated and Paraplast embedded before cutting into 8-10 μm slides by microtome. After Paraplast removing and slides rehydration, slides were mounted and directly observed by microscopy or treated with Calcofluor® to increase the cell wall signal intensity before microscopy observation.

Histological observations of cross sections of the 6th internodes indicated no differences in the sub-epidermal cell layers or vascular bundles distribution and size (figure 2.29 A and B). *br2:NC238* and the revertant line internodes are similar to the typical monocot stem organization described in literature with the vascular bundles regularly arranged. In the internodes, the course of the bundles is vertical. On the contrary at the level of the nodes they meet the horizontal strands and anastomose into elaborate plexus (Shane, 2000) (figure 2.27, C).

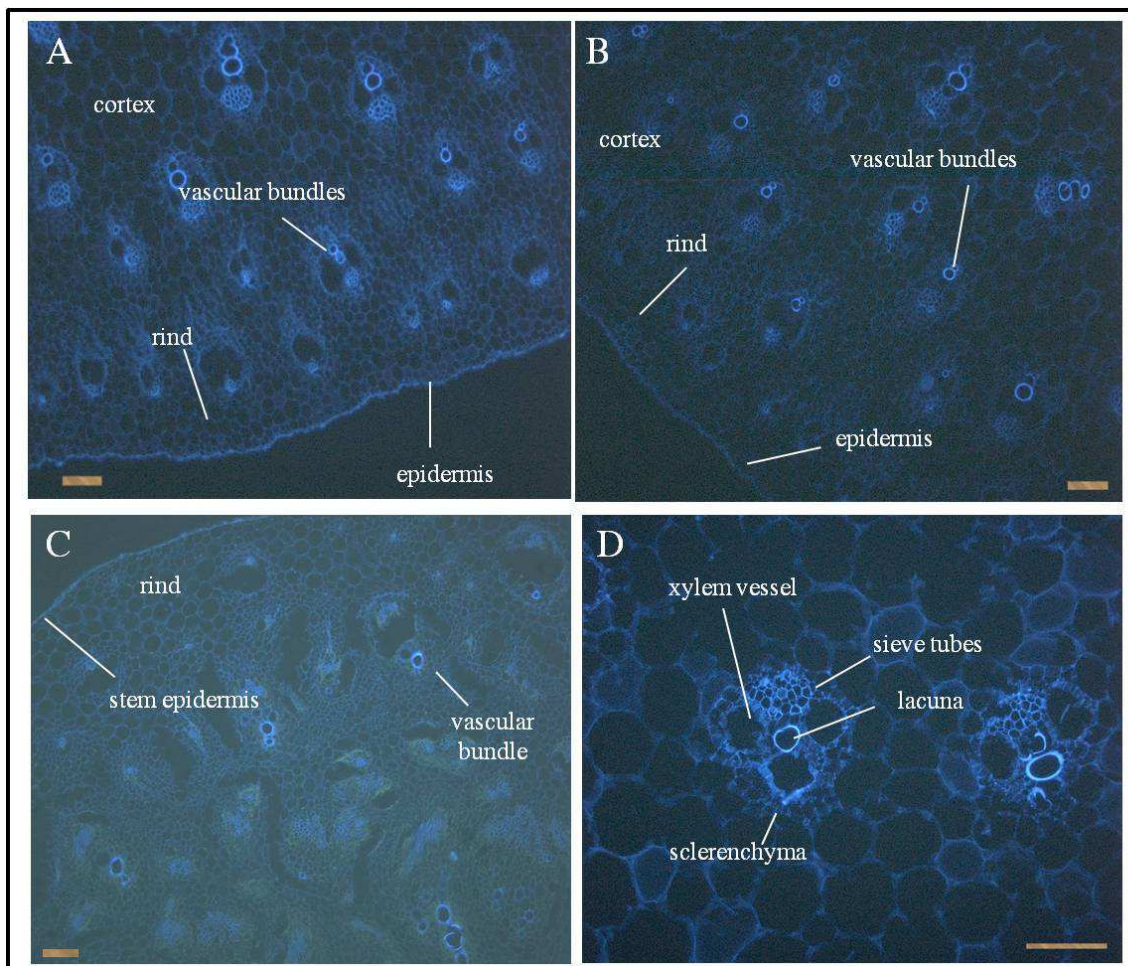


Figure 2.29. Cross section of *br2:NC238* (A) and revertant (B) 6th internode from 7-leaf-old plants. C) Cross section of 7th node of revertant plant 7-leaf-old. D) Particular of the cross section revertant 6th internode from 7-leaf-old plants. Scale bar=100 μm .

In order to verify if the shortening of the internodes of *br2:NC238* plants is due to an auxin over- or under-accumulation for a defective auxin transport, auxin localization at tissue level was observed using a anti-IAA antibody staining. Preliminary experiments of IAA immunolocalizations on longitudinal sections of young internodes of the *wild type* revertant plant indicate higher accumulation of auxin at the vascular bundles. Most auxin is probably transported away from the source tissues (young leaves and flowers) by an unregulated bulk flow in the mature phloem to the site where it is necessary (Petrásek and Friml, 2009). IAA accumulation at the vascular bundles might be due to the long-distance polar transport process. A reduction of auxin accumulation in *br2:NC238* tissues compared to its revertant was detectable.

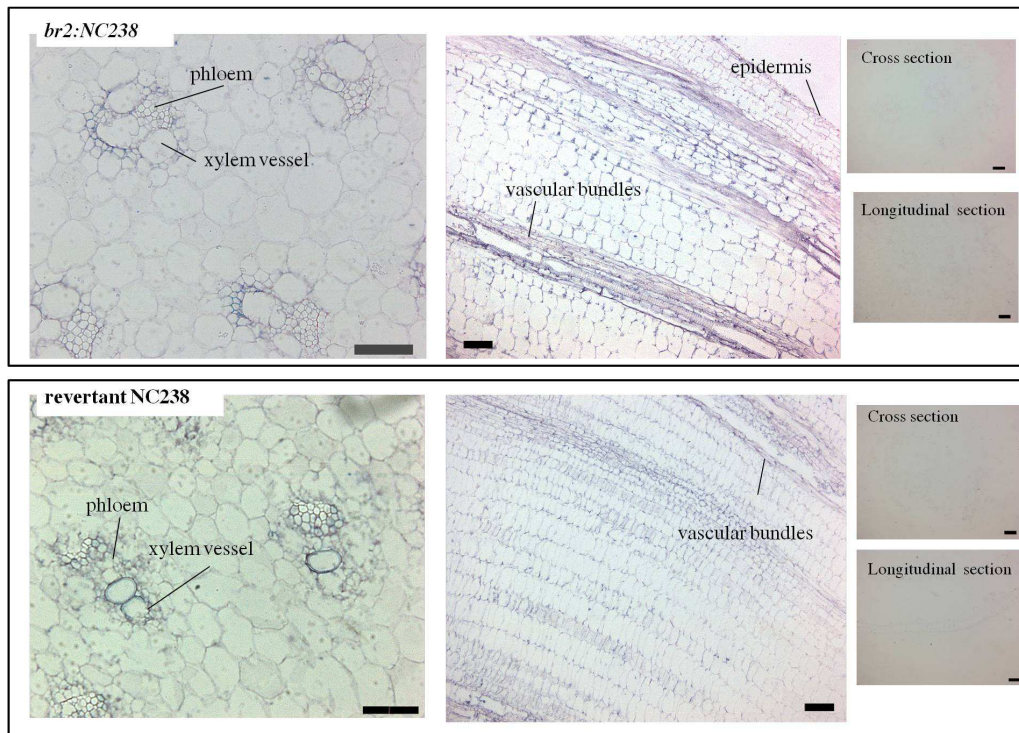


Figure 2.28. IAA-immunolocalization of transversal and longitudinal sections of 6th internodes of *br2:NC238* and revertant plants. Control refers to slides without primary antibody incubation. Bar scale=100µm.

2.4. Discussion

A few maize *brachytic2* mutants have been isolated. The literature describes the *br2* lines as altered in the lower internodes elongation (Multani et al., 2003; Pilu et al., 2007; Cassani et al., 2010), in the size of the leaf epidermal cells (Pilu et al., 2007; Cassani et al., 2010) in their width (Knöller et al., 2010), and in the stem vasculature (Knöller et al., 2010; Multani et al., 2003).

Auxin plays a major role in root development. Many works indicate the involvement of auxin in the regulation of root elongation and growing root tips of intact plants contain high IAA concentrations. The typical response of roots to exogenous auxin is inhibited elongation while low auxin concentrations applied to the growth solution may stimulate elongation growth (Aberg, 1978). Arabidopsis *pxd1* mutants are unable to produce pyridoxal phosphate, which impairs the capacity of these plants to convert tryptophan to IAA. These plants have a short primary root with a reduced root meristem size (Chen and Xiong, 2005). Overexpression of Arabidopsis microRNA160, which targets Auxin Response Factor 10, 16, and 17 leads to a reduction in primary root growth (Mallory et al., 2005). While the primary root arises from embryo, lateral roots development is post embryonic and derived from the pericycle. The role of auxin in lateral root is well known from the '50s. In particular, auxin promotes lateral roots initiation and emergence (Casimiro et al., 2001; Swarup et al., 2008). In the root, auxin derived from local synthesis at the root apex and transport from the shoot tissues and local auxin biosynthesis is required for the correct root development (Chen et al., 2014). In Arabidopsis, inactivation of auxin biosynthesis genes (YUC) that show tissue-specific expression in roots lead to very short and agravitropic primary roots. Over-expression of YUC genes localized at the shoot of the seedling increases auxin synthesis but does not rescue the root phenotype. Instead, the phenotype is rescued by adding IAA or over-expressing YUC in the roots (Chen et al., 2014).

Auxin is involved in many functions in several organs and tissues, not only roots, and a complex network of carriers guarantees its transport and presence when auxin is needed. Thus, auxin transport is a robust and redundant system. In monocots, many ABCBs and PINs are involved in auxin transport in roots and in particular ABCB1 is consider a long distance auxin transporter protein. On the contrary, PINs proteins are thought to be responsible of the fast response to environmental stimuli. In Arabidopsis, ABCB1 and ABCB19 have been shown to be responsible for the majority of rootward auxin transport, but residual fluxes to the root tip in

Arabidopsis abcb1 abcb19 double mutants implies the involvement of at least one additional auxin transporter in this process (Yang and Murphy, 2009).

The *br2:NC238* and the revertant NC238 line seedlings are phenotypically indistinguishable. The similarity of the two lines was confirmed by treating *br2:NC238* and the NC238 revertant line seedlings with auxin analog (NAA) and auxin transport or action inhibitors (NPA, PCIB, BUM) induced the same response in the two lines during all the different treatments. NAA application on *br2:NC238* and revertant line seedlings reduced the primary root growth and increased the root hair density. Moreover, NAA applications induced gravitropic defects on the primary roots of the two lines. It was previously reported root length reduction in *Arabidopsis* treated with NAA, where maximum inhibition of primary root elongation was obtained at 500nM NAA applications (Simon et al., 2013). NAA inhibits *Arabidopsis* root growth primarily through reducing the length of the growth zone rather than the maximal rate of elemental elongation and it does not reduce cell production rate (Rahman et al., 2007).

p-Chlorophenoxyisobutyric acid (PCIB), also called α -(4-chlorophenoxy) isobutyric acid, 2-(*p*-chlorophenoxy)-2-methylpropionic acid, or clofibric acid, has been most widely used to inhibit auxin action. In *br2:NC238* and revertant line seedlings, PCIB treatments from 10 to 100uM did not produce any effect on maize plants. In literature little is present about the effect of PCIB in maize plant. This compound could be less effective in maize and we cannot exclude higher concentrations are necessary to produce any effect. Many paper demonstrated PCIB inhibits auxin regulated gene expression (Okamoto et al., 1995; Klotz and Lagrimini, 1996, Oono et al., 2003). In *Arabidopsis* roots, PCIB impairs auxin-signaling pathway by regulating Aux/IAA protein stability and affecting the auxin-regulated root physiology, inhibiting lateral root production, gravitropic response of roots, and growth of primary roots (Oono et al., 2003).

1-Naphthylphthalamic acid (NPA) is a specific inhibitor of polar auxin transport that blocks carrier mediated auxin efflux from plant cells (Zettl et al., 1992). The compound caused reduced primary root length and root gravitropic defects in both *br2:NC238* and the revertant lines. Effects of NPA on maize seedlings were visible starting from 0.5uM concentration. In *Arabidopsis*, NPA causes the inhibition of root growth primarily by reducing cell production rate (Rahman et al., 2007).

The auxin transport inhibitor 2-[4-(diethylamino)-2-hydroxybenzoyl] benzoic acid (BUM), efficiently blocks auxin-regulated plant physiology and development. Treating the maize seedlings with 0.5uM did not show any effect. On the contrary, increasing the concentration to 10uM had lethal effect on the plants, for both the lines. The lethal effect on maize seedling

could have been increased by the use of DMSO to dilute BUM before doing the serial dilutions in water. In literature, physiological analysis and binding assays in Arabidopsis or yeast microsomes identified ABCBs, primarily ABCB1, as key targets of BUM and NPA, whereas PIN proteins are apparently not directly affected. BUM is complementary to NPA by having distinct ABCB target spectra and impacts on basipetal polar auxin transport in the shoot and root (Kim et al., 2010).

Also the main role of auxin in gravity response is well assured (Perrin et al., 2005; Hashiguchi et al., 2013; Morita and Tasaka, 2004; Band et al., 2012). The Cholodny-Went theory proposes auxin is transported laterally after the gravistimulus inducing the organ to curve. Defect in auxin transport generally causes defective gravitropic response (Chen et al., 1998; Friml et al., 2002). Similarity of the two maize lines were confirmed when no difference and no defect in *br2:NC238* and revertant line gravitropic response was observed. In addition, the expression profile of the auxin transporter encoding genes before and after 90°-rotation indicated similar transcriptional profile in the two lines.

The lack of a phenotype during the first developmental stages of the *br2:NC238* mutant might be due to the presence of the necessary amount of auxin, despite its defective transport due to the mutant ABCB1. Indeed, auxin might be transported by other carriers into the tissues. Together with passive diffusion, auxin can move through many other carriers (ABCBs, PINs, PIN-LIKEs and AUX/LAXes carrier types). In fact in the mutant line, an alteration of other auxin transporters expression, compared to the revertant plant tissues, was observed (figure x). Moreover, in young plant stem, auxin derives from nearby auxin biosynthetic sites. Auxin biosynthesis happens in young tissues, such as shoot apical meristem, young leaves and root apical meristem. During the first stages of stem development and elongation, young internodes are close to these sites of auxin biosynthesis. Thus, auxin transport from the uppermost part of the plant to the base of the young stem is not as long as it is in the later stages of the stem elongation process.

Roots are important to plants for a wide variety of processes, including nutrient and water uptake, anchoring and mechanical support, storage functions. Root system architecture may affect the ability to use soil nutrients more efficiently and increases stress tolerance, improving yields while decreasing the need for heavy fertilizer application. No statistically significant differences between *br2:NC238* and revertant lines root system traits were observed in plants grown in the field at anthesis stage. The *br2:NC238* and the revertant line root systems are mainly distributed in the first 40cm of soil depth and roots were thinner in the deeper horizons.

The plant total length, Root Length Density (RLD) and Root surface Density (RAD) were not statistically different than those of the revertant plant and high variability between data was observed. In fact, many factors can influence the root system development in the field: distribution of water and nutrients, oxygen diffusion to the roots, soil physical conditions such as soil strength (Bengough, 2005).

Results of the morphological traits measurements on adult plants indicated *br2:NC238* and its revertant line do not show differences in the reproductive development. The two lines reached anthesis at the same time. The number of ears per plant and the number of tassel ramification were similar in the two lines.

br2:NC238 is a semi-dwarf line. The revertant plants that do not carry the transposon insertion in ABCB1 gene shows higher stature. The shorter length and the thicker diameter of the lower internodes is the trait that mostly affects the *br2:NC238* short stature.

Plant dwarfism can be due to a reduction in leaf number. An instance, the maize *vanishing tassel 2 (vt2)* mutant exhibits a semidwarf vegetative phenotype due to the production of fewer leaves. VT2 is a co-ortholog of Arabidopsis TAA1 and encodes a grass-specific tryptophan aminotransferase that converts Trp to indole-3-pyruvic acid through a Trp-dependent auxin biosynthesis pathway (Phillips et al. 2011). The maize *vanishing tassel 2 (vt2)* mutant exhibits a semidwarf vegetative phenotype due to the production of fewer leaves. VT2 is a co-ortholog of Arabidopsis TAA1 and encodes a grass-specific tryptophan aminotransferase that converts Trp to indole-3-pyruvic acid through a Trp-dependent auxin biosynthesis pathway (Phillips et al. 2011).

Like *br2*, several other dwarf mutants are characterized by the shortening of the internode length rather than a reduction in the number of nodes. Many maize brachytic mutants are distinguishable by the length of certain internodes along the stem. For instance, *br1* internodes are all short and similar in length, while *br5* has altered length of the higher internodes while the other internodes length is normal (Johal, unpublished). A maize dwarf mutant, *nana*, exhibited dwarfism even at the seedling stage by its reduced growth of the mesocotyl. Dwarfism in *nana* plants is due to a reduction in internodes length. It has been observed *nana* produced less auxin than wild type maize plants (Van Overbeek, 1938). In monocots, the internode elongation is attributed to the development of intercalary meristems at the base of the growing internode, which are capable of cell division and cell elongation (Sauter and Kende 1992; Van der Knaap et al. 2000). The reason why *br2* mutant is characterized by severe shortening of the lower internodes in particular is still unknown. Knoller (2010) observed *abcb1* expression in *br2* nodes

and reduced free [³H]-IAA levels in *br2* internodes compared to the wild type B73 suggesting a reduced amount of auxin due to the defect in transport from the sites of synthesis - young tissues and leaves - to the lower internodes at the base of the stem (Knöller et al., 2010).

Moreover, the *br2:NC238* lower nodes are thicker than those of the revertant plant. Literature lacks description of mutants with altered node diameter. This may be an important advantage for the line increasing resistance to lodging during storms and windy weather.

The *br2:NC238* lower brace roots nodes are close to the ground or even inside the soil, while two or three brace root nodes of the revertant plants are visible above the ground. In wild type plants at optimal growth condition, brace roots emerge from above-ground stem nodes approximately 6 weeks after germination (Hochholdinger et al., 2004). Brace roots, together with the shoot-borne roots grown from nodes under the soil line - the crown roots - provide stability and support to plants, while lateral roots provide the major surface water and nutrient uptake. The *br2:NC238* dwarf stature and the short distance between brace roots and soil surface could be an advantage during windy weather increasing the anchoring of the plant to the soil. Moreover, brace roots that enter the ground can take up water and nutrients improving yields while decreasing the need for heavy fertilizer application.

Histological observations of *br2:NC238* and revertant plant stems at 7-leaf-old stage indicated no differences in the structure of the tissues: no differences in the sub-epidermal cell layers or in the vessels size or in the bundle distribution were observed. Multani (2003) observed a reduction in stalk cell size, and increase in number of sub-epidermal parenchyma cells and an alteration in vascular bundle distribution in *br2* plants. Instead, Pilu (2007) observed larger vessel elements in *br2*.

br2 nodes are very close each other (Multani et al., 2003; Pilu et al., 2007, the present thesis). Thus, it was difficult to handmade separate internodes from nodes and sampling only internodes tissues.

Differences in number or size of the cells or size and distribution of the vessels are visible between nodes and internodes of the stalk. Internodes vascular bundles are regular arranged, while at nodes vertical bundles meet the horizontal, and axial bundles at nodes are anatomically different from those in internodes (Shane, 2000). Literature lacks images of nodes cross sections in literature, mainly because of the difficulty in wax inclusion and sectioning due to the thickness and complexity of the tissue. It cannot be excluded the differences in *br2* internodes

structure described by Multani (2003) and Pilu (2007) were due to the sampling in vicinity of the nodes and thus an observation of the beginning of the node rather than the internode.

Chapter III

Genetic characterization of the *br2*:NC238 line mutation

3.1. Introduction

The ATP-binding cassette superfamily (ABC) of membrane proteins comprises hundreds of different members in plants (Kang et al., 2011). The core unit of a functional ABC transporter consists of 4 domains: two NBDs (nucleotide-binding domains) and two TMDs (transmembrane domains), each with six transmembrane segments (Ambudkar et al., 2003). The two NBDs unite to bind and hydrolyze ATP, providing the driving force for transport, while the TMDs are involved in substrate recognition and translocation across the membrane (Jasinski et al., 2003; Higgins and Linton, 2004; Bailly et al., 2011).

Subfamily B (ABCB) includes homologs of the mammalian multidrug resistance/p-glycoproteins (MDRs/PGPs), several of which are involved in auxin transport (Geisler and Murphy, 2006; Cho and Cho, 2013). MDR/PGPs were first identified in mammalian cancer lines because their over-expression confers multidrug resistance to chemotherapeutic cancer treatments (Ambudkar et al., 2003). Structural characteristics of mammalian MDR/PGPs are well conserved in plant homologs except in the predicted pore-facing helical domains thought to confer substrate specificity (Ambudkar et al., 2003).

ABCB transporters actively transport chemically diverse substrates across the lipid bilayers of cellular membranes (figure 3.1). The first ABCBs involved in auxin transport were characterized as functioning in IAA translocation in *Arabidopsis* seedlings (Sidler et al., 1998; Noh et al., 2001).

br2 gene, ID GRMZM2G315375, has also been called Hahn 6 dwarf (Leng, ER), *mi1*, Oakes dwarf (Leng, ER), *pgp1* (Multani, DS), R4 dwarf (Leng, ER), *ZmPGP1*. A recent debate on ABC protein nomenclature proposed a unified named system base on species identifier based on the Latin binomial, the ABC family, one of the eight subgroups (A to H) and the number of the subfamily member (Verrier et al., 2008). According to this nomenclature, maize BR2 most correct name is *ZmABCB1*.

Based on the B73 reference genome - version 3, *abcb1* locus is located on Chromosome 1: 202,334,824-202,342,008, forward strand. *abcb1* gene has 2 transcripts (splice variants), 42 orthologues and 16 paralogues. T01 transcript is 4672 bp, has 5 exons and 4 introns, and encodes for a 1379 amino acids protein. According to NCBI domain search web tool, ABCB1 protein is characterized by two ATP-binding cassette domains, two ABC transporter transmembrane regions, and a general multidrug resistance protein (*mdr1*) domain (figure 3.2). T02 is a truncated version of T01, is 2061 bp, has 4 exons and 3 introns, and encodes a 598 amino acids long protein.

ABCB1 is expressed in nodal meristems, and analyses of auxin transport and content indicate that ABCB1 function in monocot-specific meristems is the same as *AtABCB1* function as auxin transporter in *Arabidopsis* (Knöller, Blakeslee, Richards, Peer, & Murphy, 2010; Multani et al., 2003).

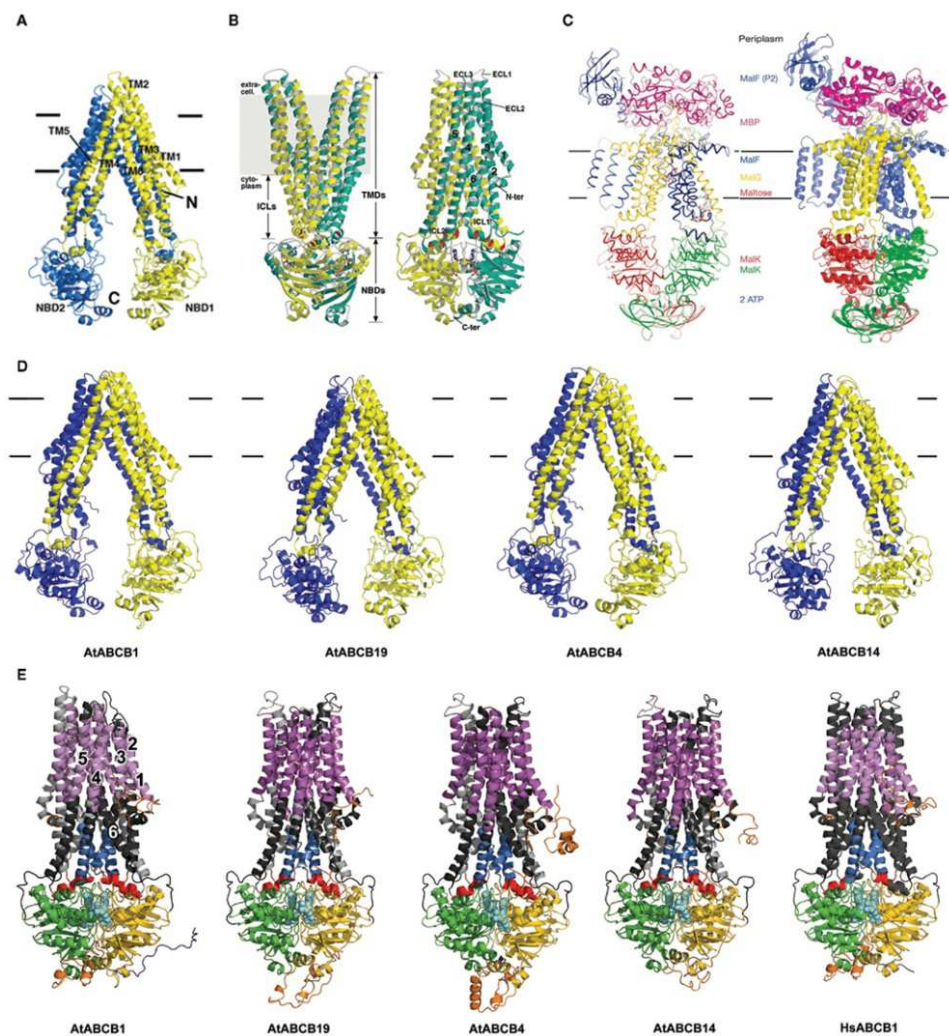


Figure 3.1.
 A) MmABCB1 (Aller et al., 2009).
 B) Sav1866 (Dawson and Locher, 2006).
 C) Maltose transporter: left, retranslocation intermediate state (Oldham and Chen, 2011a), right, translocation intermediate state (Oldham et al., 2007).
 D) Arabidopsis ABCB structural models based on MmABCB1.
 E) ABCB models based on Sav1866 including AtABCB19 and AtABCB4 models (Yang and Murphy, 2009). Adapted from Bailly (2012).

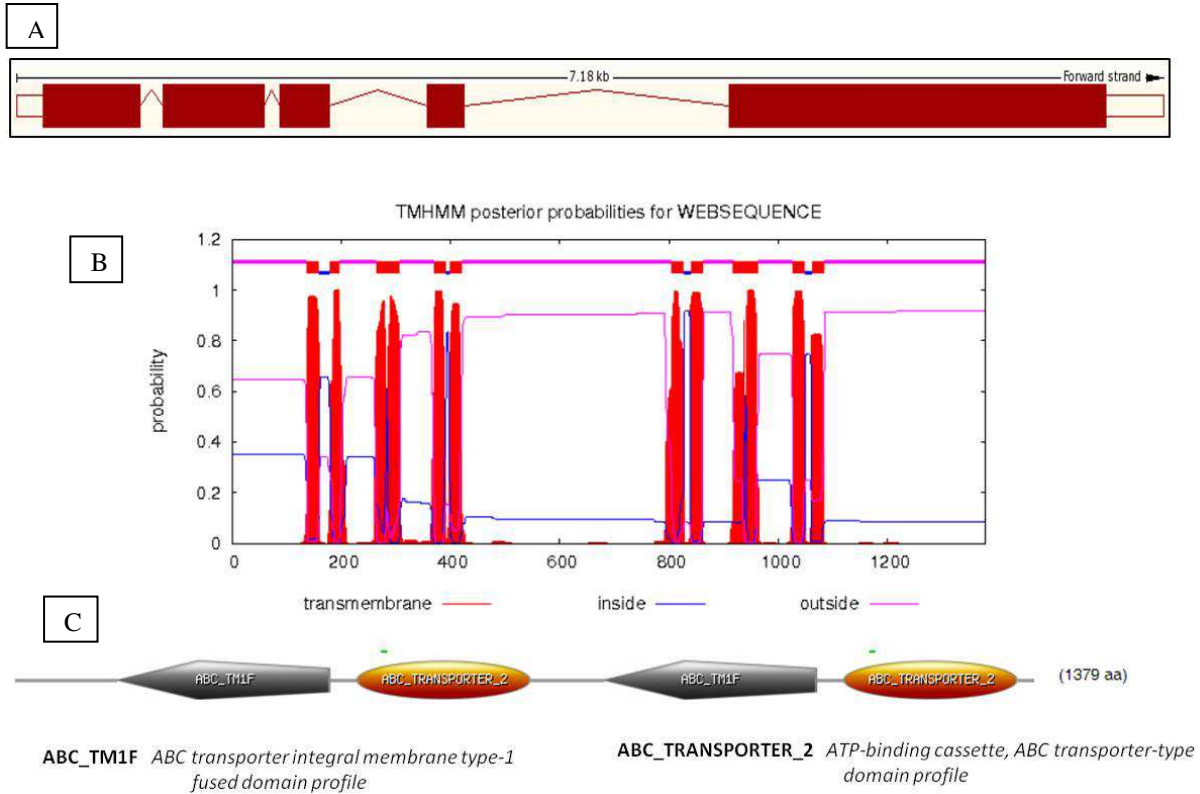


Figure 3.2. A) Intron/exon structure of *abcb1* gene (7.18Kb long) (from Gramene Data Base); B) Transmembrane structure of the ABCB1 protein (obtained from the TMHMM Server); C) Domains of the proteins (obtained from Expsy prosite Web Tool).

In addition to ABCB1, there are three putative AtABCB19 homologs: ZmABCB10-1 (GRMZM2G125424) and ZmABCB2-1 (GRMZM2G072850), present closest sequence similarity to OsABCB16, while ZmABCB10-2 (GRMZM2G085236), is more similar to the true auxin transporter OsABCB14 (Knöller et al., 2010). ZmABCB10-1 (GRMZM2G125424) is expressed in actively growing tissues, especially in pre-pollination ears at the flowering stage (Pang et al., 2013). Recently, using Arabidopsis ABCB proteins as BLAST query to search the maize genomic database, and using the hidden Markov model (HMM) profiles, 29 new ZmABCB genes were identified. Their sizes range from 388 to 1540 amino acids (Yue et al., 2015).

Several *brachytic* mutants, characterized by shortening of specific internodes along the stem - and between these, many *br2* mutants - have been isolated and characterized (Multani et al., 2003; Pilu et al., 2007; Knöllner et al., 2010; McLamore et al., 2010; Cassani et al., 2010).

Allelic tests performed crossing NC238 inbred line with other *brachytic* mutants indicated NC238 line is a *br2* mutant (Johal, unpublished). Moreover, preliminary analyses indicated the mutation was due to an insertion in the central region of *abcb1* gene (Johal, unpublished).

One of the aims of the present thesis was to study the nature of the mutation in *abcb1* gene in NC238 inbred line. To do that, amplification and sequencing of the *abcb1* gene and transcripts of NC238 were performed. Moreover, a study on the nature of the insertion responsible for the mutation in *abcb1* was performed.

3.2 Materials and methods

Plant material and growth conditions

The present study uses the following maize lines provided by Prof. Johal (Purdue University): the NC238 inbred line and a revertant NC238 line isolated in a NC238 field at Purdue University.

For gene and transcript sequencing, and expression analyses, seeds were pre-germinated in cigar-shaped rolled wet paper and grown for 3 days until DNA and RNA extraction.

For gene expression analyses plants were grown in pots (1:2 sand and general soil) in the greenhouse until 3-leaf-old stage and 7-leaf-old stage.

Genomic DNA extraction from plant tissues

1-2 g of fresh leaf was used for each preparation. Tissues were ground to a fine powder in liquid nitrogen using a mortar and pestle and resuspended in 500µl extraction buffer (NaCl 0.2M, EDTA 25mM, TRIS pH 7.5 50 mM, SDS 0.5%). The mixture was heat 10' at 56°C and centrifuged (10', 12000 rpm) using a bench centrifuge. The aqueous layer was carefully transferred to a new tube containing 400µl isopropanol. Tubes were inverted a few times and centrifuged. After centrifugation, supernatant was removed and pellet was washed with 300µl of ethanol 70%. After centrifugation, supernatant was removed. The excess liquid was drained off and the pellet was dissolved in 100µl distilled water. DNA quantity and quality was assessed through NanoDrop® spectrophotometer (NanoDrop Technologies).

Gene amplification for DNA sequencing and plant genotyping

Gene amplification for DNA sequencing and genotyping was performed by polymerase chain reaction (PCR) using Taq Polymerase (Invitrogen) according to the manufacturer's instructions. PCR mix: 10x Taq Polymerase buffer 10x (Invitrogen), MgCl₂ (Invitrogen), 10µM primer forward, 10µM primer reverse, 10mM dNTPs mix (Invitrogen), 5 U/µl Taq Polymerase (Invitrogen), 5x BIOSTAB PCR Optimizer (Sigma Aldrich), 50-100ng DNA template, and sterile distilled water to 25µl of reaction volume. Elongation was performed at 72°C. Primers annealing temperature, elongation time and number of cycles were adjusted according to the gene target. Primers are listed in table 3.1.

Electrophoresis gel run

PCR product was run on 1% agarose gel prepared by melting agarose in TEA buffer (Tris base, Acetic acid, EDTA pH 8.3). Electrophoresis was performed in 1x TAE, at 100 volts for one hour. DNA was visualized under UV light on a trans-illuminator and digitally photographed.

DNA sequencing

After amplification and electrophoresis gel run, the appropriately sized DNA fragment was excised from the gel using a clean scalpel. The gel slice was weighed in a 1.5ml tube. Purification proceeded using the gel extraction kit (QIAGEN) in accordance with the manufacturer's instructions. DNA was quantified by NanoDrop spectrophotometer (NanoDrop Technologies). DNA (200ng/100bp sequence) was sequenced with Sanger technique at BMR Genomics Centre (Padova). Resulting chromatograms were aligned using Geneous® software.

RNA extraction and cDNA synthesis

After sampling, fresh tissues were liquid nitrogen frozen and stored at -80°C in 2ml tubes until RNA extraction. Total RNA was extracted according to the RNeasy Plant Mini Kit (Qiagen) and subjected to on-column DNase treatment. RNA quantity and quality were assessed using Nanodrop 2000® spectrophotometer (Thermo Scientific).

cDNA synthesis was performed using the SuperScript III reverse transcriptase kit (Invitrogen), according to the manufacturer's instructions. One microgram of total RNA were used as template with 1µL of oligo(dT)₁₈ (0.5 µg/µL).

Expression analyses

Expression analyses were performed through RT-PCRs. Primers annealing temperature and number of cycles were adjusted, according to the target. Different numbers of cycles were tested. Three replicates were performed. Primers are listed in table x. The constitutively expressed housekeeping GAPC2 gene was used as the internal control. PCR product was run on 1% agarose gel. Electrophoresis was performed in 1x TAE, at 100 volts for one hour. DNA was visualized under UV light on a trans-illuminator and digitally photographed.

Computational analysis

BLAST (Basic Local Alignment Search Tool) developed by Altschul et al. (1990) was used to find short fragment of a query sequence that aligns perfectly with a fragment of a subject sequence found in a database. Interrogations were made at personalized parameters: somewhat similar sequences, no filter, no mask.

NCBI Conserved Domain tool: it was used to search for conserved domains within a protein or coding nucleotide sequence (Marchler-Bauer et al., 2015). Searches were made through the web interface uploading the FASTA format of the sequence of interest. Default parameters were used.

Maize GDB (Maize Genetics and Genomics Database) was used for gene sequences and data download. Maize GDB is the collection of Maize B73 genome sequences, gene annotations, stock, phenotype, genotypic and karyotypic variation, and chromosomal mapping data (Andorf et al., 2015). Searches were made through the web interface.

BLAT (BLAST Like Alignment Tool). The program was used to rapidly scan for relatively short matches (hits) to find regions in the genome likely to be homologous to the query sequence. *BLAT* performs an alignment between homologous regions and stitches together these aligned regions (often exons) into larger alignments (typically genes) (Kent, 2002). Searches were made through the web interface. Default parameters were used.

TIGR Plant Repeat Database (version 3.0) was used for transposon searches. Is a collection of repetitive DNA sequences of 12 plant genera from GenBank and other published records based on their annotation (Ouyang, 2004). Searches were made through the web interface uploading the sequence of interest. Default parameters were used.

CLUSTAL was used for multiple sequence alignment program. Searches were made through the web interface uploading the FASTA format of the sequences to align. Default parameters were used.

P-MITEs DB was used for transposon searches. The database contains MITE-related sequences of 3,527 MITE families, identified from 41 sequenced plant genomes. Search was performed through the uploading of the sequence of interest in FASTA format on the web interface. Search was also made by *BLAST* alignment of the sequence of interest to the *P-MITE* maize database downloaded from the *P-MITE* web site.

Oligo Name	Target	Strand	Sequence 5' to 3'
1F	abcb1cDNA	forward	CTCACACACACAGTCACACT
1R	abcb1cDNA	reverse	AGAAGGAGGAGGAGGAGCAG
2F	abcb1cDNA	forward	CTTTGCTCTGCCACTCTGCT
2R	abcb1cDNA	reverse	GTAGTGGATGAGGTTGCCCA
3F	abcb1cDNA	forward	CTCTTGCTGGATGTGGACCG
3R	abcb1cDNA	reverse	TCCAGCAGGATTTGCCCTG
4F	abcb1cDNA	forward	ATCTTCCGCATCATCGACCA
4R	abcb1cDNA	reverse	GTAGTAGACGCTGAGCACGG
5F	abcb1cDNA	forward	CAGCGCCATCTTCGCCTACA
5R	abcb1cDNA	reverse	ACGGGTACGAGAAGTCCACG
6F	abcb1cDNA	forward	TGCAGAAGATGTTTCATGAAGGG
6R	abcb1cDNA	reverse	CCGACTCAAACAGATCGTCAA
8F	abcb1 T02 cDNA	forward	GACGAGCATCAGGGAGAACC
8R	abcb1 T02 cDNA	reverse	GATGTGGAGCAGCTAGGCAA
4BSF	abcb1 DNA	forward	GCACATGCCTGCCATTGACC
4BSR	abcb1 DNA	reverse	ACAGGCGCCTAACAATTGCC
PIN9	pin9 cDNA	forward	CACCGTCGCCTCGCTCTCCATGCTCC
PIN9	pin9 cDNA	reverse	AAGGCCAACAGTATGTAGTAGACAATCG
AUX1	aux1 cDNA	forward	CCCGGGACATCGCCTCTC
AUX1	aux1 cDNA	reverse	GCCGCCATTAATCCCTCAGA
PIN2	pin2 cDNA	forward	AGGTGGCCAACAAGTTCGCGTCTGGG
PIN2	pin2 cDNA	reverse	CCTTCTTGCGCGGGGCCACGTACG
PIN8	pin8 cDNA	forward	ATGATCTCTTGGCCAACCATCTACCATG
PIN8	pin8 cDNA	reverse	GCACCATAACATCTTGCCGAGACTCCT
GAPC	GAPC cDNA	forward	AATGGCAAGCTCACTGGC
GAPC	GAPC cDNA	reverse	CTGTCACCGGTGAAGTCG

table 3.1. List of the primers used for expression analyses, DNA sequencing and *in situ* hybridization probe preparation: name, target to amplify, strand and sequence.

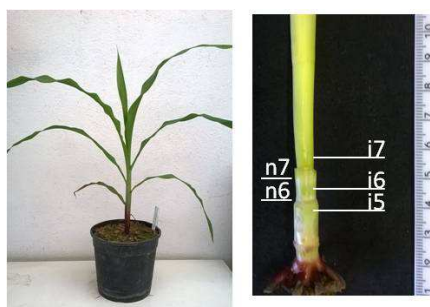


Figure 3.3. Plants at 7-leaf-old stage before (left) and after (right) leaves removal: nodes (n) and internodes (i) are labeled with their position along the stem.

3.3 Results

3.3.1 Genetic characterization of *br2:NC238* mutation

NC238 inbred line is a short stature line. Allelic tests performed crossing NC238 line with other short stature mutant lines (Prof. Johal lab mutant collection, Purdue University) indicated the NC238 line is a *br2* mutant (Johal, unpublished). *br2* gene was cloned by transposon tagging: it encodes for BR2/PGP1/ABCB1 protein, an ABC (ATP-binding cassette) transporter which belongs to the MDR (multi-drug resistant) class of P-glycoprotein homolog of Arabidopsis ABCB1 (Multani et al., 2003). A tall plant in NC238 population was isolated and self-crossed for propagation (Johal, unpublished). The isolation of the tall plant indicated the *br2* mutation in NC238 line could be due to a mobile element insertion that originated a tall revertant plant after a transposition event.

The study and characterization of *br2:NC238* mutation was performed by amplification and sequencing of the *abcb1* genomic DNA clones, both of the *br2:NC238* and its revertant line. B73 reference genome *abcb1* gene is 7kb long, composed of five exons and four introns (figure 3.3 A). The long length of the gene and its complex structure did not allowed the amplification of a full length clone. However, preliminary analyses indicated the mutation was in the central region of the gene (Johal, unpublished), thus analyses were focused on the region between exon III and the beginning of exon V (figure 3.3 A). Short sequences of the gene were amplified and sequenced. Sequence alignments between the *abcb1* sequences of *br2:NC238*, the revertant line and the B73 reference genome were performed.

Comparison of the revertant line *abcb1* gene region spanning from exon III to intron IV (from G₂₄₂₂ to T₃₅₁₁, figure 3.3) with that of the wild type B73 line corresponding gene region showed the revertant line had a 6bp long insertion (GTCGCG) in intron IV, after C₃₂₉₃. The 6bp long sequence in the revertant line *abcb1* gene flanked an identical sequence, thus it was a repetition (5'-GTCGCGGTCGCG-3').

The *abcb1* region (from G₂₄₂₂ to T₃₅₁₁) in *br2:NC238* differed from the revertant line *abcb1* corresponding region for an insertion of 572bp in intron IV. This insertion was flanked at 5' side and 3' side by the GTCGCG sequence found in the revertant line (figure 3.4).

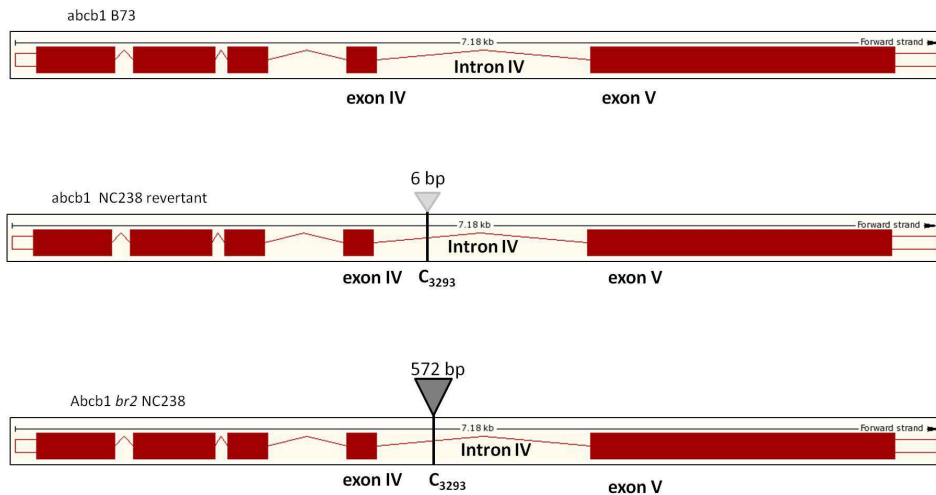


Figure 3.4. Comparison between the B73 wild type, the revertant NC238 and *br2:NC238* mutant line *abc1* gene sequences. A) The wild type *abc1* gene is characterized by 5 exons (boxes) and 4 introns (lines). B) The revertant line differs for 6 bases (triangle) from the wild type reference line gene in intron IV. C) The *br2:NC238* differs for 572 bases insertion (triangle) from its revertant line.

GTCGCG sequence is present in the B73 *abc1* sequence from G₃₂₉₄ to G₃₂₉₉. This result indicated GTCGCG is a Target Site Duplication (TSD) and the insertion in *br2:NC238* is a transposable element. TSD are characteristic traits of transposable elements which occurs upon TE integration as a result of staggered double-strand breaks at the target site (Craig, 2002). TSD are also called the transposon "footprint" as they are retained after transposition of the element.

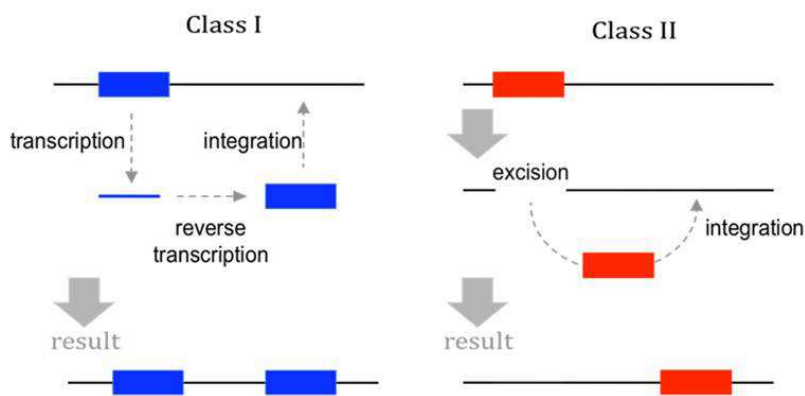
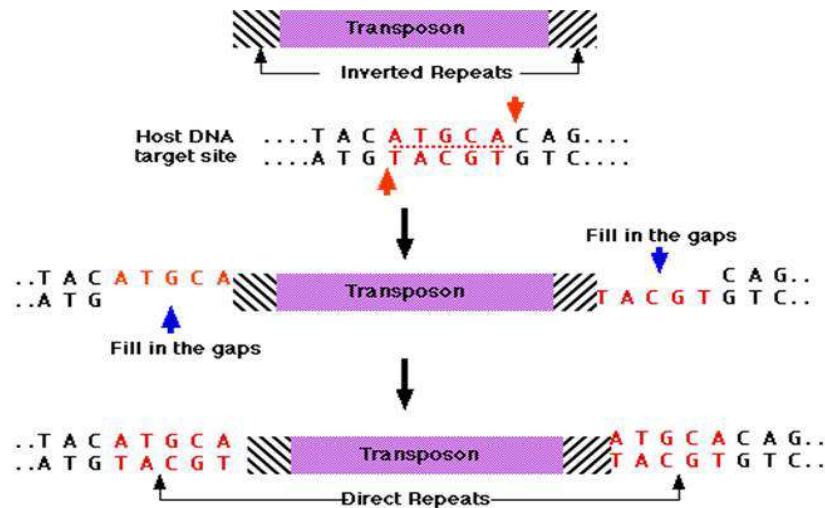


Figure 3.5. Class I transposons (left) transpose through a copy and paste mechanism that causes duplication of the transposon sequence; class II transposons transpose by excision of their sequence and integration in other locus of the genome.

<http://cubocube.com/>



<http://users.rcn.com/jkimball.ma.ultranet/BiologyPages/T/Transposons.html>

Figure 3.6. Class II transposons recognize specific target sequences of the genome. Their insertion causes the duplication of the target sequence (called Target Site Duplication, TSD). When the transposon jumped out the locus and move toward another region, TSD are retained. TSD are also called the transposon "footprint".

The insertion sequence contained in *br2:NC238* *abcb1* gene is characterized by 11 imperfect terminal inverted repeats (TIRs). TIRs are typical traits of many transposable elements groups (Feschotte et al., 2002). The GC content of the insertion sequence is 46.9%.

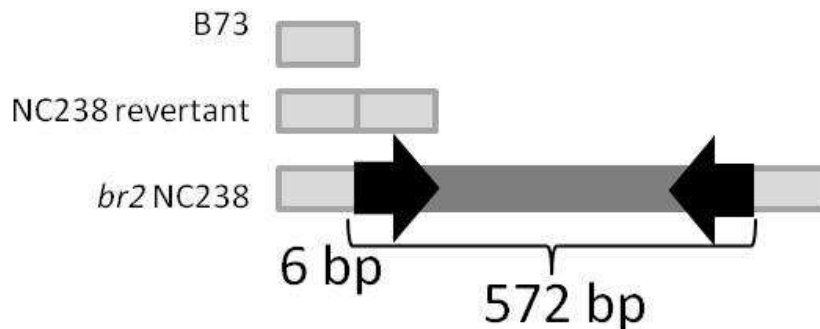


Figure 3.7. Scheme of the *br2:NC238* mutation that highlights the differences and similarities with the B73 wild type reference gene and the NC238 revertant line: *br2:NC238* is characterized by an insertion with terminal inverted repeats (TIRs, black arrows) and it is flanked by short direct repeats (grey boxes). The sequence of the direct repeat is present once in the wild type B73 *abcb1* gene while twice in the revertant line. In fact, the transposon insertion mechanism originates the duplication of the site that is retained after the transposon moving.

3.3.2 Study of the *br2:NC238* insertion

The isolation of a revertant line, together with the presence of the Target Site Duplication (TSD) in the *br2:NC238* and revertant line *abcb1* gene, and the presence of the TIRs in *br2:NC238* insertion (figure 3.7) indicated the *br2:NC238* insertion is a transposable element.

In order to identify which class and family the *br2:NC238* transposon belong to, the interrogation of the DNA and protein domains, maize genome, and transposable elements databases were performed.

The search of homologies of the *br2:NC238* insertion to DNA domains was performed using NCBI Conserved Domain tool. No significant similarities with known DNA domains were found. Also the interrogation of the protein database using the Basic Local Alignment Search Tool (BLASTx) did not find significant similarities with known domains.

Maize GDB (Maize Genetics and Genomics Database) is the collection of Maize B73 genome sequences, gene annotations, stock, phenotype, genotypic and karyotypic variation, and chromosomal mapping data (Andorf et al., 2015). Interrogation of Maize GDB - version 3 using the web BLAST tool showed that the transposon has similarities with many regions in the maize genome. Position, e-value, query identity and number of target matches are summarized in table.

Target	Chromosome	position	identity	strands
1	2	88823490-88824060	566/571 (0.9912%)	Plus minus
2	2	19875381-19874901	475/481 (0.9875%)	Plus minus
3	2	153861077-153860597	475/481 (0.9875%)	Plus minus
4	2	19874623-19874715	93/93 (1.0000%)	Plus minus
5	8	22606558- 22606996	434/439 (0.9886%)	Plus plus
6	8	22607208- 22607300	93/93 (1.0000%)	Plus plus
7	8	22607016- 22607077	62/62 (1.0000%)	Plus plus
8	4	207839332 -207839377	42/46 (0.9130%)	Plus minus
9	7	93396477- 93396518	38/42 (0.9048%)	Plus plus

Table 3.2. Summary of the search of similarities of the *br2:NC238* insertion against the Maize GDB - version 3 sequence collection. Many matches in different chromosomes were found.

The first match (table 3.2) was in a region where there is no annotation of any gene or transposable element. The second sequence aligned in plus/minus strands to a region where a low confidence gene (GRMZM2G580168_T01) was present. Its locus GRMZM2G580168_T01 was between 19,250,511 and 19,251,386 on chromosome 2, has not been physically mapped, was not associated with physically mapped probes, and was not genetically mapped. The 3rd result was a region where there was no annotation of any gene or transposable element. The 4th result aligned to another region of the previously mentioned locus GRMZM2G580168_T01. In that case, the 3'-end of the *br2:NC238* transposon aligned to the locus. The 3' of the transposon included the TIRs of the transposon. Three matches were located on chr8, one in chr4, and one in chr7 and are in regions where no genes or transposable elements have been annotated.

In order to map the transposon sequence to the maize genome, the BLAST Like Alignment Tool (BLAT) was chosen as an alternative to the BLAST tool to identify loci of the maize genome with some similarities with the query.

Many matches were found. These matches refer to position in the maize genome - version 2. Positions in the maize genome are listed in the table screen shot of the BLAT output.

Home Genomes Tables PCR Session FAQ Help											
Maize BLAT Results											
BLAT Search Results											
ACTIONS	QUERY	SCORE	START	END	QSIZE	IDENTITY	CHRO	STRAND	START	END	SPAN
browser details	YourSeq	561	1	572	572	99.2%	2	-	88193240	88193812	573
browser details	YourSeq	557	3	572	572	99.0%	2	-	19250550	19251308	759
browser details	YourSeq	520	3	572	572	99.1%	8	+	22601455	22602197	743
browser details	YourSeq	469	3	483	572	98.4%	2	-	153226078	153226557	480
browser details	YourSeq	80	389	566	572	90.0%	4	-	207663743	207664296	554
browser details	YourSeq	35	379	425	572	94.9%	2	+	27523093	27523503	411
browser details	YourSeq	33	416	456	572	90.3%	7	+	93368493	93368533	41

Figure 3.8. Summary of the search of similarities of the *br2:NC238* insertion in the Maize GDB collection using BLAT tool. The search output indicating the insertion sequence aligns to many regions of the B73 reference genome - version 2.

The third match showed that the 5' and 3' ends of the *br2:NC238* insertion aligned to the ends of class I LTR elements (figure 3.9).

Maize Genome (B73 AGPv2) on Genomaize (UCSC Genome Browser at FSU)

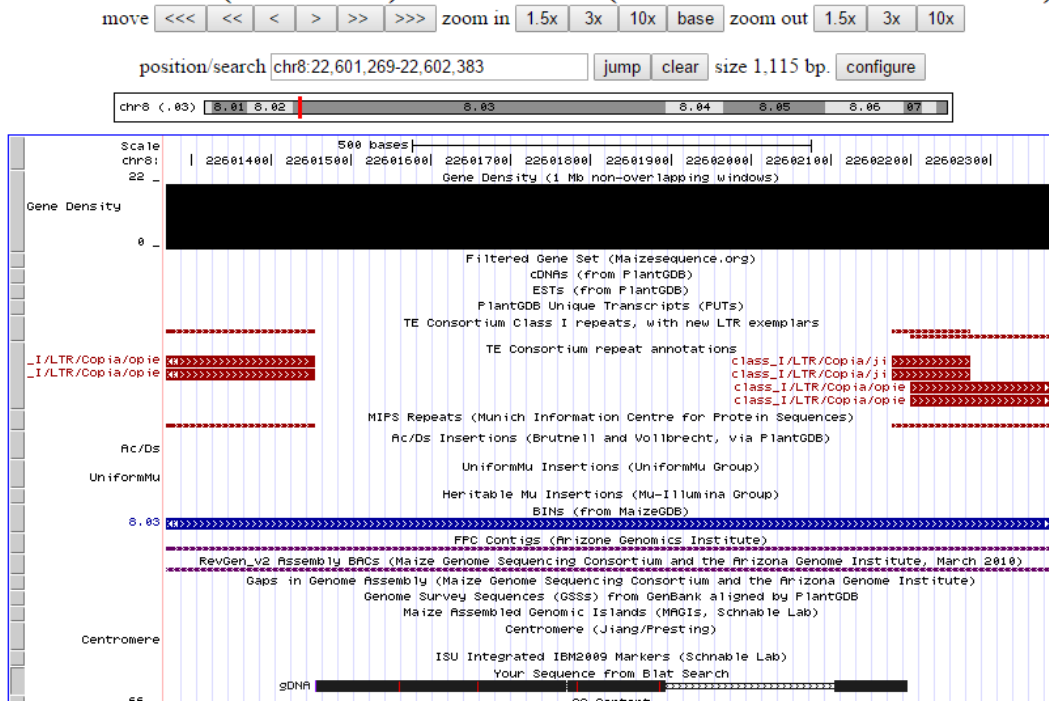


Figure 3.9. Screen shot of the output of the BLAT search: the *br2:NC238* insertion sequence (black/dotted box called gDNA) aligned with its ends to the ends of many class I transposable elements (red boxes).

The fifth match show an imperfect alignment to a class II transposable element (fig.3.10).

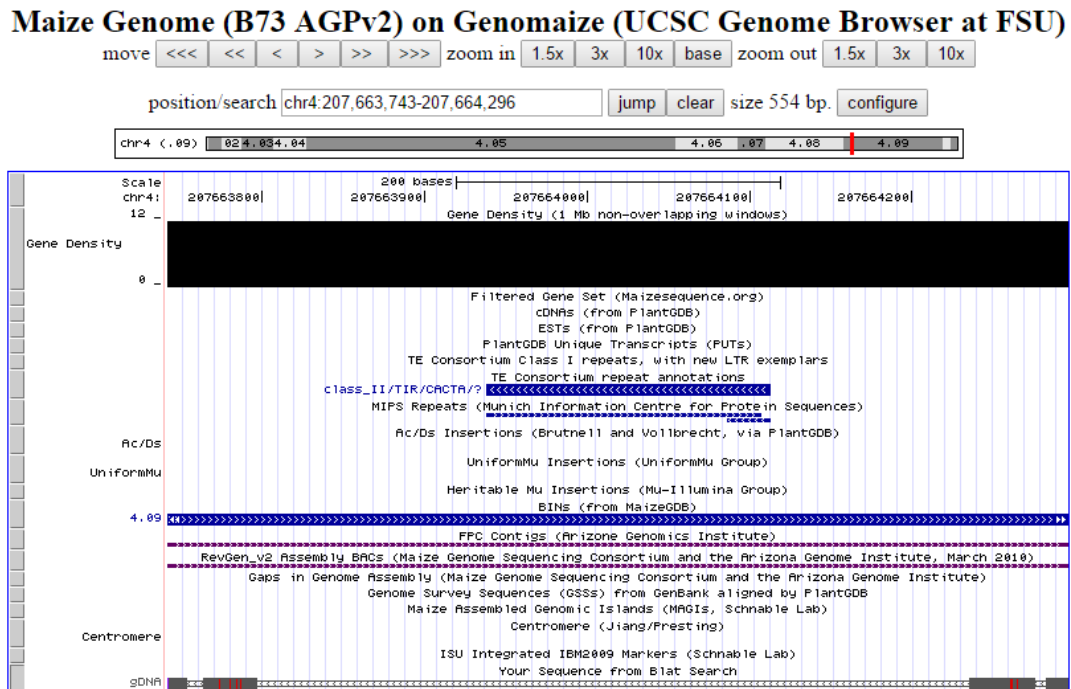


Figure 3.10. Screen shot of the output of the BLAT search: the *br2:NC238* insertion sequence (black/dotted box called gDNA) aligned with low similarity to a class II transposable element (blue box).

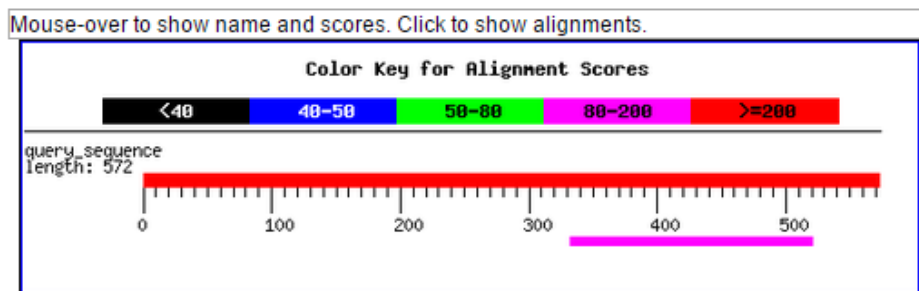
The other matches were in regions where no genes or transposable elements are annotated.

The interrogation of the DNA collections did not find significant alignments of the *br2:NC238* insertion with the Maize genome sequences. Thus a search in the databases collecting repeats and transposable element sequences was performed.

TIGR Plant Repeat Database is a collection of repetitive DNA sequences of 12 plant genera (Arabidopsis, Brassica, Glycine, Hordeum, Lotus, Lycopersicon, Medicago, Oryza, Solanum, Sorghum, Triticum and Zea) from GenBank and other published records based on their annotation (Ouyang, 2004). Interrogation of TIGR Zea Repeats DB through the Web BLAST Server - on default settings - indicated a similarity of the transposon with a Maize mPIF364 MITE element (figure 3.11). The similarity was 116/197 bases and regarded the 3'

half of the *br2:NC238* transposon. mPIF364 is 370 bp long, and belongs to the maize Tourist-like MITE family called miniature PIF (mPIF).

Distribution of Blast Hits on the Query Sequence



```
>ZRSiTEM05900009 gi|16225220|gb|AF416321.1|AF416321 Zea mays clone mPIF364
      mPIF miniature inverted-repeat transposable element
      Length = 370

Plus Strand HSPs:

Score = 148 (28.3 bits), Expect = 3.3, P = 0.96
Identities = 116/197 (58%), Positives = 116/197 (58%), Strand = Plus / Plus

Query:   332 ACGTTGCAAGGTCGACGCA-ACAAGCCAATCGAGACTGCA-GGTATGTGATCAGGAAAC- 388
          || || ||| || | || ||| ||| ||| ||| ||| ||| ||| ||| |||
Sbjct:   90  ACTTTCCAAAGTT-AT-CATATAAGTCTATCTCAAATTCATGGGGTGAGAGATGAAAATT 147

Query:   389 -ACTCCATTGTTTTT-TCCTTGCTTGCAAATTGCAATCGATAGGCAAATGATT-TACT 445
          | || ||| ||| ||| ||| ||| ||| ||| ||| ||| ||| ||| |||
Sbjct:   148 GATTCTATAGATTTACATGCTATGTTTCCGATGTATAACTTATAC-CACACTATTCTATT 206

Query:   446 TATAAACTA-AAGTT-TATGTTAGTTAATTCTCCAATCTAAATACATATGGTTAATTGC 503
          || ||| ||| ||| ||| ||| ||| ||| ||| ||| ||| ||| |||
Sbjct:   207 TACTTTGCTATAACATATATGT-AGTATATAA--CTATCTCTCTA-ATATAATTTA--G- 259

Query:   504 AATATTATATAAATATA 520
          ||| ||| ||| ||| ||| ||| ||| ||| ||| ||| ||| ||| |||
Sbjct:   260 AATAATATATAAATATA 276
```

Figure 3.11. Result of the interrogation of the TIGR DB that indicated the similarity of *br2:NC238* insertion with a mPIF element.

The search against the TIGR Zea Repeats TEs DB using the BLASTn two sequences alignment tool - at personalized parameters to find weak similarities - produced 187 BLAST HITS. Most of these were mPIF elements and sequences of copia-like retrotransposon. In some cases the query aligned many times to the transposable element sequence. All the alignments of the transposon to the genome were short partial sequences of TE, mainly 11 or

13 bp length. Most of the matches were AT-rich regions. Considering the richness in repetitive sequences of the maize genome the information obtained from this alignment may not be significantly relevant.

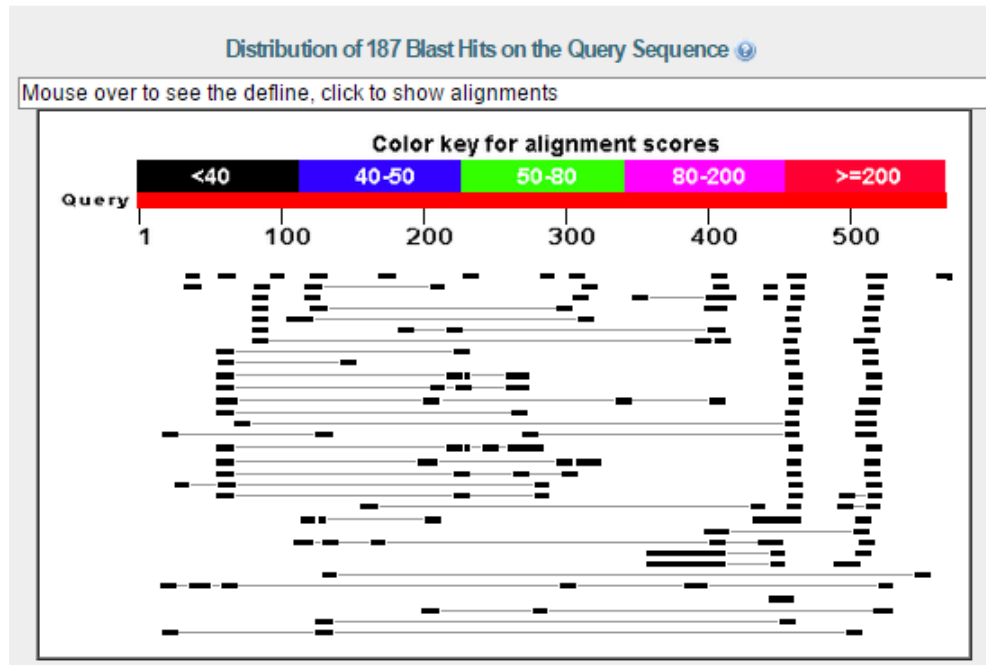


Figure 3.12. Output of the alignment against the TE sequence collection using BLASTn tool. The *br2:NC238* insertion sequence aligned with many transposons of the *Zea* collection.

Sequence	Transposable element type	Number of matches
TATATAAATATA	pPIF MITE	23
AAGTTTATGTT	copia-like retrotransposon	23
CATATACACGT	Ty1-copia type retrotransposon reverse transcriptase gene	6
AAGTTTATGTT	copia-like retrotransposon	20

Table 3.3. List of the most frequent TEs sequences that align to the *br2:NC238* insertion, their family and number of matches.

The first BLASTn output sequence was the ZRSiTEMT05700002 gi|13375369|nt96-280 *Zea mays* transposon Heart healer, a MITE transposable elements. Heart healer matched twice

along the transposon sequences: 449-AAACTAAAGTTTAT-462 and 452-CTAAAGTTTAT-462, 13/14(93%) and 11/11 (100%) identities, respectively.

A CLUSTAL alignment showed sequence similarities between the 3' end of the *br2* transposon and Heart healer and respectively in the alignment below).

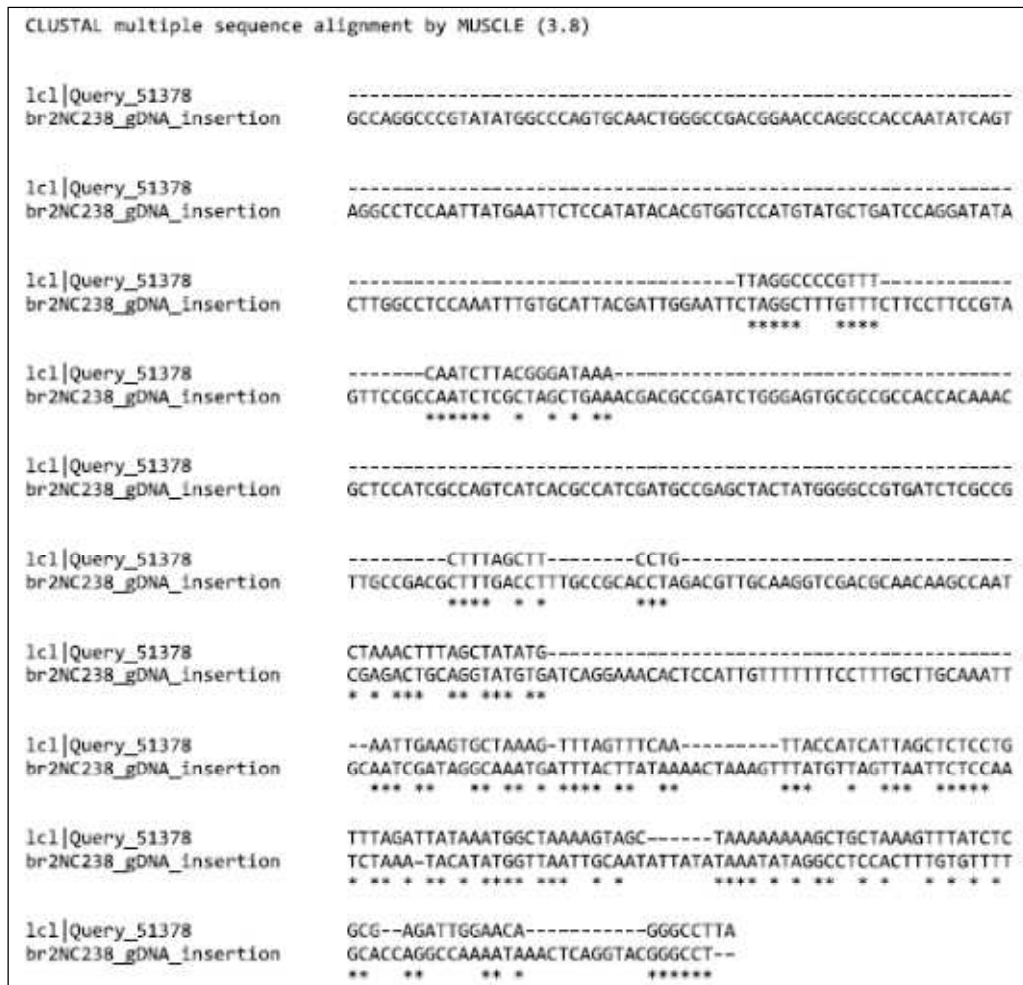


Figure 3.13. Alignment between the *br2:NC238* insertion sequence (called *br2NC238_gDNA_insertion* in the figure) and the Heart Healer transposon (called *Query_51378*) sequence.

Considering the other matches, 21 were other MITEs, 20 of these are mPIF type. Many matches were retrotransposon regions. TE families are often characterized by similarities in TIRs. However, in our cases none of the matches aligned with the TIRs of the transposon. Twenty hits were copia-like retrotransposon leader regions. These alignments were mainly located at the 3'-end of the sequence.

One hit was a copia-like retrotransposon reverse transcriptase gene-3'end that matches the two sequences TACTTGGCCTCCA and CGACGCCGATC; five results were Ty1-copia type retrotransposon reverse transcriptase gene that aligned to the sequence CATATACACGT.

Two hits were Ty1-copia type retrotransposon.

8 hits were LTR retrotransposon regions. Seven of these were 11 nucleotides long, 100% similar to the transposon sequence, the other one was 26/34 - 76% similar.

Five hits were transposase/putative transposase:

- ZRSiTETN00300014 gi|7673676|gb|AF247646.1|AF247646 Zea mays transposon Jittery transposase gene, complete cds ||Mu-like,
- ZRSiTETN00400004 gi|18419549|gb|AF432586.1| Zea diploperennis clone Zd132 transposon mariner-like transposase pseudogene, partial sequence,
- ZRSiTERTOOT00134 (gi|18568260) Zea mays clone ZMMBBb_Z195D10 putative transposase,
- ZRSiTETNOOT00019 gi|10441443:1-864 Zea mays transposon Doppia transposase DOPD and transposase DOPA mRNA, complete cds,
- ZRSiTETN00300014 gi|7673676|gb|AF247646.1|AF247646 Zea mays transposon Jittery transposase gene, complete cds ||Mu-like.

A hit was a 11 nucleotides long gag/pol region: ZRSiTERTOOT00328 gi|17082476|nt151800-150927 Zea mays Huck1a gag/pol.

The search against the Zea maize MITEs DB in particular, aligning the transposon sequence and the Zea MITE DB from the Plant Repeat DB using BLASTn web tool, showed that MITE sequences aligned mostly at the 3' side of the transposon in a AT-rich region. In fact, 30 matches were or did contain the sequence "TATATAAATATA" while the sequence "AAACTAAAGTTTAT" aligned tree times.

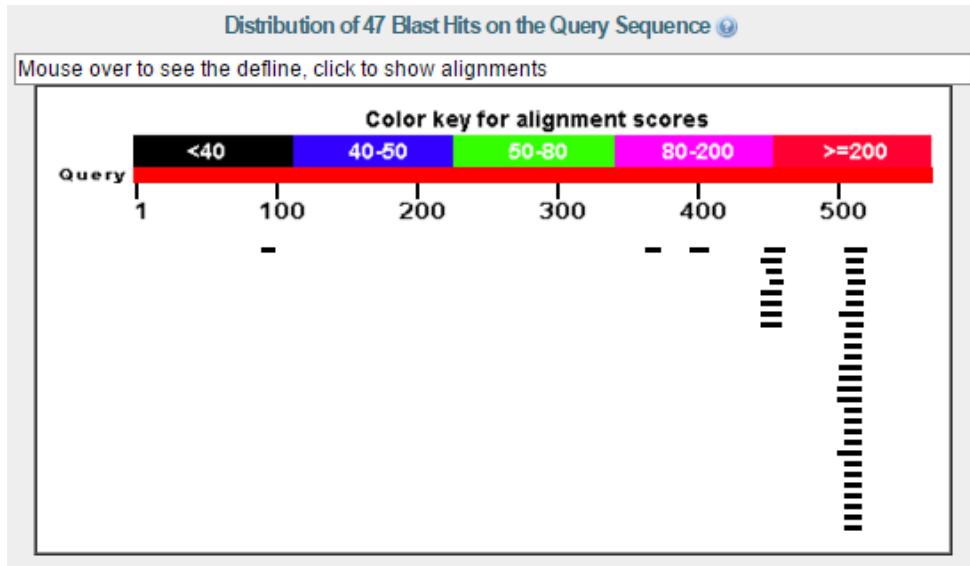


Figure 3.14. BLAST output of the search against the Zea maize MITEs DB indicated similarities of the 3' end of the *br2:NC238* insertion with many MITE elements.

The alignments with the Maize TE database found 172 similar regions. These are short regions with a maximum query coverage of 12%. The BLAST results showed similarities of many regions of the transposon, especially at the 3' end, with several transposable elements.

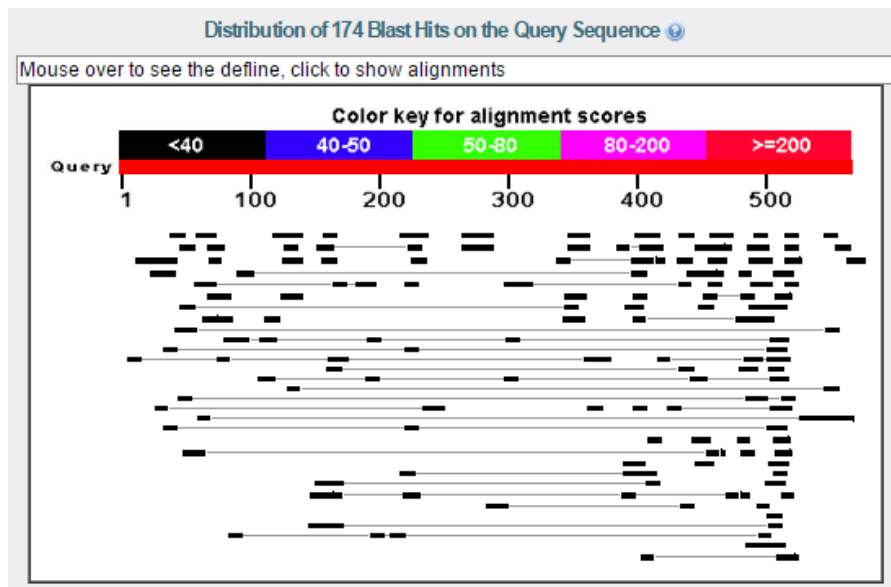


Figure 3.15. Output of the alignment of the *br2:NC238* insertion with the Maize TE database showed several matches with the TEs. In several cases, the insertion sequence aligned with many inner regions of the TE.

Results of the alignment were both DNA transposons and retrotransposons orders and superfamilies. Most of these alignments were AT-rich regions. Most of the results were hAT superfamily DNA transposons. A summary of the result is listed below (table 3.4).

Code	Class	Order	Superfamily	Number of matches
DTM	DNA	TIR	Mutator	12
DHH	DNA	Helitron	Helitron	5
DTH	DNA	TIR	Harbinger	25
RST	RNA	Non-LTR SINE	tRNA	18
RIL	RNA	Non-LTR	L1	2
DTA	DNA	TIR	hAT	53
DTC	DNA	TIR	Cacta	7
RLG	RNA	LTR	Gypsy	3
RLX	RNA	LTR	unknown	5
RLC	RNA	LTR	Copia	1

Table 3.4. Summary of the alignment of the *br2:NC238* insertion with the TEs database collection indicating the transposons classifications and the frequencies of matching.

p-MITE database contains more than 2 million MITE-related sequences of 3,527 MITE families, identified from 41 sequenced plant genomes. The interrogation of the p-MITE DB using the BLAST tool indicated 6 matches with 6 different MITE trasposable elements of *Setaria italica*.

Distribution of 6 Blast Hits on the Query Sequence

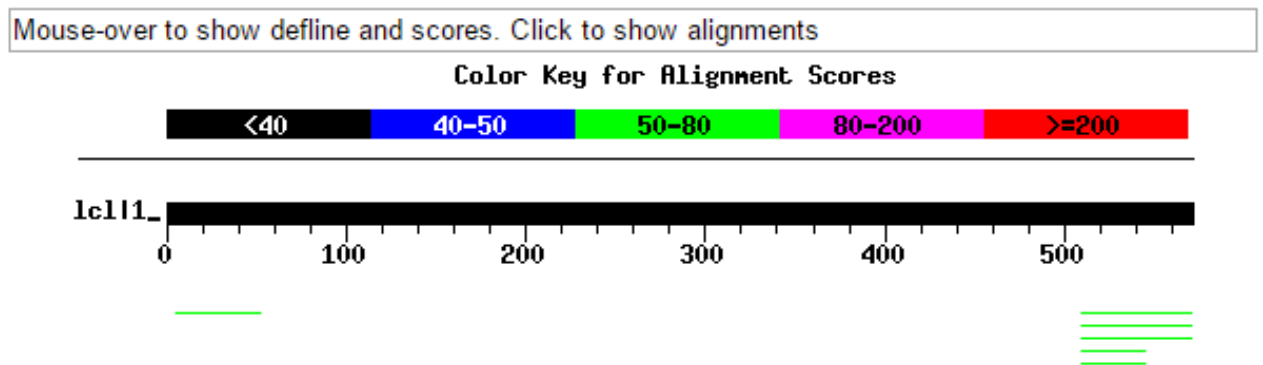


Figure 3.16. Screen shot of the output of the Plant MITE DB interrogation.

These MITE belonged all to the hAT superfamily of the TIR order. This result confirmed the previous output of the Maize TE DB search indicating similarities with many hAT MITE sequences. The first hit aligned to the 5' of the transposon, however it did not include the first six nucleotides of the TIR. The other five sequences aligned to the 3' ends of the transposon, spanning part of the central region and including the entire TIRs sequences of the transposon. However, no similarities were found between the 5'-TIRs of these elements and the transposon's ones.

Hit	Query position	Subject position	Subject length	Similarity	Strands	Transposon class/order/superfamily	Specie
1	6-53	5-52	63	43/48 (89%)	Plus plus	MITE family DTA_Sei20, SuperFamily hAT	<i>Setaria italica</i>
2	510- 571	51-112	114	53/62 (85%)	Plus plus	MITE family DTA_Sei20, SuperFamily hAT	<i>Setaria italica</i>
3	510- 571	55-115	117	54/62 (87%)	Plus plus	MITE family DTA_Sei20, SuperFamily hAT	<i>Setaria italica</i>
4	510- 571	61-121	122	54/62 (87%)	Plus plus	MITE family DTA_Sei20, SuperFamily hAT	<i>Setaria italica</i>
5	510- 546	60-95	121	35/37 (94%)	Plus plus	MITE family DTA_Sei20, SuperFamily hAT	<i>Setaria italica</i>
6	510- 546	68-103	106	35/37 (94%)	Plus plus	MITE family DTA_Sei20, SuperFamily hAT	<i>Setaria italica</i>

Table 3.5. Summary of the BLAST HITS of the P-MITE database search indicating positions, length and similarities of the TEs and their classification.

In conclusion, interrogation of DBs showed the *br2:NC238* insertion sequence aligned with many transposable element sequences. These were both class I and class II elements, from many plant species. However, none of these alignments was significant. Perfect matches were mainly short sequences 11 or 13 nucleotides long and most of the sequences were repeats. Thus, it was not possible to assign *br2:NC238* insertion to a known TE family. However, the structural traits of the *br2:NC238* insertion indicated it belongs to a MITE family: the presence of TIRs and TSD, the short length, the isolation of a revertant plant that retained the TSD.

3.3.3 Analyses of *br2:NC238* line *abcb1* transcript

The transposon that characterized the *br2:NC238* mutant is inserted inside an intron (figure 3.4). The RNA splicing removes the introns to produce the mature transcript that will be transcribed into protein. In order to verify if the transposon insertion causes alterations in gene transcription, the sequencing of *abcb1* cDNA from *br2:NC238* and its revertant line seedlings coleoptile and roots was performed

The gene structure made the amplification and sequencing of the full length *abcb1* cDNA difficult. First, the length of T01 transcript - 4672 bp - did not allow the amplification and cloning of the full-length cDNA. Second, the difficult in designing functional gene/isoform specific primers for the amplification of the *abcb1* cDNA prevented the amplification of the desired regions of the gene. In fact, the similarities of the functional transcript form T01 with the annotated alternative splicing variant T02 and the other members of the ABCB family - more than 40 genes - is very high (Yue et al., 2015). Moreover, the high GC content and the gene internal repeats further reduced the number of suitable primers.

For this reason, the analysis of *br2:NC238* and its revertant line *abcb1* transcripts was performed amplifying and sequencing short overlapped regions of the cDNAs. Positions of the primers along the *abcb1* sequence are shown in figure 3.17.

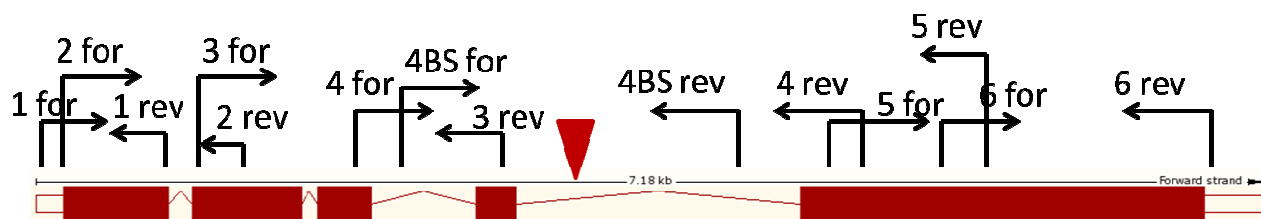


Figure 3.17. The *abcb1* gene represented with the intron/exon structure and the primers used for its sequencing (for=forward, rev= reverse). Triangle represents the position of the transposon insertion in the corresponding genomic sequence. For the primer sequences see table 3.1.

RT-PCR of both the revertant line and the *br2:NC238* cDNA to amplify the 5' side of the *abcb1* transcript (using primers 1for plus 1rev to amplify from start codon to T₄₃₄, 2for plus

2rev to amplify from C₁₀₃ to C₉₇₁, and 3for plus 3rev to amplify from C₇₇₉ to A₁₇₃₈) produced amplicons overlapping the B73 reference genome transcript. RT-PCR with 4for primer (designed on exon III, figure 3.16) and 4rev primer (designed at the beginning of exon V) was performed to amplify the central region of the transcript (from A₁₄₇₆ up to C₂₆₄₈, figure 3.16). This CDS region (from A₁₄₇₆ to C₂₆₄₈) corresponds to the genomic region that flanked intron IV, and thus the transposon insertion. The RT-PCR product from the revertant line was a single band, which sequence was 100% similar to the wild type B73, despite the presence of the 6 bp TDS in the intronic region of the gene (figure 3.7). RT-PCR of the same region in *abcb1 br2:NC238* transcript produced several bands. This suggested that the presence of the transposon in *abcb1* intron IV causes alternative splicing of the gene. Sequencing of many of these splicing variant fragments indicated they contained part of the transposon and/or part of intron IV. The similarity, close size and low expression of the splicing variants did not allowed the separation and cloning of all the bands, neither the design of specific primers was possible. Moreover, the high GC content of the isoforms - in some cases >75% - did not allow the amplification of their full length sequence.



Figure 3.18. RT-PCR with primers 4for plus 4rev to amplified the *br2:NC238 abcb1* central region (from A₁₄₇₆ up to C₂₆₄₈) produced several DNA bands corresponding to the different splicing variants of the mutated gene.

rev_cDNA_4	CTGCTGCTGGGGCGGGACAGCCAGAGCGCGACGCTGGCGGAGATGGAGGAGGCGGCCAGG
br2_cDNA_clone5	CTGCTGCTGGGGCGGGACAGCCAGAGCGCGACGCTGGCGGAGATGGAGGAGGCGGCCAGG
	Exon IV 1948
rev_cDNA_4	GTGGCCAACGCCACTCCTTCATCATCAAAC TCCCGACGGCTACGACA C -----
br2_cDNA_clone5	GTGGCCAACGCCACTCCTTCATCATCAAAC TCCCGACGGCTACGACACGCAGTTCCGC
	br2:NC238 insertion
rev_cDNA_4	-----
br2_cDNA_clone5	CAATCTCGCTAGCTGAAACGACGCCGATCTGGGAGTGCGCCGCCACCACAAACGCTCCAT
rev_cDNA_4	-----
br2_cDNA_clone5	CGCCAGTCATCAGCCATCGATGCCGAGCTACTATGGGGCCGTGATCTCGCCGTTGCCGA
rev_cDNA_4	-----
br2_cDNA_clone5	CGCTTTGACCTTTGCCGCACCTAGACGTTGCAAGGTCGACGCAACAAGCCAATCGAGACT
	1949
rev_cDNA_4	G CAGGTTGGGGAGCGCGGCTGCAGCTCTCCGGTGGGCAGAGCAGCGCATCGCCATCGC
br2_cDNA_clone5	GCAGGTTGGGGAGCGCGGCTGCAGCTCTCCGGTGGGCAGAGCAGCGCATCGCCATCGC
	Exon V

Figure 3.19. Clone of the splicing form characterized by a insertion 190bp long. The insertion aligned to the central part of the *br2:NC238* intronic insertion. Numbers indicate the position of the squared nucleotide.

A	br2_cDNA_clone2.1	-----Exon IV-----GC
	gDNA PGP1	GCGGGACAGCCAGAGCGCGACGCTGGCGGAGATGGAGGAGGCGGCCAGGGTGGCCAACGC
	T01 cDNA	GCGGGACAGCCAGAGCGCGACGCTGGCGGAGATGGAGGAGGCGGCCAGGGTGGCCAACGC
		Intron IV
	br2_cDNA_clone2.1	CCACTCCTTCATCATCAAAC TCCCGACGGCTACGACACGCAGGTCGGTCCCGTATAGCT
	gDNA PGP1	CCACTCCTTCATCATCAAAC TCCCGACGGCTACGACACGCAGGTCGGTCCCGTATAGCT
	T01 cDNA	CCACTCCTTCATCATCAAAC TCCCGACGGCTACGACACGCAGG T -----
		1954
	br2_cDNA_clone2.1	AGCTCACTAGCTGCACTGCCACTTCTCTCGCTTGTCTCCACCGTTGCTGCCTGTTGCTC
	gDNA PGP1	AGCTCACTAGCTGCACTGCCACTTCTCTCGCTTGTCTCCACCGTTGCTGCCTGTTGCTC
	T01 cDNA	-----
	br2_cDNA_clone2.1	TCCAATCCACTTGTGGTGCTGGACCACACGTCGCTGCTTGCCCTAGCTGCTCCACATCT
gDNA PGP1	TCCAATCCACTTGTGGTGCTGGACCACACGTCGCTGCTTGCCCTAGCTGCTCCACATCT	
T01 cDNA	-----	
B	br2_cDNA_clone2.1	-----Intron IV-----
	gDNA PGP1	AGGTGTGTATGCAGCGTCAAGTCATCCATCCGTCCACTCCACTCACTCATGCGCCGCGC
	T01 cDNA	-----
		br2:NC238 insertion
	br2_cDNA_clone2.1	CAGGCCCGTATATGGCCAGTGCAACTGGGCCGACGGACCAGGCCACCAATATCAGTAG
	gDNA PGP1	-----
	T01 cDNA	-----
	br2_cDNA_clone2.1	GCCTCCAATTATGAATTCTCCATATACAGTGGTCCATGTATGCTGATCCAGGATATACT
	gDNA PGP1	-----
	T01 cDNA	-----
	br2_cDNA_clone2.1	TGGCCTCCAATTGTGCATTACGATTGGAATTCTAGGCTTTGTTTCTTCCTTCCGTAGT
	gDNA PGP1	-----
T01 cDNA	-----	

Figure 3.20. Clone characterized by the retaining of part of the intron (box A) and a insertion (box B) that aligned to the central region of the *br2:NC238* intronic insertion

br2_cDNA_clone2.5	CTCCTTCATCATCAAACCTCCCGACGGCTACGACGCGCAGTTCCGCCAATCTCGCTAGCT
rev_cDNA_4	CTCCTTCATCATCAAACCTCCCGACGGCTACGAC[<u>C</u>]-----
	Exon IV 1946
br2_cDNA_clone2.5	GAAACGACGCCGATCTGGGAGTGGCCGCCACCACAAACGCTCCATCGCCAGTCATCAGC
rev_cDNA_4	-----
br2_cDNA_clone2.5	CCATCGATGCCGAGCTACTATGGGGCCGTGATCTCGCCGTTGCCGACGCTTTGACCTTTG
rev_cDNA_4	-----
br2_cDNA_clone2.5	CCGCACCTAGACGTTGCAAGGTCGACGCAACAAGCCAATCGAGACTGCAGGTTGGGGAGC
rev_cDNA_4	-----ACG[<u>C</u>]CAGGTTGGGGAGC
	1949 Exon V
br2_cDNA_clone2.5	GCGGCCTGCAGCTCTCCGGTGGGCAGAAAGCAGCGCATCGCCATCGCCCCGCCATGCTCA
rev_cDNA_4	GCGGCCTGCAGCTCTCCGGTGGGCAGAAAGCAGCGCATCGCCATCGCCCCGCCATGCTCA

Figure 3.21. Clone characterized by an insertion that aligned to the central region of the *br2:NC238* intronic insertion

		Exon III
A	br2_cDNA_clone36	-----AtCtTcCgCaTcAtCgAcCaCaGgCcG
	T01 cDNA	GCGTTCGCCAAGGCGCGTGTGGCGGCTGCCAAGATCTTCCGCATCATCGACCACAGGCCG
	gDNA PGP1	GCGTTCGCCAAGGCGCGTGTGGCGGCTGCCAAGATCTTCCGCATCATCGACCACAGGCCG
br2_cDNA_clone36	gGcAtCtCcTcGcGcGgCgGcGcGgAgCcAgAgTcGgTgAcGgGgCgGgTgGaGaTgCgG	
T01 cDNA	GGCATCTCCTCGCGCAGCGCGCGGAGCCAGAGTCGGTGACGGGGCGGGTGGAGATGCGG	
gDNA PGP1	GGCATCTCCTCGCGCAGCGCGCGGAGCCAGAGTCGGTGACGGGGCGGGTGGAGATGCGG	
br2_cDNA_clone36	gGcGtGgAcTtCgCgTaCcCgTcGcGgCcGgAcGtCcCcAtCcTgCgGcTtCtCgCtG	
T01 cDNA	GGCGTGGACTTCGCGTACCCGTCGCGGCCGACGTCCCCATCCTGCGGGCTTCTCGCTG	
gDNA PGP1	GGCGTGGACTTCGCGTACCCGTCGCGGCCGACGTCCCCATCCTGCGGGCTTCTCGCTG	
br2_cDNA_clone36	aGcGtGcCcGcCgGgAaGcCcAtCgCgCtGgTgGgCaGcTcCgGcTcCgGgAaGcAcG	
T01 cDNA	AGCGTGCCCGCGGGAAGACCATCGCGCTGGTGGGCAGCTCCGGCTCCGGGAAGAGCACG	
gDNA PGP1	AGCGTGCCCGCGGGAAGACCATCGCGCTGGTGGGCAGCTCCGGCTCCGGGAAGAGCACG	
		Intron III
br2_cDNA_clone36	gTgTgTcGtCtCaTcGaGaGtTtCtAcGaCcCcAgC-----	
T01 cDNA	GTGGTGTGCTCATCGAGAGATTCTACGACCCAGC-----	
gDNA PGP1	GTGGTGTGCTCATCGAGAGATTCTACGACCCAGCAGGTATACTAGTACTGTTACT	
		Exon IV
B	br2_cDNA_clone36	-----aCaGgGcAaAt
	T01 cDNA	-----GCAGGGCAAAT
	gDNA PGP1	TCAGACAAAAAAGAAGAAGAACGAGATGAAGTCTGCAATTCGGTTTTGGCAGGGCAAAT
br2_cDNA_clone36	CcTgCtGgAcGgGcAcGaCcTcAgGtCgCtGgAgCtGcGgTgGcTgCgGcGgCaGaTcGg	
T01 cDNA	CCTGCTGGACGGGCACGACCTCAGGTCGCTGGAGCTGCGGTGGCTGCGGCGCAGATCGG	
gDNA PGP1	CCTGCTGGACGGGCACGACCTCAGGTCGCTGGAGCTGCGGTGGCTGCGGCGCAGATCGG	
br2_cDNA_clone36	GcTgGtGgAcCaGgAgCcGgCgCtGtTcGcGcGgAgCaTcAgGgAgAaCcTgCtGcTgGg	
T01 cDNA	GCTGGTGAGCCAGGAGCCGGCGCTGTTCCGCGACGAGCATCAGGGAGAACCCTGCTGCTGGG	
gDNA PGP1	GCTGGTGAGCCAGGAGCCGGCGCTGTTCCGCGACGAGCATCAGGGAGAACCCTGCTGCTGGG	
br2_cDNA_clone36	GcGgGaCaGcCaGaGcGcGaCgCtGgCgGaGgTgGgAgGcGgCcAgGgTgGcCaAcGc	
T01 cDNA	GCGGGACAGCCAGAGCGCGACGCTGGCGGAGATGGAGGAGGCGCCAGGGTGGCCAAACGC	
gDNA PGP1	GCGGGACAGCCAGAGCGCGACGCTGGCGGAGATGGAGGAGGCGCCAGGGTGGCCAAACGC	
		Intron IV
br2_cDNA_clone36	CcAcTcTcTcAtCaTcAaAcTcCcCgAcGgCtAcGaCaCgCaGgTcCgTcCcGtAtAgCt	
T01 cDNA	CCACTCCTTCATCATCAAACCTCCCGACGGCTACGACAC-----	
gDNA PGP1	CCACTCCTTCATCATCAAACCTCCCGACGGCTACGACACGACGAGGTCCGTCCCGTATAGCT	

		Intron IV
br2_cDNA_clone36		CcAcTcCtTcAtCaTcAaAcTcCcCgAcGgCtAcGaCaCgCaGgTcCgTcCcGtAtAgCt
T01 cDNA		CCACTCCTTCATCATCAAACCTCCCCGACGGCTACGACAC-----
gDNA PGP1		CCACTCCTTCATCATCAAACCTCCCCGACGGCTACGACACGCAGGTCCGTCCCGTATAGCT
br2_cDNA_clone36		AgCtCaCtAgCtGcAcTgCcAcTtCtCtCgCtTgCtCcCcAcCgTtGcTgCcTgTtGcTc
T01 cDNA		-----
gDNA PGP1		AGCTCACTAGCTGCACTGCCACTTCTCTCGCTTGCTCCCCACCGTTGCTGCCTGTTGCTC
br2_cDNA_clone36		TcCaAtCcAcTtGtCgGtGtCtGgAcCaCaCgTgCcTgCtTgCcTaGcTgCtCcAcAtCt
T01 cDNA		-----
gDNA PGP1		TCCAATCCACTTGTGCGGTGTCTGGACCACACGTGCCTGCTTGCTTAGCTGCTCCACATCT
br2_cDNA_clone36		GcTtTcCcTgTcCaAcCtTaTgCaAcTcAcTcTaAtAcTaTaTcAaAtAcAtTtCtAgAg
T01 cDNA		-----
gDNA PGP1		GCTTCCCTGTCCAACCTTATGCAACTCACTCTAATACTATATCAAATACATTTCTAGAG
br2_cDNA_clone36		TtTaAaGcTtAtCtTaGaAtAaAtGcAtCtTtAgCtAcGaGaCaAcCtAaCtTcAgTtGt
T01 cDNA		-----
gDNA PGP1		TTTAAAGCTTATCTTAGAATAAATGCATCTTTAGCTACGAGACAACCTAACTTCAGTTGT

		Intron IV
br2_cDNA_clone36		AgGtGtGtAtGcAgCgTcAaGtCaTcCaTcCgTtCcAcTcCaCtCaCtCaTgCgTcGcGc
T01 cDNA		-----
gDNA PGP1		AGGTGTGTATGCAGCGTCAAGTCATCCATCCGTTCCACTCCACTCACTCATGCGTCGCGC
br2_cDNA_clone36		br2:NC238 insertion
T01 cDNA		CaGgCcCgTaTaTgGcCcAgTgCaAcTgCcAgTgCaAcTgGgCcGaCgGaAcCaGgCcAc
gDNA PGP1		-----
br2_cDNA_clone36		CaAtAtCaGtAgGcCtCcAaTtAtGaAtTcTcCaTaTaCaCgTgGtCcAtGtAtGcTgAt
T01 cDNA		-----
gDNA PGP1		-----
br2_cDNA_clone36		CcAgGaTaTaCtTgGcCtCcAaAtTtGtGcAtTaCgAtTgGaAtTcTaGgCtTtGtTtCt
T01 cDNA		-----
gDNA PGP1		-----

Figure 3.22. Clone that retained part of intron IV (box B, box C) and had a insertion that partially aligned to the *br2:NC238* intronic insertion (box D).

Amplification of the 3'-end of *abcb1* transcript of the *br2:NC238* (primers 5for plus 5rev from C₅₁₁₃ to T₆₀₇₆, and 6for plus 6rev from T₅₅₅₆ to G₆₉₉₅, figure 3.17) produced two different sequences: the wild type 3'-end sequence and a sequence that lacks 860 bases.

Also amplification of the 3'-end of *abcb1* transcript of the revertant plant produced two different sequences: the wild type 3'-end sequence and a sequence characterized by a 967 base long gap.

In order to exclude a tissue-specific splicing form localization, RT-PCR were repeated on both roots and aerial part of seedlings. The same DNA forms were obtained.

GRAMENE maize sequence database annotated a putative ABCB1 splicing variant sequence (figure 3.23). This transcript is a truncated version of ABCB1 that contains only four out of five exons and its last exon is 230 bp longer than the canonical ABCB1 transcript (figure 3.23, B). Amplification using gene-specific primers (for8 plus rev8, figure 3.17) of the cDNA from seedling coleoptile and root RNA, and sequencing of the amplicons, confirmed the presence of the splicing form in *br2:NC238* tissues.

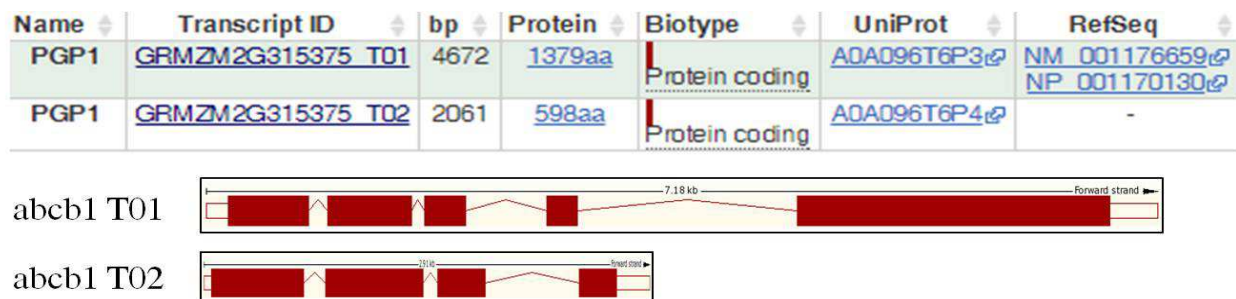


Figure 3.23. The *abcb1* T01 and the predicted splicing variant T02. A) Data from Gramene DB. B) Comparison between the intron/exon structure of *abcb1* T01 (top) and its splicing variant T02 (bottom).

3.3.4 Expression analyses of *abcb1* and other auxin transporter encoding genes

br2:NC238 mutant is characterized by the shortening of the lower internodes of the stem. The mutation is due to a transposon insertion in *abcb1* gene that led to alter its transcription producing several splicing forms that include or not intron IV and/or part of the transposon sequence. A predicted splicing variant, *abcb1* T02, is annotated in the Maize Genome Database.

Expression analyses of *abcb1* and other auxin transporter encoding genes were performed in order to:

1. identify the tissues and the stages of *abcb1* expression, as well as its T02 splicing form expression;
2. verify alterations in auxin transporter expression profiles in the *br2:NC238* plant.

RT-PCR on 7-leaf-old revertant plant tissues indicated *abcb1* mRNA was highly expressed at nodal tissues compared to internode, shoot apical meristem, and leaf (figure 3.24). This result suggests a function of the ABCB1 protein in exporting auxin from the upper internode to the lower one, as previously suggested by Knöller (Knöller et al., 2010).

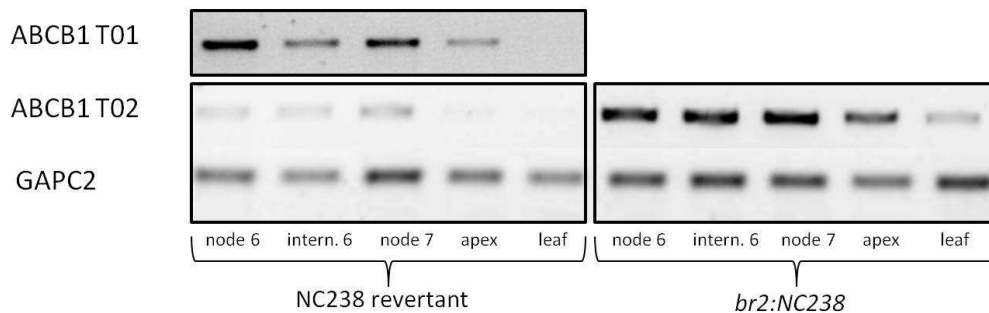


Figure 3.24. Expression analyses of *abcb1* transcript at 7-leaf-old stage.

abcb1 transcript was also detected at 3-leaf-old stage, suggesting a role of ABCB1 protein starting from the early stages of the stem development (figure 3.25).

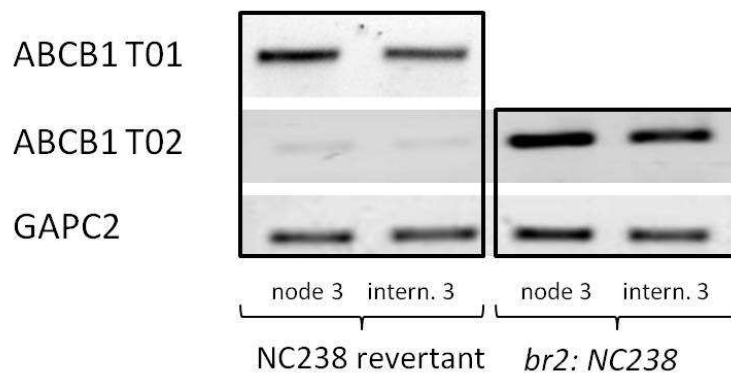


Figure 3.25. Expression analyses of *abcb1* transcript at 3-leaf-old stage.

The mutant phenotype was not visible until the *br2* plants were 7-leaf-old. Thus, the mutant phenotype was evident at a much more later development stage than the stage the mutated gene transcript was detectable.

The lack of a phenotype during the first developmental stages of the *br2:NC238* mutant might be due to the presence of the necessary amount of auxin, despite its defective transport due to the mutant ABCB1. Indeed, auxin might also be transported by other carriers in the tissues. Together with passive diffusion, auxin can move through many other carriers: ABCBs, PINs, PIN-LIKEs and AUX/LAXes carrier types. In fact, in the mutant line, an alteration of other auxin transporters expression profiles, compared to the revertant plant tissues, was observed. A general increased in the transcription levels of AUX1, PIN1a, -2, -8 and -9 was observed (figure 3.26).

Alteration in the expression levels of PIN mRNAs was already observed in *br2* mutant roots (Forestan et al., 2012). Moreover, it was previously demonstrated that IAA treatment alters auxin transporter expression, increasing many PIN genes expression levels in maize shoot, while reducing the expression of other PINs, LAXes and ABCBs (Yue et al., 2015). Higher AUX1 expression levels, especially in the 6th internode, were recorded in *br2* plants. Little is known about AUX/LAX carriers. Five AUX/LAX have been recently identified in maize (Yue et al., 2015). In *Arabidopsis thaliana*, AUX1 belongs to a small multigene family comprising four highly conserved genes that have all auxin uptake functions, but regulate distinct auxin dependent developmental processes (Péret et al., 2012). AUX1 is the most characterized AUX/LAX gene in plant. In *Arabidopsis*, mutations within the AUX1 gene confer an auxin-resistant root growth phenotype and abolish root gravitropic curvature (Bennett et al., 1996).

AUX1 transcript is expressed in Arabidopsis root epidermal cells and thus it is supposed to be associated to the basipetal auxin transport (Bennett et al., 1996). The transcript of PIN9, a monocot specific gene, was more expressed in the *br2:NC238* 6th internode compared to the revertant line tissue. Previous expression analyses showed PIN9 was typically expressed in in maize roots and nodes and transcript localization experiments showed it is expressed in the endodermis, pericycle, and in phloem of the central cylinder. Moreover, treating *br2* seedling with the auxin analog NAA resulted in the up-regulation of PIN9 in the root apex (Forestan et al., 2012).

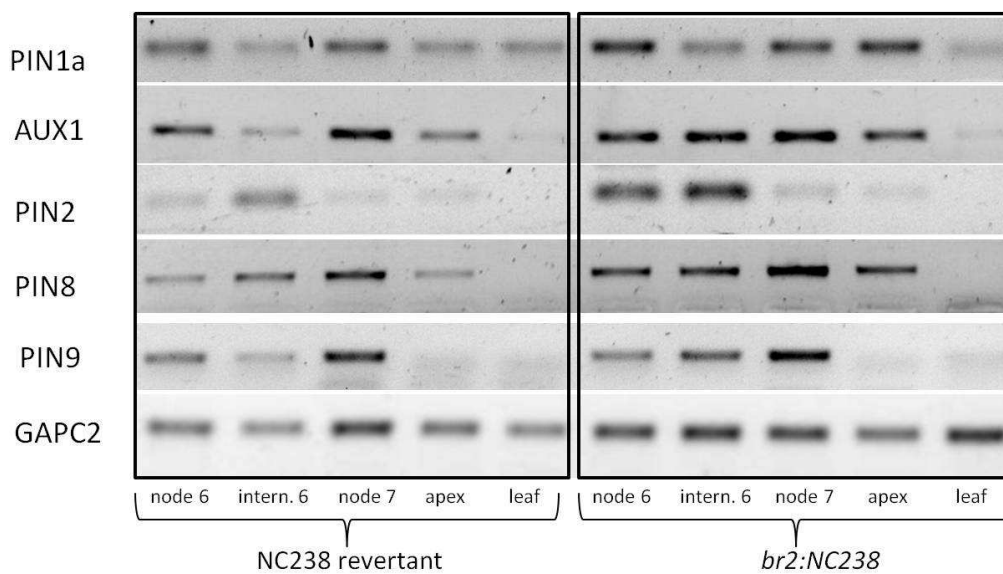


Figure 3.26. Expression analyses of auxin transporters transcript at 7-leaf-old stage.

On the contrary, at 3-leaf-old stage, similar expression profiles of auxin transporters genes were observed in *br2:NC238* and the revertant line tissues (figure 3.27). This is consistent with the normal phenotype of the *br2:NC238* plants at this stage.

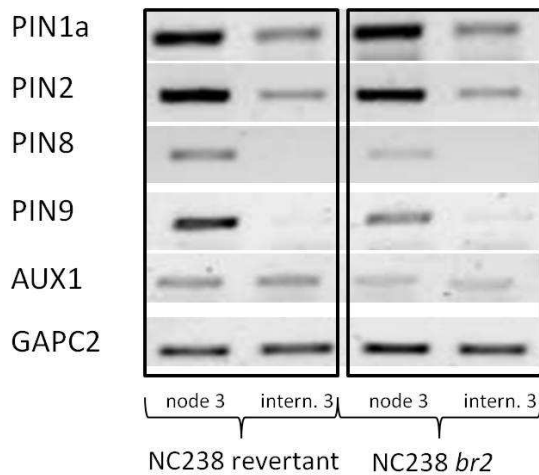


Figure 3.27. Expression analyses of auxin transporters transcript at 3-leaf-old stage.

Moreover, in young plants stem, auxin derives from nearby auxin biosynthetic sites. Auxin biosynthesis happens in young tissues, such as shoot apical meristem, young leaves and root apical meristem. During the first stages of stem development and elongation, young internodes are close to these sites of auxin biosynthesis. Thus, auxin transport from the uppermost part of the plant to the base of the young stem is not as long as it is in the later stages of the stem elongation process. ABCBs are thought to be responsible for the long-distance auxin transport and PINs, as well as AUX/LAX, are thought to be involved in short distance transport and rapid auxin flux redirection, as during the gravitropic response. It is thought that the generally apolar localization of ABCBs is not compatible with the plasticity and the complexity of the terrestrial plants that required dynamic redirection of auxin fluxes. ABCBs transport system is more ancient than PINs one, as shown by phylogenetic analyses that also indicated PINs arose with vascular plants (reviewed in Zazimalová, Murphy, Yang, Hoyerová, & Hosek, 2010). About the predicted *abcb1* splicing variant T02, it was detected in *br2:NC238* plant tissues at both 3- and 7-leaf-old stages. The strong expression of T02 in *br2:NC238* tissues and its low expression in the revertant tissues suggests its increased transcription was an effect of the presence of the mutation in *br2:NC238* line that prevents the normal maturation of the primary transcript.

Altogether the present results suggest:

1. ABCB1 is expressed from the early stages of the stem development, particularly at node level. A minor role of ABCB1 in the first steps of the elongation of the stem is suggested, as plants younger than 6-7-leaf-old showed normal internode length, despite the early transcription of *abcb1* gene in the wild type plant. Expression analyses indicated high levels of the predicted Maize GDB splicing form T02 in *br2:NC238* tissues, rather than the revertant line tissues.
2. Altered expression profiles of other auxin carriers were observed, suggesting other proteins might become (more) involved in auxin transport when the transport through ABCB1 is defective and auxin over or down accumulates.

3.4 Discussion

Allelic tests performed crossing NC238 inbred line with *brachytic* mutants indicated NC238 line is a *br2* mutant (Johal, unpublished). Moreover, preliminary analyses indicated the mutation was due to an insertion in the central region of *abcb1* gene (Johal, unpublished). One of the aims of the present thesis was to study the nature of the mutation in *abcb1* gene in NC238 inbred line.

The characterization of the mutation was performed by amplification and sequencing of the *abcb1* genomic DNA from *br2:NC238* plants and aligning it with the *abcb1* genes of the revertant NC238 line and the wt B73 line reference genome.

The revertant line *abcb1* gene is characterized by a 6bp long insertion (GTCGCG) in intron IV that creates a direct repeat with an adjacent similar existing region. These sequences are also both present twice in *br2:NC238*, where they flank a 572bp inner sequence. The inner sequence corresponds to the duplicated target site (target site duplication, TSD) of the transposon. This region was presumably duplicated in the insertion event and retained after the transposon excision. The length and/or the sequence of the TSDs reflect the enzymatic cleavage properties of transposases and can be used to classify cut-and-paste transposons into different superfamilies. For instance, the *Tc1/Mariner* superfamily is characterized by 5'-TA-

3' TSD (Shao and Tu 2001), and the *piggyBac* superfamily by 5'-TTAA-3' (Sarkar et al. 2003; Mitra et al. 2008). Many hAT elements are characterized by the generation of 8bp target-site duplications after the transposition event, 3bp in the *PIF/Harbinger* superfamily (Zhang et al. 2001), whereas the *Mutator/MuDR* superfamily is associated with TSD ranging in size from 9 to 12bp (Lisch 2002; Marquez and Pritham 2010). However, the class I - transposons of the *Spy* family possess TIRs and encode for a transposase, but do not generate TSD.

The insertion sequence is also characterized by 11bp of imperfect terminal inverted repeats (TIRs).

The presence of 10-30bp TIRs, the TSD, and the short length of the sequence suggested the insertion was a Miniature inverted-repeat transposable element (MITE).

The presence of the insertion and the isolation of its revertant line confirm the capacity of this insertion of moving to other location in the genome, in a way that is typical of the class II transposable elements.

The sequence analysis on NCBI domain database indicated the lacking of known DNA domains. In particular, the lacking of transposase coding sequence, indicates the element is non-autonomous and relies on an autonomous longer transposon for its transposition, reinforcing the hypothesis that the transposon is a MITEs. In fact, MITEs are believed to be "deletion derivatives" of DNA transposons. The best characterized deletion derivative of an autonomous element is the MITE element *mPing*, a rice *Tourist*-like MITE, deletion derivative of the autonomous *Ping* element (Kikuchi et al., 2003; Yang et al., 2007). MITEs are often located in gene-rich euchromatic regions and are associated with genes (Tu, 1997; Han and Wessler, 2010). When close to genes, MITEs can affect their expression. For instance, MITE Kiddo in rice was shown to up-regulate the expression of Ubiquitin2 when inserted in its promoter region (Yang et al., 2005).

Interrogation of the *br2:NC238* transposon sequence against the Maize GDB version 3 by the BLAST tool showed the transposon has similarities with many sequences in the maize genome. These matches are short sequences that do not span any TE and are located in chromosome 2, 8, 4 and 7. One of these output sequence is a locus where a low confidence gene (GRMZM2G580168_T01) is present.

The transposon BLAT search identified many sequences with some similarities of the query in the maize genome database - version 2.

Interrogation of the Zea repeats collection of the TIGR Plant Repeat Database (TIGR_Zea_Repeats.v3.0) through the Web BLAST Server on default settings indicated a similarity of the transposon with a Maize mPIF364 MITE element that belong to the maize Tourist-like MITE family called miniature PIF (mPIF).

Searching against the TIGR Zea Repeats TEs DB using the BLASTn two sequences alignment tool - at personalized parameters to find weak similarities - indicated, also in this search, many similarities with mPIFs. Moreover similarities with copia-like retrotransposon and copia-like reverse transcriptase gene were found. Copia-like or copia elements, together with gypsy, are one of the major subclasses of LTR retrotransposons. Differently from DNA - copy and paste - TEs, LTR TEs propagate through RNA intermediate, they are transcribed and reverse transcribed into a new location by their own encoded reverse transcriptase. They are characterize by terminal inverted repeats but these are much longer than MITEs ranging in size from a few hundred bp to almost 5 kb, depending on the repeat family.

The most significant TIGR Zea Repeats TEs DB output sequence was a Heart healer transposon. Heart healer is classified as MITE transposable elements. Little is known about this transposon in the literature. Investigation on Maize transposon transcription patterns showed Heart healers were expressed in the leaf, flower, shoot apical meristem and endosperm, while no expression was observed in the embryo, ovary, pericarp, root and cell culture (Vicent, 2010).

Similarities with transposase/putative transposases were found: two are *Zea mays* transposon Jittery transposase gene, *Zea diploperennis* clone Zd132 transposon mariner-like transposase pseudogene, *Zea mays* clone ZMMBBb_Z195D10 putative transposase, *Zea mays* transposon Doppia transposase DOPD and transposase DOPA. One match aligns to the *Zea mays* Huck1a gag/pol region.

The search against the Zea maize MITEs DB indicated many similarities with the transposon 3'-side, in a AT-rich region. Several matches regard the "TATATAAATATA" and "AAACTAAAGTTTAT" regions. No literature information is present about these sequences.

Alignment with the Maize TE database showed 172 similar regions of both DNA transposons and retrotransposons orders and super families. Most of these alignments were AT-rich

regions. Many results were hAT superfamily DNA transposons. DNA transposons in the hAT superfamily are widespread in plants and animals and include a number of active, well-studied elements such as the Ac transposon of *Zea mays*, the *hobo* transposon of *Drosophila melanogaster*, the *Hermes* transposon of the housefly *Musca domestica*, and the *Tol2* transposon of the Japanese Medaka fish, *Oryzias latipes* (Mc Clintock, 1950, Blackman 1989, Kawakami and Shima 1999) hAT transposons are also found in mammalian genomes including humans where they are the most abundant DNA transposons and comprise 1.55% (195 Mb) of the total genome (Lander, 2001). hAT elements in plants, animals, and fungi are characterized by six conserved blocks of amino acids and by a weak consensus for TIRs (Rubin et al., 2001).

Interrogating the p-MITE database using the BLAST on-line tool indicated 6 matches with 6 different MITE transposable elements *Setaria italica* specie, all belonging to the hAT superfamily of the TIR order.

***br2:NC238 abcb1* cDNA sequencing**

Amplification and sequencing of the 5'-side of the transcript produced a single band, which sequence was 100% similar to the wild type B73, for both the revertant and the *br2:NC238* transcript.

Amplification of the 3'-side of *abcb1* transcript of the revertant plant produced two different sequences: the wild type sequence and a sequence characterized by a 967 base long gap. This isoform is not annotated in B73 genome database and could be a region amplified from another abc superfamily member that is similar to *abcb1* in its 3'-side. Also, this splicing form could be a typical isoform of NC238 genetic background.

Amplification of the 3'-side of *abcb1* transcript of the *br2:NC238* produced two different sequences: the wild type 3'-side sequence and a splicing form that lacks 860 bases, in both roots and aerial part of seedlings. The shorter isoform the gap could be the 3'-side of one of the splicing variant caused by the transposon. RT-PCR of the central region of *abcb1 br2:NC238* transcript produced several bands corresponding to different splice variants as consequence of the presence of the transposon in *abcb1* intron IV causes several. It is well known that transposons play a role in alternative splicing creation. Splicing is the mechanism of removing intronic sequences defined by short conserved sequence motifs at the 5' and 3' of the introns to

join the neighboring exons and generate an uninterrupted open reading frame (ORF) for translation. This is catalyzed by the spliceosome, a high molecular weight complex that is assembled at every intron. The *cis* sequences in the pre-mRNA include splice sites, branch point, polypyrimidine tract, enhancer, and suppressor sequences. In addition, in plants UA-richness of introns contributes to their recognition and is essential for efficient splicing. It has been reported transposon insertion in introns can create alternative splicing forms of the gene. In contrast, transposon insertion in exons can function as new introns and be removed by splicing (Varagona et al., 1992).

Alternative splicing can be caused by single base mutation, as in the case of *Waxy* (*Wx*) gene of rice (*Oryza sativa*) that encodes a granule-bound starch synthase that controls grain amylose content. The *wx* mutant (*wxb*) has a guanosine to uridine mutation at the 5' splice site of intron 1, activates two cryptic splice sites in exon 1 and reduces splicing efficiency resulting in lower levels of amylose to generate “sticky” rice (Cai et al., 1998; Isshiki et al., 1998).

Through alternative splicing different transcript variants with different stabilities and different regulatory motifs can be generated, leading to variation in the transcriptome. The importance of alternative splicing in plants has been increasingly recognized in the last decade. Recently, high-throughput RNA-seq has allowed the identification of previously unknown transcript isoforms (Alamancos et al., 2014).

An alternative splicing variant of *abcb1* gene was already annotated in the Maize Genome database (GRMZM2G315375-T02). Domain analyses indicate this form encodes a truncated version of the protein with one of the two ATP-binding cassettes and one of the two transmembrane regions.

This form is present in both *br2NC238* and the revertant plant at 7-leaf-old stage in stem tissues. A higher expression of the transcript was observed in *br2NC238* line.

This transcript is not related to the transcripts originated by the transposon insertion in *br2NC238* *abcb1* intron IV, and its over expression in the mutant may derived by lacking of the normal T01 transcript that is replaced by many other abnormal transcripts, and eventually proteins.

In conclusion, the *br2:NC238* insertion share many structural characteristics with MITE TEs: short sequence, presence of Terminal Inverted Repeats (TIRs), flanked by short direct Target Site Duplication (TSD), and the isolation of a revertant plant that retained the extra copy of a TSD.

However, the databases interrogations did not allow the assignment of the sequence to any known TE family or superfamily. Searches outputs showed several similarities with both DNA and RNA transposable elements as well as similarities with transposases or putative transposases regions. Many of these outputs are MITEs. However, all these matches are short sequences, mainly consisting of 11 or 13 nucleotides, and considering the richness in repetitive sequences of the maize genome this information may not be significantly relevant.

Moreover, the majority of MITEs were classified into five superfamilies, including Tc1/Mariner, PIF/Harbinger, CACTA, hAT and Mutator. MITE families were assigned into superfamilies based on their TIR and TSD sequences. None of the results align with the TIRs of the transposon. However, alignments mainly localized at the 3'-end of the sequence.

RT-PCRs indicated *abcb1* is expressed from early stages of stem development, however, a minor role of ABCB1 protein in the first steps of the elongation of the stem is suggested, as plants younger than 6-7-leaf-old showed normal internode length. The presence of the insertion in *abcb1* gene in *br2:NC238* was associated with high levels of the predicted Maize GDB splicing form T02. Moreover, alteration in the profile of other auxin transporters encoding genes was observed. Results indicated other proteins might become (more) involved in auxin transport, when the transport through ABCB1 is defective, and auxin over or down accumulates.

Chapter IV

The br2NC238:B73 line

4.1 Introduction

Little is known about the NC238 inbred line in the literature. Allelic tests indicated the inbred line is a brachytic 2 type mutant (Johal, unpublished): the mutation is due to a transposon insertion in *abcb1* intronic region. BR2/ABCB1 was clone by transposon tagging: it encodes for a auxin transporter protein (Multani et al., 2003; Knöller et al., 2010). Other *br2* alleles have been later isolated (Pilu et al., 2007). *br2* lines were described as altered in the lower internodes elongation (Multani et al., 2003; Pilu et al., 2007; Cassani et al., 2010), in the size of the leaf epidermal cell (Pilu et al., 2007; Cassani et al., 2010) and leaf cells width (Knöller et al., 2010), and in the stem vasculature (Knöller et al., 2010; Multani et al., 2003).

NC238 inbred line measurements indicated it is characterized by the shortening and thickness of the lower internodes. The phenotype arise when plants were 6-7 collared leaves. The other stem traits (number of nodes per plant, days to anthesis, tassel length, ears per plant) did not differ from the tall revertant plant traits (present thesis results).

In order to verify the transpon insertion was the true cause of the short stature of the NC238 plant, the NC238 *abcb1* mutant allele was introgressed in the B73 line - the maize reference genome (figure 4.1) (Schnable et al., 2009). *br2NC238* short line is homozygous for the the *abcb1* mutant recessive allele (*abcb1 abcb1*). The *br2NC238* line was crossed with the B73 line. The heterozygous F1 progeny (*Abcb1 abcb1*) was backcrossed 5 times. The obtained line was self-crossed to obtained a progeny composed by 50% short homozygous plants. This short br2NC238:B73 line carrying the mutant allele *br2/abcb1* was used in the experiments.

Amplification and sequencing of *abcb1* gene in the new line were made in order to confirm the presence of the allele in the line. RT-PCR was performed in order to verify the

transcription of the gene in this line. Finally, the morphological traits measurements were made to confirm the allele confers the br2 type phenotype.

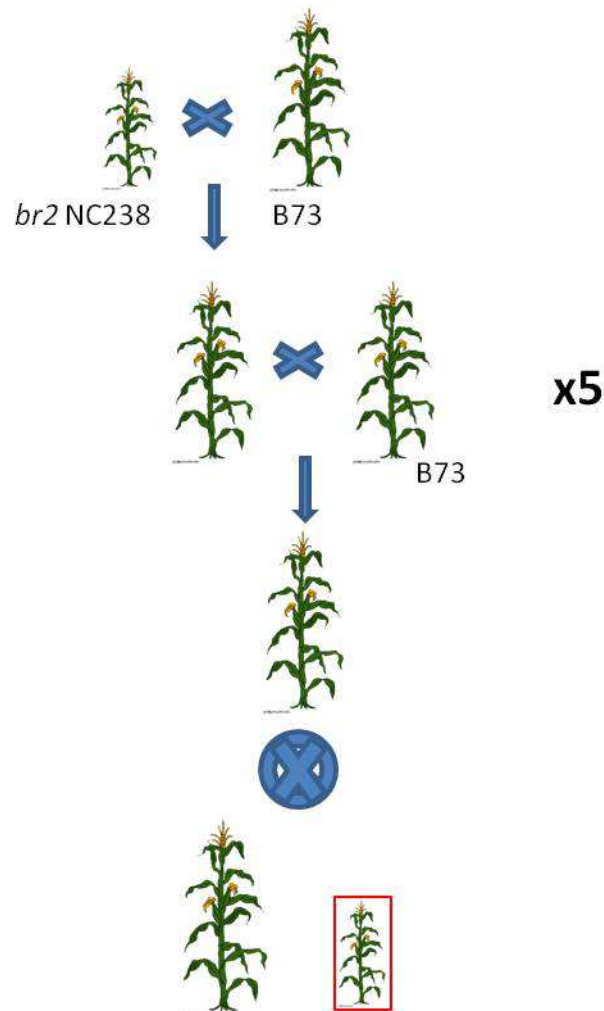


Figure 4.1. *br2NC238* was homozygous for the the *abcb1* mutant allele (*abcb1 abcb1*). The *abcb1* allele was introgressed in the wild type B73 reference genome line (*Abcb1 Abcb1*). After 5 cycles of crossing the line carrying the *br2NC238 abcb1* allele with the wild type B73, a selfed crossing of the resulting line (*Abcb1 abcb1*) allowed to obtained a progeny 50% homozygous plant (*abcb1 abcb1*, red squared in the figure). This *br2NC238:B73* line carrying the mutant allele *abcb1 abcb1* was used in the experiments.

4.2 Materials and methods

Plant material

br2:B73 was provided by prof.Johal (Purdue University). B73 wild type line was available at Prof.Varotto lab, originally obtained from the Maize Stock Centre and propagated at the "L.Toniolo" farm of the University of Padua. The two lines were grown in pots in the greenhouse of the University of Padua until anthesis stage.

Molecular biology techniques and statistical analyses

DNA and RNA extraction, gene amplification, DNA sequencing, gene expression analyses and statistical analyses were performed as described in Chapters II and III "Materials and methods" sections.

4.3. Results

4.3.1 Genetic analyses of the *br2NC238:B73* line

After an introgression of *br2NC238 abcb1* allele in the wild type B73 that consisted in multiple cycles of crossing of *br2NC238* with B73, self crossing of the resulting line and selection of the short plant (homozygous *abcb1 abcb1*) a B73 genetic background line carrying the mutant allele *br2/abcb1* was obtained (figure 4.1).

Amplification and sequencing of the genomic clone of *br2NC238:B73* line using primers 4BS (see Chapter III figure 3.17) confirmed the presence of the NC238 insertion and the homozygosity of the line. RT-PCRs on seedling coleoptile using primers 4 forward plus 4 reverse (see Chapter III figure 3.17, from A₁₄₇₆ up to C₂₆₄₈ and 11 forward plus 5 reverse (see Chapter III figure 3.17, from A₁₈₅₅ to T₃₅₆₄) to amplify the central region of the transcript, produced multiple bands confirming the presence of the insertion causes an alteration of the transcription of the gene. Amplification was performed on two plants (plant 1 and plant 2 in figure 4.2).

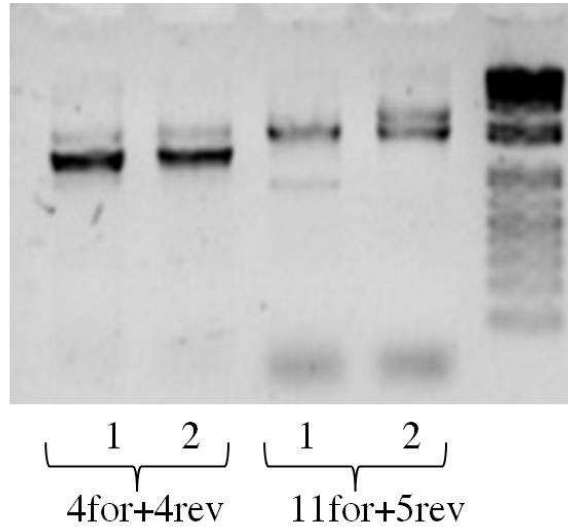


Figure 4.2. Gel of the RT-PCR on two seedlings of the *br2NC238:B73* line (named 1 and 2) using primers 4forward plus 4reverse and 11forward plus 5reverse.

4.3.2 Morphological traits measurements

br2NC238:B73 and wild type B73 plants were grown in pots in greenhouse at controlled temperature and lightening. Measurements were performed at anthesis. 19 B73 plants and 18 *br2NC238:B73* plants were measured. Plant stature was measured from soil level to the uppermost node. Position of the node carrying the uppermost ear was counted. Number of tassel branches and number of leaves per plant were counted. Internode length and node diameters were recorded.

In *br2NC238:B73* line, the typical phenotype arise when plants had 5-6 collared leaves (figure 4.3). Previous observation of *br2NC238* line indicated the *br2* phenotype arise when plants were 6-7 collared leaves.



Figure 4.3. *br2NC238:B73* (left) and B73 plants (right) were visible different starting from the stage plants had 5-6 collared leaves.



Figure 4.4. B73 wt (A, D) and *br2NC238:B73* (B, C) at anthesis after leaves removal, plant stems (A, B) and particular of the lower internodes (C, D).

At anthesis, on average, *br2NC238:B73* plants stature was 70cm tall - 31% lower than B73 stature. Short stature was due to the shortening of the lower internodes. The first and the second internodes above the uppermost crown root node were visible different (figure 4.4). Number of leaves per plant did not differ in the two lines ($p\text{-value}>0.01$).

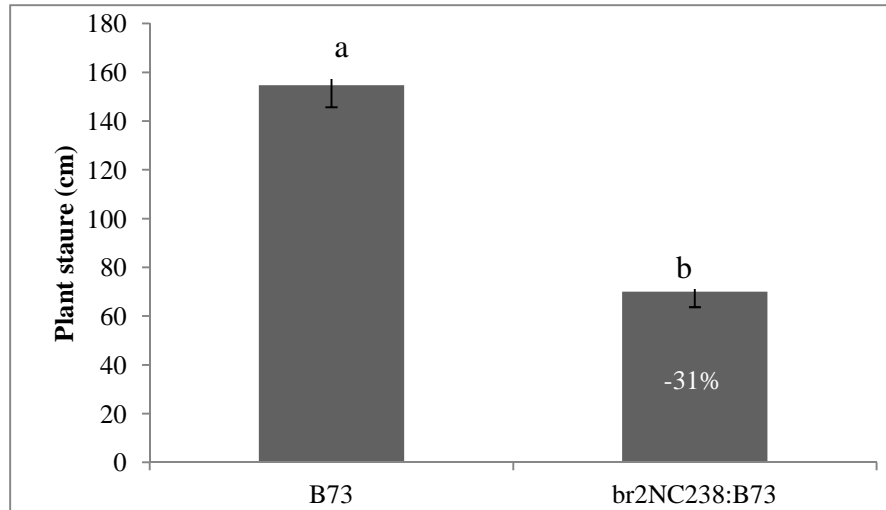


Figure 4.5. Stature of B73 and the *br2NC238:B73* plants.

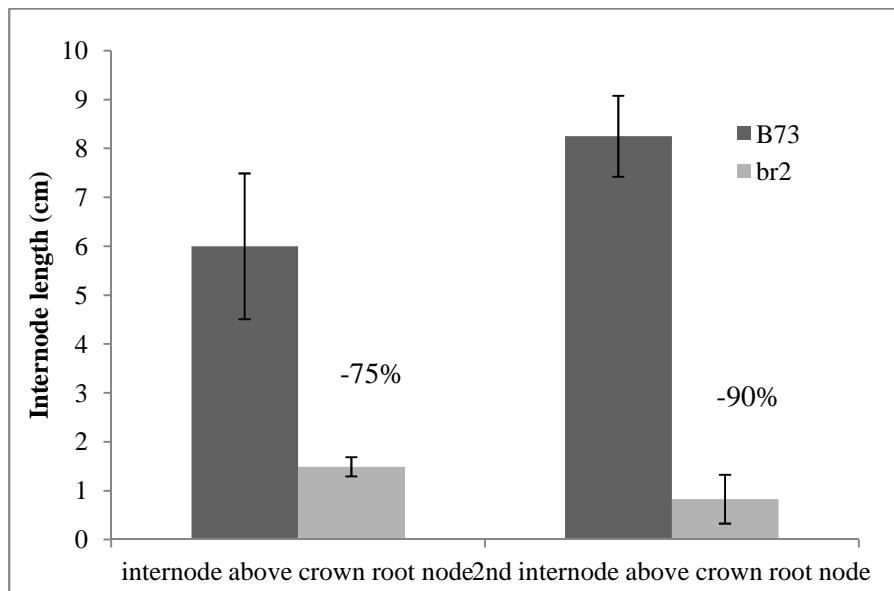


Figure 4.6. Internode lengths: *br2* lower internodes were shorter than the B73 line

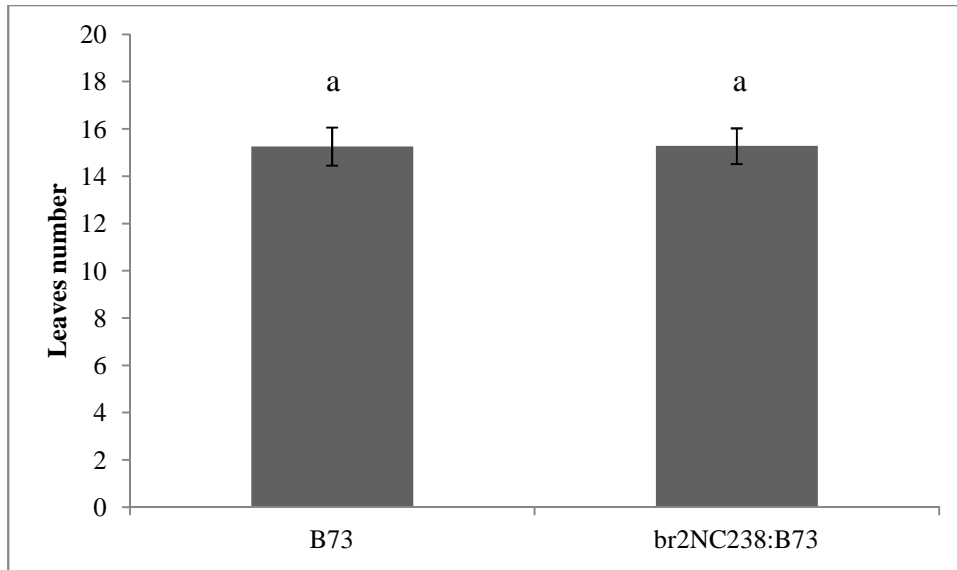


Figure 4.7. Number of leaves per plant of B73 and the *br2NC238:B73* are similar. Short stature was due to the shortening of the lower internodes.

In order to detect differences in the reproductive growth, the number of tassel branches was observed. Differences in the number of tassel branches were observed in the two lines: the average number of branches of *br2NC238:B73* tassel was slightly higher than those of the B73 line (Figure 4.8, T-test p -value <0.01). The position of the uppermost ear along the stem was recorded: no statistically significant difference was observed between the two lines (figure 4.10).

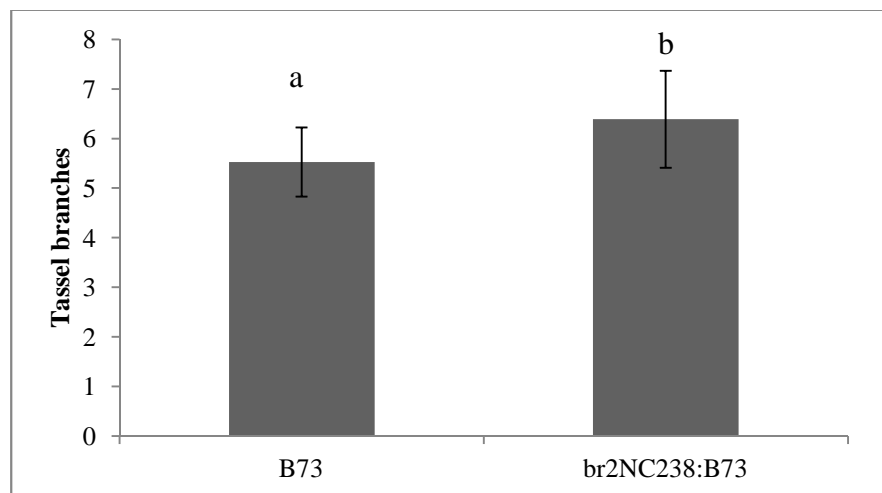


Figure 4.9. Number of tassel branches of the *br2NC238:B73* plants were slightly higher than those of B73 plant.

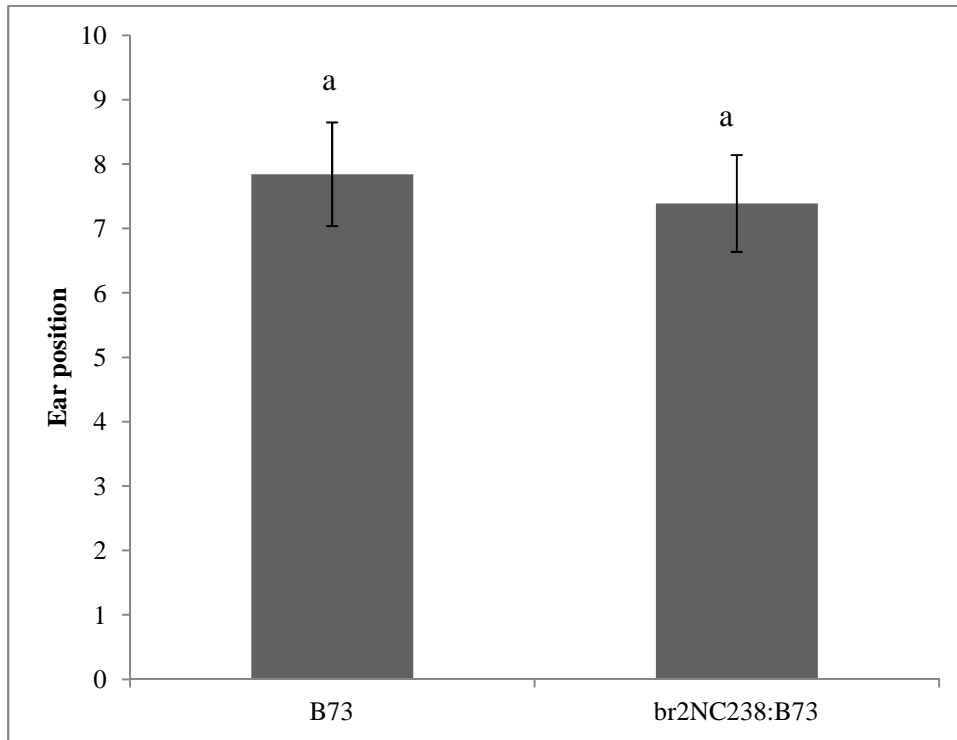


Figure 4.10. Position of the node with the uppermost ear of the *br2NC238:B73* and the B73 plant.

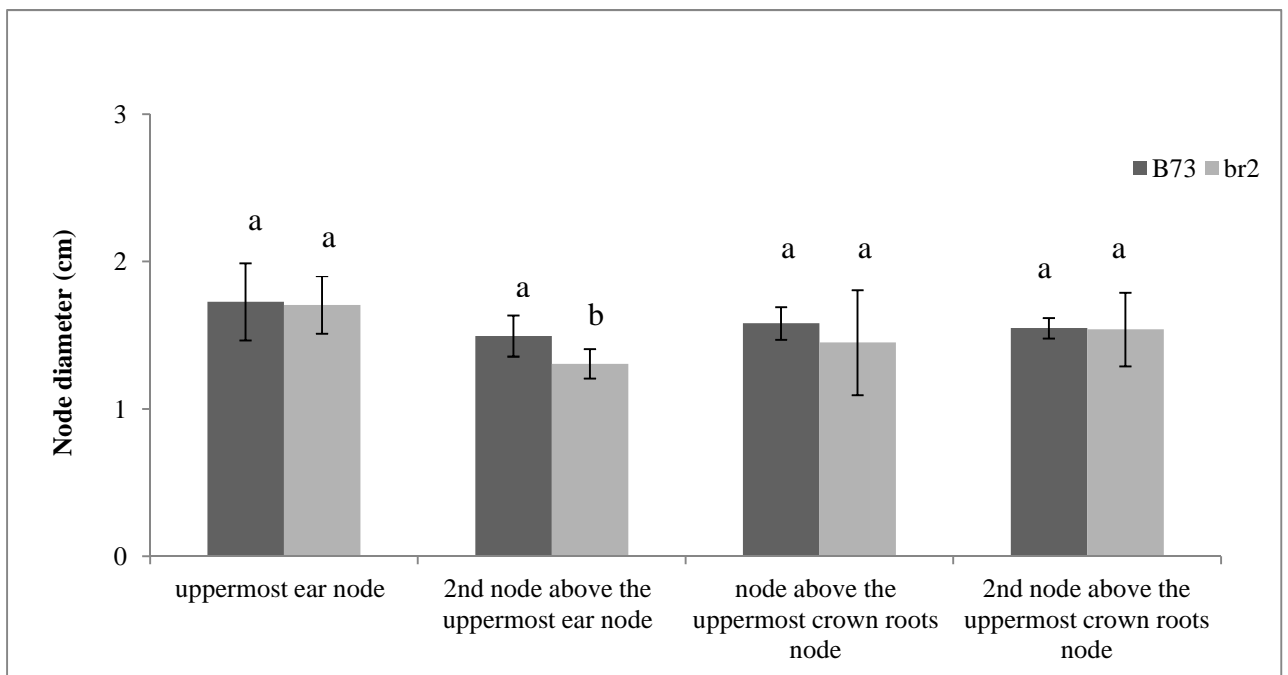


Figure 4.11. Node diameters of B73 and *br2NC238:B73* line (named *br2* in the figure). Only the second node above the uppermost ear node differed in the two lines: *br2* node was thicker than B73 node.

The shortening of the lower internodes caused the crown root nodes to be close to the ground leaves or even inside (figure 4.12). This characteristic could influence the plant anchoring to the soil. However, differently from *br2:NC238*, in B73 mutants the lower internodes diameters were not thicker than the wild type B73. This observation suggest that the genetic background affects the phenotype of the mutant.

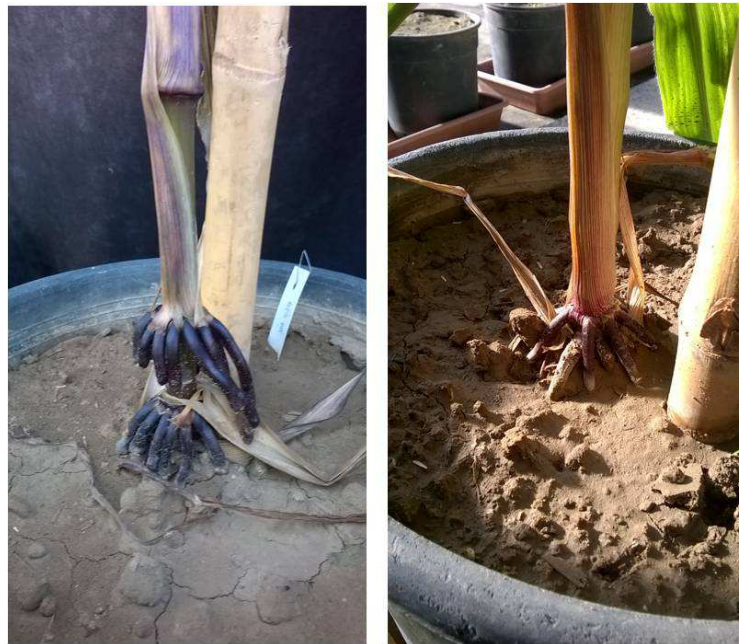


Figure 4.12. The shortening of the lower internodes of *br2:NC238:B73* (right) caused the crown roots node to be close to the soil, while the wild type plants (right) are characterized by the two or three crown root nodes.

In conclusion, introgression of the NC238 *br2* mutant allele in the reference genome B73 caused the typical phenotype characterized by the shortening of the lower internodes. However, other traits observed in *br2:NC238* line were not present in B73: the lower node diameters were similar between *br2* and B73 lines. Moreover, differently from *br2:NC238*, *br2* in B73 caused an increased in tassel branches. These traits appear to be related to the genetic background.

However, results indicate the *abcb1* mutant allele derived from *br2:NC238* line was responsible for the shortening of the stature in B73 mutant and suggest that the allele might be used in breeding programs to obtain lines with reduced height.

4.4 Discussion

NC238 inbred line measurements indicated it is characterized by the shortening and thickness of the lower internodes while no differences in the other stem traits (number of nodes per plant, days to anthesis, tassel length, ears per plant) compared to the tall revertant plant were observed (present thesis results).

Introgression of *br2:NC238 abcb1* mutant allele in B73 line allowed to verify the effects of the *br2:NC238 abcb1* mutation in another genetic background. B73 line was chosen as it represented the maize reference line (Strable and Scanlon, 2009). Morphological traits measurements indicated the mutation in B73 caused the shortening of the lower internodes. This trait was observed also in all the other *br2* line previously characterized.

However, the *br2:NC238 abcb1* mutation had some different effects in B73 compared to the *br2:NC238* line. These two differences may be due to the differences in the genetic background.

First, the increased thickness of the lower nodes observed in *br2:NC238* was not observed in *br2:NC238:B73*. The thickness of the stem base is an important trait as it could confer resistance to lodging during storms and windy weather.

Second, *br2:NC238:B73* is characterized by an increased number of tassel branches. Tassel branches development is regulated by auxin, thus the alteration in tassel branches number in *br2* was consistent with an alteration of auxin transport. The inflorescence meristem (IM) first produces a series of axillary meristems, named branch meristems (BMs), that will make the long basal branches of the mature tassel. Auxin starts to accumulate from the stem epidermis at the site of primordium initiation. Once the primordium starts to grow out, auxin is depleted from the surrounding area and a new auxin sink forms at the site of the next primordium (Reinhardt et al., 2003; Heisler et al., 2005).

RT-PCRs on seedling coleoptile to amplify the central region of the transcript, produced multiple bands confirming the presence of the insertion caused an alteration of the transcription of the gene.

Results indicate the *abcb1* mutant allele derived from *br2:NC238* line was responsible for the shortening of the stature in B73 mutant and suggest that the allele might be used in breeding programs to obtain lines with reduced height.

5. General discussion and conclusions

Dwarfism or semi-dwarfism confers many advantages to crop species, such as increased allocation of energy to seed rather than stem, denser growth, increased resistance to storm damages and reduced loss during harvesting. A defect in polar auxin transport (PAT) causes the sorghum mutant *dwarf3* (*dw3*) and the maize *brachytic2* (*br2*) mutations (Multani et al., 2003). Both *dw3* and *br2* are mutations affecting the gene orthologue of *A. thaliana ABCB1*, which functions in auxin PAT.

Auxin is a key regulator of plant growth: local biosynthesis, degradation and conjugation contribute to the modulation of IAA homeostasis at the cellular level. ABCBs, together with the PIN FORMED, the AUX1/LAX and the PILS auxin transporters, create a directional auxin flux from the site of synthesis - young tissues - to the site of action (Zazimalová et al., 2010b; Smith, 2008; Xu et al., 2006; Cho and Cho, 2012; Balzan et al., 2014). Indeed, auxin transport, with local biosynthesis and conjugation, allows the establishment of an auxin gradient, and the local auxin maxima regulates many aspects of the embryonic development, stem cell maintenance, shoot architecture, and tropic growth responses, root development and gravitropism (Peer et al., 2011; Gallavotti et al., 2008; Gallavotti, 2013; Müller et al., 1998; Zhao, 2010; Kuhlemeier, 2007; Marchant et al., 2002; Debi et al., 2003; Blilou et al., 2005; Kramer and Bennett, 2006; Rojas-Pierce et al., 2007; Terasaka et al., 2010; Barbez et al., 2012; Wang and Ruan, 2013).

The NC238 inbred line is a *br2* mutant line, characterized by both a reduced stature and wider lower nodes diameter. No other altered phenotypic traits, included root system traits, were detected in the present study.

Many brachytic mutants (*br*) were previously isolated: these *br* lines appear to differ for the position of the inode/nternodes affected by the mutation. In the case of *br2:NC238* the shortening of the internodes regarded mainly the base of the stem. Importantly, the lower nodes are those where ear primordia initiate, but the mutation does not affect the ear differentiation and development.

In our work, the mutant allele was introgressed in the B73 line. In this reference inbred line floral transition is usually observed at V4-V5 stage (Meng et al., 2011). In the first stages of development, *br2* and the revertant plants were indistinguishable and the mutant phenotype

became visible when plants were 6/7-collared-leaves, thus after floral transition, suggesting that the mutation does not affect the differentiation of the inflorescence meristem.

In addition, the introgression of the *br2:NC238* *abcb1* mutant allele in the B73 genetic background confirmed the mutation in *abcb1* was the cause of the short stature phenotype. However, in this genetic background no thickness of the lower nodes was observed. Moreover, an alteration in tassel branches number was recorded. This is the first time that an alteration in tassel branch number is observed in a *br2* line. It is well known that in plants, the genetic background influences the penetrance (whether or not a mutant phenotype is detected) and expressivity (the intensity of the mutant phenotype) of mutations. The *br2:NC238* *abcb1* mutant allele may induce other (minor) effects - in addition to the severe shortening of the lower plant internodes - when expressed in other genetic backgrounds.

An intronic insertion characterized the *br2:NC238* *abcb1* mutant allele. *abcb1* gene is expressed from the early stages of the stem development, particularly at nodes level. A minor role of ABCB1 in the first steps of the elongation of the stem is suggested, as *br2* plants younger than 6-7-leaf-old showed normal internode length. The *br2:NC238* *abcb1* insertion sequence aligned to many transposable elements of both class I and class II, but all matches were short sequences. However, the analyses could not be significant as most of the maize genome is composed of repeats and transposons. Though, many structural traits suggested the insertion was a MITE type DNA transposon. The presence of the insertion in an intronic region in *br2:NC238* caused alteration in the splicing of the pre-RNA of the gene: several splicing forms were consequently produced. Moreover, expression analyses indicated high levels of the Maize GDB annotated predicted splicing form T02 and altered expression profiles of other auxin carriers, mainly up-regulated, in *br2:NC238* tissues. Alterations in the expression of auxin transporters and the *abcb1* T02 splicing variant in *br2* mutant might suggest the presence of a compensatory mechanism aims at restoring the defective auxin transport. However, this compensatory mechanism is not completely successfully considering the *br2* severe phenotype.

In conclusion, NC238*br2* allele could be useful for breeding programs aiming at obtaining lines with reduced height.

Further analyses have to be performed in order to study the nature and the transposition mechanism, and particularly to determine the stability of the *br2:NC238* insertion element in the genome. Moreover, the effects of the *br2:NC238 abcb1* allele on the plant yield need to be evaluated as well as the effect of the variation in the numbers tassel branches in pollen production.

References

- Abel, S., and Theologis, a (1996). Early genes and auxin action. *Plant Physiol.* 111, 9–17. doi:10.1104/pp.111.1.9.
- Aloni, R., Aloni, E., Langhans, M., and Ullrich, C. I. (2006). Role of cytokinin and auxin in shaping root architecture: regulating vascular differentiation, lateral root initiation, root apical dominance and root gravitropism. *Ann. Bot.* 97, 883–93. doi:10.1093/aob/mcl027.
- Ambudkar, S. V., Kimchi-Sarfaty, C., Sauna, Z. E., and Gottesman, M. M. (2003). P-glycoprotein: from genomics to mechanism. *Oncogene* 22, 7468–7485. doi:10.1038/sj.onc.1206948.
- Ananiev, E. V., Phillips, R. L., and Rines, H. W. (1998). Complex structure of knob DNA on maize chromosome 9: Retrotransposon invasion into heterochromatin. *Genetics* 149, 2025–2037.
- Andorf, C. M., Cannon, E. K., Portwood, J. L., Gardiner, J. M., Harper, L. C., Schaeffer, M. L., Braun, B. L., Campbell, D. A., Vinnakota, A. G., Sribalusu, V. V., et al. (2015). MaizeGDB update: new tools, data and interface for the maize model organism database. *Nucleic Acids Res.*, gkv1007. doi:10.1093/nar/gkv1007.
- Avila Bolivar, L., Lukens L. (2015). Positional cloning and characterization of a gene required for normal cellular elongation in maize (*Zea Maize*). in *Annual Maize Genetics Meeting*.
- Bailly, A., Yang, H., Martinoia, E., Geisler, M., and Murphy, A. S. (2011). Plant lessons: exploring ABCB functionality through structural modeling. *Front. Plant Sci.* 2, 108. doi:10.3389/fpls.2011.00108.
- Balzan, S., Johal, G. S., and Carraro, N. (2014). The role of auxin transporters in monocots development. *Front. Plant Sci.* 5, 393. doi:10.3389/fpls.2014.00393.
- Band, L. R., Wells, D. M., Larrieu, A., Sun, J., Middleton, A. M., French, A. P., Brunoud, G., Sato, E. M., Wilson, M. H., Péret, B., et al. (2012). Root gravitropism is regulated by a transient lateral auxin gradient controlled by a tipping-point mechanism. *Proc. Natl. Acad. Sci. U. S. A.* 109, 4668–73. doi:10.1073/pnas.1201498109.
- Barbez, E., Kubeš, M., Rolčík, J., Béziat, C., Pěnčík, A., Wang, B., Rosquete, M. R., Zhu, J., Dobrev, P. I., Lee, Y., et al. (2012). A novel putative auxin carrier family regulates intracellular auxin homeostasis in plants. *Nature* 485, 119–22. doi:10.1038/nature11001.
- Barker, M. S., Baute, G. J., and Liu, S. (2012). Plant Genome Diversity Volume 1. *Plant Genome Divers.*, 155–169. doi:10.1007/978-3-7091-1130-7.
- Benfey, P. N., and Schiefelbein, J. W. (1994). Getting to the root of plant development: the genetics of *Arabidopsis* root formation. *Trends Genet.* 10, 84–8. Available at: <http://www.ncbi.nlm.nih.gov/pubmed/8178369>.
- Bengough, A. G. (2005). Root responses to soil physical conditions; growth dynamics from field to cell. *J. Exp. Bot.* 57, 437–447. doi:10.1093/jxb/erj003.
- Bennett, M. J., Marchant, a, Green, H. G., May, S. T., Ward, S. P., Millner, P. a, Walker, a R., Schulz, B.,

- and Feldmann, K. a (1996). Arabidopsis AUX1 gene: a permease-like regulator of root gravitropism. *Science* 273, 948–50. Available at: <http://www.ncbi.nlm.nih.gov/pubmed/18627499>.
- Bennetzen, J. L. (2000). Transposable element contributions to plant gene and genome evolution. 251–254.
- Bhalerao, R. P., Eklöf, J., Ljung, K., Marchant, A., Bennett, M., and Sandberg, G. (2002). Shoot-derived auxin is essential for early lateral root emergence in Arabidopsis seedlings. *Plant J.* 29, 325–332. doi:10.1046/j.0960-7412.2001.01217.x.
- Blilou, I., Xu, J., Wildwater, M., Willemsen, V., Paponov, I., Friml, J., Heidstra, R., Aida, M., Palme, K., and Scheres, B. (2005). The PIN auxin efflux facilitator network controls growth and patterning in Arabidopsis roots. *Nature* 433, 39–44. doi:10.1038/nature03184.
- Boeke, J. D., and Devine, S. E. (1998). Yeast retrotransposons: Finding a nice quiet neighborhood. *Cell* 93, 1087–1089. doi:10.1016/S0092-8674(00)81450-6.
- Bommert, P. (2005). Genetics and Evolution of Inflorescence and Flower Development in Grasses. *Plant Cell Physiol.* 46, 69–78. doi:10.1093/pcp/pci504.
- Bureau, T. E., Ronald, P. C., and Wessler, S. R. (1996). A computer-based systematic survey reveals the predominance of small inverted-repeat elements in wild-type rice genes. *Proc. Natl. Acad. Sci. U. S. A.* 93, 8524–8529. doi:10.1073/pnas.93.16.8524.
- Bureau, T. E., and Wessler, S. R. (1992). Tourist: a large family of small inverted repeat elements frequently associated with maize genes. *Plant Cell* 4, 1283–1294. doi:10.1105/tpc.4.10.1283.
- Casacuberta, J. M., and Santiago, N. (2003). Plant LTR-retrotransposons and MITEs: control of transposition and impact on the evolution of plant genes and genomes. *Gene* 311, 1–11. doi:10.1016/S0378-1119(03)00557-2.
- Casimiro, I., Marchant, a, Bhalerao, R. P., Beeckman, T., Dhooge, S., Swarup, R., Graham, N., Inzé, D., Sandberg, G., Casero, P. J., et al. (2001). Auxin transport promotes Arabidopsis lateral root initiation. *Plant Cell* 13, 843–852. doi:10.1105/tpc.13.4.843.
- Cassani, E., Villa, D., Durante, M., Landoni, M., and Pilu, R. (2010). The brachytic 2 and 3 maize double mutant shows alterations in plant growth and embryo development. *Plant Growth Regul.* 64, 185–192. doi:10.1007/s10725-010-9556-8.
- Celenza, J. L., Grisafi, P. L., and Fink, G. R. (1995). A pathway for lateral root formation in Arabidopsis thaliana. *Genes Dev.* 9, 2131–2142. doi:10.1101/gad.9.17.2131.
- Charlesworth, D., and Willis, J. H. (2009). The genetics of inbreeding depression. *Nat. Rev. Genet.* 10, 783–796. doi:10.1038/nrg2664.
- Chen, H., and Xiong, L. (2005). Pyridoxine is required for post-embryonic root development and tolerance to osmotic and oxidative stresses. *Plant J.* 44, 396–408. doi:10.1111/j.1365-313X.2005.02538.x.
- Chen, Q., Dai, X., De-paoli, H., Cheng, Y., Takebayashi, Y., Kasahara, H., Kamiya, Y., and Zhao, Y. (2014). Auxin Overproduction in Shoots Cannot Rescue Auxin Deficiencies in Arabidopsis Roots. 55, 1072–1079. doi:10.1093/pcp/pcu039.

- Chen, R., Hilson, P., Sedbrook, J., Rosen, E., Caspar, T., and Masson, P. H. (1998). The *Arabidopsis thaliana* AGR1 gene encodes a component of the polar-auxin-transport efflux carrier. *Proc. Natl. Acad. Sci. U. S. A.* 95, 15112–7.
- Cheng, Y., Dai, X., and Zhao, Y. (2006). Auxin biosynthesis by the YUCCA flavin monooxygenases controls the formation of floral organs and vascular tissues in *Arabidopsis*. *Genes Dev.* 20, 1790–9. doi:10.1101/gad.1415106.
- Cho, M., and Cho, H.-T. (2013). The function of ABCB transporters in auxin transport. *Plant Signal. Behav.* 8, e22990. doi:10.4161/psb.22990.
- Cho, M., and Cho, H.-T. (2012). The function of ABCB transporters in auxin transport. *Plant Signal. Behav.* 8, 2–4. Available at: <http://www.ncbi.nlm.nih.gov/pubmed/23221777>.
- Comas, L. H., Becker, S. R., Cruz, V. M. V., Byrne, P. F., and Dierig, D. A. (2013). Root traits contributing to plant productivity under drought. *Front. Plant Sci.* 4, 1–16. doi:10.3389/fpls.2013.00442.
- Comfort, N. C. (2001). From controlling elements to transposons : Barbara McClintock and the Nobel Prize *. *Genetics* 17, 475–478.
- Crow, J. F. (1998). Anecdotal , Historical and Critical Commentaries on Genetics 90 Years Ago : The Beginning of Hybrid Maize.
- Debi, B. R., Mushika, J., Taketa, S., Miyao, A., Hirochika, H., and Ichii, M. (2003). Isolation and characterization of a short lateral root mutant in rice (*Oryza sativa* L.). *Plant Sci.* 165, 895–903. doi:10.1016/S0168-9452(03)00293-0.
- Elliott, T. a, and Gregory, T. R. (2015). Do larger genomes contain more diverse transposable elements? *BMC Evol. Biol.* 15, 1–10. doi:10.1186/s12862-015-0339-8.
- Feschotte, C., Jiang, N., and Wessler, S. R. (2002). Plant transposable elements: where genetics meets genomics. *Nat. Rev. Genet.* 3, 329–41. doi:10.1038/nrg793.
- Feschotte, C., and Wessler, S. R. (2002). Mariner-like transposases are widespread and diverse in flowering plants. *Proc. Natl. Acad. Sci. U. S. A.* 99, 280–5. doi:10.1073/pnas.022626699.
- Feschotte, C., Zhang, X., and Wessler, S. R. (1870). *Miniature Inverted-repeat Transposable Elements (MITEs) and their Relationship with Established DNA Transposons.*
- Finnegan, D. J. (2012). Retrotransposons. *Curr. Biol.* 22, 432–437. doi:10.1016/j.cub.2012.04.025.
- Forestan, C., Farinati, S., and Varotto, S. (2012). The maize PIN gene family of auxin transporters. *Front. Plant Sci.* 3, 16. doi:10.3389/fpls.2012.00016.
- Fournier, C. (2000). Dynamics of the Elongation of Internodes in Maize (*Zea mays* L.): Analysis of Phases of Elongation and their Relationships to Phytomer Development. *Ann. Bot.* 86, 551–563. doi:10.1006/anbo.2000.1217.
- Friml, J., Wiśniewska, J., Benková, E., Mendgen, K., and Palme, K. (2002). Lateral relocation of auxin efflux regulator PIN3 mediates tropism in *Arabidopsis*. *Nature* 415, 806–9. doi:10.1038/415806a.

- Gallavotti, A. (2013). The role of auxin in shaping shoot architecture. *J. Exp. Bot.* 64, 2593–608. doi:10.1093/jxb/ert141.
- Gallavotti, A., Yang, Y., Schmidt, R. J., and Jackson, D. (2008). The Relationship between auxin transport and maize branching. *Plant Physiol.* 147, 1913–23. doi:10.1104/pp.108.121541.
- Gao, K., Chen, F., Yuan, L., Zhang, F., and Mi, G. (2015). A comprehensive analysis of root morphological changes and nitrogen allocation in maize in response to low nitrogen stress. *Plant. Cell Environ.* 38, 740–750. doi:10.1111/pce.12439.
- Geisler, M., and Murphy, A. S. (2006). The ABC of auxin transport: the role of p-glycoproteins in plant development. *FEBS Lett.* 580, 1094–102. doi:10.1016/j.febslet.2005.11.054.
- Grzebelus, D., Lasota, S., Gambin, T., Kucherov, G., and Gambin, A. (2007). Diversity and structure of PIF/Harbinger-like elements in the genome of *Medicago truncatula*. *BMC Genomics* 8, 409. doi:10.1186/1471-2164-8-409.
- Guan, J. C., Koch, K. E., Suzuki, M., Wu, S., Latshaw, S., Petruff, T., Goulet, C., Klee, H. J., and McCarty, D. R. (2012). Diverse Roles of Strigolactone Signaling in Maize Architecture and the Uncoupling of a Branching-Specific Subnetwork. *Plant Physiol.* 160, 1303–1317. doi:10.1104/pp.112.204503.
- Guilfoyle, T. J. (2015). The PB1 Domain in Auxin Response Factor and Aux/IAA Proteins: A Versatile Protein Interaction Module in the Auxin Response. *Plant Cell Online* 27, 33–43. doi:10.1105/tpc.114.132753.
- Guilfoyle, T. J., and Hagen, G. (2007). Auxin response factors. *Curr. Opin. Plant Biol.* 10, 453–60. doi:10.1016/j.pbi.2007.08.014.
- Han, M.-J., Xiong, C.-L., Zhang, H.-B., Zhang, M.-Q., Zhang, H.-H., and Zhang, Z. (2015). The diversification of PHIS transposon superfamily in eukaryotes. *Mob. DNA* 6, 12. doi:10.1186/s13100-015-0043-7.
- Han, M.-J., Xu, H.-E., Zhang, H.-H., Feschotte, C., and Zhang, Z. (2014). Spy: a new group of eukaryotic DNA transposons without target site duplications. *Genome Biol. Evol.* 6, 1–27. doi:10.1093/gbe/evu140.
- Han, Y., and Wessler, S. R. (2010). MITE-Hunter: a program for discovering miniature inverted-repeat transposable elements from genomic sequences. *Nucleic Acids Res.* 38, e199. doi:10.1093/nar/gkq862.
- Hartwig, T., Chuck, G. S., Fujioka, S., Klempien, a., Weizbauer, R., Potluri, D. P. V., Choe, S., Johal, G. S., and Schulz, B. (2011). Brassinosteroid control of sex determination in maize. *Proc. Natl. Acad. Sci.* 108, 19814–19819. doi:10.1073/pnas.1108359108.
- Hashiguchi, Y., Tasaka, M., and Morita, M. T. (2013). Mechanism of higher plant gravity sensing. *Am. J. Bot.* 100, 91–100. doi:10.3732/ajb.1200315.
- Havecker, E. R., Gao, X., and Voytas, D. F. (2004). The diversity of LTR retrotransposons.
- Hay, A., and Tsiantis, M. (2010). KNOX genes: versatile regulators of plant development and diversity. *Development* 137, 3153–65. doi:10.1242/dev.030049.

- Hayashi, K. (2012). The interaction and integration of auxin signaling components. *Plant Cell Physiol.* 53, 965–75. doi:10.1093/pcp/pcs035.
- Hayward, A., Stirnberg, P., Beveridge, C., and Leyser, O. (2009). Interactions between auxin and strigolactone in shoot branching control. *Plant Physiol.* 151, 400–12. doi:10.1104/pp.109.137646.
- Heckwolf, S., Heckwolf, M., Kaeppler, S. M., de Leon, N., and Spalding, E. P. (2015). Image analysis of anatomical traits in stalk transections of maize and other grasses. *Plant Methods* 11, 26. doi:10.1186/s13007-015-0070-x.
- Higashiyama, T., Noutoshi, Y., Fujie, M., and Yamada, T. (1997). Zepp, a LINE-like retrotransposon accumulated in the Chlorella telomeric region. *EMBO J.* 16, 3715–3723. doi:10.1093/emboj/16.12.3715.
- Higgins, C. F., and Linton, K. J. (2004). The ATP switch model for ABC transporters. *Nat. Struct. Mol. Biol.* 11, 918–26. doi:10.1038/nsmb836.
- Hochholdinger, F., and Tuberosa, R. (2009). Genetic and genomic dissection of maize root development and architecture. *Curr. Opin. Plant Biol.* 12, 172–177. doi:10.1016/j.pbi.2008.12.002.
- Hochholdinger, F., Woll, K., Sauer, M., and Dembinsky, D. (2004). Genetic dissection of root formation in maize (*Zea mays*) reveals root-type specific developmental programmes. *Ann. Bot.* 93, 359–68. doi:10.1093/aob/mch056.
- Hochholdinger, F., Wulff, D., Reuter, K., Park, W. J., and Feix, G. (2000). Tissue-specific expression of AUX1 in maize roots. *J. Plant Physiol.* 157, 315–319. doi:10.1016/S0176-1617(00)80053-X.
- Holyoake, A. J., and Kidwell, M. G. (2003). Vege and Mar: Two novel hAT MITE families from *Drosophila willistoni*. *Mol. Biol. Evol.* 20, 163–167. doi:10.1093/molbev/msg023.
- Huang, C. R. L., Burns, K. H., and Boeke, J. D. (2012). Active transposition in genomes. *Annu. Rev. Genet.* 46, 651–75. doi:10.1146/annurev-genet-110711-155616.
- Huang M.L, Wattanachaisaerekul S., Han Y.J. , Vongsangnak W., (2014), In silico analysis of plant and animal transposable elements, International Journal of Bioinformatics Research and Applications, 10:3, DOI: 10.1504/IJBRA.2014.060763
- Irwin, P. A., and Voytas, D. F. (2001). Expression and processing of proteins encoded by the *Saccharomyces* retrotransposon Ty5. *J. Virol.* 75, 1790–1797. doi:10.1128/JVI.75.4.1790-1797.2001.
- Jasinski, M., Ducos, E., Martinoia, E., and Boutry, M. (2003). The ATP-Binding Cassette Transporters : structure , function , and gene family comparison between rice and Arabidopsis. *Plant Physiol.* 131, 1169–1177. doi:10.1104/pp.102.014720.ABC.
- Jiang, N., Bao, Z., Zhang, X., and Hirochika, H. (2003). An active DNA transposon family in rice. 55, 163–167.
- Jung, H. G., and Casler, M. D. (2006). Maize Stem Tissues. *Crop Sci.* 46, 1793. doi:10.2135/cropsci2005.02-0085.
- Jurka, J., Kapitonov, V. V., Pavlicek, a., Klonowski, P., Kohany, O., and Walichiewicz, J. (2005). Repbase

- Update, a database of eukaryotic repetitive elements. *Cytogenet. Genome Res.* 110, 462–467. doi:10.1159/000084979.
- Kalendar, R., Vicent, C. M., Peleg, O., Anamthawat-jonsson, K., Bolshoy, A., and Schulman, A. H. (2004). Large Retrotransposon Derivatives : Abundant , Conserved but Nonautonomous Retroelements of Barley and Related Genomes.
- Kang, J., Park, J., Choi, H., Burla, B., Kretzschmar, T., Lee, Y., and Martinoia, E. (2011). Plant ABC Transporters. *Arab. B.* 9, e0153. doi:10.1199/tab.0153.
- Kapitonov, V. V, and Jurka, J. (2001). Rolling-circle transposons in eukaryotes. *Proc. Natl. Acad. Sci. U. S. A.* 98, 8714–8719. doi:10.1073/pnas.151269298.
- Kazazian, H. H. (2014). Processed pseudogene insertions in somatic cells. *Mob. DNA* 5, 20. doi:10.1186/1759-8753-5-20.
- Kempken, F., and Windhofer, F. (2001). The hAT family: a versatile transposon group common to plants, fungi, animals, and man. *Chromosoma* 110, 1–9. doi:10.1007/s004120000118.
- Kent, W. J. (2002). BLAT — The BLAST -Like Alignment Tool. *Genome Res.*, 656–664. doi:10.1101/gr.229202.
- Kikuchi, K., Terauchi, K., Wada, M., and Hirano, H.-Y. (2003). The plant MITE mPing is mobilized in anther culture. *Nature* 421, 167–170. doi:10.1038/nature01218.
- Kim, J. Y., Henrichs, S., Bailly, A., Vincenzetti, V., Sovero, V., Mancuso, S., Pollmann, S., Kim, D., Geisler, M., and Nam, H. G. (2010). Identification of an ABCB/P-glycoprotein-specific inhibitor of auxin transport by chemical genomics. *J. Biol. Chem.* 285, 23309–23317. doi:10.1074/jbc.M110.105981.
- King, J. J., Stimart, D. P., Fisher, R. H., and Bleecker, A. B. (1995). A mutation altering auxin homeostasis and plant morphology in Arabidopsis. *Plant Cell Online* 7, 2023. Available at: papers3://publication/uuid/11FDA9E2-CC88-4C04-819A-F04FD07D21C2.
- Kitomi, Y., Inahashi, H., Takehisa, H., Sato, Y., and Inukai, Y. (2012). OsIAA13-mediated auxin signaling is involved in lateral root initiation in rice. *Plant Sci.* 190, 116–22. doi:10.1016/j.plantsci.2012.04.005.
- Knöller, A. S., Blakeslee, J. J., Richards, E. L., Peer, W. A., and Murphy, A. S. (2010). Brachytic2/ZmABCB1 functions in IAA export from intercalary meristems. *J. Exp. Bot.* 61, 3689–96. doi:10.1093/jxb/erq180.
- Korasick, D. a., Enders, T. a., and Strader, L. C. (2013). Auxin biosynthesis and storage forms. *J. Exp. Bot.* 64, 2541–2555. doi:10.1093/jxb/ert080.
- Kramer, E. M., and Bennett, M. J. (2006). Auxin transport: a field in flux. *Trends Plant Sci.* 11, 382–386. doi:10.1016/j.tplants.2006.06.002.
- Kuang, H., Padmanabhan, C., Li, F., Kamei, A., Bhaskar, P. B., Ouyang, S., Jiang, J., Robin Buell, C., and Baker, B. (2009). Identification of miniature inverted-repeat transposable elements (MITEs) and biogenesis of their siRNAs in the Solanaceae: New functional implications for MITEs. *Genome Res.* 19, 42–56. doi:10.1101/gr.078196.108.

- Kuhlemeier, C. (2007). Phyllotaxis. *Trends Plant Sci.* 12, 143–50. doi:10.1016/j.tplants.2007.03.004.
- Lisch, D. (2013). How important are transposons for plant evolution? *Nat. Rev. Genet.* 14, 49–61. doi:10.1038/nrg3374.
- Lux, A., and Rost, T. L. (2012). Plant root research: the past, the present and the future. *Ann. Bot.* 110, 201–204. doi:10.1093/aob/mcs156.
- Ma, J., and Bennetzen, J. L. (2006). divergence in a centromeric region of rice. 103.
- Maeght, J.-L., Rewald, B., and Pierret, A. (2013). How to study deep roots—and why it matters. *Front. Plant Sci.* 4, 1–14. doi:10.3389/fpls.2013.00299.
- Makarevitch, I., Thompson, A., Muehlbauer, G. J., and Springer, N. M. (2012). Brd1 Gene in Maize Encodes a Brassinosteroid C-6 Oxidase. *PLoS One* 7, e30798. doi:10.1371/journal.pone.0030798.
- Mallory, A. C., Bartel, D. P., and Bartel, B. (2005). st Re vis e Fir Re e. *Development* 17, 1–16. doi:10.1105/tpc.105.031716.1.
- Marchant, A., Bhalerao, R., Casimiro, I., Eklöf, J., Casero, P. J., Bennett, M., and Sandberg, G. (2002). AUX1 Promotes Lateral Root Formation by Facilitating Indole-3-Acetic Acid Distribution between Sink and Source Tissues in the Arabidopsis Seedling. 14, 589–597. doi:10.1105/tpc.010354.2.
- Marchler-Bauer, A., Derbyshire, M. K., Gonzales, N. R., Lu, S., Chitsaz, F., Geer, L. Y., Geer, R. C., He, J., Gwadz, M., Hurwitz, D. I., et al. (2015). CDD: NCBI’s conserved domain database. *Nucleic Acids Res.* 43, D222–D226. doi:10.1093/nar/gku1221.
- Matsuoka, Y., Vigouroux, Y., Goodman, M. M., Sanchez G, J., Buckler, E., and Doebley, J. (2002). A single domestication for maize shown by multilocus microsatellite genotyping. *Proc. Natl. Acad. Sci. U. S. A.* 99, 6080–6084. doi:10.1073/pnas.052125199.
- McCLINTOCK, B. (1950). The origin and behavior of mutable loci in maize. *Proc. Natl. Acad. Sci. U. S. A.* 36, 344–355. doi:10.1073/pnas.36.6.344.
- McLamore, E. S., Diggs, A., Calvo Marzal, P., Shi, J., Blakeslee, J. J., Peer, W. a, Murphy, A. S., and Porterfield, D. M. (2010). Non-invasive quantification of endogenous root auxin transport using an integrated flux microsensor technique. *Plant J.* 63, 1004–16. doi:10.1111/j.1365-313X.2010.04300.x.
- McSteen, P. (2010). Auxin and monocot development. *Cold Spring Harb. Perspect. Biol.* 2, a001479. doi:10.1101/cshperspect.a001479.
- Meng, X., Muszynski, M. G., and Danilevskaya, O. N. (2011). The FT-Like ZCN8 Gene Functions as a Floral Activator and Is Involved in Photoperiod Sensitivity in Maize. *Plant Cell* 23, 942–960. doi:10.1105/tpc.110.081406.
- Momose, M., Abe, Y., and Ozeki, Y. (2010). Miniature inverted-repeat transposable elements of Stowaway are active in potato. *Genetics* 186, 59–66. doi:10.1534/genetics.110.117606.
- Moreno-Vázquez, S., Ning, J., and Meyers, B. C. (2005). hATpin, a family of MITE-like hAT mobile elements conserved in diverse plant species that forms highly stable secondary structures. *Plant Mol. Biol.* 58, 869–86. doi:10.1007/s11103-005-8271-8.

- Morita, M. T., and Tasaka, M. (2004). Gravity sensing and signaling. *Curr. Opin. Plant Biol.* 7, 712–8. doi:10.1016/j.pbi.2004.09.001.
- Muehlbauer, G. J., Bhau, B. S., Syed, N. H., Heinen, S., Cho, S., Marshall, D., Pateyron, S., Buisine, N., Chalhoub, B., and Flavell, A. J. (2006). A hAT superfamily transposase recruited by the cereal grass genome. *Mol. Genet. Genomics* 275, 553–63. doi:10.1007/s00438-006-0098-8.
- Müller, a, Guan, C., Gälweiler, L., Tänzler, P., Huijser, P., Marchant, a, Parry, G., Bennett, M., Wisman, E., and Palme, K. (1998). AtPIN2 defines a locus of Arabidopsis for root gravitropism control. *EMBO J.* 17, 6903–11. doi:10.1093/emboj/17.23.6903.
- Multani, D. S., Briggs, S. P., Chamberlin, M. a, Blakeslee, J. J., Murphy, A. S., and Johal, G. S. (2003). Loss of an MDR transporter in compact stalks of maize br2 and sorghum dw3 mutants. *Science* 302, 81–4. doi:10.1126/science.1086072.
- Murray, J. a. H., Jones, a., Godin, C., and Traas, J. (2012). Systems Analysis of Shoot Apical Meristem Growth and Development: Integrating Hormonal and Mechanical Signaling. *Plant Cell* 24, 3907–3919. doi:10.1105/tpc.112.102194.
- Naseem, M., Kaldorf, M., and Dandekar, T. (2015). The nexus between growth and defence signalling: auxin and cytokinin modulate plant immune response pathways. *J. Exp. Bot.* 66, 4885–4896. doi:10.1093/jxb/erv297.
- Noh, B., Murphy, A. S., and Spalding, E. P. (2001). Multidrug Resistance – like Genes of Arabidopsis Required for Auxin Transport and Auxin-Mediated Development. 13, 2441–2454. doi:10.1105/tpc.010350.Mammalian.
- Noma, K., Ohtsubo, E., and Ohtsubo, H. (1999). Non-LTR retrotransposons (LINEs) as ubiquitous components of plant genomes. *Mol. Gen. Genet.* 261, 71–79. doi:10.1007/s004380050943.
- Oono, Y., Ooura, C., Rahman, A., Aspuria, E. T., Hayashi, K., Tanaka, A., and Uchimiya, H. (2003). p - Chlorophenoxyisobutyric Acid Impairs Auxin Response in Arabidopsis Root 1. 133, 1135–1147. doi:10.1104/pp.103.027847.auxin-induced.
- Ouyang, S. (2004). The TIGR Plant Repeat Databases: a collective resource for the identification of repetitive sequences in plants. *Nucleic Acids Res.* 32, 360D–363. doi:10.1093/nar/gkh099.
- Pang, K., Li, Y., Liu, M., Meng, Z., and Yu, Y. (2013). Inventory and general analysis of the ATP-binding cassette (ABC) gene superfamily in maize (*Zea mays* L.). *Gene* 526, 411–28. doi:10.1016/j.gene.2013.05.051.
- Patel, M., Jung, S., Moore, K., Powell, G., Ainsworth, C., and Abbott, a. (2004). High-oleate peanut mutants result from a MITE insertion into the FAD2 gene. *Theor. Appl. Genet.* 108, 1492–1502. doi:10.1007/s00122-004-1590-3.
- Peer, W. A., Blakeslee, J. J., Yang, H., and Murphy, A. S. (2011). Seven things we think we know about auxin transport. *Mol. Plant* 4, 487–504. doi:10.1093/mp/ssr034.
- Pereira, V. (2004). Insertion bias and purifying selection of retrotransposons in the Arabidopsis thaliana genome. *Genome Biol.* 5, R79. doi:10.1186/gb-2004-5-10-r79.

- Péret, B., Swarup, K., Ferguson, A., Seth, M., Yang, Y., Dhondt, S., James, N., Casimiro, I., Perry, P., Syed, A., et al. (2012). AUX/LAX genes encode a family of auxin influx transporters that perform distinct functions during Arabidopsis development. *Plant Cell* 24, 2874–85. doi:10.1105/tpc.112.097766.
- Perrin, R. M., Young, L.-S., Murthy U M, N., Harrison, B. R., Wang, Y., Will, J. L., and Masson, P. H. (2005). Gravity signal transduction in primary roots. *Ann. Bot.* 96, 737–43. doi:10.1093/aob/mci227.
- Petersen, G., and Seberg, O. (1999). Phylogenetic Evidence for Excision of Stowaway Miniature Inverted-Repeat Transposable Elements in Triticeae (Poaceae). 1589–1596.
- Petrásek, J., and Friml, J. (2009). Auxin transport routes in plant development. *Development* 136, 2675–88. doi:10.1242/dev.030353.
- Phillips, K. a, Skirpan, A. L., Liu, X., Christensen, A., Slewinski, T. L., Hudson, C., Barazesh, S., Cohen, J. D., Malcomber, S., and McSteen, P. (2011). Vanishing Tassel2 Encodes a Grass-Specific Tryptophan Aminotransferase Required for Vegetative and Reproductive Development in Maize. *Plant Cell* 23, 550–66. doi:10.1105/tpc.110.075267.
- Piégu, B., Bire, S., Arensburger, P., and Bigot, Y. (2015). A survey of transposable element classification systems – A call for a fundamental update to meet the challenge of their diversity and complexity. *Mol. Phylogenet. Evol.* 86, 90–109. doi:10.1016/j.ympev.2015.03.009.
- Pilu, R., Cassani, E., Villa, D., Curiale, S., Panzeri, D., Badone, F. C., and Landoni, M. (2007). Isolation and characterization of a new mutant allele of brachytic 2 maize gene. *Mol. Breed.* 20, 83–91. doi:10.1007/s11032-006-9073-7.
- Quittenden, L. J., McAdam, E. L., Davies, N. W., and Ross, J. J. (2014). Evidence that Indole-3-Acetic Acid is Not Synthesized Via the Indole-3-Acetamide Pathway in Pea Roots. *J. Plant Growth Regul.* 33, 831–836. doi:10.1007/s00344-014-9431-3.
- Rahman, A., Bannigan, A., Sulaman, W., Pechter, P., Blancaflor, E. B., and Baskin, T. I. (2007). Auxin, actin and growth of the Arabidopsis thaliana primary root. *Plant J.* 50, 514–528. doi:10.1111/j.1365-313X.2007.03068.x.
- Rahman, A., Takahashi, M., Shibasaki, K., Wu, S., Inaba, T., Tsurumi, S., and Baskin, T. I. (2010). Gravitropism of Arabidopsis thaliana roots requires the polarization of PIN2 toward the root tip in meristematic cortical cells. *Plant Cell* 22, 1762–76. doi:10.1105/tpc.110.075317.
- Rojas-Pierce, M., Titapiwatanakun, B., Sohn, E. J., Fang, F., Larive, C. K., Blakeslee, J., Cheng, Y., Cutler, S. R., Cuttler, S., Peer, W. a, et al. (2007). Arabidopsis P-glycoprotein19 participates in the inhibition of gravitropism by gravacin. *Chem. Biol.* 14, 1366–76. doi:10.1016/j.chembiol.2007.10.014.
- Ross, J. J., O'Neill, D. P., Wolbang, C. M., Symons, G. M., and Reid, J. B. (2001). Auxin-Gibberellin Interactions and Their Role in Plant Growth. *J. Plant Growth Regul.* 20, 336–353. doi:10.1007/s003440010034.
- Rubin, E., Lithwick, G., and Levy, A. a. (2001). Structure and evolution of the hAT transposon superfamily. *Genetics* 158, 949–957.
- Sanmiguel, P., and Bennetzen, J. L. (1998). Evidence that a Recent Increase in Maize Genome Size was

- Caused by the Massive Amplification of Intergene Retrotransposons. 82, 37–44.
- Schmidt, T. (1999). LINEs , SINEs and repetitive DNA : non-LTR retrotransposons in plant genomes. 903–910.
- Schnable, P., Ware, D., Fulton, R., and Stein, J. (2009). The B73 maize genome: complexity, diversity, and dynamics. *Science* (80-). Available at: <http://www.sciencemag.org/content/326/5956/1112.short> [Accessed June 16, 2015].
- Schoof, H., Lenhard, M., Haecker, A., Mayer, K. F. X., Ju, G., Laux, T., Pflanz, M., Der, Morgenstern, A., Der, Jürgens, G., and Laux, T. (2000). The stem cell population of Arabidopsis shoot meristems is maintained by a regulatory loop between the CLAVATA and WUSCHEL genes. *Cell* 100, 635–44. doi:10.1016/S0092-8674(00)80700-X.
- Schulman, A. H. (2013). Retrotransposon replication in plants. *Curr. Opin. Virol.* 3, 604–614. doi:10.1016/j.coviro.2013.08.009.
- Shane, M. (2000). The Vascular System of Maize Stems Revisited: Implications for Water Transport and Xylem Safety. *Ann. Bot.* 86, 245–258. doi:10.1006/anbo.2000.1171.
- Shen, W.-H., and Xu, L. (2009). Chromatin remodeling in stem cell maintenance in Arabidopsis thaliana. *Mol. Plant* 2, 600–609. doi:10.1093/mp/ssp022.
- Sidler, M., Hassa, P., Hasan, S., Ringli, C., and Dudler, R. (1998). Involvement of an ABC transporter in a developmental pathway regulating hypocotyl cell elongation in the light. *Plant Cell* 10, 1623–36. Available at: <http://www.pubmedcentral.nih.gov/articlerender.fcgi?artid=144355&tool=pmcentrez&rendertype=abstract>.
- Simon, S., Kubeš, M., Baster, P., Robert, S., Dobrev, P. I., Friml, J., Petrášek, J., and Zažímalová, E. (2013). Defining the selectivity of processes along the auxin response chain: A study using auxin analogues. *New Phytol.* 200, 1034–1048. doi:10.1111/nph.12437.
- Smith, R. S. (2008). The role of auxin transport in plant patterning mechanisms. *PLoS Biol.* 6, e323. doi:10.1371/journal.pbio.0060323.
- Smith, S., and De Smet, I. (2012). Root system architecture: insights from Arabidopsis and cereal crops. *Philos. Trans. R. Soc. Lond. B. Biol. Sci.* 367, 1441–52. doi:10.1098/rstb.2011.0234.
- States, U. (1994). Roots and Root Systems.
- Strable, J., and Scanlon, M. J. (2009). Maize (*Zea mays*): a model organism for basic and applied research in plant biology. *Cold Spring Harb. Protoc.* 2009, pdb.emo132. doi:10.1101/pdb.emo132.
- Swarup, K., Benková, E., Swarup, R., Casimiro, I., Péret, B., Yang, Y., Parry, G., Nielsen, E., De Smet, I., Vanneste, S., et al. (2008). The auxin influx carrier LAX3 promotes lateral root emergence. *Nat. Cell Biol.* 10, 946–54. doi:10.1038/ncb1754.
- Szak, S. T., Pickeral, O. K., Landsman, D., and Boeke, J. D. (2003). Identifying related L1 retrotransposons by analyzing 3' transduced sequences. *Genome Biol.* 4, R30. doi:10.1186/gb-2003-4-5-r30.

- Terasaka, K., Blakeslee, J. J., Titapiwatanakun, B., Peer, W. A., Bandyopadhyay, A., Makam, S. N., Lee, R., Richards, E. L., Murphy, A. S., Sato, F., et al. (2010). PGP4 , an ATP Binding Cassette P-Glycoprotein , Catalyzes Auxin Transport in Arabidopsis thaliana Roots. *Plant Cell* 17, 2922–2939. doi:10.1105/tpc.105.035816.2.
- Thon, M. R., Pan, H., Diener, S., Papalas, J., Taro, A., Mitchell, T. K., and Dean, R. a (2006). The role of transposable element clusters in genome evolution and loss of synteny in the rice blast fungus *Magnaporthe oryzae*. *Genome Biol.* 7, R16. doi:10.1186/gb-2006-7-2-r16.
- Tiwari, S. B., Wang, X., and Guilfoyle, T. J. (2013). AUX / IAA Proteins Are Active Repressors , and Their Stability and Activity Are Modulated by Auxin Author (s): Shiv B . Tiwari , Xiao-Jun Wang , Gretchen Hagen and Tom J . Guilfoyle Published by : American Society of Plant Biologists (ASPB) Stable URL. *Plant Cell* 13, 2809–2822. doi:10.1105/tpc.010289.The.
- Tsuda, K., Ito, Y., Sato, Y., and Kurata, N. (2011). Positive autoregulation of a KNOX gene is essential for shoot apical meristem maintenance in rice. *Plant Cell* 23, 4368–81. doi:10.1105/tpc.111.090050.
- Tu, Z. (1997). Three novel families of miniature inverted-repeat transposable elements are associated with genes of the yellow fever mosquito, *Aedes aegypti*. *Proc. Natl. Acad. Sci. U. S. A.* 94, 7475–7480. doi:10.1073/pnas.94.14.7475.
- Varagona, M. J., Purugganan, M., and Wessler, S. R. (1992). Alternative Splicing Induced by Insertion of Retrotransposons into the Maize waxy Gene. *Plant Cell* 4, 1–10.
- Verrier, P. J., Bird, D., Burla, B., Dassa, E., Forestier, C., Geisler, M., Klein, M., Kolukisaoglu, Ü., Lee, Y., Martinoia, E., et al. (2008). Plant ABC proteins – a unified nomenclature and updated inventory. *Trends Plant Sci.* 13, 151–159. doi:10.1016/j.tplants.2008.02.001.
- Vert, G., Walcher, C. L., Chory, J., and Nemhauser, J. L. (2008). Integration of auxin and brassinosteroid pathways by Auxin Response Factor 2. *Proc. Natl. Acad. Sci. U. S. A.* 105, 9829–9834. doi:10.1073/pnas.0803996105.
- Vicient, C. M. (2010). Transcriptional activity of transposable elements in maize. *BMC Genomics* 11, 601. doi:10.1186/1471-2164-11-601.
- Wang, C., Liu, Y., Li, S.-S., and Han, G.-Z. (2015). Insights into the Origin and Evolution of the Plant Hormone Signaling Machinery. *Plant Physiol.* 167, 872–886. doi:10.1104/pp.114.247403.
- Wang, H., Xing, J., Grover, D., Hedges Kyudong Han, D. J., Walker, J. a., and Batzer, M. a. (2005). SVA elements: A hominid-specific retroposon family. *J. Mol. Biol.* 354, 994–1007. doi:10.1016/j.jmb.2005.09.085.
- Wang, L., and Ruan, Y.-L. (2013). Regulation of cell division and expansion by sugar and auxin signaling. *Front. Plant Sci.* 4, 163. doi:10.3389/fpls.2013.00163.
- Wang, Y., Wang, J., Shi, B., Yu, T., Qi, J., Meyerowitz, E. M., and Jiao, Y. (2014). The Stem Cell Niche in Leaf Axils Is Established by Auxin and Cytokinin in Arabidopsis. *Plant Cell* 26, 2055–2067. doi:10.1105/tpc.114.123083.
- Went, F. (1926). On growth-accelerating substances in the coleoptile of *Avena sativa*. *Proc. K. Ned. Akad.*

van Wet. 30, 10–19.

- Wicker, T., Sabot, F., Hua-van, A., Bennetzen, J. L., Capy, P., Chalhoub, B., Flavell, A., Leroy, P., Morgante, M., Panaud, O., et al. (2007). A unified classification system for eukaryotic transposable elements.
- Winkler, R. G., and Freeling, M. (1994). Physiological Genetics of the Dominant Gibberellin-Nonresponsive Maize Dwarfs, Dwarf-8 and Dwarf-9. *Planta* 193, 341–348. doi:10.1007/BF00201811.
- Witte, C. P., Le, Q. H., Bureau, T., and Kumar, a (2001). Terminal-repeat retrotransposons in miniature (TRIM) are involved in restructuring plant genomes. *Proc. Natl. Acad. Sci. U. S. A.* 98, 13778–83. doi:10.1073/pnas.241341898.
- Woodward, A. W., and Bartel, B. (2005). Auxin: regulation, action, and interaction. *Ann. Bot.* 95, 707–35. doi:10.1093/aob/mci083.
- Wright, D. A., Ke, N., Smalle, J., Hauge, B. M., Goodman, H. M., and Voytas, D. F. (1996). Multiple non-LTR retrotransposons in the genome of *Arabidopsis thaliana*. *Genetics* 142, 569–78. Available at: <http://www.pubmedcentral.nih.gov/articlerender.fcgi?artid=1206989&tool=pmcentrez&rendertype=abstract>.
- Xu, J., Seifertova, D., Brewer, P. B., Ru, K., Scheres, B., Blilou, I., and Rouquie, D. (2006). Polar PIN Localization Directs Auxin. 312, 2006.
- Xu, N., York, K., Miller, P., and Cheikh, N. (2004). Co-regulation of ear growth and internode elongation in corn. *Plant Growth Regul.* 44, 231–241. doi:10.1007/s10725-004-5935-3.
- Yang, G., Lee, Y.-H., Jiang, Y., Shi, X., Kertbundit, S., and Hall, T. C. (2005). A two-edged role for the transposable element *Kiddo* in the *rice ubiquitin2* promoter. *Plant Cell* 17, 1559–1568. doi:10.1105/tpc.104.030528.1.
- Yang, G., Zhang, F., Hancock, C. N., and Wessler, S. R. (2007). Transposition of the rice miniature inverted repeat transposable element mPing in *Arabidopsis thaliana*. *Proc. Natl. Acad. Sci. U. S. A.* 104, 10962–7. doi:10.1073/pnas.0702080104.
- Yang, H., and Murphy, A. S. (2009). Functional expression and characterization of *Arabidopsis* ABCB, AUX1 and PIN auxin transporters in *Schizosaccharomyces pombe*. *Plant J.* 59, 179–91. doi:10.1111/j.1365-313X.2009.03856.x.
- Yue, R., Tie, S., Sun, T., Zhang, L., Yang, Y., Qi, J., Yan, S., Han, X., Wang, H., and Shen, C. (2015). Genome-wide identification and expression profiling analysis of ZmPIN, ZmPILS, ZmLAX and ZmABCB auxin transporter gene families in maize (*Zea mays* L.) under various abiotic stresses. *PLoS One* 10, e0118751. doi:10.1371/journal.pone.0118751.
- Zazimalová, E., Murphy, A. S., Yang, H., Hoyerová, K., and Hosek, P. (2010a). Auxin transporters--why so many? *Cold Spring Harb. Perspect. Biol.* 2, a001552. doi:10.1101/cshperspect.a001552.
- Zazimalová, E., Murphy, A. S., Yang, H., Hoyerová, K., and Hosek, P. (2010b). Auxin transporters--why so many? *Cold Spring Harb. Perspect. Biol.* 2, a001552. doi:10.1101/cshperspect.a001552.
- Zenser, N., Ellsmore, a, Leasure, C., and Callis, J. (2001). Auxin modulates the degradation rate of Aux/IAA

- proteins. *Proc. Natl. Acad. Sci. U. S. A.* 98, 11795–800. doi:10.1073/pnas.211312798.
- Zettl, R., Feldwisch, J., Bolandt, W., Schell, J., and Palme, K. (1992). probe for naphthylphthalamic acid receptor proteins from higher plants : Identification of a 23-kDa protein from maize coleoptile plasma membranes. 89, 480–484.
- Zhang, X., Feschotte, C., Zhang, Q., Jiang, N., Eggleston, W. B., and Wessler, S. R. (2001). P instability factor: an active maize transposon system associated with the amplification of Tourist-like MITEs and a new superfamily of transposases. *Proc. Natl. Acad. Sci. U. S. A.* 98, 12572–7. doi:10.1073/pnas.211442198.
- Zhao, Y. (2010). Auxin biosynthesis and its role in plant development. *Annu. Rev. Plant Biol.* 61, 49–64. doi:10.1146/annurev-arplant-042809-112308.
- Zhou, F., Tran, T., and Xu, Y. (2008). Nezha, a novel active miniature inverted-repeat transposable element in cyanobacteria. *Biochem. Biophys. Res. Commun.* 365, 790–794. doi:10.1016/j.bbrc.2007.11.038.